Heat shock protein 90 is a master regulator of HIV-1 latency

Somaya NoorSaeed

Thesis submitted for the degree of

Doctor of Philosophy

Division of Infection and Immunity

University College London

February 2025

Declaration

I, Somaya NoorSaeed, confirm that the work presented in this thesis is my own. Where information has been derived from other sources, I confirm that this has been indicated in the thesis.

Abstract

An estimated 39.9 million people live with HIV-1 globally. While combined antiretroviral therapy has significantly reduce the mortality rate of HIV-1 patients by controlling the virus and preventing its spreading, interrupting the treatment causes the virus to rebound from a latent reservoir that is mostly present in memory CD4+ T cells. Therefore, treatment is not curative but rather lifelong. Alternative treatment strategies involve the use of pharmacological agents to Induce deep latency or stimulation of latently infected cells to facilitate immune-mediated clearance. The multifactorial nature of HIV-1 latency is associated with the infected CD4+ T cell's activation status. Hence to perturb latency, it is necessary to target several pathways simultaneously without compromising CD4+ T cell activity and function. HIV-1 latency has been demonstrated to be regulated by Hsp90, although knowledge on the pathways is limited. However, Hsp90 known to enhance the proper folding of numerous cellular proteins required for HIV-1 gene expression, for this reason, we hypothesized that Hsp90 might be a master regulator of latency. We tested this hypothesis using a polyclonal Jurkat cell model of latency and *ex-vivo* latently infected primary CD4+ T cells. Here we showed that Hsp90 is necessary for HIV-1 reactivation in the Jurkat model, which is mediated via the T-cell receptor, agonists of TLR-7 and TLR-8, phorbol esters, TNF-α, and FOXO-1 suppression. Additionally, in primary cells, targeting Hsp90 reduced HIV-1 gene expression induced by stimulation the TCR or in the presence of IL7/IL15 or a FOXO-1 inhibitor. The activation of the NF-kB, NFAT, and AP-1 signal transduction pathways was inhibited by chemically inhibiting Hsp90. We showed that Hsp90 inhibition for HIV-1 was mostly significant within the CD4+ T cell

population, CDRA45+ CCR7+ “naïve” and CD45RA- CCR7- “effector memory” which did not perturb their phenotype or activation state. Our results indicate that Hsp90 is a master regulator of HIV-1 latency that can potentially be targeted in cure strategies.

Impact statement

HIV-1 continues to be a significant global health challenge. Although combined antiretroviral therapy (cART) effectively suppresses viral replication, it is not a cure. Interruption of treatment often leads to a rapid viral rebound due to the persistence of a latent reservoir in memory CD4+ T cells, necessitating lifelong therapy and driving the search for alternative cure strategies.

This thesis highlights the role of heat shock protein 90 (Hsp90) in regulating HIV-1 latency and reactivation. Using both a polyclonal Jurkat cell latency model and *ex-vivo* latently infected primary CD4+ T cells, the study reveals that Hsp90 is essential for HIV-1 reactivation triggered by various stimuli. Inhibiting Hsp90 significantly disrupted the activation of critical signal transduction pathways, including NF-kB, NFAT, and AP-1, all of which are essential for viral reactivation.

Furthermore, Hsp90 inhibition did not significantly alter the phenotype or activation state of CD4+ T cells, suggesting that targeting Hsp90 can suppress HIV-1 reactivation while preserving the functional integrity of these immune cells. This finding positions Hsp90 as a promising therapeutic target for developing functional cure strategies. By inhibiting Hsp90, it may be possible to enforce a "block-and-lock" strategy, keeping the virus in a deeply latent state and preventing reactivation, even in the absence of cART. Alternatively, Hsp90 inhibition could improve the effectiveness of latency-reversing agents by disrupting pathways critical for viral persistence.

Overall, this research highlights the central role of Hsp90 in maintaining HIV-1 latency and its potential as a therapeutic target. These findings provide valuable insights into latency mechanisms and open new avenues for noval strategies aimed at targeting latent HIV-1 reservoirs, bringing us closer to the goal of achieving a functional cure.

UCL Research Paper Declaration Form: referencing the doctoral candidate's own published work(s)

1. For a research manuscript that has already been published (if not yet published, please skip to section 2):

1. (a) What is the title of the manuscript?
2. (b) Please include a link to or doi for the work:
3. (c) Where was the work published?
4. (d) Who published the work?
5. (e) When was the work published?
6. (f) List the manuscript's authors in the order they appear on the publication:
7. (g) Was the work peer reviewed?
8. (h) Have you retained the copyright?
9. (i) Was an earlier form of the manuscript uploaded to a preprint server (e.g. medRxiv)? If 'Yes', please give a link or doi

   If 'No', please seek permission from the relevant publisher and check the box next to the below statement:

□ I acknowledge permission of t he publisher named under 1d t o i nclude in t his t hesis portions of t he publication named as i ncluded i n 1c.

2. For a research manuscript prepared for publication but that has not yet been published (if already published, please skip to section 3):

(a) What is the current title of the manuscript? *Heat shock protein 90 is a master regulator of HIV-1 latency*

(b) Has the manuscript been uploaded to a preprint server e.g. medRxiv' ?

If 'Yes', please please give a link or doi:

doi: https://doi.org/10.1101/2024.08.23.609311

(c) Where is the work intended to be published? PLOS Pathogens

(d) List the manuscript's authors in the intended authorship order:

Somaya Noorsaeed, Nawal AlBurtamani, Ahmed Rokan, Ariberto Fassati

(e) Stage of publication: under redivision

3. For multi-authored work, please give a statement of contribution covering all authors (if single-author, please skip to section 4): I performed the experimental work for this publication with exception of Figure 3.1, performed by Nawal AlBurtamani. Ahmed Rokan helped in data analysis and reviewed the manuscript. I prepared all figures for this publication and Ariberto Fassati supervised the project and wrote the paper.

4. In which chapter(s) of your thesis can this material be found?

Chapter 3

e-Signatures confirming that the information above is accurate (this form should be co-signed by the supervisor/ senior author unless this is not appropriate, e.g. if the paper was a single-author work):

Candidate: Somaya Noorsaeed  Date: 28 January 2025

Supervisor/Senior Author signature (where appropriate): Ariberto Fassati

 Date: 28 January 2025

Acknowledgements

I would like to express my deepest gratitude to my supervisor, Prof. Ariberto Fassati, for giving me the opportunity to pursue my PhD in his laboratory. I am deeply thankful for his mentorship throughout my research and the writing of this thesis. I extend my appreciation to the Fassati group for fostering such an inspiring and collaborative environment.

Completing this PhD would not have been possible without the incredible support of the amazing people in my life. I am especially thankful to my husband, Ahmed, who believed in me throughout this journey and was always there to support me whenever I needed it.

I dedicate this thesis to my wonderful mother, whose constant support and encouragement have been the foundation of my education. I would also like to thank my family, especially my siblings (Ashraf, Sally, Soha, and Dr. Sondos) who have always been there for me. Without their support, I would not be where I am today.

Lastly, I would like to thank Prof. Clare Jolly and Prof. Benedict Seddon for their continued advice and guidance throughout my research. I am also grateful to everyone in the division who has offered their help along the way.

Statement of contributions

Chapter 3

Generation of Jurkat model of latency (section 3.1) done by Nawal AlBurtamani (PhD student in Prof. Ariberto Fassati's lab).

Chapters 4-5

These chapters are solely my work, with input from my supervisor Prof. Ariberto Fassati.

Table of contents

List of Figures

List of Tables

Abbreviations

cART	Combined antiretroviral therapy
ART	Antiretroviral therapy
Hsp90	Heat shock protein 90
PLWH	People are living with HIV
AIDS	Acquired immunodeficiency syndrome
PrEP	Pre-exposure prophylaxis
PWID	People who inject drugs
MSM	Men who have sex with men
SIV	Simian immunodeficiency virus
CRFS	Circulating recombinant forms
NNRTIS	Non-nucleoside reverse transcriptase inhibitors
PIS	Protease inhibitors
INSTIS	Integrase strand transfer inhibitors
LTRS	Long terminal repeats
MA	Matrix
CA	Capsid
PR	Protease
RT	Reverse transcriptase
IN	Integrase
RT	Reverse transcriptase
NC	Nucleocapsid
PIC	Pre-integration complex
MTOC	Microtubule organizing center
FEZ1	Fasciculation and elongation protein zeta 1
BICD2	Bicaudal D homolog 2
CypA	Cyclophilin A
NPC	Nuclear pore complex
TNPO3	Transportin 3
SPADs	Speckle-associated chromatin domains

LAD	Lamina-associated domain
LEDGF	Lens epithelium-derived growth factor
Pol II	RNA polymerase II
ssRNA	Single-stranded RNA
dsDNA	Double-stranded DNA
cDNA	Complementary DNA
mRNA	Messenger RNA
PBS	Primer binding site
tRNA	Transfer RNA
PPT	Polypurine tract
AZT	Zidovudine
3TC	Lamivudine
TDF	tenofovir disoproxil fumarate
EFV	efavirenz
NVP	nevirapine
DOR	doravirine
LEDGF/p75	lens epithelium-derived growth factor
IBD	Integrase-binding domain
CPSF6	Cleavage and Polyadenylation Specificity factor subunit 6
DSIF	DRB Sensitivity-Inducing factor
NELF	Negative elongation factor
TAR	Transactivation response element
P-TEFb	Positive transcription elongation factor b
CDK9	Cyclin-dependent kinase 9
CTD	C-terminal domain
7SK snRNA	7SK Small nuclear RNA
SEC	Super elongation complex
Rev	Response element
PI(4,5)P2	Phosphatidylinositol-4,5-bisphosphate
ALIX	Apoptosis-linked gene 2-interacting protein X
Vif	Viral infectivity factor

Vpr	Viral protein R
Vpu	Viral protein U
Nef	Negative factor
TAT	Trans-activator of transcription
FITM	The interferon-induced transmembrane
REAF	RNA-associated early-stage antiviral factor
Tcm	T cells
Ttm	Transitional memory T cells
HDACs	Histone deacetylases
TF	Transcription factors
TCR	T cell receptor
CBF-1	C-promoter binding factor-1
HATs	Histone acetyltransferases
PBAF	Polybromo-associated factor
Nuc-1	Repositions nucleosome 1
TSS	Transcription start site
HMTs	Histone methyltransferases
ECs	Elite controllers
HDACis	Histone deacetylase inhibitors
LRAs	Latency reversing agents
TLR	Toll-like receptor
PKC	Protein kinase C
STAT5	Signal transducer and activator of transcription 5
LPAs	Latency-promoting agents
dCA	Didehydro-cortistatin A
BLT	Bone marrow-liver-thymus
BRD4	Bromodomain-containing protein 4
mTOR	Mechanistic Target of Rapamycin
PTCs	Post-treatment controllers
ZNF	Zinc-finger
ZFN)	Zinc-finger nucleases

TALENs	Transcription activator-like effector nucleases
bNAbs	Broadly neutralizing antibodies
ADCC	Antibody-dependent cellular cytotoxicity
CDC	Complement-dependent cytotoxicity
ATI	Antiretroviral therapy interruption
NHPs	Non-human primates
Hsps	Heat shock proteins
ER	Endoplasmic reticulum
NTD	N-terminal domain
MD	Middle domain
MEEVD	Met-Glu-Glu-Val-Asp
TPR	Tetratricopeptide repeat
HAT	Histone acetyltransferases
HSF1	Heat shock factor 1
HSEs	Heat shock elements
NSCLC	Non-small cell lung cancer
GIST	Gastrointestinal stromal tumours
17-AAG	17-allylamino-17-demethoxygeldanamycin
PTMs	Post-translational modifications
HIF-1α	Hypoxia-inducible factor 1α
ChIP	Chromatin immunoprecipitation
PBMCs	Peripheral blood mononuclear cells
EV-71	Human enterovirus 71
DENV	Dengue virus
HBV	Hepatitis B virus
CHIKV	Chikungunya virus
EBOV	Ebola virus
SARS	Severe acute respiratory syndrome coronavirus 2
VSV	Vesicular stomatitis virus
PDK1	Phosphoinositide kinase 1
VICE foci	Virus-induced chaperone-enriched foci

HSV-1	Human herpesvirus-1
EBV	Epstein-Barr virus
KSHV	Kaposi's sarcoma-associated herpesvirus
VZV	Varicella-zoster virus
TNFα	Tumour necrosis factor α
PMA	Phorbol myristate acetate
MFI	Mean fluorescence intensity
PHA	Phytohemagglutinin
ITAMs	Immunoreceptor tyrosine-based activation motifs
LAT	Linker for T cell activation
TAK1	Transforming-growth-factor- β-activated kinase-1
MAPK	Mitogen-activated protein kinase
AP-1	Activator protein complex 1
HIF-1α	Hypoxia-Inducible Factor 1-alpha
PRRs	Pattern recognition receptors
TGF-β	Transforming Growth Factor-beta
IKK complex	Iκb kinase complex
TPR	Triple parameter reporter
RCAN1	Regulator of Calcineurin 1
FMO	Fluorescence minus one
tSNE	T-distributed stochastic neighbour embedding
Tscm	T memory stem cells
AhR	The aryl hydrocarbon receptor

Chapter 1: Introduction

1.1 Epidemiology of HIV-1

HIV remains one of the most serious global health challenges. As of 2023, it is estimated that approximately 39.9 million people are living with HIV (PLWH) worldwide, with the vast majority infected by HIV-1 [1]. The HIV-1 pandemic began in the early 1980s, with the first cases of what would later be termed AIDS (Acquired Immunodeficiency Syndrome) reported in 1981 [2]. Since its discovery, HIV-1 has caused millions of deaths globally and continues to exert a significant negative impact on health and the economy. However, mortality rates have dropped significantly with the introduction and widespread use of antiretroviral therapy (ART), reaching their lowest levels since the 1980s [1]. Public health achievements have dramatically increased the life expectancy of PLWH, reducing AIDS-related mortality to its lowest point since the peak in 2004 [1].

In Sub-Saharan Africa, where the epidemic has been most severe, these advancements have led to an increase in average life expectancy from 56.3 years in 2010 to 61.1 years in 2023 [1]. Globally, the incidence of new HIV infections in 2023 was 39% lower than in 2010. Sub-Saharan Africa saw the most significant decline, with new infections decreasing by 56% over this period. Despite these encouraging developments, approximately 1.3 million people (with estimates ranging from 1.0 million to 1.7 million) were newly diagnosed with HIV in 2023, underscoring the ongoing need for sustained prevention and treatment initiatives [1].

HIV is classified into two main types: HIV-1 and HIV-2. Both viruses originate from cross-species transmission events involving simian immunodeficiency viruses (SIVs) from non-human primates to humans [2]. The majority of infections globally are caused by HIV-1, but HIV-2 is more regional, with the highest prevalence in West Africa, especially in countries such as Guinea-Bissau and Senegal [2]. It is estimated that between 1 and 2 million people are living with HIV-2 globally [2].

HIV-1 and HIV-2 are transmitted through similar pathways, including heterosexual contact, mother-to-child transmission (MTCT) during pregnancy, childbirth, or breastfeeding, and exposure to contaminated blood or needles. However, HIV-2 is less infectious than HIV-1 and typically progresses to disease more slowly [2].

HIV-1 is transmitted mostly through heterosexual contact, which accounts for the vast majority of infections worldwide, almost 85% of all cases [3]. Sub-Saharan Africa is the epicentre of the epidemic, accounting for approximately 70% of global infections [3]. This region has been severely impacted by a variety of social, economic, and structural reasons, including restricted access to healthcare, gender inequity, and stigma [3]. In contrast, high-income countries have seen marked declines in new infections and AIDS-related deaths, largely attributable to the widespread availability of antiretroviral therapy (ART) and the implementation of comprehensive prevention programs, including pre-exposure prophylaxis (PrEP) and harm reduction strategies [4]. However, even in these situations, discrepancies remain, notably among marginalised populations such as men who have sex with men (MSM), people who inject drugs (PWID), and racial and ethnic minorities [5].

HIV-1 exhibits extensive genetic diversity, which significantly impacts both its epidemiology, and the strategies used for therapeutic management. The virus is classified into four distinct groups: M (major), N, O, and P, each representing a separate zoonotic transmission event from non-human primates to humans [2,6]. The most prevalent group, Group M, is responsible for the global HIV-1 pandemic [2,6]. Since its discovery, Group M has infected over 60 million people and led to more than 25 million deaths [2,5]. This group originated from the simian immunodeficiency virus (SIVcpz) found in the chimpanzee subspecies Pan troglodytes in Central Africa, with the cross-species transmission likely occurring in southeastern Cameroon [2,6]. Group N also emerged from the same chimpanzee subspecies, while Groups O and P are linked to the SIVgor strain, which infects western lowland gorillas (*Gorilla gorilla gorilla*) [2,6]. These findings suggest a more complex transmission history, where the virus initially jumped from chimpanzees to gorillas before ultimately being transmitted to humans. This complex evolutionary pathway underscores the dynamic nature of HIV-1's origins and the critical role of primate species in the emergence of the virus [2].

Group M has evolved into nine different subtypes (A through K) as well as several circulating recombinant forms (CRFs) [7]. These CRFs, which result from recombination events between various subtypes, are common in locations where multiple subtypes co-circulate [7]. The dynamic nature of HIV-1 diversity is particularly evident in regions with high rates of circulating recombinant forms, where recombinant strains can account for up to 20% of infections. In Southeast Asia, for

example, CRF01_AE is the prevalent strain, frequently associated with heterosexual transmission networks [7]. Emerging research suggests that those infected with several HIV-1 strains or recombinant forms may have more rapid disease development, highlighting the clinical importance of viral diversity [3]. This has consequences for treatment options, because increased genetic variability can influence medication resistance and the efficiency of antiretroviral regimens [3].

HIV-2 exhibits considerable genetic diversity, though it has not been studied as extensively as HIV-1 [2]. HIV-2 is classified into multiple groups, labelled A to H, with Groups A (prevalent in West Africa) and B (common in Côte d'Ivoire) being the most frequently observed in humans. The origin of HIV-2 is traced to the simian immunodeficiency virus (SIVsmm), which infects sooty mangabey monkeys (*Cercocebus atys*) [2]. The virus is believed to have jumped to humans through activities like the hunting and butchering of bushmeat, which exposed individuals to the blood of infected primates [2,6].

HIV-2 infections generally progress to AIDS more slowly than HIV-1. However, once the disease advances, the clinical outcomes and mortality rates become comparable to those seen in late-stage of HIV-1 infections. Diagnosing and treating HIV-2 poses unique challenges, primarily because many standard diagnostic tests are optimized for HIV-1 detection, which can lead to underdiagnosis of HIV-2. Additionally, HIV-2 exhibits natural resistance to non-nucleoside reverse transcriptase inhibitors (NNRTIs), necessitating the use of alternative treatments such as protease inhibitors (PIs) and integrase strand transfer inhibitors (INSTIs) [8].

The epidemiology of HIV-1 and HIV-2 is governed by transmission dynamics, genetic variation, and inequities in healthcare access. While great progress has been made in managing the epidemic, challenges such as viral recombination, regional differences, and stigma remain significant. Addressing these concerns through targeted treatments, improved healthcare infrastructure, and continuous research is crucial to lowering the global HIV-1 load and bringing us closer to the goal of eliminating AIDS as a public health danger [3,7].

1.2 Clinical features of HIV-1 infection

The progression of HIV-1 infection to AIDS is marked by a series of defined stages **(Figure 1.1)**, beginning with the acute infection phase, during which the virus replicates rapidly and spreads throughout the body [3,4,9,10]. This phase typically occurs within two to four weeks following exposure and is often associated with flu-like symptoms [4]. During acute infection, HIV-1 rapidly depletes CD4+ T cells in peripheral blood, and a high viral load is observed. Although the immune system mounts a strong response, HIV-1 is not eradicated and instead establishes latent reservoirs in memory CD4+ T cells, which will later contribute to long-term persistence of the virus [3].

Following the acute phase, HIV-1 enters a period of clinical latency (Asymptomtic but progressive phase), which can last several years or even decades. Although asymptomatic, this stage is not a true latency but rather a period of chronic low-level replication. CD4+ T cell counts gradually decline, and the immune system remains

in a state of chronic activation, partly due to ongoing viral replication and immune responses to HIV-1. This prolonged activation exhausts immune resources, reducing the effectiveness of CD8+ T cells in fighting infections. Chronic immune activation also drives bystander apoptosis of uninfected T cells, further depleting the CD4+ T cell population and accelerating the decline in immune function [9,10].

AIDS, the final stage of HIV-1 infection, is defined by severe immunosuppression, reflected by CD4+ T cell counts falling below 200 cells/mm³ or by the presence of AIDS-defining opportunistic infections or cancers [4]. At this stage, the immune system is profoundly compromised, unable to mount effective responses against pathogens or to suppress malignancies (**Figure 1.1**). Common opportunistic infections associated with AIDS include Pneumocystis jirovecii pneumonia, tuberculosis, and fungal infections, while cancers such as Kaposi's sarcoma and lymphomas also frequently occur [4]. In untreated individuals, AIDS-related complications are the primary causes of morbidity and mortality [3,4].

The rate of disease progression varies significantly among individuals, influenced by multiple viral, host, and environmental factors. Certain viral strains, such as those using the CXCR4 coreceptor, are associated with more rapid CD4+ T cell decline. Host genetics also play a role; for example, individuals with specific HLA alleles, such as *HLA-B57 and HLA-B*27, exhibit slower disease progression [11]. Additionally, genetic mutations affecting the CCR5 coreceptor (e.g., CCR5-Δ32) confer resistance to R5-tropic HIV-1 strains, highlighting the importance of host factors in modulating HIV-1 pathogenesis [12].

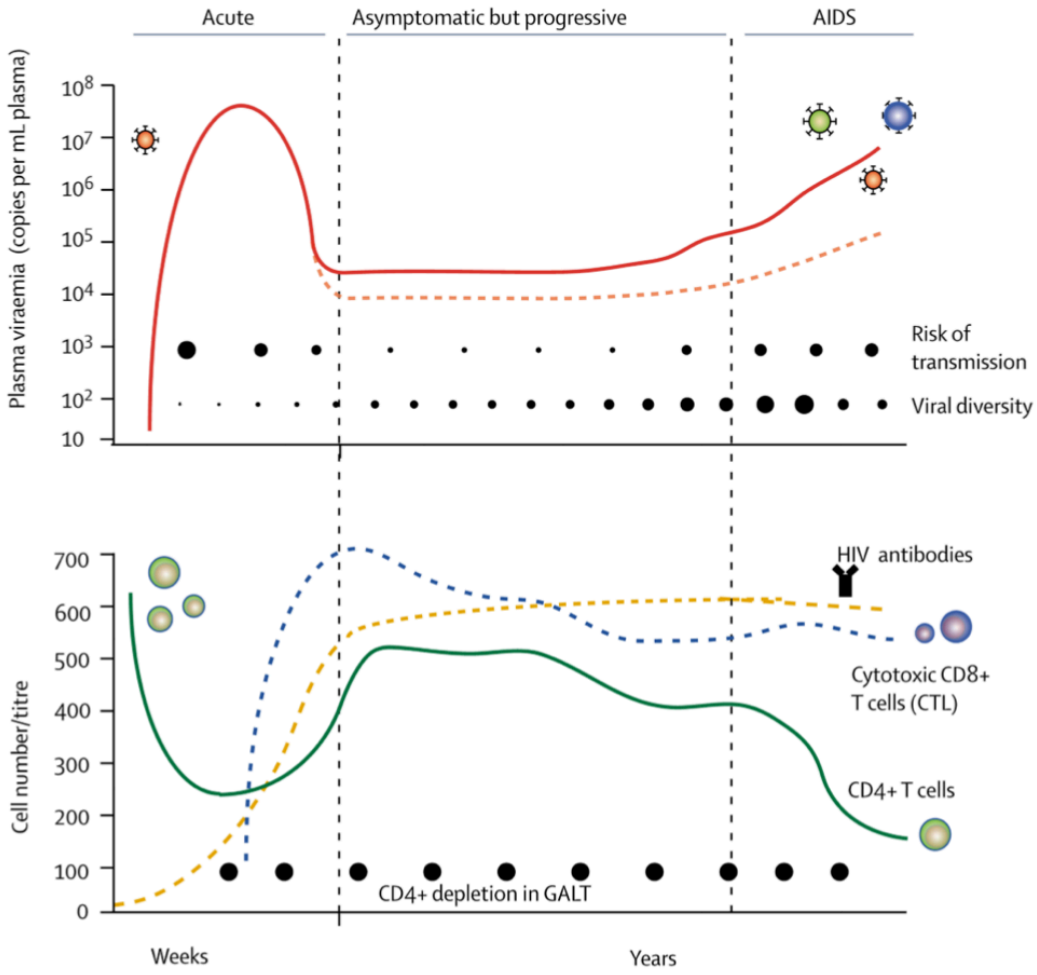

Figure 1.1 Clinical features of HIV-1 infection. The progression of HIV-1 infection is defined by levels of viral replication and changes in CD4+ T-cell populations. During acute infection, plasma viraemia peaks (red line, top panel), accompanied by a significant decline in CD4+ T-cell counts (green line, bottom panel) and the absence of HIV-1-specific antibodies (yellow dashed line, bottom panel). As the immune system responds, cytotoxic CD8+ T lymphocytes (CTLs) expand (blue dashed line, bottom panel), leading to a reduction in viraemia and the establishment of an individual viral load set point during the chronic phase. This set point varies widely among individuals (red dashed line, top panel) and serves as a predictor of disease progression. Over time, viral diversity increases (indicated by closed circles, top panel), reflecting ongoing viral evolution. The risk of transmission is particularly high in the early weeks of infection when viraemia reaches its peak. GALT (gut-associated lymphoid tissues) is also significantly impacted during this phase. Taken from Simon V et al., 2006 [3].

1.3 HIV-1 structure and life cycle

1.3.1 HIV-1 Genome and virion structure

The HIV-1 genome is a compact and efficient genetic system, consisting of approximately 9 kilobases (kb) of single-stranded, positively sensed RNA. This genome contains all the information required to encode 15 proteins essential for the virus's replication and assembly within host cells [13] **(Figure 1.2).** In its encapsulated virion form, the genome exists as a dimer of two identical RNA molecules, ensuring redundancy and stability during infection.

The HIV-1 genome is structured around nine distinct ORFs (Open reading frame), which include the gag, pol, and env genes encoding structural and enzymatic components of the virus, as well as accessory genes such as tat (Trans-activator of transcription), regulator of virion expression (Rev), viral infectivity factor (Vif), viral protein R (Vpr), viral protein U (Vpu), and negative factor (Nef) which play critical roles in viral replication and immune evasion [13]. Flanking the genome are long terminal repeats (LTRs), which are critical regulatory regions divided into U3, R, and U5 elements. These LTRs contain the viral promoter and other regulatory elements necessary for gene expression, integration into the host genome, and reverse transcription. This tightly organized and multifunctional genomic architecture underscores the adaptability and resilience of HIV-1 in overcoming host defenses and establishing infection [13].

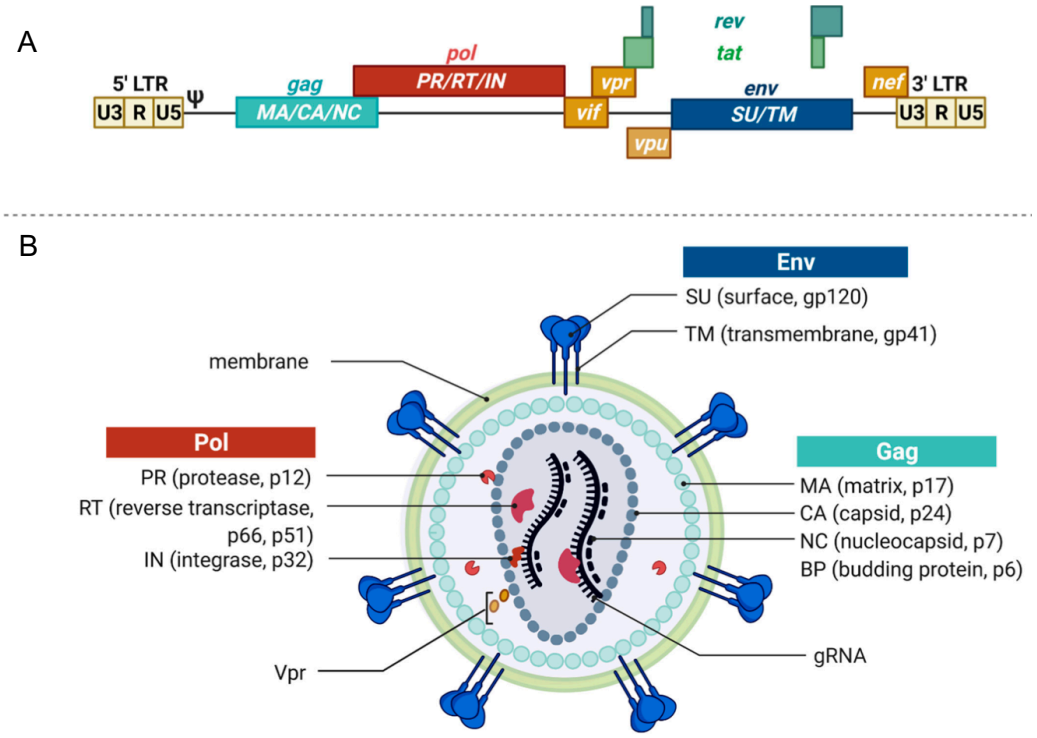

Figure 1.2 HIV-1 genome and virion structure. A) The HIV-1 genome is organized to encode structural, regulatory, and accessory proteins essential for viral replication and assembly. It consists of a linear, dimeric single-stranded RNA (ssRNA) approximately 9 kb in length, flanked by 5′ and 3′ LTRs. The LTRs contain crucial sequences, including the viral promoter and elements required for reverse transcription, integration, and gene expression. The LTR regions are divided into the U3, R, and U5 segments, followed by the packaging signal Psi (ψ). The Gag gene encodes structural proteins such as matrix (MA), capsid (CA), and nucleocapsid (NC), which form the viral core. The Pol gene encodes the viral enzymes protease (PR), reverse transcriptase (RT), and integrase (IN). Adjacent to Pol are the regulatory genes rev and tat, and the accessory genes vif, vpr, and vpu. The Env gene encodes the envelope glycoproteins, including the surface unit (gp120) and the transmembrane unit (gp41), which facilitate host cell entry. The genome also contains the accessory gene nef, located downstream of Env. B) The mature virion is spherical and enveloped by a lipid bilayer derived from the host cell membrane, incorporating 7–35 trimeric envelope glycoproteins. Beneath the membrane, the Gag-derived MA proteins form an inner layer, which also contains Vpr and PR. At the center of the virion is the capsid, housing two copies of the ssRNA along with RT, IN, and NC proteins, which stabilize the RNA. These structural and enzymatic components are critical for the infectivity and replication of the virus. Taken from Heuvel et al. 2022 [13].

1.3.2 HIV-1 life cycle virus entry to the target cells

The process of viral entry begins when the HIV-1 envelope glycoprotein, gp120, binds to the CD4 receptor on the surface of target cells [3,14]. This interaction induces conformational changes in gp120, exposing binding domains for one of two chemokine coreceptors: CCR5 or CXCR4. The specific coreceptor engaged determines the virus's tropism and cellular targets [3,15–17].

HIV-1 displays distinct tropism profiles depending on the host cell type, with notable differences between monocytes/macrophages and CD4+ T cells. These variations in cellular tropism significantly influence the dynamics of viral replication, the establishment and maintenance of latent reservoirs, and the overall pathogenesis of the infection [4].

R5-tropic strains of HIV-1, which use the CCR5 coreceptor, have a strong preference for infecting macrophages and monocytes. These cells typically express lower levels of CD4 yet are still susceptible to R5 viruses due to the efficient use of CCR5. R5-tropic viruses are predominantly involved in the early stages of HIV infection and are the primary variants transmitted across mucosal barriers [4]. In contrast, CD4+ T cells can be infected by both R5- and X4-tropic variants. X4-tropic viruses utilize the CXCR4 coreceptor and tend to emerge during later stages of infection. Their emergence is often associated with higher viral replication rates, enhanced cytopathicity, syncytium formation, and accelerated depletion of CD4+ T cells, which contributes to rapid disease progression [18].

Upon HIV-1's attachment to both CD4 and a coreceptor, the transmembrane protein gp41 facilitates the fusion of the viral envelope with the host cell membrane, enabling the viral capsid to enter the cell [19]. Once the viral core enters the cytoplasm, it is directed toward the nucleus, and viral RNA undergoes reverse transcription by the virus's reverse transcriptase (RT) to form DNA, the absence of proofreading function in this enzyme results in an increased mutation rate, facilitating viral diversity and supporting immune evasion [4].

The core, either intact or partially disassembled, is transported through the nuclear pores. After reverse transcription is finalized within the nucleus, the core structure fully disassembles in a process known as uncoating. At this point, the pre-integration complex (PIC), which includes the IN, facilitates the integration of viral DNA into the host genome. This integration step is critical for establishing a persistent infection and enabling subsequent viral replication [20] .

In addition to differences in entry mechanisms and coreceptor usage, HIV-1 also demonstrates cell type specific preferences in its integration sites within the host genome, further contributing to the differences in viral persistence between macrophages and T cells. In CD4+ T cells, HIV-1 tends to integrate into gene-dense, transcriptionally active regions often within introns of actively transcribed genes thereby promoting high levels of viral gene expression and replication [21]. Conversely, in macrophages and monocytes, the virus preferentially integrates into

gene-poor regions or heterochromatin, leading to reduced transcriptional activity and promoting a more latent state [22]. This low level of viral gene expression allows macrophages to serve as long-lived reservoirs, particularly in tissues such as the central nervous system (CNS), lungs, and gut-associated lymphoid tissue (GALT).

These combined differences in both tropism and integration site preference have significant implications for HIV-1 pathogenesis and long-term persistence [22,23].

1.3.3 Capsid structure and function

The HIV-1 capsid is a cone-shaped structure made up of hexamers and pentamers of the capsid protein (CA, p24) subunits [24]. These subunits form a fullerene cone with a tiny tip and a wider base that encloses the viral RNA genome [24] **(Figure 1.3)**. The capsid is essential for several phases of the viral life cycle, such as reverse transcription, viral entry, and viral genome integration into host DNA [25]. When it enters the host cell, its main function is to shield the viral RNA from cellular immune sensors so that it can pass through the cytoplasm and enter the nucleus without triggering an immunological reaction [25].

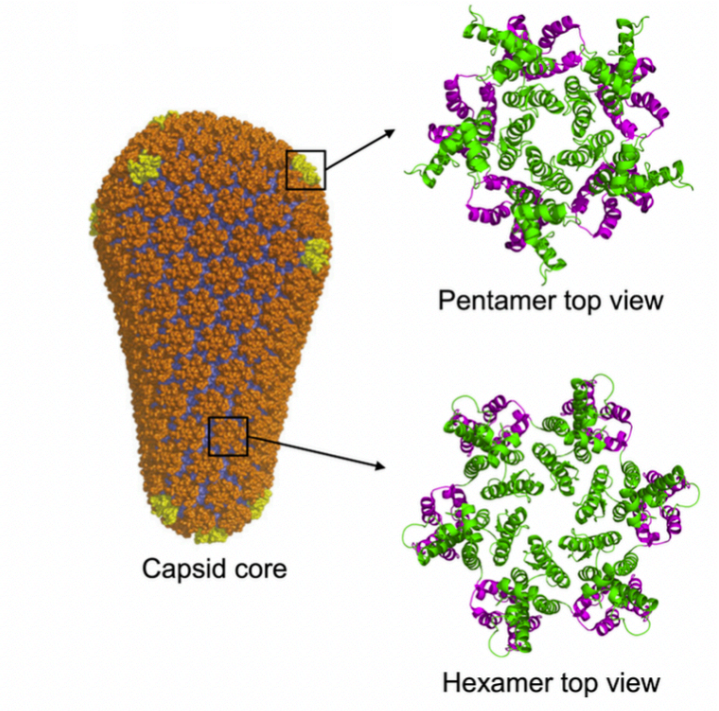

Figure 1.3 Capsid Core Structure. The mature HIV-1 capsid core adopts a fullerene cone shape, comprising a total of 125 hexameric units (in orange) and 12 pentameric units (in yellow). Taken from Toccafondi et al. 2021 [26].

In order to facilitate its effective passage through the cytoplasm and into the nucleus, the HIV-1 capsid has evolved to establish particular interaction with host cellular components. The capsid uses the host's cytoskeletal network, especially the microtubule system, to travel in a targeted manner towards the nucleus once the virus has fused with the membrane of the host cell. α-tubulin and β-tubulin dimers, which give microtubules their structural polarity, combine to form dynamic filaments [27]. Their minus ends are grouped at the microtubule organizing center (MTOC), which is close to the nucleus, while their plus ends stretch towards the cell periphery [27] **(Figure 1.4)**. The capsid's transport along microtubules is driven by the dynein motor protein complex, which moves toward the minus-ends of microtubules [27].

Dynein function is supported by its co-factor, dynactin, a multi-component protein complex that enhances dynein's activity. Additionally, several host adaptor proteins regulate this interaction by linking the capsid to the dynein motor complex. Among these adaptors, fasciculation and elongation protein zeta 1 (FEZ1) is particularly important, as it connects the capsid to dynein, enabling efficient transport [27,28]. Another key adaptor, bicaudal D homolog 2 (BICD2), strengthens the interaction between dynein and dynactin, significantly increasing the motility of the complex and facilitating long-distance transport of the capsid along microtubules [27,28].

The interaction between the HIV-1 capsid and cyclophilin A (CypA) also plays a crucial role in facilitating successful trafficking during these early stages of infection [25]. CypA binds to a conserved loop on the capsid and stabilizes its structure, protecting it from premature disassembly and ensuring efficient reverse transcription. In primary CD4+ T cells, this interaction also helps shield the viral capsid from host restriction factors like TRIM5α, which can disrupt capsid integrity [27].

As the capsid approaches the nucleus, it interacts with the nuclear pore complex (NPC) to enter the nucleus. Host nuclear transport proteins, including nucleoporins NUP358 and NUP153, as well as transportin 3 (TNPO3), guide the capsid through the nuclear envelope [27]. During this critical phase, the capsid undergoes partial disassembly, or uncoating, allowing the release of the PIC into the nucleus. The PIC, which contains integrase and other viral components, then facilitates the integration of the viral DNA into the host cell genome, a key step in establishing infection [27] **(Figure 1.4)**.

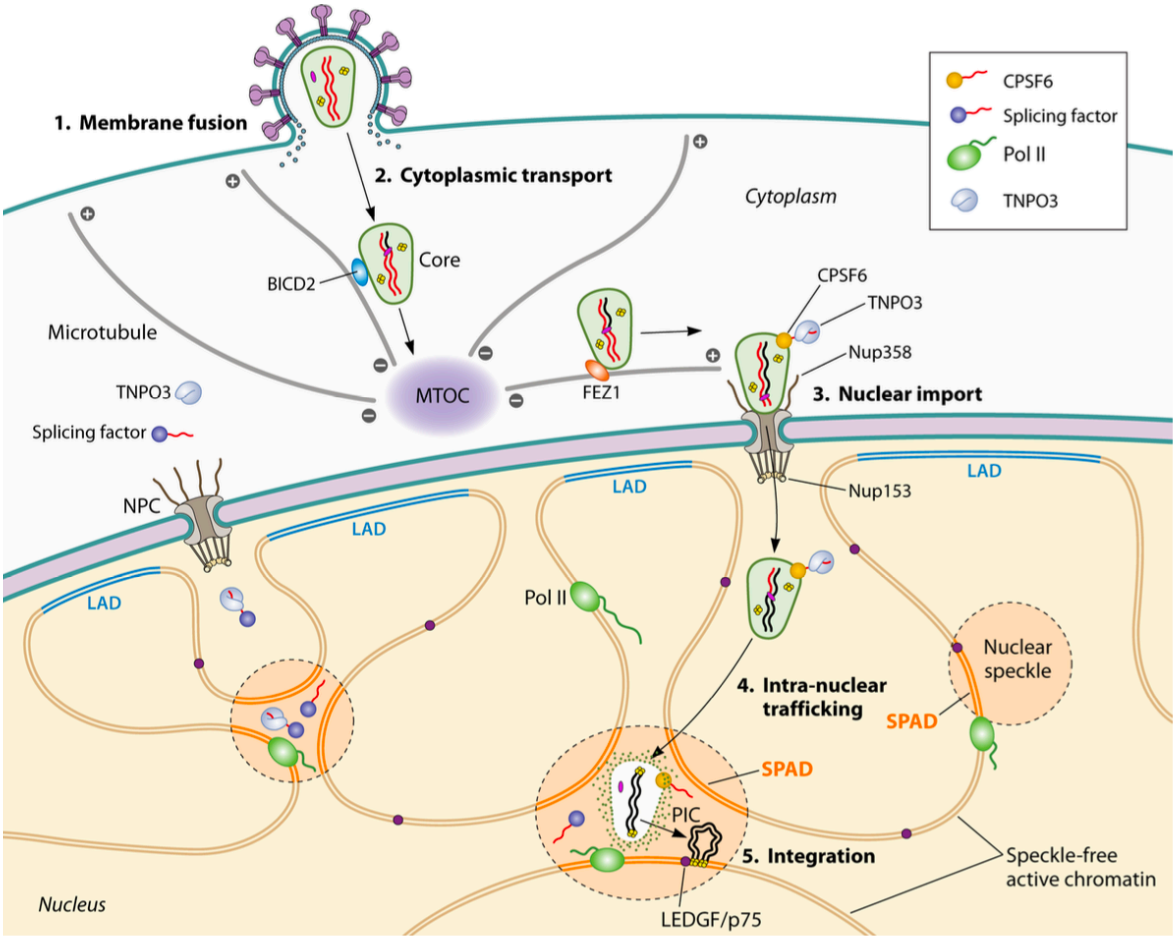

Figure 1.4 Schematic of HIV-1 ingress. HIV-1 entry into the host cell begins with the fusion of the viral and cellular membranes (step 1), allowing the viral core to enter the cytoplasm. Once inside, the core associates with motor complex adapter proteins, including BICD2 and FEZ1, facilitating its transport along microtubules (step 2) toward the MTOC and nuclear membrane. The core interacts with host cell proteins such as cleavage and polyadenylation specificity factor subunit 6 (CPSF6), NUP358, and NUP153, which support its passage through the NPC (step 3). The interaction between the viral CA and CPSF6 enables the core to access the nucleoplasm (step 4), guiding it to speckle-associated chromatin domains (SPADs) for the integration of viral DNA into the host genome (step 5). In uninfected cells, the β-karyopherin TNPO3 plays a role in transporting pre-mRNA splicing factors into the nucleus and directing them to nuclear speckles. This steady-state mechanism contrasts with the virus-specific adaptations that enable HIV-1 to exploit these cellular pathways for its replication. Abbreviations include LAD (lamina-associated domain), LEDGF (lens epithelium-derived growth factor), PIC, and Pol II (RNA polymerase II) which will disuses in section (1.3.5). Taken from Jang et al. 2023 [27].

1.3.4 Reverse transcription

Reverse transcription is the process by which HIV-1 transforms its single-stranded RNA (ssRNA) genome into double-stranded DNA (dsDNA), a crucial step for its integration into the host cell's genome. This transformation is carried out by the viral enzyme RT and occurs in several stages. The process begins with the synthesis of complementary DNA (cDNA) for the negative (-) strand and concludes with the production of a complete double-stranded proviral DNA, flanked by LTRs at both ends. This step is essential for establishing a stable infection within the host [29].

The genomic viral ssRNA has a polyadenylated tail and a 5′ cap, just like a messenger RNA (mRNA). LTRs flank the dsDNA, and HIV-1 sequences consist of around 634 base pairs that are divided into three parts called U3 (unique 3′), R (repeat), and U5 (unique 5′). The integration of the dsDNA into the host genome is facilitated by the LTR ends [29] **(Figure 1.5)**. The viral enzyme RT initiates the synthesis of DNA at the primer binding site (PBS), a structured RNA element located near the 5′ end of the RNA genome within the untranslated leader region. At this site, a cellular transfer RNA (tRNA) molecule binds to the PBS, and the 3′ hydroxyl group (-OH) of the tRNA acts as a primer for RNA-dependent DNA synthesis.

Using the RNA genome as a template, RT begins generating the complementary negative (-) strand of DNA, known as cDNA. This synthesis pauses once RT reaches the 5′ end of the RNA genome, resulting in the production of a short DNA fragment called the (-) strand strong stop DNA [29]. At this point, a strand transfer, or the first template exchange, occurs. During this process, the R region of the newly synthesized (-) strand DNA aligns with the complementary R sequence at the 3′ end of the RNA genome. This alignment enables RT to resume elongation [29].

As the (-) strand DNA synthesis progresses, the RNase H activity of reverse transcriptase degrades the RNA portion of the RNA-DNA hybrid. Most of the RNA genome is removed during this process, leaving behind only short RNA fragments. One of these fragments, the polypurine tract (PPT) located near the 3′ end of the RNA genome, is resistant to degradation and remains intact. The PPT is critical in the next stages of replication, serving as the primer for synthesizing the complementary positive (+) strand of DNA [29,30].

Reverse transcriptase continues elongating the (-) strand DNA until the entire RNA genome is transcribed into a complementary DNA strand. At this point, the synthesis of the (+) strand DNA begins, using the PPT as a primer. Reverse transcriptase extends the (+) strand DNA along the (-) strand template until it reaches the tRNA primer positioned at the 5′ end of the (-) strand DNA. This temporary halt produces a fragment known as the (+) strand strong stop DNA.

Subsequently, the tRNA primer is removed by the RNase H activity of reverse transcriptase, exposing the PBS on the (-) strand DNA. The PBS regions on both the (-) and (+) strands then anneal to one another, circularizing the developing DNA molecule. This annealing step allows the second template exchange to occur, enabling reverse transcriptase to resume and complete the synthesis of both DNA strands, forming the full-length double-stranded viral DNA [29,30] **(Figure 1.5).** This fully formed proviral DNA is incorporated into the PIC and transported to the nucleus, where it integrates into the host cell's genome.

Notably, reverse transcription is a highly error-prone process because reverse transcriptase lacks proofreading mechanisms. This inherent lack of fidelity leads to

a high mutation rate, contributing to the extensive genetic variability observed in HIV-1 [29,31].

Moreover, reverse transcription is a key process targeted in HIV-1 treatment, with two primary classes of antiretroviral drugs designed to inhibit reverse transcriptase activity: NRTIs and NNRTIs. NRTIs, such as zidovudine (AZT), lamivudine (3TC), and tenofovir disoproxil fumarate (TDF), function as nucleotide analogs that disrupt DNA synthesis by prematurely terminating the elongation process. In contrast, NNRTIs, including efavirenz (EFV), nevirapine (NVP), and more recently developed options like doravirine (DOR), bind to reverse transcriptase at a non-active site. This binding induces structural changes in the enzyme, preventing it from effectively synthesizing viral DNA. These two drug classes are essential components of cART, which is the cornerstone of modern HIV treatment [32].

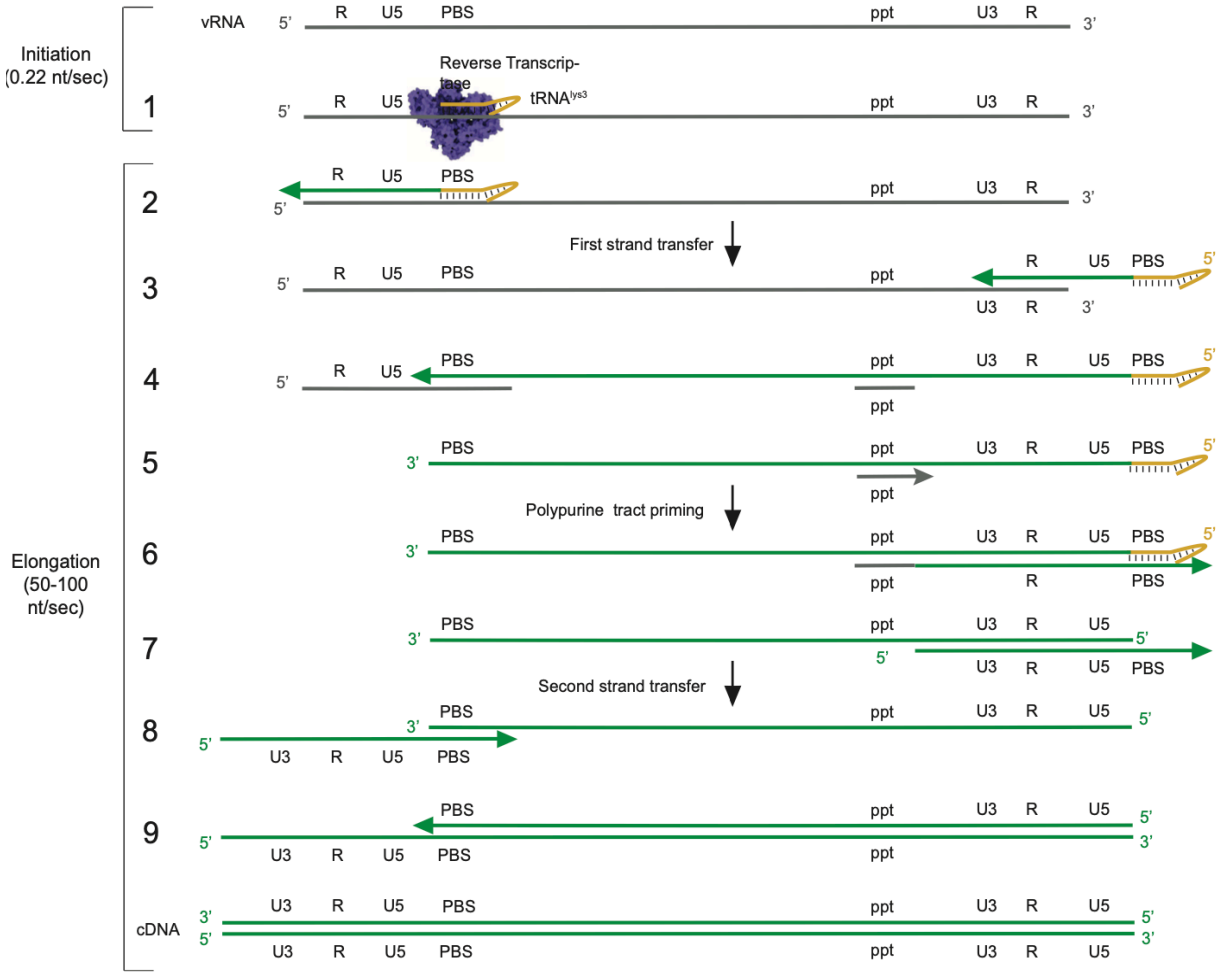

Figure 1.5 Schematic representation of the reverse transcription process in HIV-1 replication. (1) Reverse transcription begins with the synthesis of the minus strand of cDNA, extending to the repetitive R region at the 5' end of the viral RNA (vRNA) template. (2) The first strand transfer occurs, allowing the extended primer to anneal to the complementary R region at the 3' end of the vRNA template. (3) cDNA synthesis resumes, with the vRNA template being degraded except for the polypurine tract (ppt). (4) Plus-strand synthesis is initiated, with RT using the remaining ppt as a primer. (5) The plus strand extends to the PBS. (6) All remaining RNA is degraded. (7) Complementary PBS sequences enable the second strand transfer, allowing plus-strand synthesis to proceed. (8) The PBS region of the minus strand is extended to copy the U3, R, and U5 regions. (9) The final product is a double-stranded DNA molecule, flanked by U3, R, and U5 regions on either side of the protein-coding segment of the genome. Taken from Krupkin et al. 2020 [30].

1.3.5 Integration

HIV-1 genome integration into host DNA is a critical step in the viral lifecycle that results in a chronic infection in the host. The viral enzyme integrase mediates this process and inserts the viral DNA into the host genome at specific sites that are conducive to viral transcription [4,14,33,34]. HIV-1 integration shows a distinct preference for genomic regions characterized by active chromatin. These regions include areas rich in genes, transcriptionally active sites, zones with activating epigenetic marks, speckle-associated domains (SPADs), and topologically associating domains (TADs). This targeted integration is largely directed by specific virus-host interactions [27] **(Figure 1.4).**

A key host factor that significantly influences HIV-1 integration is lens epithelium-derived growth factor (LEDGF/p75). This protein directly interacts with the viral integrase through its integrase-binding domain (IBD), tethering the PIC to chromatin [27]. LEDGF/p75 guides the integration process toward transcriptionally active genomic regions, particularly within gene-rich areas marked by open chromatin and elevated gene transcription [27]. This targeting ensures that the virus integrates into sites optimal for efficient viral gene expression.

Another crucial determinant of HIV-1 integration specificity is the interaction between the viral CA and CPSF6 [19,27]. CPSF6 plays a role in directing the PIC to nuclear speckles, subnuclear structures rich in transcriptional and splicing activity. These nuclear speckles provide an environment that facilitates viral replication by supporting integration into transcriptionally active sites, enhancing both viral gene

expression and replication efficiency [27]. Together, these virus-host interactions shape the genomic integration landscape of HIV-1, favouring regions that optimize viral transcription and replication [19,27].

1.3.6 Viral gene expression

After integration of the viral DNA into the host genome, HIV-1 utilizes the host's transcriptional machinery to express its genes, producing the proteins necessary for virus assembly and release. The viral genome encodes nine genes organized in a compact manner, allowing the virus to maximize its coding capacity. These genes are transcribed and spliced to produce a wide array of mRNAs, which are subsequently translated into viral proteins.

The integrated proviral DNA serves as a template for transcription by host RNA polymerase II, where transcription is initiated at the R region of the 5' LTR and ends at the R region within the 3' LTR, which acts as the promoter region. Within the U3 element, there are binding sites for key host transcription factors such as NF-kB, SP1, AP-1, and NFAT, along with the TATA box, which is critical for transcription and recruitment of RNA polymerase II [35–37]. Upon cell activation, host transcription factors such as NF-kB, NFAT, and Sp1 bind to specific sites within the 5′ LTR, initiating the transcription of viral RNA [35,38]. However, only a small amount of viral RNA is produced by basal transcription alone [3,4] and this is because of the pausing of RNA Pol II.

RNA Pol II plays a crucial role in transcription regulation, where it pauses momentarily after initiating RNA synthesis but before entering the productive elongation phase. This regulatory mechanism is mediated by negative elongation factors such as DRB Sensitivity-Inducing Factor (DSIF) and Negative Elongation Factor (NELF), which stabilize the paused Pol II and inhibit further transcription. This pausing step is critical for precise gene expression, as it allows time for proper RNA capping and the recruitment of elongation factors required for efficient transcription. HIV-1 exploits Pol II pausing to regulate its transcription [39]. The viral protein Tat is essential in this process, as it interacts with the transactivation response element (TAR), a stem-loop structure present in the nascent viral RNA at the 5' end. Tat facilitates the recruitment of the host cell's positive transcription elongation factor b (P-TEFb) to overcome the pause and drive productive elongation. P-TEFb is composed of cyclin-dependent kinase 9 (CDK9), the catalytic subunit, and Cyclin T1 or T2, the regulatory subunits. Cyclin T1/T2 activates CDK9 and helps target P-TEFb to the transcriptional machinery, enabling Pol II to resume elongation and ensuring efficient transcription of the HIV-1 genome.

P-TEFb enhances RNA Pol II activity by phosphorylating serine 2 residues within its C-terminal domain (CTD). This modification allows Pol II to transition into productive elongation while also facilitating the recruitment of RNA processing factors essential for efficient transcription. Furthermore, P-TEFb phosphorylates the SPT5 subunit of DSIF, transforming it from a negative elongation factor into a positive one. Similarly, P-TEFb phosphorylates NELF, causing its dissociation from the transcriptional complex. These combined actions release Pol II from its paused state. This release

leads to a marked increase in transcription elongation, resulting in significantly higher production of viral RNA [4,39]. This mechanism is crucial for regulating gene expression, enabling rapid responses to stimuli, and maintaining transcriptional fidelity.

P-TEFb activity is tightly regulated through sequestration and stabilization mechanisms. In its inactive state, P-TEFb is bound in a complex with 7SK small nuclear RNA (7SK snRNA), along with associated proteins such as HEXIM1, LARP7, and MePCE [39]. This sequestration inhibits CDK9 activity, preventing unregulated transcription elongation. Activation of P-TEFb occurs in response to cellular or viral signals that release it from the 7SK snRNP complex. Stabilization of P-TEFb in its active form is also achieved through interactions with proteins such as BRD4, which recruits P-TEFb to chromatin, and the super elongation complex (SEC), which enhances its efficiency at active transcription sites [40,41].

The expression of the HIV-1 gene is further controlled at the RNA processing level. The HIV-1 genome is compact, thus in order to maximise its coding potential, the virus uses alternative splicing to create a range of mRNA transcripts from a single precursor RNA [4]. Over the course of the lifecycle, the ordered expression of several viral proteins depends on this splicing. HIV-1 produces three primary types of RNA transcripts: unspliced, singly spliced, and multiple spliced [42]. The unspliced RNA serves as the genetic material for new virions and is also translated to produce the Gag and Gag-Pol polyproteins, which are essential for viral assembly and the production of viral enzymes. Singly spliced RNA, on the other hand, produces

several structural and accessory proteins, including Env, Vif, Vpu, and Vpr [42–44]. The Env protein is very important because it encodes the precursor protein gp160, which is cleaved into the envelope glycoproteins gp120 and gp41, which are required for viral attachment and host cell entry. Regulatory proteins like Tat, Rev, and Nef are encoded by multiple spliced RNA [43,44]. Each of these proteins has a distinct function in controlling host cell activity and viral replication.

1.3.7 Export of RNA from the nucleus

The export of HIV-1 RNA from the nucleus to the cytoplasm is tightly regulated and facilitated by the viral protein Rev [45]. Early in the infection, only multiply spliced transcripts are exported to the cytoplasm because these spliced RNA species are compatible with the host's nuclear export machinery [44]. As HIV-1 replication progresses, Rev binds to the Rev response element (RRE), a structured RNA sequence located within the env region of unspliced and singly spliced transcripts [45]. This interaction allows Rev to bind to the host nuclear export factor CRM1 (exportin 1), which mediates the transport of these RNA species from the nucleus to the cytoplasm. This process ensures the production of the full complement of viral proteins, including those encoded by unspliced RNA, such as Gag and Gag-Pol, as well as envelope glycoproteins derived from singly spliced RNA transcripts [4].

1.3.8 Translation and protein production

Once in the cytoplasm, the HIV-1 RNA functions as a template for viral protein synthesis. A highly regulated ribosomal frameshifting mechanism is required for the translation of unspliced HIV-1 RNA, which regulates the production of Gag and Gag-Pol polyproteins. This process occurs at a specific slippery sequence within the viral RNA, where approximately 5–10% of ribosomes undergo a -1 frameshift during translation. As a result, most ribosomes synthesize the Gag polyprotein, while a smaller fraction produce Gag-Pol. This tightly controlled balance between Gag and Gag-Pol production is critical for the proper assembly and maturation of infectious viral particles, as each polyprotein contributes distinct structural and enzymatic components necessary for the HIV-1 lifecycle [46]. The Gag polyprotein contains structural elements crucial for viral assembly, including the MA, CA, and NC proteins. In contrast, the Gag-Pol polyprotein encodes key enzymatic components necessary for viral replication, such as reverse transcriptase, integrase, and protease [46]. After translation, the viral protease, which is part of the Gag-Pol polyprotein, cleaves both Gag and Gag-Pol into their individual functional components. This cleavage is a critical step for the maturation and infectivity of the viral particles [4].

The singly spliced HIV-1 RNA directs the production of the envelope protein precursor gp160, which is initially synthesized in the rough endoplasmic reticulum. Once synthesized, gp160 is transported to the Golgi apparatus, where it undergoes glycosylation and is subsequently cleaved by the cellular protease furin into two distinct subunits, gp120 and gp41 [47]. These subunits form the mature envelope glycoprotein complex, which is subsequently transported to the host cell membrane

and incorporated into budding virions. The modified envelope glycoproteins are essential for the virus's ability to bind to and fuse with target cells, identifying them as vital components in viral infectivity [4,47].

1.3.9 Assembly, budding and maturation

1.3.9.1 Assembly of HIV-1 at the plasma membrane

HIV-1 assembly starts when the Gag polyprotein targets particular areas of the host cell membrane. Gag comprises several domains that are necessary for assembly, including the p6 regions, CA, NC, MA. Each of these domains plays a distinct role in the creation of new virions. Gag travels to the plasma membrane via the matrix domain, where it attaches itself to phosphatidylinositol-4,5-bisphosphate (PI(4,5)P2), a lipid that is abundant in some membrane microdomains known as lipid rafts [48,49]. These lipid rafts serve as assembly sites, concentrating Gag and other viral proteins to facilitate efficient viral particle formation [48].

As Gag molecules accumulate at the membrane, they multimerize through CA-CA interactions, forming a curved lattice structure that begins to shape the viral particle. This lattice structure provides a scaffold for the growing virion and enables encapsulation of the viral RNA genome [48]. The nucleocapsid domain of Gag binds specifically to the viral RNA packaging signal, ensuring that two copies of the unspliced viral RNA genome are selectively incorporated into the nascent virion. This process also recruits Gag-Pol polyproteins [48].

Env proteins, which have been trafficked to the plasma membrane after cleavage in the Golgi, are also incorporated into the budding particle. The matrix domain of Gag interacts with the cytoplasmic tail of gp41 (part of Env), securing Env in the viral envelope [48].

1.3.9.2 Budding of HIV-1 from the host cell

Once assembly is complete, the nascent virion must bud from the host cell to complete the viral replication cycle. This critical step is orchestrated by the p6 domain of the Gag polyprotein, which hijacks the host's endosomal sorting complexes required for transport (ESCRT) pathway. The ESCRT machinery, typically involved in cellular processes like multivesicular body (MVB) formation, cytokinesis, and membrane repair, is exploited by HIV-1 to mediate the scission of the budding virion from the plasma membrane [48]. The p6 domain directly interacts with specific ESCRT components, notably through its late domain motifs. These motifs, such as the PTAP (Pro-Thr-Ala-Pro) sequence, bind to Tsg101, a key component of the ESCRT-I complex [48]. Additionally, a secondary motif, YP(X)nL, interacts with ALIX (apoptosis-linked gene 2-interacting protein X), facilitating recruitment of downstream ESCRT machinery. These interactions initiate a cascade of events that lead to the assembly and activation of ESCRT-III, the core complex responsible for membrane scission. ESCRT-III subunits, such as CHMP4, oligomerize at the neck of the budding virion and, with the help of VPS4, a AAA ATPase, mediate the final scission event [48]. This process is energy-dependent, as ATP hydrolysis by VPS4

is required to disassemble and recycle ESCRT-III components after membrane fission, ensuring efficient release of the virion [48].

Mutations in the p6 domain have significant consequences for the budding process [50]. Viruses with p6 mutations fail to recruit the necessary ESCRT components, leading to defects in membrane scission. These p6 mutant viruses often remain binding to the host cell surface, significantly reducing their release efficiency [48]. Even when such virions are released, they are typically non-infectious due to improper assembly and maturation [48].

1.3.9.3 Maturation: protease-mediated cleavage and viral infectivity

The final step in the production of an infectious HIV-1 particle is maturation **(Figure 1.6),** a process driven by the viral protease. During maturation, the HIV-1 protease cleaves the Gag and Gag-Pol polyproteins into their individual components in a precise and sequential manner. The order of cleavage begins with the release of the MA protein from the CA, followed by the separation of nucleocapsid NC and p6, as well as the processing of spacer peptides such as SP1 and SP2 [9,48]. The Gag-Pol polyprotein is similarly processed to release the viral enzymes PR, RT, and IN. This ordered cleavage ensures that the structural and enzymatic components are correctly assembled and functional. Approximately 1,500 CA proteins are generated during this process, which are essential for forming the mature virion.

Protease-mediated cleavage of Gag reorganizes the virion's internal structure, converting the immature spherical shape into the mature conical core characteristic

of infectious HIV-1 particles. This structural transformation involves the reassembly of the CA into a stable, cone-shaped shell surrounding the viral RNA and associated enzymes. Inside this shell, the viral RNA, reverse transcriptase, and integrase are arranged in a conformation that is ready for delivery to a new host cell upon infection [9,48].

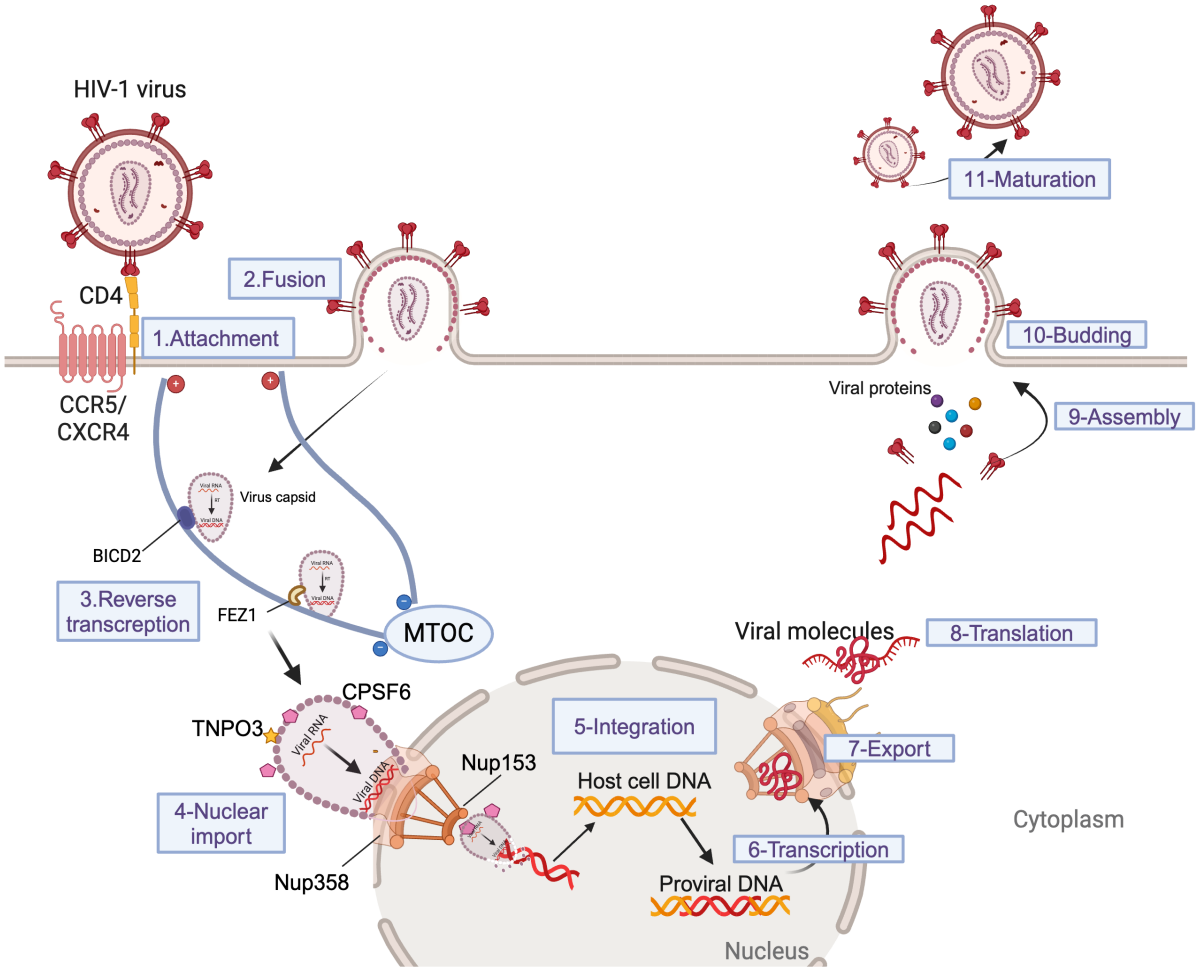

Figure 1.6 Summary of HIV-1 lifecycle. Created by Biorender.com

1.4 Restriction factors targeting HIV-1 and their counteraction

To prevent HIV-1 from replicating and spreading, the human immune system has evolved a number of intrinsic antiviral defences. Important restriction factor families, including APOBEC, IFITM, SERINC, Tetherin, MxB, TRIM5α, REAF and SAMHD1, have unique and vital functions in the fight against HIV-1. As a result, viruses have evolved defence mechanisms against the innate immune system that guarantee their survival and ability to replicate. To get past the host's immune system, HIV-1 uses four accessory proteins: viral infectivity factor Vif, Vpr, Vpu, and Nef [51]. The ability of these accessory proteins to neutralize host antiviral factors underscores the critical role that restriction mechanisms play in controlling viral infections.

1.4.1 APOBEC3 Family

The APOBEC family includes several cytidine deaminases, notably APOBEC3 proteins like A3G and A3F. These enzymes interfere with HIV by incorporating themselves into budding virions, where they introduce hypermutations in the viral DNA during reverse transcription [52]. This mutagenesis leads to the production of non-functional or defective proviruses. APOBEC3 proteins act primarily on the (-) strand of viral DNA, converting cytosine to uracil, which eventually results in G-to-A mutations in the viral genome. Despite their potent antiviral effects, the HIV accessory protein Vif counteracts APOBEC3 by targeting it for ubiquitination and subsequent proteasomal degradation, allowing the virus to escape this restriction [51,52].

1.4.2 Tetherin (BST-2)

Tetherin, also known as BST-2, is a host protein that physically tethers budding virions to the surface of infected cells, preventing their release into the extracellular space. This retention inhibits the spread of the virus. HIV's Vpu protein counteracts Tetherin by inducing its degradation through ubiquitination pathways, thereby facilitating virion release and spread [53].

1.4.3 TRIM5α

TRIM5α is an E3 ubiquitin ligase that restricts HIV-1 by binding to the viral capsid and forming a hexagonal lattice around it, which disrupts capsid stability and prevents successful reverse transcription. This process often leads to the degradation of the capsid through proteasomal pathways. While effective in non-human primates, human TRIM5α has limited activity against HIV-1 due to evolutionary adaptations in the virus [54].

1.4.4 SERINC Family (SERINC3 and SERINC5)

SERINC3 and SERINC5 are transmembrane proteins that impede HIV infectivity by reducing the efficiency of viral fusion with target cells. They are incorporated into the viral envelope during assembly and hinder the functionality of the envelope glycoproteins. HIV combats this restriction through its accessory protein Nef, which downregulates SERINC3 and SERINC5 from the cell surface, preventing their incorporation into virions [54,55].

1.4.5 SAMHD1

SAMHD1 is a deoxynucleoside triphosphohydrolase that depletes the cellular pool of dNTPs, the building blocks required for reverse transcription. By lowering dNTP levels, SAMHD1 effectively inhibits the synthesis of viral cDNA in non-dividing cells such as macrophages and dendritic cells. HIV-2 and certain SIV strains use the Vpx accessory protein to degrade SAMHD1, but HIV-1 lacks this mechanism, relying on other strategies to evade restriction [56].

1.4.6 MxB (Myxovirus Resistance Protein B)

MxB inhibits HIV-1 by targeting the pre-integration complex, reducing the efficiency of proviral integration into the host genome. It binds to the viral capsid and disrupts its proper uncoating and nuclear import. MxB's activity is upregulated by interferon responses, highlighting its role in the innate immune defense against HIV [56].

1.4.7 IFITM Proteins (Interferon-Induced Transmembrane Proteins)

IFITM proteins, specifically IFITM1, IFITM2, and IFITM3, inhibit HIV entry into host cells. They interfere with the viral membrane fusion process, either by altering the lipid composition of the cellular membrane or directly disrupting the fusion machinery. IFITM proteins localize to different cellular compartments, such as the plasma membrane and endosomes, where they restrict HIV entry depending on its tropism. For instance, IFITM1 is effective against CCR5-tropic strains at the plasma membrane, while IFITM2 and IFITM3 target CXCR4-tropic strains within endosomes [56].

1.4.8 REAF (RNA-associated early-stage antiviral factor)

The REAF also known as RPRD2, restricts HIV replication particularly during the reverse transcription stage. REAF is a constitutively expressed protein that limits the completion of proviral DNA synthesis and inhibits integration into the host genome. Its antiviral activity is especially pronounced in macrophages and specific cell lines, where it acts to impede the production of reverse transcripts shortly after viral entry. HIV-1 employs its accessory protein Vpr to counteract REAF's restriction [57].

1.5 HIV-1 latency

HIV-1 latency is a state in which the virus becomes dormant within certain infected cells, especially in long-lived memory CD4+ T cells. Latently infected CD4+ T cells escape immune clearance by HIV-specific CD8+ T cells and natural killer (NK) cells primarily due to the absence of viral antigen expression.

Latent HIV-1 is transcriptionally silent, meaning that viral proteins are not produced and thus not presented on MHC class I molecules, which makes the infected cells invisible to cytotoxic immune responses [58,59]. Additionally, latently infected cells may exhibit impaired antigen processing and presentation or upregulate inhibitory ligands such as PD-L1 and HLA-E [60]. These ligands engage immune checkpoint receptors on CD8+ T cells and NK cells, thereby suppressing effector function and facilitating viral persistence. The ability of latent cells to evade the immune system is further reinforced by their localization in immune-privileged tissues such as lymphoid

follicles and the central nervous system, where access by cytotoxic effector cells is restricted.

Moreover, latent HIV-1 predominantly resides in resting memory CD4+ T cells, which are metabolically inactive and non-proliferative. This quiescent state makes them inherently less detectable by the immune system, which preferentially targets activated or dividing cells. Collectively, these features create a sanctuary for latent HIV-1, allowing the virus to persist despite antiretroviral therapy and ongoing immune surveillance, and pose a major barrier to achieving a functional cure.

Importantly, HIV-1 latency is reversible, meaning that under specific conditions, such as cellular activation, the virus can reactivate and resume active replication, leading to the production of new viral particles [40,41]. This reversible dormancy poses a significant obstacle to treating HIV-1, as latent reservoirs persist even during prolonged antiretroviral therapy, serving as a source of potential viral rebound if treatment is interrupted [40,41,59].

The concept of HIV-1 latency was initially explored through *in-vitro* studies on transformed cell lines, where it was observed that infected cells exhibited minimal or no viral gene expression [59]. However, this dormant state could be reactivated by specific stimuli, such as T-cell activation. These early findings suggested that HIV-1 transcription relies heavily on host transcription factors like NF-kB, which are transiently activated during immune responses. This led to the hypothesis that latent HIV-1 infection might occur in resting CD4+ T cells that had previously been activated

and then returned to a quiescent state [59]. By the mid-1990s, significant progress was made in understanding latency. Research conducted in 1995 provided conclusive evidence that resting CD4+ T cells could harbor integrated HIV-1 DNA in a transcriptionally silent state [59,61]. This dormant virus was shown to persist for extended periods in memory T cells, evading immune detection and remaining unaffected by ART [59].

Structured therapy interruption has since been studied extensively, and certain individuals, such as those in the VISCONTI cohort, have demonstrated prolonged viral control without ART [62]. This phenomenon, while rare, highlights potential immune or virological factors that could be leveraged for functional cures. Latent reservoirs are remarkably stable, with a half-life of approximately 44 months, making their eradication a daunting challenge [39].

Latent HIV-1 reservoirs are predominantly found within memory CD4+ T cells, particularly central memory T cells (Tcm) and transitional memory T cells (Ttm) [63–65]. These subsets are key to the virus's persistence due to their long lifespan and capacity for proliferation. In addition to circulating memory T cells, tissue-resident memory T cells (Trm) have been identified as important contributors to HIV-1 latency [64,65]. These cells reside permanently in non-lymphoid tissues such as the gut-associated lymphoid tissue (GALT), lymph nodes, lungs, and genital tract, where they participate in localized immune defense [65]. In contrast to their circulating counterparts, Trm cells are confined to specific tissues and do not re-

enter the bloodstream, limiting their exposure to immune effector mechanisms and antiretroviral therapy (ART) [63–65].

Although memory T cells represent the primary reservoir for latent HIV-1, additional cell types of the myeloid lineage such as monocytes, macrophages, and dendritic cells also contribute to viral persistence [59]. Tissue-resident macrophages, including microglia in the brain, Kupffer cells in the liver, and macrophages found in the lungs and spleen, are capable of harboring latent virus and supporting low-level replication. These reservoirs are particularly problematic in individuals undergoing long-term ART, as they may maintain residual viremia and chronic inflammation, posing a significant barrier to eradication and cure strategies [60–62].

The establishment of latency occurs early in the course of infection, notably during the acute phase when viral replication is highly active. During this stage, a considerable number of infected cells evade immune clearance by entering a quiescent state, allowing the virus to persist undetected for extended periods, often decades [36].

1.5.1 Molecular mechanisms of latency

Latency is primarily maintained through multiple molecular mechanisms that suppress viral gene expression and evade the host immune response [21]. A key factor is the integration site of the provirus within the host genome [66]. Although HIV-1 prefers to integrate into gene-rich areas, not all integration sites are equally

favourable to active transcription. Some integration sites position the viral genome in regions that are less accessible for transcription factors [21], either due to the chromatin structure or the local nuclear environment. This site-specific variability contributes to the possibility that some integrated viral genomes will remain latent rather than actively transcribed [21].

Chromatin remodelling plays a pivotal role in establishing and maintaining latency. Once HIV-1 has integrated into the host genome, the host cell's machinery can change the chromatin structure around the viral DNA through histone modifications, which are essential for gene silencing [39,59]. In addition to chromatin remodelling, the viral genome itself is positioned within specific nucleosome structures—referred to as Nuc-0, Nuc-1, and Nuc-2—that play an important role in regulating transcription [39]. These nucleosomes are precisely placed along the viral genome, with Nuc-1, in particular, positioned at the 5' LTR, where it acts as a significant barrier to transcription. This arrangement allows either repressive or stimulatory host transcription factors to bind, depending on the nucleosome state, influencing whether the viral genome remains silent or becomes transcriptionally active [39].

Histone deacetylation, facilitated by histone deacetylases (HDACs) [21,40], removes acetyl groups from histones, leading to a more compact chromatin structure that limits access to transcriptional machinery and represses gene activation. Similarly, histone methylation, particularly at specific CpG sites associated with gene silencing, further contributes to this compacted structure, effectively silencing the viral promoter within the LTR regions [21,40]. Together, HDACs and methyltransferases play significant roles in creating and maintaining a condensed chromatin state around the

proviral DNA, effectively inhibiting transcription and reinforcing viral latency [21,40] **(Figure 1.7).**

1.5.2 Transcriptional regulation and host factors

HIV-1 transcription is tightly regulated by the availability of host transcription factors required for viral gene expression [21,40]. For the HIV-1 promoter in the 5′ LTR to drive transcription, it requires specific host transcription factors (TF), such as NF-kB, NFAT, and AP-1 [40]. In resting memory CD4+ T cells these TFs are sequestered in the cytoplasm preventing viral transcription [40]. Activating latently infected CD4+ T cells stimulate intracellular signalling pathways, increasing the nuclear availability these TF. For instance, T cell receptor (TCR) stimulation triggers a signaling cascade that activates protein kinases, which in turn activate NF-kB and NFAT. Once active, these transcription factors translocate into the nucleus and bind to specific binding sites within the HIV-1 genome's 5′ LTR. This binding significantly enhances the viral promoter's transcriptional activity, resulting viral RNA production [39].

Additionally, In the absence of Tat certain cellular proteins, such as NELF and DSIF, can halt RNA polymerase II during the early stages of transcription elongation, further reducing viral mRNA production [21,39,58].

Additionally, the host factor BRD4, a bromodomain-containing protein, plays a key role in maintaining latency by competing with Tat for binding to P-TEFb. In this latent state, BRD4 binds P-TEFb, blocking Tat from accessing it and recruiting it to the viral promoter, effectively silencing HIV-1 gene expression [21,41,59] **(Figure 1.7).**

1.5.3 Role of epigenetic and cellular factors

Beyond chromatin remodelling and transcriptional repression, cellular proteins also play an active role in maintaining latency. Certain host factors, such as YY1, LSF1, and C-promoter binding factor-1 (CBF-1), represses HIV through epigenetic silencing by binding directly to the viral LTR and recruit HDAC-1 which suppress transcription and stabilizing the latent state [41,67,68].

This complex interplay of host and viral factors establishes a highly regulated latent state that enables HIV-1 to persist in the host for prolonged periods **(Figure 1.7).**

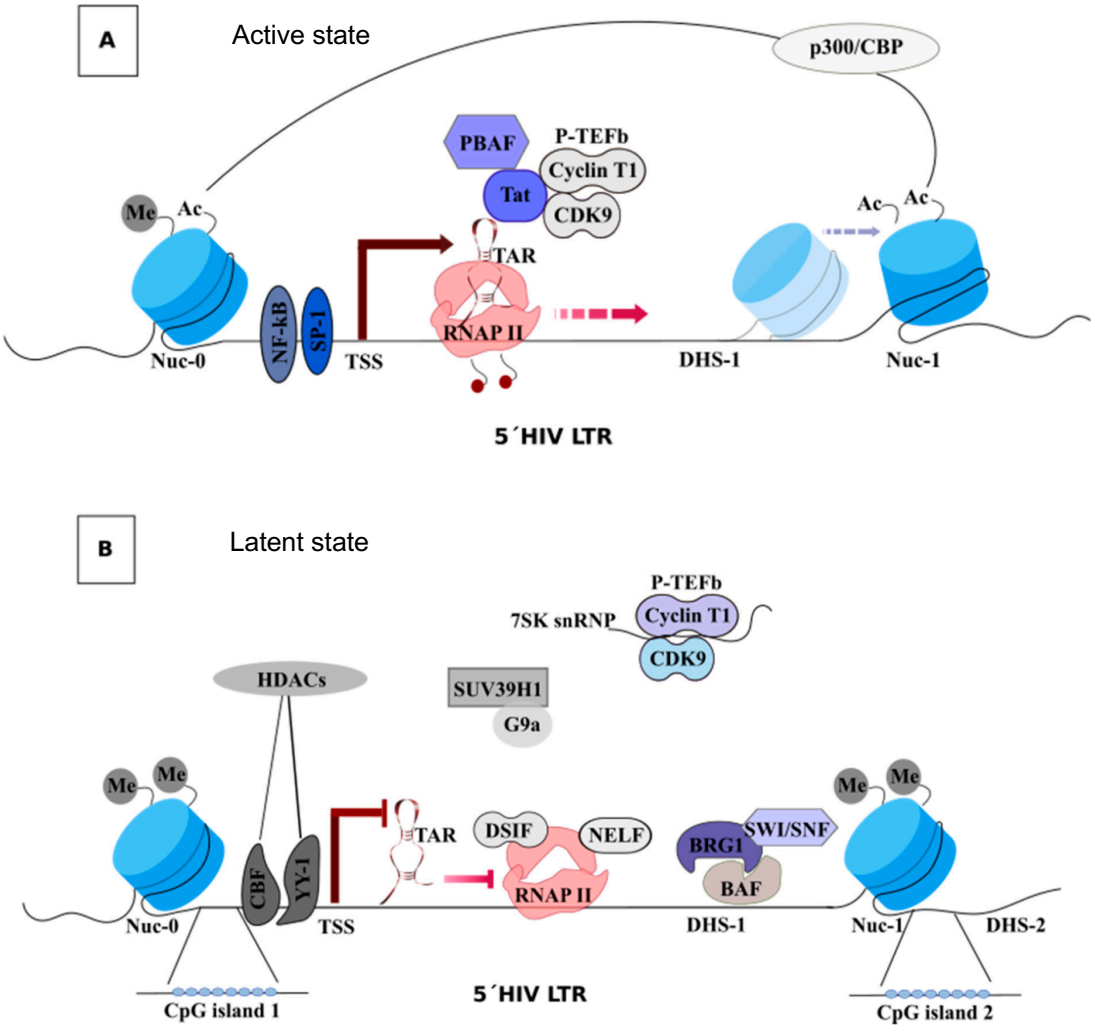

Figure 1.7 Molecular Mechanisms of HIV-1 Latency. A) HIV-1 transcription is regulated through Tat-mediated mechanisms involving several host factors. Transcription is initiated by activators like NF-kB, SP-1, and HATs, including p300/CBP (CREB-binding protein). HATs facilitate the formation of open chromatin, promoting the recruitment of polybromo-associated factor (PBAF), which repositions nucleosome 1 (Nuc-1) downstream of the transcription start site (TSS). This chromatin remodelling enhances the efficiency of transcriptional elongation. Simultaneously, the secondary structure of the TAR RNA, formed at the 5' end of nascent transcripts, becomes accessible for Tat protein binding. Tat recruits the P-TEFb, which contains (CDK9). CDK9 phosphorylates the CTD of RNA polymerase II at serine 2 residues, facilitating the transition from paused to active elongation. This process ensures the production of full-length HIV-1 transcripts, including those necessary for synthesizing Tat, thereby establishing a positive feedback loop for transcription elongation. B) The establishment of HIV-1 latency is mediated by several host proteins and transcription factors that suppress viral gene expression. Key transcription factors, such as YY1 and CBF, play a critical role by recruiting histone HDACs. HDACs remove acetyl groups from histones, particularly at Nuc-1, resulting in tighter chromatin compaction. This restricted chromatin state limits the accessibility of transcriptional activators to the viral promoter, thereby promoting viral latency. Additionally, histone methyltransferases (HMTs) such as SUV39H1 and G9a contribute to latency by modifying histones at the HIV-1 promoter. SUV39H1 induces trimethylation at lysine 9 of histone H3 (H3K9me3), while G9a promotes dimethylation (H3K9me2), both of which are associated with transcriptional repression. Furthermore, transcriptional elongation is blocked through the cooperative actions of DSIF (DRB Sensitivity-Inducing Factor) and NELF, which induce pausing of RNAPII. Together, these mechanisms ensure the silencing of HIV-1 transcription and the maintenance of a latent state. Taken from Moranguinho et al. 2020 [69]

1.5.4 HIV-1 latency transcriptional regulation by Vpr

Vpr is a multifunctional accessory protein encoded by HIV-1 that plays a central role in supporting viral replication, evading host immune defenses, and modulating a range of host cellular functions, including transcriptional control. One of the ways Vpr

enhances HIV-1 transcription is by influencing host signaling pathways and altering the chromatin landscape to favor viral gene expression.

A major mechanism by which Vpr promotes transcription is through activation of the NF-kB signaling pathway. Vpr can trigger DNA damage responses by activating the ATM/ATR kinase cascade, which in turn leads to the phosphorylation and degradation of IkB, the inhibitor of NF-kB. This allows NF-kB to translocate to the nucleus, where it binds to the LTR region of the HIV-1 genome, enhancing transcriptional activity [70].

In addition to NF-kB activation, Vpr facilitates transcriptional activation through its interaction with host coactivators such as p300 and CBP, which
possess histone acetyltransferase (HAT) activity. These coactivators promote histone acetylation and chromatin remodeling at the HIV-1 promoter, making it more accessible for transcription [71]. Vpr also modulates transcription driven by the Sp1 transcription factor, which binds to the LTR and regulates basal levels of HIV-1 gene expression [71,72]

Vpr has been shown to recruit the Cullin 4-RING E3 ubiquitin ligase complex (CRL4DCAF1), which leads to the degradation of host restriction factors that would otherwise suppress viral transcription. This degradation of cellular proteins can enhance viral gene expression by relieving transcriptional repression [71].

Beyond its direct effects on the HIV-1 promoter, Vpr influences host cell gene expression profiles, promoting the induction of genes associated with cell cycle arrest, apoptosis, and immune modulation. Vpr-induced arrest at the G2/M phase of

the cell cycle is particularly beneficial to the virus, as transcription from the HIV-1 LTR is enhanced during this phase [71].

Together, Vpr's diverse regulatory roles not only facilitate efficient HIV-1 transcription and replication but also contribute to viral persistence and pathogenesis, making it a potential target for future therapeutic strategies.

1.6 HIV-1 treatment

1.6.1 Combination antiretroviral therapy and limitations

cART has profoundly transformed the management of HIV-1 infection, changing it from a fatal disease to a manageable chronic condition. This approach involves the simultaneous administration of three or more drugs, each targeting a different stage of the HIV-1 lifecycle. This combination approach aims to suppress viral replication and reduce the viral load to undetectable levels, thereby preserving immune function and improving patient outcomes. Listed below are cART drug classes and their mechanisms of action.

1.6.1.1 Nucleoside reverse transcriptase inhibitors (NRTIs)

These drugs, such as zidovudine (AZT), lamivudine (3TC), and tenofovir (both disoproxil fumarate and alafenamide forms), mimic natural nucleotides. By being incorporated into the growing viral DNA chain, they act as chain terminators, halting the action of the reverse transcriptase enzyme and preventing further DNA synthesis [32].

1.6.1.2 Non-nucleoside reverse transcriptase inhibitors (NNRTIs)

Also target the reverse transcription step but through a different mechanism. Drugs like efavirenz (EFV), nevirapine (NVP), and newer agents such as rilpivirine (RPV) bind to a distinct non-active site pocket on the reverse transcriptase enzyme. This interaction induces conformational changes that inhibit the enzyme's ability to synthesize viral DNA. NNRTIs are particularly valued for their ease of use and efficacy but are often paired with other drug classes to prevent resistance [32].

1.6.1.3 Protease inhibitors (PIs)

These agents, such as lopinavir/ritonavir (LPV/r), atazanavir (ATV), and darunavir (DRV), target the HIV-1 protease enzyme. This enzyme is critical for cleaving Gag and Gag-Pol polyproteins into functional components necessary for the maturation of viral particles. By blocking this process, PIs prevent the production of infectious virions [32].

1.6.1.4 Integrase strand transfer inhibitors (INSTIs)

INSTIs have revolutionized HIV-1 therapy by targeting the integration of viral DNA into the host genome. Drugs like raltegravir (RAL), dolutegravir (DTG), and bictegravir (BIC) inhibit the strand transfer step mediated by the integrase enzyme. By blocking this critical process, INSTIs prevent the establishment of a stable proviral state, effectively halting the progression of infection [32].

1.6.1.5 Entry and fusion inhibitors (ENFs)

These drugs block HIV-1 from entering host cells by targeting specific stages of the entry process. For example, enfuvirtide (T-20) prevents the fusion of the viral envelope with the host cell membrane, while maraviroc (MVC) inhibits the CCR5 co-

receptor, which is essential for viral entry in CCR5-tropic strains of HIV-1. Though less commonly used than other drug classes, these inhibitors offer valuable options, particularly in treatment-experienced patients with drug resistance [32].

1.6.1.6 Capsid inhibitors

These drugs represent a more recent addition to the arsenal against HIV-1. Drugs like lenacapavir disrupt capsid stability, interfering with several stages of the viral lifecycle, including reverse transcription, nuclear transport, and assembly. This long-acting drug class shows promise in clinical trials, particularly for heavily treatment-experienced individuals [32].

The introduction of cART has been pivotal in reducing the progression of HIV-1 infection to AIDS, increasing CD4+ T cell counts, lowering viral loads, and improving overall survival rates [32,73]. However, cART is not without its challenges. The persistence of latent viral reservoirs in long-lived cells, such as memory CD4+ T cells, poses a significant barrier to curing HIV-1. These reservoirs remain dormant and unaffected by cART, only to reactivate and cause viral rebound if treatment is interrupted [73]. Moreover, long-term use of cART can lead to adverse effects, including cardiovascular diseases, metabolic disorders like obesity and type 2 diabetes, and non-HIV-related cancers. Such complications can impact adherence to therapy and overall quality of life. Another major concern is the emergence of drug-resistant HIV-1 strains [73], which undermine the efficacy of existing treatments and necessitate the development of new therapeutic options. While cART has transformed HIV-1 from a fatal disease into a manageable chronic condition, these

challenges highlight the need for continued advancements in HIV-1 treatment strategies.

Some exceptional cases, such as the "Berlin Patient" [74], the "London Patient [75], “the Duesseldorf patient” [76] and “the New York Patient” [77] have achieved what is termed "functional cure," but this was not due to cART alone. These patients underwent allogeneic stem cell transplantation using donor cells with a mutation in the CCR5 co-receptor (CCR5Δ32), which HIV-1 uses to enter cells. This mutation renders the cells resistant to HIV-1 infection, and the combination of transplantation and the donor's CCR5Δ32 genotype led to long-term viral remission. However, these methods remain experimental, with significant risks, high costs, and limited scalability.

1.6.2 Emerging Strategies and Cure Research

The concept of a functional cure has emerged as a central focus in "Emerging Strategies and Cure Research" for HIV-1. This innovative approach shifts the emphasis from complete eradication of the virus to achieving long-term viral suppression without the need for ongoing ART. Unlike a sterilizing cure, which aims to eliminate every trace of the virus, a functional cure acknowledges the persistence of latent reservoirs but ensures they remain inactive and incapable of causing disease.

Elite controllers (ECs) provide a unique real-world model for understanding functional cures. These individuals, comprising approximately 1 in 500–1000 people living with HIV, can naturally suppress HIV-1 viremia to levels undetectable by PCR assays without the aid of ART or hematopoietic stem cell transplantation. Despite harboring viral reservoirs, ECs maintain long-term viral control, which prevents the progression of disease [78,79]. Their ability to sustain normal CD4+ T cell counts and avoid the clinical manifestations of HIV infection highlights the immune system's potential to achieve a functional cure [80]. Researchers can develop treatment approaches to replicate this occurrence in the larger HIV-positive community by better understanding the immunological and genetic mechanisms driving natural viral suppression through the study of ECs. A few of these treatment strategies will be discussed in more detail below.

1.6.2.1 Shock and Kill Strategies

This approach aims to eliminate latent HIV-1 reservoirs by intentionally reactivating the dormant virus using compounds or cytokines known as latency reversing agents (LRAs), in combination with ongoing cART treatment [81]. LRAs stimulate the reactivation and replication of the latent virus, which can theoretically result in the death of reactivated cells through direct viral cytopathic effects or immune-mediated clearance of infected cells [81,82]. Meanwhile, cART prevents the newly produced viral particles from infecting uninfected cells, ensuring continued viral suppression [82] **(Figure 1.8)**.

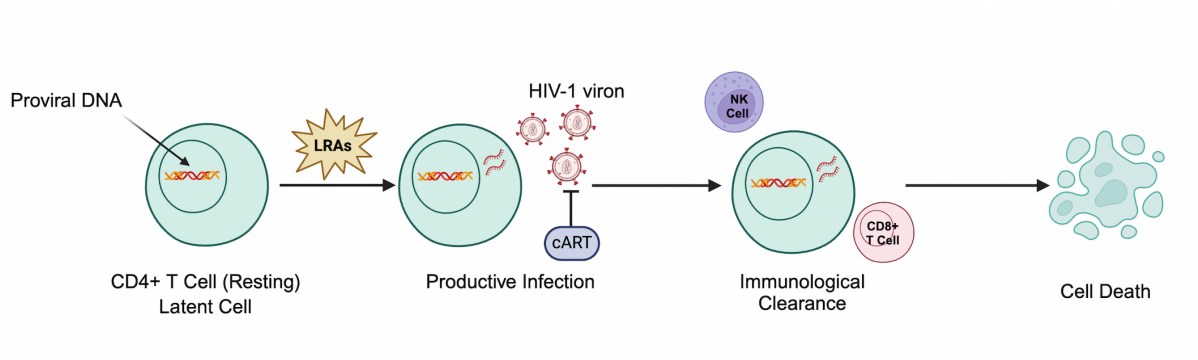

Figure 1.8 The shock and kill strategy. During HIV-1 infection, most CD4+ T cells are destroyed through cytopathic effects, while a small subset of infected cells survives by reverting to a resting memory state, harboring latent proviruses. The "shock-and-kill" strategy employs LRAs to reactivate these latent viruses, promoting HIV-1 replication, and virion production. Reactivation triggers the elimination of infected cells either through direct cell death or immune-mediated clearance. At the same time, cART prevents the infection of new cells, ensuring that the reactivated virus is unable to establish further spread. Schematic created by Biorender.com

A wide variety of LRAs have been identified and studied for their ability to reactivate latent HIV reservoirs *in-vitro*, *ex-vivo*, and in animal models [83–85] **(Table1.1).** While these LRAs have shown promising results in experimental settings, their efficacy in clinical trials involving people with HIV (PWH) on suppressive ART has been more limited [84]. Several classes of LRAs which act on different pathways **(Figure 1.9)** including histone deacetylase inhibitors (HDACis), protein kinase C (PKC) agonists, Toll-like receptor (TLR) agonists, have been investigated in human trials which have successfully induced viral transcription and virion production in clinical trials, but these effects have not translated into a significant reduction in the size of the latent reservoir. This gap underscores the challenge of achieving meaningful reservoir depletion in humans.

HDACis such as vorinostat [86,87], Panobinostat [88], and romidepsin [89] have demonstrated their ability to increase HIV transcription in clinical studies, but their impact on reservoir clearance remains minimal. Similarly, the PKC agonist bryostatin-1 [90,91] has been evaluated for its latency-reversing properties, showing some activation of latent HIV without substantial reservoir depletion. Toll-like receptor agonists, such as lefitolimod (a TLR-9 agonist), have also been investigated for their potential to reactivate HIV by stimulating innate immune pathways, with modest success in promoting viral transcription [92].

Table 1.1 Different Latency-Reversing Agents. Taken from Jean et al. 2019 [82]

Compound/class of compounds	Mechanism of action
Histone deacetylase inhibitors. (e.g., vornistat, romidepsin, panobinostat)	Inhibit HDACs
Histone methylation inhibitors (e.g., BIX-01294, GSK-343, AZ391)	Inhibit HMTs
DNA methylation inhibitors (e.g., 5-aza-CdR)	Inhibit DNMTs
Protein kinase C agonists (e.g., prostratin, bryostratin-1, ingenol-B)	Promote NF-kB-mediated transcription of HIV-1, increase active P-TEFb levels and its release form 7SKsnRNP
Bromodomain extra-terminal motif inhibitors BETis (e.g., JQ1, I-BET, UMB136)	Block the interaction of BRD4 with P-TEFb and release active P-TEFb from 7SKsnRNP, other mechanism proposed as well
Disulfram	Unclear but may involve the Akt/PTEN pathway
Hexamethylbisacetamide HMBA	Promotes recruitement of active P-TEFb at 5' LTR
Benzotriazoles	Block the proper turnover of STAT5

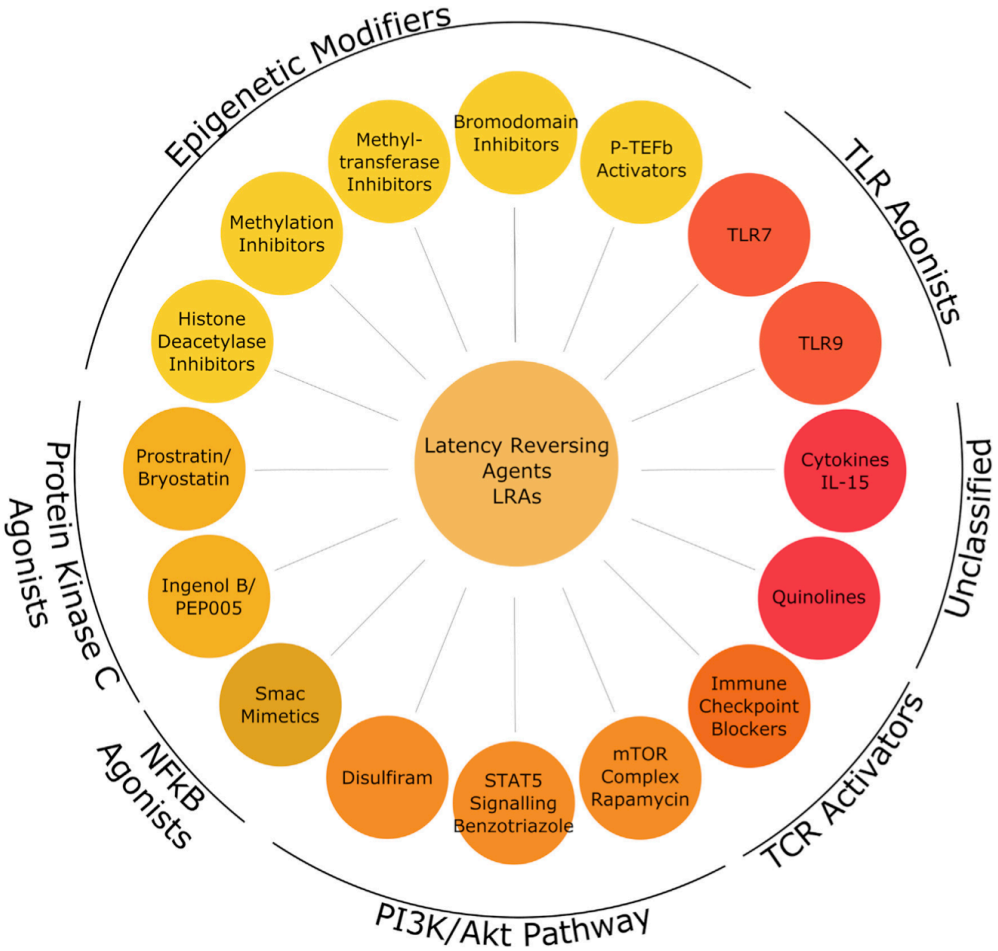

Figure 1.9 LRAs Pathways. LRAs function through various cellular pathways to enhance HIV transcription and/or the production of virions. These pathways involve critical factors such as P-TEFb, TLRs, TCR, the mechanistic target of rapamycin (mTOR), signal transducer and activator of transcription 5 (STAT5), and interleukin-15 (IL15). Each of these components plays a key role in reactivating latent HIV, facilitating the expression of viral genes and the production of infectious particles. Taken from Kim et al [81].

1.6.2.2 Block and Lock Strategies

The block and lock approach seeks to achieve a functional cure for HIV-1 by using latency-promoting agents (LPAs) **(Table 1.2)** to push the virus into a deeply silenced, irreversible state of latency, often referred to as "deep latency" [82,93]. By keeping

the virus from reactivating, this strategy seeks to stop its replication and essentially make the reservoirs ineffective[93]. Over time, the viral reservoirs are expected to decay naturally, as the replenishment of these reservoirs and the risk of reactivation would be effectively eliminated [82,93]. This strategy may provide an effective way to long-term remission without requiring ongoing antiretroviral treatment by keeping the virus latent indefinitely **(Figure 1.10).**

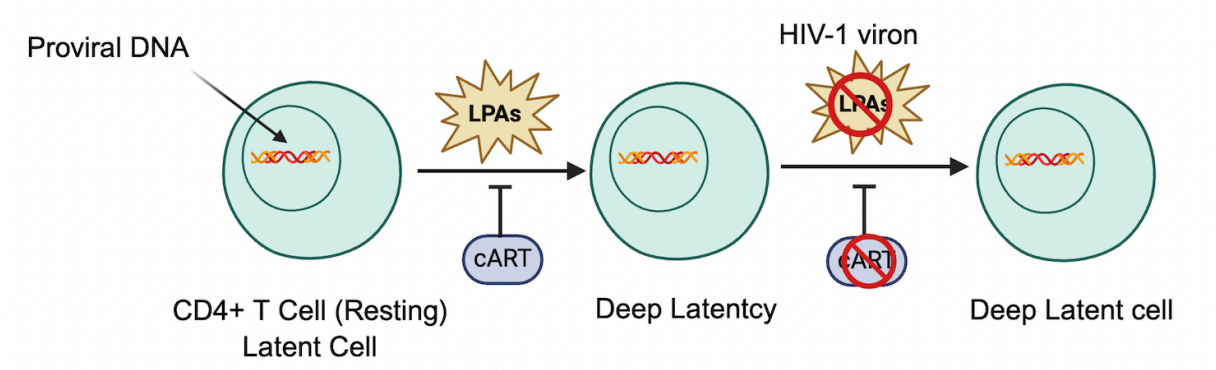

Figure 1.10 The block-and-lock strategy. Aims to achieve long-lasting suppression of HIV gene expression. By cART with a LPA, this approach seeks to inhibit ongoing viral transcription, establish epigenetic modifications that reinforce gene silencing, and push the virus into a state of "deep latency." This durable suppression reduces or prevents viral rebound when ART is discontinued. This schematic was created by Biorender.com

One approach involves targeting the Tat protein, which plays a pivotal role in viral transcription. Tat inhibitors, such as didehydro-cortistatin A (dCA), disrupt the interaction between Tat and TAR RNA, silencing HIV transcription and reducing residual viral activity [94]. Preclinical studies using primary CD4+ T cells isolated from ART-suppressed individuals have shown that dCA effectively suppresses viral replication [95]. Moreover, studies utilizing the humanized bone marrow-liver-thymus

(BLT) mouse model for HIV-1 latency have demonstrated that treatment with dCA significantly reduces viral RNA levels in tissues and prolongs the time to viral rebound following the cessation of ART [96].

Bromodomain-containing protein 4 (BRD4) is a critical regulator of HIV-1 transcription and a potential target for the block-and-lock strategy. As an epigenetic reader, BRD4 plays a dual role: it stimulates general gene expression by interacting with various proteins but inhibits HIV transcription by competing with Tat for binding to the P-TEFb complex, which is essential for transcriptional elongation [97]. This duality makes BRD4 an attractive target for therapeutic intervention. Research by Niu et al. identified a small molecule, ZL0580, that targets bromodomain 1 of BRD4 to suppress HIV transcription [98]. ZL0580 inhibits Tat-mediated transactivation and transcription elongation while inducing a repressive chromatin environment at the HIV-1 LTR promoter [98]. This small molecule demonstrated significant potential in preclinical studies. In PBMCs from a viremic HIV-infected individuals, treatment with ZL0580, alongside ART, delayed viral rebound following therapy cessation [98]. These findings position BRD4 modulators like ZL0580 as a promising new class of compounds for the block-and-lock strategy, aiming to permanently silence HIV transcription. However, while ZL0580 significantly delayed viral rebound, it did not entirely prevent it. This limitation suggests that combining BRD4 modulators with other therapeutic approaches may be necessary to achieve a more robust and durable functional cure [98].

The mTOR complex has been identified as a significant player in the regulation of HIV-1 latency, offering new avenues for therapeutic intervention under the block-and-lock strategy. The involvement of this pathway in HIV-1 latency was uncovered through genome-wide screens and subsequent experiments that demonstrated its role in maintaining latency by controlling HIV transcription. mTOR inhibitors, such as Torin1 and pp242, have shown effectiveness in both primary CD4+ T cells and patient-derived cells [99]. These inhibitors suppress the reactivation of latent HIV by targeting both mTORC1 and mTORC2 complexes. Mechanistically, they downregulate CDK9 phosphorylation, a crucial cofactor for Tat-dependent transcription, thereby halting both Tat-dependent and Tat-independent activation of the HIV promoter [99]. Moreover, mTOR inhibition can also repress latent HIV reactivation triggered by strong T-cell stimulants, further highlighting its potential utility in preventing viral rebound [99]. These findings support the integration of mTOR inhibitors into block-and-lock strategies, where stable latency maintenance could offer a functional cure for HIV-1.

Hsp90**,** a heat-shock chaperone, plays a critical role in regulating HIV-1 transcription by localizing at the viral promoter and modulating key cellular pathways. Research has shown that the cytosolic isoform of Hsp90 is essential for HIV-1 replication, as its inhibition through RNA interference effectively blocks viral replication in primary human T cells [100]. Study by our lab showed that Hsp90 controls HIV-1 reactivation by inhibiting the NF-kB signaling pathway in J-Lat cell model of latency [101]. Studies in humanized mouse models has highlighted the therapeutic potential of Hsp90 inhibitors in latency control, showing that treatment with Hsp90 inhibitors such as

AUY922 or 17-AAG, in combination with a reverse transcriptase inhibitor (EFdA), delayed viral rebound for up to 11 weeks following ART interruption. Although latent viruses could be reactivated through heat shock or cellular activation from PBMCs and spleen, the study emphasized the potential of Hsp90 inhibition in maintaining deep latency [102]. These findings underline the significant role of Hsp90 in NF-kB activity and HIV-1 transcriptional regulation, positioning Hsp90 inhibitors as potential LPAs for achieving a functional cure.

An interesting approach in HIV-1 cure research explores the mechanisms underpinning the functional control observed ECs. ECs and post-treatment controllers (PTCs) maintain undetectable viral loads without the need for cART, despite harboring persistent HIV reservoirs. The integration sites of intact HIV proviruses in ECs and PTCs are predominantly located in transcriptionally repressive chromatin regions, such as centromeric regions, LADs, and zinc-finger (ZNF) gene loci [80]. This pattern contrasts with the more permissive euchromatin regions associated with viral replication in other populations [80]. Recent findings suggest that immune-mediated selection, rather than differences in initial integration site preferences, drives the localization of HIV proviruses to these repressive regions [80]. This natural positioning effectively silences the proviruses, shielding them from immune detection and ensuring their persistence. Importantly, however, this transcriptional silencing is not irreversible, as proviruses in heterochromatic regions can be reactivated under certain conditions. This reversible silencing aligns directly with the principles of the block-and-lock strategy, which aims to maintain HIV in a

deeply latent, transcriptionally inactive state to prevent reactivation and viral rebound [80].

Therapies targeting integration sites or mimicking the immune-mediated selection observed in ECs and PTCs could improve the effectiveness of block-and-lock strategies. One promising example is LEDGINs, small molecules that, by antagonizing the interactions between integrase and LEDGF, redirect integration to transcriptionally inert regions of the host genome [103,104]. By directing proviruses to heterochromatic regions, LEDGINs significantly reduce the likelihood of viral reactivation [103–105]. However, further research is needed to translate these findings into clinical applications. These findings highlight the potential of transcriptional silencing strategies to achieve drug-free remission, offering a promising pathway toward a functional cure for HIV.

Table 1.2 Summary of Potential Latency-Promoting Agents. Taken from Jean et al. 2019 [82]

Compound/class of compounds	Mechanism of action
TAR inhibitors (e.g., WMN5, HM13)	Interfere with proper Tat/TAR interaction by binding to TAR RNA
Tat inhibitors, dehydrocorticostatin (dCA)	Interferes with proper Tat/TAR interaction by binding to TAR-binding domain of Tat, epigenetically repress the 5'LTR, inhibits Tat-mediated neurotoxicity
Tat inhibitors, Trilopide	Promotes proteasomal degradation of Tat
CDK9 inhibitors (e.g., CR8#13, F07#13, IM)	Inhibit CDK9 kinase activity, disrupts proper Tat/CDK9 interaction
Cyclin T1 inhibitors (e.g., C3)	Disrupt proper Tat/cyclinT1 interaction
Histone acetyltransferases inhibitors HAT inhibitors (e.g., curcumin, LTK14)	Inhibit HAT
Histone demethylases inhibitors HDMis (e.g., LSD1)	Inhibit HDMs
NFAT inhibitors (e.g., CsA, FK506)	Inhibit NFAT-mediated HIV-1 transcription
NF-kB inhibitors (e.g., IKK inhibitors, 17- AAG, AUY922, GV1001)	Inhibit different steps of NF-kB pathway to suppress HIV-1 transcription, indirect inhibition of NF-kB through targeting of Hsp90 chaperone
mTORis (e.g., pp242, Torin1)	Inhibit mTOR signaling

1.6.2.3 Gene Therapy

Gene therapy has emerged as a promising strategy for achieving a functional or complete cure for HIV-1 by targeting the virus and its interaction with host cells. This innovative approach involves precise genetic modifications to infected or susceptible cells, aiming to disrupt HIV-1 replication, prevent viral entry, or eliminate latent reservoirs. By either rendering cells resistant to infection or eradicating the virus from latent reservoirs, gene therapy holds the potential to achieve a functional or sterilizing cure [106]. Below are some key mechanisms of gene therapy.

1. Targeting CCR5 and CXCR4 Coreceptors

One notable strategy involves targeting the CCR5 co-receptor, which is essential for HIV-1 entry into host cells. A naturally occurring mutation, CCR5Δ32, renders cells resistant to HIV-1 infection by disrupting the receptor's functionality. The success of the "Berlin Patient," who achieved long-term viral remission following a CCR5Δ32-homozygous stem cell transplantation, highlighted the potential of this approach. However, this case remains unique, as most patients experience viral rebound after ART interruption [106].

Gene-editing tools, such as zinc-finger nucleases (ZFNs), transcription activator-like effector nucleases (TALENs), and CRISPR-Cas9, have been developed to mimic the CCR5Δ32 mutation by knocking out CCR5 co-receptor expression in host cells. These tools have shown remarkable efficiency *in-vitro*, successfully rendering cells resistant to HIV-1 infection [106]. However, translating this success into *in-vivo* applications presents significant challenges. Safe and effective delivery systems for

these gene-editing tools remain a major challenge, and the high costs associated with transplantation procedures further limit their widespread use. Additionally, the potential for HIV-1 to switch tropism from CCR5 to CXCR4 presents another route for viral escape, complicating the efficacy of this approach [106].

2. Targeting the HIV-1 genome

Targeting the proviral DNA within latently infected cells offers a theoretical solution to prevent viral rebound following the discontinuation of treatment. Recent research has concentrated on highly conserved regions of the HIV-1 genome, as these are critical for viral replication and less prone to genetic variation [107]. Studies have demonstrated that gene-editing technologies, such as CRISPR/Cas9, can effectively suppress HIV-1 replication in T-cell lines and primary CD4+ T cells [107]. However, a significant challenge remains: HIV-1's ability to rapidly develop resistance. The virus can quickly mutate, allowing it to escape the targeted effects of the CRISPR/Cas9 system, thereby limiting the long-term effectiveness of these approaches [107].

1.6.2.4 Immunotherapy

Immunotherapy, including broadly neutralizing antibodies (bNAbs) offers strategies to expose and eliminate the HIV-1 reservoirs. For instance, when paired with LRAs, bNAbs can target reactivated HIV-infected cells.

Broadly neutralizing antibodies (bNAbs)

bNAbs fight HIV-1 by binding to specific epitopes on the virus, blocking its entry into host cells. In addition to this direct neutralization, bNAbs can activate immune effector mechanisms, such as antibody-dependent cellular cytotoxicity (ADCC) and complement-dependent cytotoxicity (CDC), to target and eliminate HIV-infected cells more effectively [106,108].

The administration of single bNAbs has consistently demonstrated the ability to suppress viremia for several weeks following antiretroviral therapy interruption (ATI) in both non-human primates (NHPs) and humans, however, viral rebound inevitably occurred. These findings highlight the need for bNAbs to be combined with other therapeutic strategies to achieve sustained, long-term viral suppression [108].

Studies in both humans and NHPs have demonstrated the ability of bNAbs to reduce viral loads. For example, combinations of bNAbs such as 3BNC117 and 10-1074 have shown significant success in suppressing viremia in SHIV-infected macaques and HIV-infected individuals [108]. However, when used as monotherapy, bNAbs often fail to achieve long-term viral suppression due to the rapid emergence of resistant viral strains [108].

To address these limitations, researchers are investigating combination therapies involving multiple bNAbs that target distinct epitopes on the HIV envelope protein (Env). This approach aims to provide broader protection against the genetic diversity of HIV-1 and minimize the risk of viral escape. Despite their potential, bNAbs face

several challenges, including the need for improved delivery systems, prolonged half-lives, and cost-efficient production methods [106].

Future clinical developments are expected to focus on combining bNAbs with other therapeutic modalities, such as latency-reversing agents or antiretroviral therapy, to achieve durable viral suppression and move closer to a functional cure for HIV-1. These efforts aim to harness the full potential of bNAbs in addressing the complexities of HIV infection and its persistence [106,108].

1.7 Hsp90

The discovery of heat shock proteins (Hsps) originated from an observation by Ferruccio Ritossa, who noticed unusual chromosomal puffing in *Drosophila melanogaster* exposed to elevated temperatures. This "puffing" was attributed to the activation of genes responsible for producing specific proteins, later named Hsps, as part of a cellular stress response [109]. This physiological mechanism is conserved across most living organisms and is characterized by the upregulation of Hsps, including Hsp90, to protect cells by preventing protein damage or aggregation and ensuring survival under stress [110].

While heat shock is a primary trigger for Hsp expression, other factors can also induce their overexpression. These include environmental stressors such as toxins, UV radiation, and oxidative stress, as well as chemical exposures and various physiological and pathological conditions [111]. Collectively, these stimuli activate

the cellular stress response, resulting in increased Hsp production to maintain proteostasis and cellular integrity [109].

1.7.1 Hsp90 types

The Hsp90 protein family consists of highly conserved and widely distributed molecules, each with an approximate molecular weight of 90 kDa. These proteins function as molecular chaperones, helping in the proper folding of newly synthesized proteins or correcting misfolded proteins, thereby preventing their aggregation. Hsp90 proteins are present across all living organisms, except archaea, and constitute approximately 1–2% of the total cellular protein content in mammalian cells under normal, non-stress conditions [112].

In mammals, Hsp90 chaperones are encoded by four primary genes **(Figure 1.11)**, producing isoforms that are distributed across different cellular compartments. These isoforms, which include cytosolic, endoplasmic reticulum (ER), and mitochondrial variants, exhibit distinct localization, expression patterns, and specialized functions, each Taken to meet the specific requirements of their respective environments [109,113,114].

1. **HSP90α and HSP90β (Cytosolic Isoforms):**
    - **HSP90α (*HSP90AA1 or HSPC1)*:** This is an inducible isoform of Hsp90, expressed at low levels under normal conditions but highly upregulated in response to stress. HSP90α primarily assists in folding

stress-induced or damaged proteins and is often associated with cancer, where it stabilizes oncogenic proteins [109].

- **HSP90α A2 (*HSP90AA2 or HSPC2):*** This is an inducible isoform of Hsp90, is a less characterized but functionally significant member of the Hsp90 family, contributing to cellular homeostasis and stress responses. Further research into its specific roles and interactions may provide insights into novel therapeutic strategies.
- **HSP90β (*HSP90AB1 or HSPC3*):** is constitutively expressed and essential for sustaining proteostasis in normal physiological conditions. It is necessary for the folding of housekeeping proteins and is involved in overall cellular maintaining [109].

2. **GRP94 (Endoplasmic Reticulum Isoform) (*HSP90B1 or HSPC4)*:** GRP94, or glucose-regulated protein 94, is the ER-resident isoform of HSP90. It specializes in folding and assembling proteins destined for secretion or insertion into membranes, such as immunoglobulins and integrins. GRP94 also contributes to the unfolded protein response (UPR), a critical pathway for managing ER stress [109].
3. **Mitochondrial Isoform (*TRAP1 or HSPC5)*:** TRAP1, or tumor necrosis factor receptor-associated protein 1, is the mitochondrial variant of Hsp90. It is involved in maintaining mitochondrial proteostasis by stabilizing key mitochondrial proteins and protecting against oxidative stress. TRAP1 has also been implicated in metabolic regulation and apoptosis, particularly in cancer cells, where it supports mitochondrial function under stressful conditions [109].

The elevated expression of Hsp90 has been associated with numerous pathological conditions, including various cancers, viral infections, inflammatory responses, and neurodegenerative disorders. This suggests that Hsp90 may play a significant role in the development and progression of these diseases [115–117].This thesis will focus on the cytosolic form of Hsp90, with particular emphasis on the inducible isoform, which has been reported to play a significant role in influencing HIV-1 infection [100,101].

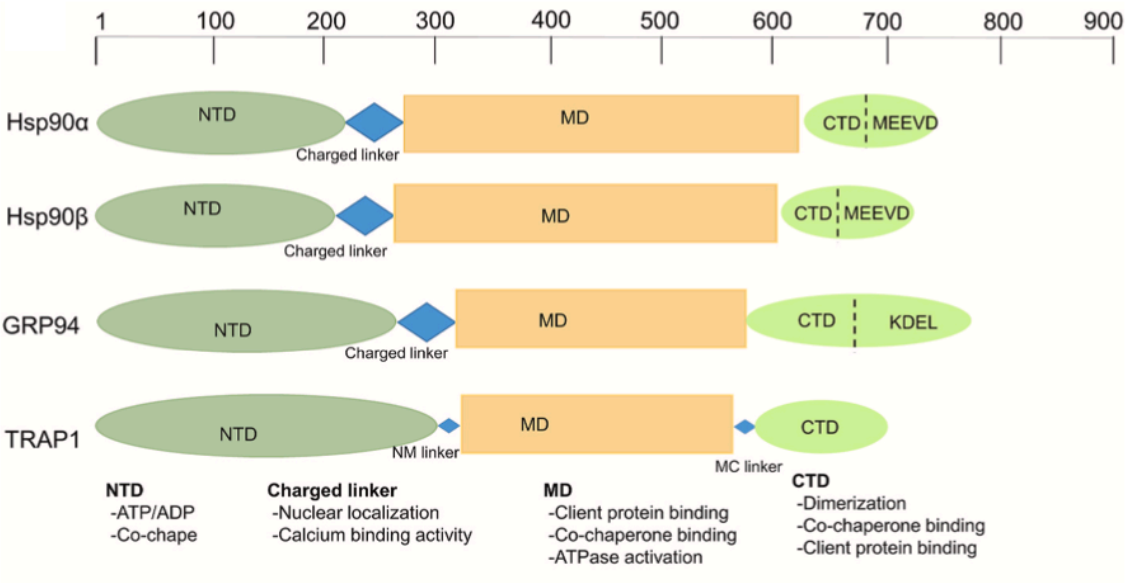

Figure 1.11 Schematic diagram showing structural domains of HSP90 isoforms. HSP90α, HSP90β, GRP94, and TRAP1**.** Taken from Li et al. 2024 [118].

1.7.2 Hsp90 structure

Hsp90 is a dimeric chaperone that relies on ATP to drive its activity through a tightly controlled conformational cycle. Each monomer is composed of three primary domains which has specific function: the N-terminal domain (NTD), it is the ATP-

binding site; the middle domain (MD), responsible for interacting with client proteins, both linked by variable charger linker domain in eukaryotes which increase the flexibility and dynamicity; CTD which enables dimerization and supports chaperone functionality. CTD also includes a Met-Glu-Glu-Val-Asp (MEEVD) motif or (KDEL, in GRP94 isoform), critical for binding co-chaperones with tetratricopeptide repeat (TPR) domains [119].

ATP binding and hydrolysis induce conformational changes in Hsp90, which is essential for its functionality. Structurally, the ATPase pocket is highly conserved across species and comprises residues that specifically recognize and bind the adenine and phosphate groups of ATP. Upon ATP binding, Hsp90 undergoes a conformational shift, transitioning from an open to a closed state, which promotes interaction with client proteins and co-chaperones. The hydrolysis of ATP to ADP subsequently releases energy that drives further structural rearrangements, leading to the release or folding of the client protein [119] **(Figure 1.12)**. The ATPase pocket is also a prime target for Hsp90 inhibitors such as geldanamycin and its derivatives, which compete with ATP for binding (will be discussed later in details).

The structural transitions between closed and open conformational enable Hsp90 to effectively engage with a diverse range of client proteins and co-chaperones, which regulate and optimize its chaperone activity [119]. Hsp90's affinity for unstable, partially folded, or misfolded client proteins accounts for its exceptional capacity to interact with a broad variety of proteins. Hsp90 stabilises proteins in a nearly natural state and gets them ready for functional activation by acting on later stages of folding

pathway maturation [120]. Hsp90 client proteins include kinases, transcription factors, and other signaling molecules that are critical for cellular homeostasis.

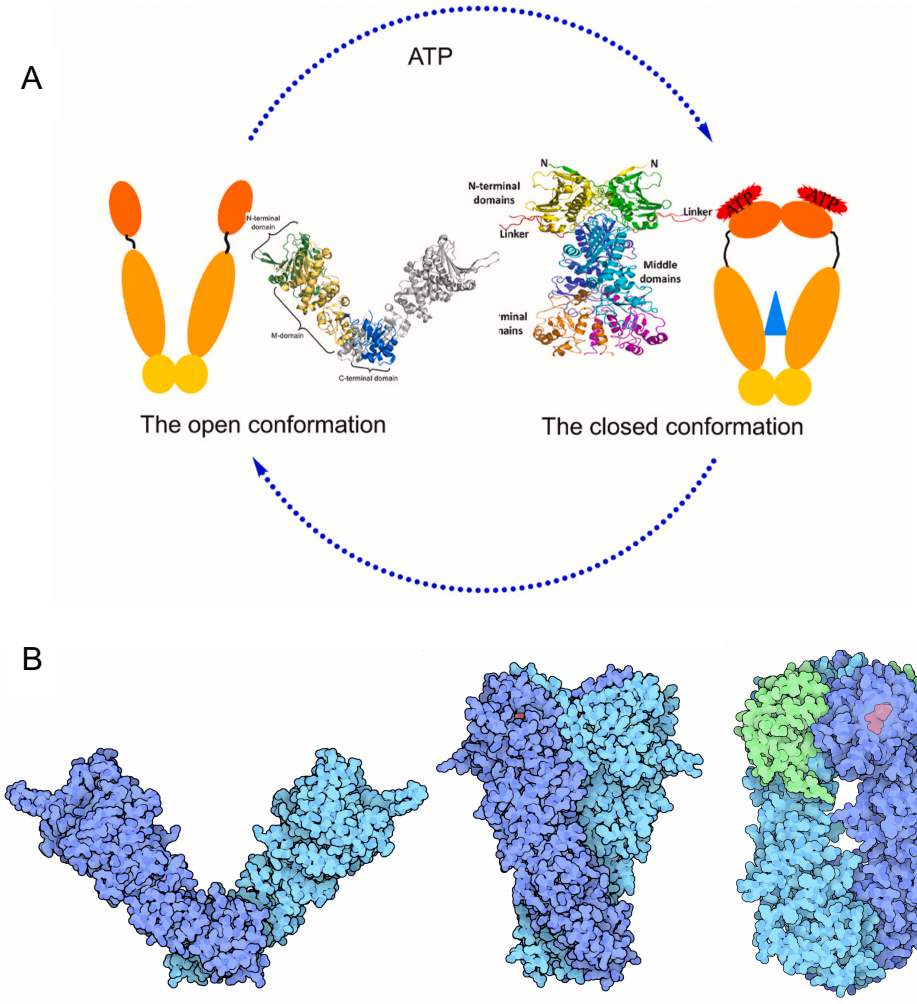

Figure 1.12 ATPase cycle of Hsp90 A) Schematic representation of the ATPase cycle of Hsp90 begins with the protein in its predominantly adopting an open state, V-shaped conformation. When ATP binds to the N-terminal domain, it triggers a structural rearrangement of the lid segment, transitioning Hsp90 into an intermediate state. This change facilitates the formation of a compact closed state, characterized by dimerization of the N-terminal domains and their interaction with the middle (M) domains. In this configuration, ATP is hydrolyzed, leading to the dissociation of the N-terminal domains and the subsequent release of ADP and inorganic phosphate (Pi). Following this, Hsp90 reverts to its original open conformation, completing the cycle. Taken from Li et al. 2024 [118]. B) Conformational changes of Hsp90. Hsp90 (blue) and cochaperone Sba1 (green), with bound ATP (red). https://pdb101.rcsb.org/motm/108

Hsp90 is one of the most conserved proteins across species, reflecting its critical role in cellular function and stress responses. Its structure and sequence are remarkably preserved from prokaryotes to eukaryotes, underscoring its evolutionary importance. In yeast, *Saccharomyces cerevisiae* expresses two homologs, Hsc82 and Hsp82, which are very similar to human Hsp90 and essential for cellular viability, particularly during stress. In bacteria, the Hsp90 homolog HtpG performs a similar role in stabilizing unfolded proteins under heat stress, although it is less essential under normal conditions [112]. Despite variations in function and co-chaperone interactions, the core ATP-binding domain and the dimerization domain of Hsp90 are conserved across all species. This universality highlights Hsp90's central role in proteostasis and stress response mechanisms, making it a key focus of research across evolutionary biology and medicine [112].

1.7.3 Hsp90 Regulation

The Hsp90 activity is tightly regulated through post-translational modifications and interactions with a diverse set of co-chaperones [119,121]. Modifications such as phosphorylation and acetylation influence Hsp90’s ATPase activity, stability, and binding to client proteins, enabling it to adapt to changing cellular conditions [119].

1.7.3.1 Post-translational modifications.

Post-translational modifications (PTMs) are crucial for regulating Hsp90's functional flexibility and activity. Various PTMs, including phosphorylation, acetylation, and

ubiquitination, have been extensively studied, as they significantly influence Hsp90's chaperone cycle, client protein interaction, and co-chaperone recruitment [121].

1. **Phosphorylation** plays a dominant role in modulating Hsp90 activity. It occurs on serine, threonine, and tyrosine residues, with specific modifications either enhancing or inhibiting its ATPase activity. For instance, phosphorylation at Thr90 by protein kinase A increases ATP binding affinity and alters co-chaperone interactions. However, phosphorylation at residues such as Thr22 (by CK2) reduces the binding affinity for co-chaperones like Aha1, potentially slowing down the chaperone cycle [121].
2. **Acetylation** of Hsp90**,** mediated by histone acetyltransferases (HAT) and reversed by histone deacetylases (e.g., HDAC6), further regulates its function. Acetylation at lysine residues, such as Lys294, can diminish ATP-binding affinity, suppressing the chaperone cycle. Conversely, deacetylation supports client protein stabilization by enhancing ATP hydrolysis efficiency and promoting complex formation with co-chaperones like p23 [121].
3. **Ubiquitination** adds another layer of regulation by tagging Hsp90 for proteasomal degradation or altering its interaction dynamics. Specific ubiquitination sites may lead to either functional alterations or clearance of Hsp90 under stress conditions [121].

1.7.3.2 Hsp90 co-chaperones

Co-chaperones play a crucial role in regulation of Hsp90 [119]. Approximately 20 structurally diverse co-chaperones regulate the activity of Hsp90, with many functioning as modulators of its chaperone cycle, adaptor proteins to facilitate client

protein recruitment, or serving both roles simultaneously. These co-chaperones play a crucial role in adjusting Hsp90's activity and expanding its functional versatility in cellular processes. A significant number of these cofactors bind to the C-terminal MEEVD motif of Hsp90 through their TPR domains [119]. Unlike Hsp90, which interacts with hundreds or thousands of client proteins, these co-chaperones demonstrate a much more selective and specific binding pattern [121]. Some of these cofactors simultaneously bind both Hsp90 and specific client proteins, facilitating the formation of multimeric protein complexes and enhancing the chaperone's functional precision [121,122].

For instance, the co-chaperon Hop facilitates the transfer of client proteins from Hsp70 to Hsp90, creating a coordinated chaperone system, while p23 stabilizes the ATP-bound conformation of Hsp90, ensuring prolonged interaction with client proteins. CDC37 is specifically important for kinases maturation. These co-chaperones act as regulatory adaptors, ensuring that Hsp90 performs its diverse functions with precision [119,123].

1.7.3.3 Transcriptional Regulation

Hsp90 levels rise significantly under stress conditions due to the activation of heat shock factor 1 (HSF1). When activated, HSF1 binds to specific regions in the HSP gene promoter, known as heat shock elements (HSEs) [121]. This binding facilitates the recruitment of RNA polymerase, enhancing the transcription of the HSP90 gene and increasing its expression to support cellular proteostasis. According to the

current model, HSP90, along with HSP70, interacts with HSF1 to maintain it in an inactive state under non-stress conditions [121].

1.7.4 Hsp90 Inhibitors: Mechanisms and Therapeutic Potential

By blocking the action of Hsp90, these drugs cause the destabilisation and subsequent destruction of client proteins that are crucial for different cellular processes. Hsp90 inhibitors are classified according to their chemical structure and mechanism of action. Each class has specific characteristics that contribute to their therapeutic potential.

1.7.4.1 Inhibition of ATPase Activity

Most Hsp90 inhibitors bind to the N-terminal ATP pocket and block ATP binding and hydrolysis. This interference disturbs the conformational changes essential for Hsp90 function, causing client proteins to be destabilised and degraded by proteasomes. This mechanism supports the efficacy of drugs such as geldanamycin and its derivatives [124]. These inhibitors divided into four classes according to the main scaffold including ansamycin-based, resorcinol-based, purine- based, and benzamide-based.

1. **Ansamycin-Based Inhibitors:** This family contains geldanamycin, one of the first Hsp90 inhibitors discovered, which binds to Hsp90's N-terminal ATP-binding site [118,124,125]. By reducing ATPase activity, geldanamycin interrupts the chaperone cycle, causing client protein degradation. Although

early ansamycin inhibitors, such as geldanamycin, showed great potency as Hsp90 inhibitors, their therapeutic value was limited due to excessive toxicity. This challenge resulted in the invention of safer compounds, such as 17-AAG (17-allylamino-17-demethoxygeldanamycin, commonly known as tanespimycin or KOS-953) [124] **(Figure 1.13A).** 17-AAG began Phase I clinical trials in 1999, with multiple intravenous formulations undergoing thorough Phase I testing [126]. Initial studies revealed promise therapeutic activity in a variety of malignancies, including melanoma, breast cancer, prostate cancer, and multiple myeloma [126]. Furthermore, 17-AAG has undergone evaluation in several Phase II clinical trials, despite showing limited and short-lived anti-Hsp90 activity, faced challenges such as poor solubility and low bioavailability, restricting its clinical progress. Its derivative, 17-DMAG, improved on these limitations with better solubility, bioavailability, and antitumor efficacy. However, clinical trials for 17-DMAG were largely delayed or terminated, with none advancing to Phase III [127].

2. **Resorcinol-Based Inhibitors:** Through high-throughput screening, researchers discovered a resorcinol-based inhibitor [128]. To enhance its solubility, modifications were made by adding specific substituents, resulting in the development of AUY922 (luminespib) [129] Figure **(1.13B)**. This novel compound showed significant biological activity, effectively suppressing tumor proliferation, invasion, and metastasis *in-vivo* [130,131], AUY922 was evaluated in Phase II trials for a variety of cancers, including non-small cell lung cancer (NSCLC), HER2-positive breast cancer, and gastrointestinal

stromal tumours (GIST). In NSCLC patients with ALK rearrangements, AUY922 exhibited encouraging antitumor activity, particularly in cases resistant to ALK inhibitors like Crizotinib. In HER2-positive breast cancer, it showed potential as a monotherapy and in combination with existing therapies, demonstrating its ability to target therapy-resistant cancer cells. However, despite its promising preclinical and early clinical results, AUY922 faced challenges in demonstrating consistent efficacy across broader cancer types. In terms of side effects, AUY922 treatment can lead to temporary loss of colour vision, which is reversible upon discontinuation of the drug. Additionally, it may cause gastrointestinal symptoms such as diarrhea, as well as fatigue and anorexia, though these side effects are generally manageable [132].

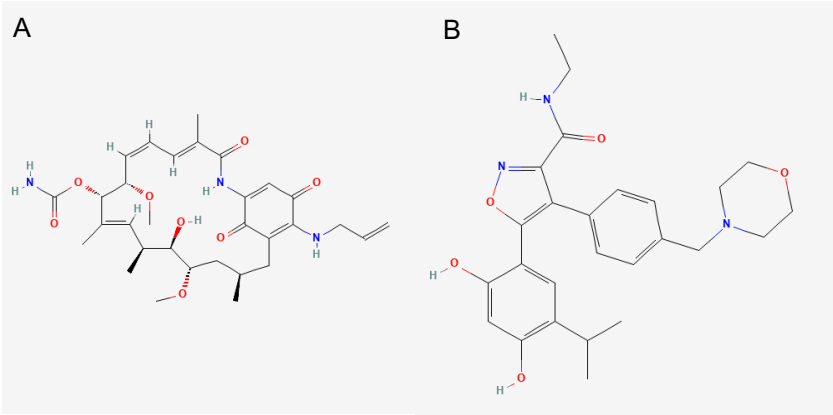

Figure 1.13 Chemical structure of 17-AAG and AUY922. A) Chemical structure of 17-AAG (PubChem ID: 6505803). B) Chemical structure of AUY922 (PubChem ID:135539077).

3. **Purine-Based Inhibitors:** Purine analogs are designed to mimic ATP and competitively bind to the ATP-binding site of Hsp90. Hsp90 inhibitors interfere with the chaperone's ability to stabilise its client proteins by inhibiting ATPase activity, resulting in their breakdown [124]. Notable examples are PU-H71 and PU-DZ8, which are currently undergoing advanced preclinical assessments for their medicinal potential. Another promising compound, CNF-2024, an orally bioavailable 9-benzyl purine derivative with high potency at nanomolar concentrations, has progressed to Phase I clinical trials [126]. It is being tested for its efficacy in treating various cancers, including chronic lymphocytic leukaemia, advanced solid tumours, lymphomas, and, more recently, advanced breast cancer [126].

4. **Benzamide-based inhibitors:** represent a more refined class of Hsp90 inhibitors, addressing limitations like poor solubility and high toxicity seen in earlier compounds. These inhibitors offer improved pharmacokinetics and reduced side effects, enhancing their therapeutic potential [127]. One such compound, SNX-5422, a pyrazole-derived inhibitor, was purified using an ATP-affinity column. It has shown potent antiproliferative activity at low nanomolar concentrations and excellent oral bioavailability in clinical trials, making it a promising candidate for Hsp90-targeted therapies [127].

1.7.4.2 Inhibitors Targeting the Hsp90 C-Terminus

CTD inhibitors interfere with co-chaperone and client protein interactions, offering a distinct mechanism of action. These inhibitors prevent Hsp90 dimerization or destabilize the Hsp90 complex, thus interrupting its chaperone functions. Notable CTD inhibitors include novobiocin and its derivatives. Novobiocin binds specifically to the ATP-binding site of the CTD, which is structurally and functionally distinct from the well-characterized ATP-binding site in the N-terminal domain (NTD), blocking Hsp90's chaperone activity and leading to the degradation of client proteins [127]. Derivatives like KU-32 and KU-569 enhance ATP binding and hydrolysis, improving therapeutic potential. These compounds show promise in inducing apoptosis and inhibiting tumour growth in preclinical models [127]. Another example is LB76, a CTD-targeting inhibitor designed to disrupt interactions with co-chaperones, specifically by binding to the MEEVD motif in the CTD. Preclinical studies using LB76-loaded nanoparticles have shown improved delivery and antitumor activity, demonstrating potential for clinical applications [127].

1.7.4.3 Disruption of Hsp90-Co-Chaperone Interactions

Some inhibitors preferentially impair the interactions of Hsp90 and its co-chaperones, such as p23 and CDC37. These interactions are required for the correct folding and activation of client proteins. By targeting these complexes, inhibitors can degrade specific oncogenic proteins involved in tumour growth and other illnesses [124,126].

1.7.4.4 Targeting Post-Translational Modifications (PTMs)

PTM, such as acetylation and phosphorylation, affect Hsp90 function and interaction with client proteins. While this area of research is still in its early stages, addressing these alterations provides a fresh technique for modulating Hsp90 activity and potentially disrupting its role in disease [124].

Hsp90 client proteins are linked to a variety of illnesses, particularly those involving dysregulated protein homeostasis and signalling pathways, some of which are discussed below.

While Hsp90 inhibitors show great potential, issues such as drug resistance, toxicity, and delivery constraints persist. Ongoing research attempts to improve these drugs' safety, specificity, and therapeutic efficacy [118,124,126].

1.7.5 Hsp90 in Disease

Hsp90's role in maintaining proteostasis becomes particularly relevant in the context of disease, where its chaperone activity can both promote and hinder pathological processes. Dysregulation of Hsp90 function is implicated in various diseases, including cancer, neurodegenerative disorders, and viral Infections.

1.7.5.1 Hsp90 in Cancer:

Hsp90 is frequently overexpressed in cancer cells, where it plays a critical role in maintaining the stability and functionality of numerous oncogenic client proteins, such as mutated kinases like HER2, which is associated with breast cancer [114].

Studies have shown a correlation between elevated Hsp90 expression in breast cancer and poorer patient survival outcomes [133]. Additionally, Hsp90 is essential for stabilizing transcription factors such as hypoxia-inducible factor 1α (HIF-1α). This factor regulates the expression of genes involved in angiogenesis and metabolic adaptation to hypoxic environments, processes that contribute to tumour growth and metastatic progression [134]. This allows cancer cells to survive under the harsh conditions of the tumour microenvironment [134].

Because of its pivotal role in cancer progression, Hsp90 has emerged as a promising therapeutic target. Inhibitors like AUY922 and 17-AAG, currently undergoing clinical trials, function by binding to the ATP-binding domain of Hsp90, thereby disrupting its activity. This disruption results in the degradation of client proteins essential for tumour survival, ultimately leading to cancer cell death. However, the limited success of Hsp90 inhibitors in clinical trials has been linked to drug-induced toxicity [133,135–137].

1.7.5.2 Hsp90 in Neurodegenerative Disorders:

Hsp90's involvement in neurodegenerative diseases is complex, as it can both reduce and contribute to pathological processes. In conditions such as Alzheimer's disease, Parkinson's disease, and Huntington's disease, Hsp90 interacts with misfolded and aggregated proteins, such as amyloid-beta, tau, and alpha-synuclein. While Hsp90 can promote the refolding or clearance of these proteins, it can also stabilize toxic protein conformations, thereby contributing to disease progression [116]. Modulating Hsp90 activity in neurodegeneration is an area of ongoing

research, with the goal of enhancing its protective effects while minimizing its contribution to pathological aggregation [116].

1.7.5.3 Hsp90 in Viral Infections

Hsp90 is a critical host factor exploited by numerous viruses to facilitate their replication, stability, and survival within host cells.

1. **Hsp90 and HIV-1**

In the context of HIV-1 infection, proteomic and microarray studies have identified elevated levels of Hsp90 expression following viral infection. However, it remains uncertain whether this upregulation is directly triggered by HIV-1 or if it represents a generalized cellular response to the stress induced by infection [138,139].

Hsp90 plays a pivotal role in supporting HIV-1 replication by promoting viral gene expression. This is achieved through its interaction with the viral promoter, a process demonstrated in detail by chromatin immunoprecipitation (ChIP) experiments [100]. These findings highlight Hsp90's involvement in regulating the transcriptional machinery at the HIV-1 promoter, underscoring its critical function in facilitating the HIV-1 replication [100]. The importance of Hsp90 was further confirmed in conditions of hyperthermia (39.5°C), which enhanced HIV-1 replication by increasing viral gene expression. Under these elevated temperatures, both Hsp70 and Hsp90 levels were upregulated in CD4+ T cells [140]. However, specific Hsp90 inhibitors effectively suppressed the hyperthermia-induced replication, confirming Hsp90's central role in this process. Confocal microscopy studies supported these findings by revealing that

hyperthermia recruits Hsp90 to the viral transcriptional site, further linking Hsp90 activity to increased HIV-1 gene expression [140].

Beyond its role in active replication, Hsp90 is also implicated in the reactivation of latent HIV-1. It facilitates this process by interacting with P-TEFb, a critical regulator of transcription elongation. Hsp90 stabilizes and maintains the functionality of CDK9, a key component of P-TEFb, protecting it from proteasomal degradation [141]. Furthermore, Hsp90 is part of the HSP90-CDC37-P-TEFb complex, which is essential for transitioning RNA polymerase II from a paused state to active elongation, thereby promoting HIV-1 gene expression. A recent study demonstrated that the recruitment of this complex is mediated by HSF-1 and that treatment with JQ1, a compound known to activate transcription, led to increased levels of the HSP90-CDC37-P-TEFb complex. Importantly, knockdown of Hsp90 or CDC37 significantly reduced HIV-1 reactivation, highlighting the critical role of this complex in latent HIV-1 reactivation [142].

In addition to its interactions with the transcriptional machinery, Hsp90 plays a role in controlling HIV-1 reactivation via the NF-kB pathway. By stabilizing key components of this pathway, Hsp90 ensures efficient signaling that supports the reactivation of latent HIV-1 [101].

A recent study investigated the effects of the Hsp90 inhibitor tanespimycin on peripheral blood mononuclear cells (PBMCs) obtained from PLWH in an *ex-vivo* setting. The findings revealed that tanespimycin significantly suppressed HIV-1 latency reactivation and transcriptional elongation within 24 hours of activation and

reduced the levels of initiated HIV transcripts after six days of treatment. Additionally, the inhibitor effectively blocked the production of viral RNA in supernatants following T cell activation across multiple participants. These results highlight tanespimycin's ability to inhibit HIV transcription at both initiation and elongation stages, presenting it as a promising candidate for therapeutic strategies targeting HIV [143].

Collectively, these findings demonstrate the multifaceted role of Hsp90 in HIV-1 biology, making it a promising target for therapeutic strategies aimed at controlling HIV-1 replication and reactivation.

2. Hsp90 and other viruses

Hsp90 plays a pivotal role in the lifecycles of a diverse range of viruses, contributing to processes such as viral entry, replication, protein maturation, and gene expression. Its involvement underscores its potential as a therapeutic target in antiviral strategies [144].

Hsp90 is essential for the internalization of several viruses into host cells. Notable examples include human enterovirus 71 (EV-71) [145], dengue virus (DENV) [146], hepatitis B virus (HBV), and coxsackievirus A9 (CAV-9), where Hsp90 facilitates early stages of infection by supporting viral entry [144].

In terms of replication, Hsp90 is exploited by numerous RNA viruses, including respiratory syncytial virus (RSV) [147], human parainfluenza virus 2 (HPIV-2) [148], vesicular stomatitis virus (VSV) [148], simian virus 40 (SV40), Ebola virus (EBOV) [149], Severe acute respiratory syndrome coronavirus 2 (SARS-CoV-2) [150] and chikungunya virus (CHIKV) [144]. It stabilizes viral replication complexes and

ensures efficient genome replication. Hepatitis C virus (HCV) also depends on Hsp90 for its replication [151], leveraging its stabilizing effects on viral polymerases, such as NS5B, and kinases involved in replication, including phosphoinositide kinase 1 (PDK1) [144]. Moreover, Hsp90 ensures the proper folding and maturation of HCV proteins like NS2/3, supporting their cleavage into functional units essential for viral replication [117,144,151,152].

Influenza viruses exploit Hsp90 to stabilize the activity of their RNA-dependent RNA polymerase, particularly the PB2 subunit [144,153]. This interaction facilitates the assembly and nuclear transport of the polymerase complex, which is essential for the synthesis of viral RNA. Additionally, Hsp90 supports the functionality of viral ribonucleoprotein complexes, critical for replication and transcription within the nucleus [144].

Hsp90's role extends to DNA viruses as well. For example, human herpesvirus-1 (HSV-1) relies on Hsp90 during the formation of virus-induced chaperone-enriched foci (VICE foci) within the host nucleus [117] . These structures are closely associated with viral replication compartments, where Hsp90 manages the cellular stress response and ensures proper protein folding. Other DNA viruses, such as Epstein-Barr virus (EBV), Kaposi’s sarcoma-associated herpesvirus (KSHV), and varicella-zoster virus (VZV), use Hsp90 to regulate viral gene expression. By interacting with viral and host factors, Hsp90 enhances the transcription and translation of viral genes, promoting effective infection [144].

Hsp90 also contributes to protein maturation and virion formation in poliovirus, rhinovirus, and coxsackievirus. By stabilizing viral proteins during their synthesis and assembly, it ensures the production of infectious virions [144].

In summary, Hsp90 is a versatile chaperone that various viruses exploit to support their lifecycle. Whether aiding in entry, replication, protein folding, or gene expression, Hsp90's multifunctionality highlights its potential as a universal target in antiviral research.

1.8 Research questions

Novel therapeutic approaches are needed to eradicate HIV-1 from latent viral reservoirs and cure HIV-1 infection. To develop cure strategies for HIV-1, it is crucial to identify host factors that play an essential role in both virus replication and silencing.

Previous research conducted by our group and others has established that host factor Hsp90 plays a pivotal role in HIV-1 gene expression and reactivation from latency in CD4+ T cells. Additionally, Hsp90 inhibitors, such as 17-AAG and AUY922, were found to disrupt the interaction of Cdc37 with the IKK complex, reduce the degradation of IκBα, and impair nuclear translocation of NF-kB. Since NF-kB is a crucial transcription factor for activating the HIV-1 LTR, these inhibitors ultimately suppress HIV-1 reactivation from latency, even under potent stimulatory conditions.

Based on the above, I hypothesize that Hsp90 functions as a master regulator of HIV-1 reactivation from latency. I began by identifying which signaling pathways are dependent on Hsp90. To address this, I screened a panel of latency-reversing agents (LRAs) for their ability to induce HIV-1 reactivation in a Jurkat latency model. I then tested whether the reactivation observed through specific pathways was dependent on Hsp90 by treating cells with Hsp90 inhibitors, including AUY922 and 17-AAG.

Next, I aimed to identify key components of signaling pathways that depend on Hsp90, with a particular focus on client proteins shared across multiple pathways. To achieve this, I reviewed relevant literature and available databases to compile a comprehensive list of Hsp90-dependent targets.

I then investigated whether inhibiting Hsp90 alters the phenotype and differentiation of primary CD4+ T cells, as well as the efficacy of latency-reversing agents (LRAs) in reactivating latent HIV in a CD4+ T cell model. To this end, I designed a panel of antibodies to profile the phenotype of primary CD4+ T cells, assessing key markers of activation and immune inhibition.

Chapter 2: Materials and methods

2.1 Ethics statement

Blood samples were obtained from healthy volunteers after written informed consent, or from the National Health Service Blood and Transplant (NHS-BT) according to the approved protocol of the University College London Research Ethics Committee reference REC 3138/001 and NHS-BT reference R140.

2.2 Chemical compounds

NVP-AUY922 was purchased from LKT Laboratories; 17-AAG (tanespimycin) from Merck Life Science UK Ltd. Phorbol 12-myristate 13-acetate (PMA), 5Z were obtained from Cayman Chemical; TNF-α was purchased from Life Technologies Limited. Imiquimod (TLR7 agonist) was purchased from SAlfaAesar, CL075 (TLR8 agonist) from Sigma-Aldrich (MREK). FOXO-1inh (AS1842856) was purchased from MedChemExpress LLC, PHA and Ionomycin were obtained from Thermo Fisher Scientific. Compounds were dissolved in DMSO to obtain 1000x stock solutions (v/v) and stored in aliquots at −20 °C in the dark. Purified anti-human CD3 antibody (OKT) and anti-human CD28 antibody (CD28.2) were purchased from Biolegend; Recombinant human IL7, rhIL-2, IL6 and IL15 were obtained from Peprotech. The concentrations used are shown in Table 3.2 for each compound.

2.3 PBMC isolation

Whole blood was collected in heparin-coated tubes and peripheral blood mononuclear cells (PBMCs) were isolated by density gradient centrifugation; briefly blood was diluted 1:1 with 1xPBS and layered over Ficoll Paque Plus and centrifuged at 800 xg for 20 minutes at room temperature (with centrifuge break off). The layer of PBMCs that forms was aspirated, washed once in 10ml 1xPBS in 15ml tubes and centrifuged at 600 xg for 7 minutes at room temperature. PBMCs were resuspended in 1xPBS, stained with trypan blue and counted using a haemocytometer. If not used directly, PBMCs were cryopreserved in liquid nitrogen (-180 °C) in 1ml aliquots at $50x10^6$ PBMCs per vial in freezing medium (90% FBS and 10% DMSO) after freezing in “Mr frosties” at -80°C overnight. When needed, vials of PBMCs were warmed at 37 °C in a water bath until partially thawed and then were diluted gradually in 10mls of X-VIVO™15 Serum-free media supplemented with 5% fetal bovine serum and 100 U/mL penicillin/streptomycin, pelleted, and then resuspend.

2.4 Isolation of CD4+ cells

Human CD4+ T lymphocytes were isolated from PBMCs using MojoSort Human CD4+ T Cell Isolation Kit (BioLegend, 480010) following the manufacturer’s instructions. Briefly, PBMCs were first filtered with a 70 μm cell strainer, centrifuged at 300xg for 5 minutes, and resuspend in an 3ml MojoSort Buffer (BioLegend, 480017). Cells were counted and adjusted to the concentration of 1 x 10^8 cells/mL then 100μL of the Biotin-Antibody Cocktail was added, mixed well and incubated on ice for 20 minutes**.** After that, the same amount of magnetic Streptavidin Nanobeads

was added, mixed well and incubated for 20 minutes on ice. Finally, 2.5mL of MojoSort™ Buffer was added to the tube. Non CD4+ T cells were subsequently removed using a magnetic separator (Mojosort). Tubes were placed in the magnet for 15 minutes. The magnetically labelled fraction remained in the tube and CD4+ T cells were collected by pouring the solution into a new tube. Isolated CD4+ T cells were cultured in X-VIVO™ 15 Serum-free Hematopoietic Cell Medium (Lonza), supplemented with 5% fetal bovine serum and 100 U/mL penicillin/streptomycin

2.5 Cell lines and tissue culture

The Jurkat cell line E6-1 was obtained from the American Type Culture Collection (ATCC) and cultured in RPMI media (Gibco) supplemented with 10% fetal bovine serum, 100 U/mL penicillin/streptomycin, and maintained at 37°C in a 5% CO_2 incubator HEK-293T cells were obtained from the ATCC and maintained in DMEM media (Gibco) supplemented with 10% fetal bovine serum, 100 U/mL penicillin/streptomycin. Once confluent (every 2-3 days), the medium was aspirated off and the adherent cell monolayer was gently washed with PBS before being disrupted by trypsin/EDTA (Gibco) and diluted with complete DMEM. Triple parameter reporter (TPR) Jurkat-derived cells were kindly provided by Prof. Peter Steinberger (Medical University of Vienna) and cultured in RPMI as above.

2.6 Bacterial culture and plasmid preparation

2.6.1 Transformation

The plasmids pNL4-3-Δ6-drEGFP, pCMV-VSV-G envelope, and pCMV-Gag/Pol were transformed into One Shot™ Stbl3™ Chemically Competent E. coli cells (invitrogen) following the manufacturer's protocol. For unstable plasmids, the incubation temperature was adjusted to 30°C post-transformation. Bacteria were cultured LB agar plates supplemented with the ampicillin antibiotic and incubated overnight 37°C or 30°C (for unstable plasmids). Next day, single bacterial colonies were picked and inoculated into 5 mL of LB broth containing 100 µg/mL ampicillin. These cultures were incubated overnight at either 37°C or 30°C (for unstable plasmids) in a shaking incubator set at 200 rpm (Kuhner ISF-1-W Incubator Shaker Pred ISF1-X/Z). Subsequently, the starter cultures were expanded into 100 mL LB broth with antibiotics in an Erlenmeyer flask and incubated overnight at 37°C or 30°C (for unstable plasmid) under the same shaking conditions.

2.6.2 DNA Extraction and Glycerol Stock Preparation

Plasmid DNA was extracted from the bacterial cultures using a QIAGEN Plasmid DNA Midiprep Kit, following the manufacturer's instructions. The DNA concentration was quantified using a Nanodrop spectrophotometer. To ensure long-term storage, glycerol stocks were prepared by mixing equal volumes of bacterial culture and 80% glycerol, followed by storage at -80°C.

LB Agar

To prepare LB agar, 20 g of Luria-Bertani (LB) agar granules (Sigma) were dissolved in 1 L of deionized water (dH2O) and sterilized in an autoclave at 121°C for 15 minutes. The medium was then cooled before use.

LB Broth

For LB broth preparation, 20 g of LB broth powder (Sigma) was dissolved in 1 L of deionized water (dH2O) and sterilized in an autoclave at 121°C for 15 minutes. The broth was allowed to cool before use.

2.7 Virus production

Production of the Single-Cycle HIV-1 Vector (Δenv)

The single-cycle HIV-1 vector (Δenv) was produced by transfecting 293T cells with FuGENE Transfection Reagent, following previously described protocols [22, 45]. The transfection process was carried out as follows:

2.7.1 Transfection

FuGENE Transfection Reagent was mixed with a plasmid DNA mixture comprising the following plasmids:

- pNL4-3-Δ6-drEGFP 1.5 μg
- pCMV-VSV-G envelope 2 μg
- pCMV-Gag/Pol packaging vectors 1 μg

The DNA mixture was prepared in TE buffer up to 15μl then mixed 18 μl FuGENE (Promega) Plus 200μl Opti-MEM (Gibco). The mixture was incubated at room

temperature for 15 minutes to allow the formation of DNA-FuGENE complexes. Then transfection complex was added dropwise to the culture medium of 293T cells, which had been plated the day prior. Before transfection, the existing medium was replaced with fresh culture medium (DMEM). The cells were maintained at 60–70% confluency at the time of transfection. Following the addition of the transfection complex, the cells were incubated under standard conditions (37°C, 5% CO_2) to facilitate the uptake of the DNA-FuGENE complexes. After 24 hours, the culture medium was replaced with fresh DMEM.

2.7.2 Viral Supernatant Collection and Processing

Supernatants containing the virus were collected at 48 and 72 hours post-transfection. These supernatants were filtered through a 0.45 µm filter to remove debris and subsequently concentrated by ultracentrifugation at 25,000 rpm for 2 hours at 4°C through a 25% sucrose cushion [116]. The resulting viral pellet was resuspended in RPMI or X-VIVO medium and stored at -80°C.

2.7.3 Titration of Virus Stock

The virus stock titer was determined by infecting $1x10^5$ Jurkat cells with serial dilutions of the viral supernatants. Two days post-infection, GFP expression was measured by flow cytometry to assess the efficiency of transduction.

2.8 Generation of latently infected Jurkat cells

Jurkat cells were infected with NL4.3Δ6-drGFP viral stock at an MOI of 0.2. Forty-eight hours post-infection, GFP+ (infected) cells were sorted using BD FACSAria II

and the GFP+ population was maintained in culture and regularly monitored by flow cytometry for GFP expression until latent infection was established (2-3 weeks).

2.9 Stimulation/ inhibition of Jurkat Latent cells

To stimulate latently infected Jurkat cells, 1×10^5 cells were treated with the indicated concentrations of LRAs listed in Table 3.2 for 24 hours. For the FOXO-1 inhibitor, cells were treated for 48 hours. Hsp90 inhibitors (AUY922 or 17-AAG) and the TAK1 inhibitor (5Z-7-Oxozeaenol) were dissolved in DMSO and applied in different concentrations, as shown in the figures. These inhibitors were added simultaneously with the corresponding stimuli at their specified concentrations.

2.9.1 Assessment of Drug Toxicity and Cell Activation

Following stimulation or inhibition, cell viability was evaluated by staining with LIVE/DEAD Fixable Blue Dead Cell Stain (Thermo Fisher Scientific). To assess cell activation, cells were stained with anti-CD69 APC antibody (BioLegend).

Flow cytometry was performed to measure the percentage of GFP+ cells and the activation marker CD69. Fluorescence data were acquired using a BD LSR Fortessa cytometer, BD FACS Diva9 software and analyzed with FlowJo software version 10.8.1.

2.10 Infection of primary CD4+ T cells and generation of latently infected cells.

CD4+ T cells were activated by anti-CD3/CD28 monoclonal antibodies. Tissue culture plates were precoated with anti-CD3 (OKT) Ab at 1 µg/mL then cells were added to the plate together with soluble anti-CD28 Ab (CD28.2) at 2 µg/mL and 100 U/mL IL-2 in X-VIVO media supplemented with 5% FBS and 100 U/mL penicillin/streptomycin. On day 3, the activated CD4+ T cells were infected with the NL4.3Δ6-drGFP virus at an MOI of 2 in the presence of 4 µg/mL polybrene and 100 U/mL IL-2. The cells were incubated overnight on a shaker in the incubator. After removing them from the shaker, the cells were incubated for an additional 24 hours. An aliquot of the cells was then stained with CD3, CD4, CD45RA, CD45RO, CD25, and CD69 and analysed by flow cytometry to assess infection by measuring GFP+ cells within the CD45RO+ population. The cells were subsequently monitored for latency establishment by measuring GFP+ cells every other day. Once latency was established, the cells were reactivated using different LRAs. To reactivate latently infected CD4+ T cells, 1×10^5 cells were cultured in 96-well plates in 100uL media and treated with different LRAs, including anti-CD3/CD28 Abs (1µg/mL /2 µg/mL), IL7 + IL15 (20 ng/mL of each), AS1842856 (200 nM), TLR7 agonist (5 µg/mL). Cells were treated with each LRA in the presence of either DMSO, AUY922 (25 nM), or AUY922 (50 nM) and incubated for 48 hours before staining and analysis by flow cytometry. Additionally, the supernatant of these cells was collected for cytokine analysis.

2.11 Cell Surface Staining for Flow Cytometry

2.11.1 Compensation controls

BD anti-Ig compensation beads were prepared for individual antibodies by adding the Ab to the beads (one antibody per FACS tube containing one drop of beads) and incubating for 30 mins in the dark. For Live cell stain control dead cells were used, cells were heated for 10 mins before staining with Live/dead blue stain.

2.11.2 Fluorescence minus one (FMO)

FMO controls were used to set the gates of the 18-color panel. A comparison of stains with and without a particular antibody was used to design the gating technique. Cells of interest were stained using the entire antibody panel with the exception of one antibody.

2.11.3 Surface cell staining

Live dead blue stain (1 µL in 1000 µL PBS) was prepared and 40 µL was added per sample and left to incubate for 20 mins, protected from light. The panel of antibodies listed in the table below was used to identify T cell subset, activation and inhibitory markers. For cell staining, Abs were then prepared, in the dark, diluted 1:100 in FACS buffer. Cells were washed with PBS before adding 50 µL of Abs stain per $2x10^5$ cells and incubating for 30 mins at 4 ^oC in the dark. Finally, cells were washed with 1x PBS twice and then resuspended in FACS buffer. Unstained PBMCs were kept aside as a control.

Fluorochrome	Specificity (Marker)	Supplier (catalogue number)
BV510	TIGIT	BD (747842)
BV711	Tim-3	BD (747959)
BV786	CD197(CCR7)	BD (566758)
BV421	CD196(CCR6)	BD (562515)
BV605	CD71	BD (745096)
APC/fire 810	CD25	BioLegend (356150)
APC	CD69	Biolegend (310910)
Alexa fluor 700	CD 127	BioLegend (351344)
APC/Cyanine 7	CD4+5RO	BioLegend (304228)
BUV805	HLA-DR	BD (748338)
UV (450) live dead blue	Live/Dead	ThermoFisher (L34961)
BUV 395	CD4+5RA	BD (740315)
BUV737	CD183	BD (741866)
Spark NIR 685	CD38	BioLegend (303552)
PE-Dazzle	PD-1	BioLegend (367434)
PE cy7	CD4+	Biolegend (317414)
PE/fire 810	CD194(CCR4)	BioLegend (359433)
GFP	GFP reporter	
Percp cy5.5	CD3	Biolegend (317336)

2.11.4 Phospho-flow

CD4+ T cells were pre-treated with AUY922 inhibitors or DMSO for 1 hour. Following this, the cells were placed on ice to pre-chill before being centrifuged at 600g for 5 minutes at 4°C. After centrifugation, the supernatant was discarded, and 1 µg/ml of anti-CD3 OKT3 antibody in 100 µl was added to all tubes except the unstimulated control. The samples were incubated on ice for 20 minutes. Subsequently, the cells

were centrifuged again at 600g for 5 minutes at 4°C, the supernatant was removed, and 1 µg/ml of anti-mouse antibody in 100 µl of cold media was added. Additionally, 2 µg/ml of anti-CD28 antibody prepared in the same media was included. The cells were resuspended on ice for 15 minutes and then transferred directly to a 37°C water bath for 10 minutes to stimulate. The reaction was stopped by adding 250 µl of pre-warmed Cytofix buffer (BD, catalogue number 554655) to each tube, followed by gentle mixing and incubation for 12 minutes in the water bath. After incubation, the samples were centrifuged at 600g for 5 minutes, the supernatant was discarded, and the cells were permeabilized by adding 500 µl of pre-chilled Perm III buffer (BD, catalogue number 558050). The tubes were vortexed or pipetted thoroughly to mix and incubated on ice for 30 minutes. Post-incubation, the cells were washed twice with PBS at 600g for 5 minutes each. Specific antibodies (as listed in the corresponding table) were then added, and the samples were incubated for 1 hour. Finally, the cells were washed, resuspended in FACS buffer and analyzed using a flow cytometer.

Fluorochrome	Specificity (Marker)	Supplier (catalogue number)
PE	NF-kB p65 (pS529)	BD (558423)
Pacific Blue	p38 MAPK (pT180/pY182)	BD (560313)
PerCP-Cy™5.5	ERK1/2 (pT202/pY204)	BD (560115)
Alexa Fluor® 647	JNK (pT183/pY185)	BD (562481)

FACS buffer

1% FBS, 0.05% sodium azide, 5mM EDTA in PBS (1L):

10ml FBS, 500ul NaN_3, 10ml 0.5M EDTA, 1L PBS

2.12 qPCR for proviral quantification in HIV-1 infected Jurkat cells.

2.12.1 DNA extraction for Jurkat cells

Total DNA from 1.5 × 10^6 infected Jurkat cells was extracted at each week after sorting according to the manufacturer's instructions using the Qiagen DNeasy Blood & Tissue Kit. Briefly, the sample was centrifuged at 300 x g for 5 min. Pellet was then re-suspended in 200 µl of PBS. Then, 20 µl of proteinase K was used to lyse the cells. Then 200 µl of buffer AL was added, and mixture was vortexed very well, then incubate it for 10 minutes at 56°C. 200 µl of ethanol was added to the sample, which was well mixed by vortexing. the mixture from the previous step was transferred into the DNeasy Mini spin column and placed in a 2 ml collection tube and centrifuged. The flow-through was discarded, and the DNeasy Mini spin column was placed in a new 2 ml collection tube. 500 µl Buffer AW1 was then added, centrifuged at ≥6000 x g for 1 min, the flow-through discard once again and 500 µl of AW2 buffer was added after transferring the DNeasy Mini spin column to new collection tube, and then centrifuged for 3 minutes at 20,000 x g. DNeasy Mini spin column was put in a clean 1.5 ml microcentrifuge tube, flow-through was removed, and 200 µl Buffer AE was then added directly onto the DNeasy membrane. After 1 minute of RT incubation, the sample was centrifuged to elute for 1 minute at ≥6000 x g. DNA concentration and purity were measured by Nonodrop, and each DNA sample was normalized to 100ng/µl.

2.12.2 Real-time qPCR

The real-time qPCR reaction was performed using a Real-Time PCR machine (Applied Biosystems) in a final volume of 20 ml containing 1x Power-Up SYBR green master mix (Applied Biosystems), to detect GFP expression, GFP 200ng of DNA in 2µl and 0.2µM of each primer:

forward GFP primer AAGCTGACCCTGAAGTTCATCTGC and reverse GFP primer CTTGTAGTTGCCGTGGTCCTTGAA. Cycling parameters were 95^{o} C for 2 min followed by 95^{o} C for 1 min, 55^{o} C for 1 min and 68^{o} C for 1 min repeated for 40 cycles. Quantification was done using a standard curve that was generated by serial dilutions of the NL4.3Δ6-drEGFP plasmid.

To detect IL-2 expression in different samples 10ng cDNA and 600 nM of IL-2 primers (IL-2 Forword primer CCCAAACTCACCAGGATGCTC and reverse IL-2 primer ATTGCTGATTAAGTCCCTGGGT) were added to PowerUp SYBR Green Master Mix for a final volume of 20 µl, Amplification was performed using QuantStudio 5 real-time PCR at the following conditions: 50°C 2 minutes. 95°C 2 minutes. Denature 95°C 15 seconds and anneal/extend 60°C 1 minute for 40 cycles.

2.13 Quantification of HIV-1 integration

2.13.1 DNA extraction using phenol chloroform

for primary cells, DNA was extracted using the phenol/chloroform method. Initially, cells were digested overnight at 55°C in a tissue lysis buffer containing Proteinase K (100 µg/mL) to lyse the cells and release nucleic acids. Following digestion, an equal volume of phenol-chloroform-isoamyl alcohol (25:24:1) was added to the lysate, and

the mixture was gently inverted several times to ensure thorough mixing. The tubes were then centrifuged at 14,000 RPM for 15 minutes at 4°C to separate the aqueous and organic phases. The aqueous phase, containing the DNA, was carefully transferred to a new tube, and two volumes of chilled 100% ethanol were added to precipitate the DNA. The tubes were again centrifuged at 14,000 RPM for 15 minutes at 4°C. After discarding the supernatant, 150 µL of chilled 70% ethanol was added to wash the DNA pellet. This was followed by a brief centrifugation at 14,000 RPM for 5 minutes at 4°C. The supernatant was carefully removed, and any residual ethanol was removed using a pipette without disturbing the pellet. Finally, molecular-grade water was added to dissolve the DNA, and the concentration was measured using a Nanodrop spectrophotometer.

Tissue Lysis Buffer (20 mL):

Tris-Cl (1 M, pH 8.0-8.5): 2.0 mL, NaCl (5 M): 0.8 mL, SDS (10% in sterile H2O): 0.4 mL, EDTA (0.5 M): 0.2 mL and Sterile dH2O: 16.6 mL

2.13.2 Alu-LTR quantitative PCR

To quantify the integration of HIV-1 in CD4+ T cells, nested Alu-LTR quantitative PCR was performed as previously described [112]. Briefly, DNA was isolated from infected CD4+ T cells 48 hours post-infection, 6/8 days post-infection, and from a negative sample (uninfected) using the phenol chloroform. Integrated DNA was pre-amplified using 50 nM Alu forward primer, 150 nM HIV-1 LTR reverse primer, 25 µL PCR Master Mix (2X) (ThermoFisher), and 200 ng DNA in 50 µL reactions. Cycling conditions were: 95°C for 8 min x 1 cycle, followed by 18 cycles of 95°C for 1 min,

52°C for 1 min, and 72°C for 3 min. A second round real-time TaqMan quantitative PCR was performed using the pre-amplified DNA. These samples were run alongside a standard curve of known dilutions of infected Jurkat cells containing integrated HIV-1 DNA. Reactions contained 0.5 μM Alu forward primer, 0.5 μM Alu-LTR2 reverse primer, 0.15 μM probe, 10 μL 2x TaqMan Gene Expression Master Mix, and 2 μL of 1:20 diluted pre-amplified DNA. Cycling conditions were: 50°C for 2 min, 95°C for 15 min x 1 cycle, followed by 45 cycles of 95°C for 15 s, and 60°C for 1 min. Reactions were performed using a QuantStudio real-time PCR system. Below is the list of primers used:

ALU-FW: AAC TAG GGA ACC CAC TGC TTA AG

LTR1-RV: TGC TGG GAT TAC AGG CGT GAG

LTR2-RV: TGC TAG AGA TTT TCC ACA CTG ACT

ALU- Probe: FAM—TAG TGT GTG CCC GTC TGT TGT GTG AC—TAMRA

2.14 RNA extraction

Total RNA was extracted from latent infected jurkat cells stimulated with IL-2 or anti-CD3CD28 Abs and treated with AUY922, DMSO for 48h using the RNAeasy kit following the manufacturer's instructions. $2X10^5$ cells were collected from cell culure and washed in PBS. 380 μL of RLT buffer was added and mixture was vortexed very well with pipetting. One volume of 70% ethanol was added, the lysate was mixed, loaded onto an RNaesy spin colum and centrifuged for 30 second at 13000 rpm. The flowthrough was disposed of and the column was washed with 700 μL RW buffer and

500 µL RPE buffer twice. RNA was eluted from the column using nuclease-free water and kept at -80 °C for storage.

2.15 cDNA preparation

cDNA synthesis was performed from total RNA according to the manufacturer's instructions using the SuperScript III kit (thermofisher). The reaction began by adding 1 µL of random primers (250 ng) and 1 µL of dNTP mix (10 mM) to the RNA sample, followed by the addition of 9 µL of nuclease-free water. The mixture was incubated at 65°C for 5 minutes to denature the RNA and then placed on ice for at least 1 minute, followed by a brief centrifugation. Next, 4 µL of 5× First Strand Buffer, 1 µL of 0.1 M DTT, 1 µL of RNaseOUT Recombinant RNase Inhibitor, and 1 µL of SuperScript III Reverse Transcriptase were added to the tube. The reaction was incubated at room temperature for 5 minutes to initiate primer annealing, followed by incubation at 50°C for 45 minutes for cDNA synthesis. The reaction was terminated by heating the mixture to 70°C for 15 minutes to inactivate the reverse transcriptase enzyme. The resulting cDNA was used for downstream applications.

2.16 Western Blot

$1x10^6$ cells were collected from cell culture and washed with cold PBS then incubated with 1X RIPA buffer and a protease inhibitor cocktail for 30 minutes on ice. Samples were centrifuged for 20 minutes at 4 ^oC ,≥8000 x g and the cell lysate was stored at -20^o C. Cell lysate diluted in 6X SDS buffer and 12 µl of cell lysate loaded onto a Mini-PROTEAN TGX Stain-Free Precast gel (4-20 %) (Bio-Rad). Samples were run

for 1 hour at 120V, the proteins were transferred to a 0.2 m Nitrocellulose membrane (Bio-Rad) at 25V, 2.5A, for 7 minutes using Trans-Blot Turbo system. The membrane was blocked for 2 hours with 5% skim milk in Tris-buffered saline with Tween 20 (TBST) and incubated overnight at 4°C with the primary antibodies for TAK1, or alpha-actin diluted in 1% skim milk in TBST. The next day, the membrane was washed with TBST 3 times for 10 mins each time before incubation with the HRP-conjugated secondary antibody for 1 hour at room temperature. The membrane was washed in TBST 3 times for 10 mins each time and the signal were detected using Chemiluminescence (ECL, Thermo Scientific) following the manufactirer's instructions. Images were collected by ChemiDoc Imaging system (Bio-Rad) and analyzed by the Image Lab program.

Tris-buffered saline with Tween 20 (TBST)

150 mM NaCl, 20 mM Tris base, 0.1 % Tween 20.

2.17 Cytokine analysis

LEGEND plex assay

Supernatants from CD4+ T cells isolated from five different donors were collected on the day of cells analysis. These supernatants were then analysed for IFN-γ, IL-4, IL-17A, IL-10, and TNF-α levels using the LEGENDplex™ Human Essential Immune Response Panel Mix and Match (Cat #740932, BioLegend) following the manufacturer's protocol. The measurements were taken using a BD LSRFortessa flow cytometer, and the data were analysed with the LEGENDplex™ Data Analysis Software.

2.18 Statistical analysis

Means ± SE or SD, n, and the statistical test used are shown in the Figure legends. Statistical analyses were conducted using GraphPad Prism software. The levels of statistical significance are indicated as follows: *$p \leq 0.05$; **$p \leq 0.01$; ***$p \leq 0.001$; ****$p < 0.0001$.

Chapter 3: Screening for stimuli that induce HIV-1 reactivation from latency in a Hsp90-dependent way.

3.1 Introduction

The HIV-1 promoter, located within the LTR region, is a complex regulatory element that plays a pivotal role in the activation of HIV viral replication. This promoter region contains various DNA elements that bind specific transcription factors, including NF-kB, AP-1, SP-1, and NFAT. These interactions are critical for initiating and regulating the transcription of the viral genome in response to specific activating signals [154–156]. A well-established example is cytokine tumour necrosis factor (TNF)α, which can stimulate latently infected cells and activate viral expression through several mechanisms including: activation of NF-kB signalling pathway and upregulation of transcription factors such as NFAT [157]. Another potent activator of the HIV-1 LTR is PMA [158], which induces several signaling pathways, including the mitogen-activated protein kinase (MAPK) pathway. This activation leads to the recruitment of the AP-1 transcription factor complex to the LTR, further enhancing its activity [159]. Additionally, stimulation of the TCR triggers a kinase cascade that activates transcription factors NF-kB and NFAT. These factors translocate to the nucleus and bind to specific sites within the 5′ LTR of the HIV-1 genome, significantly enhancing the transcriptional activity of the viral promoter and driving the production of viral RNA [39].

Hsp90 is a highly conserved molecular chaperone that is responsible for folding, stabilizing, and activating a broad variety of client proteins, many of which are essential for cell growth, differentiation, and survival [160]. Hsp90 is known to play essential roles in many cellular processes, including protein homeostasis, signal transduction, and stress response [160]. Hsp90 operates as part of a large protein

complex that includes co-chaperones, such as Hsp70, and other regulatory factors that control the activity and stability of client proteins [160].

Hsp90 function is regulated through interactions with other proteins and nucleic acids as well as several post-translational changes, including phosphorylation, acetylation, and ubiquitination [119]. In addition, Hsp90 can be targeted by a variety of small molecule inhibitors that disrupt its function and lead to the degradation of client proteins [125,136]. The best characterized Hsp90 inhibitors are small compounds that antagonize the Hsp90 ATPase activity, which causes Hsp90 client proteins to become unstable and degrade. These inhibitors have shown promise as potential therapeutics for cancer and other diseases, due to their ability to target specific oncogenic pathways and to overcome drug resistance [125,136].

Our lab has shown that Hsp90 is critical for HIV-1 gene expression and reactivation from latency in CD4+ T cells [100,101] ,and that hyperthermia 39.5C (fever) enhances HIV-1 replication by an Hsp90-mediated mechanism [140]. In CD4+T cells, Hsp90 binds to IKKγ, a component of the IKK complex that regulates NF-kB. Hsp90 is required to recruit the co-chaperone Cdc37, which is important for IKK function [101]. Hsp90 inhibitors such as 17-AAG and AUY922 displace Cdc37 from the IKK complex, reduce degradation of IkBα and lower nuclear translocation of the transcription factor NF-kB (p65/p50). Ultimately, this impairs HIV-1 reactivation from latency, even after potent stimulation of the infected cells, because NF-kB is a critical transcription factor that binds to the HIV-1 LTR. These observations have been independently confirmed by other *in-vitro* and *in-vivo* studies [102,161].

HIV-1 latency is multifactorial and linked to the overall quiescence state of the infected memory CD4+ T cell. Similarly, HIV-1 exit from latency is promoted by the activation of memory CD4+ T cells [59,162,163]. Underlining the multifactorial nature of HIV-1 latency, individual LRA that target a specific pathway fail to trigger significant HIV-1 reactivation, and multi-drug interventions are more effective [164]. Thus, there is a clear rationale to develop pharmacological interventions that target multiple pathways simultaneously to either reactivate HIV-1 from latency, or repress reactivation, provided that these interventions do not perturb the overall T cell function.

In this regard, Hsp90 may be a good candidate because it is required for HIV-1 reactivation from latency, it regulates multiple cellular pathways and yet potent and selective Hsp90 inhibitors have been tested in phase II clinical trials to treat malignancies [131,132,135,165]. The favourable pharmacological properties and toxicity profile of these Hsp90 inhibitors are well known and suggest they might be repurposed to treat HIV-1 infection. Here, I have investigated which of the known HIV-1 reactivation pathways depend on Hsp90 and if selective Hsp90 inhibitors blunt HIV-1 reactivation from latency. I have used a Jurkat cell line model of HIV-1 latency for the initial screening of the Hsp90-depedent latency reversing stimuli. The results show that several known latency reactivating stimuli are Hsp90-dependent, and their activity can be blunted by small molecule Hsp90 antagonists.

3.2 Results

3.2.1 Assessing Stimuli for Activation of Latent Virus in a Jurkat Model.

In order to better understand how Hsp90 regulates HIV-1 reactivation from latency, I first sought to identify which of the pathways known to reactivate HIV-1 from latency can activate the virus in our model of latency. To address this aim, I used latently infected polyclonal Jurkat cells, established in our lab **(Figure 3.1A)**. In this model, Jurkat cells were infected with a single cycle HIV-1 vector (Δenv) pseudotyped with VSV-G that expresses a destabilized GFP from the viral promoter (LTR). Infected cells were sorted to select GFP+ cells, which were expanded for 2-3 weeks until latency (GFP- cells) was apparent **(Figure 3.1C)**. Quantitative PCR showed no loss of proviral DNA during passaging and sorting **(Figure 3.1C)**, demonstrating actual viral latency. In contrast to the well-established J-Lat model of latency [166], our model is polyclonal and therefore better represents the situation *in-vivo*, in which latently infected cells contain proviruses integrated into different chromosomal locations.

First, I started by evaluating a panel of stimuli that mimic physiological conditions. I chose twelve stimuli **(Table 3.1)** which were previously shown to reactivate latent HIV-1 in different cell models and patients' cells through different receptor engagement and different pathways such as anti-CD3/CD28 Abs (TCR stimulation) [166] , IL7 (homeostatic stimulus) [167], IL15 [168], pro-inflammatory cytokines such as TNF-α [169], IL6, and IL2 [169], PMA, ionomycin [166], FOXO-1 inhibitor [170] and TLRs agonist [171]. Because the integrated viral genome encodes GFP, viral

reactivation can be conveniently monitored by flow cytometry. I titrated each stimulant to ensure reactivation of the provirus was significant but did not reach saturation, which would affect the titration of Hsp90 antagonists [100] ,and was not toxic to cells **(Table 4.1)**.

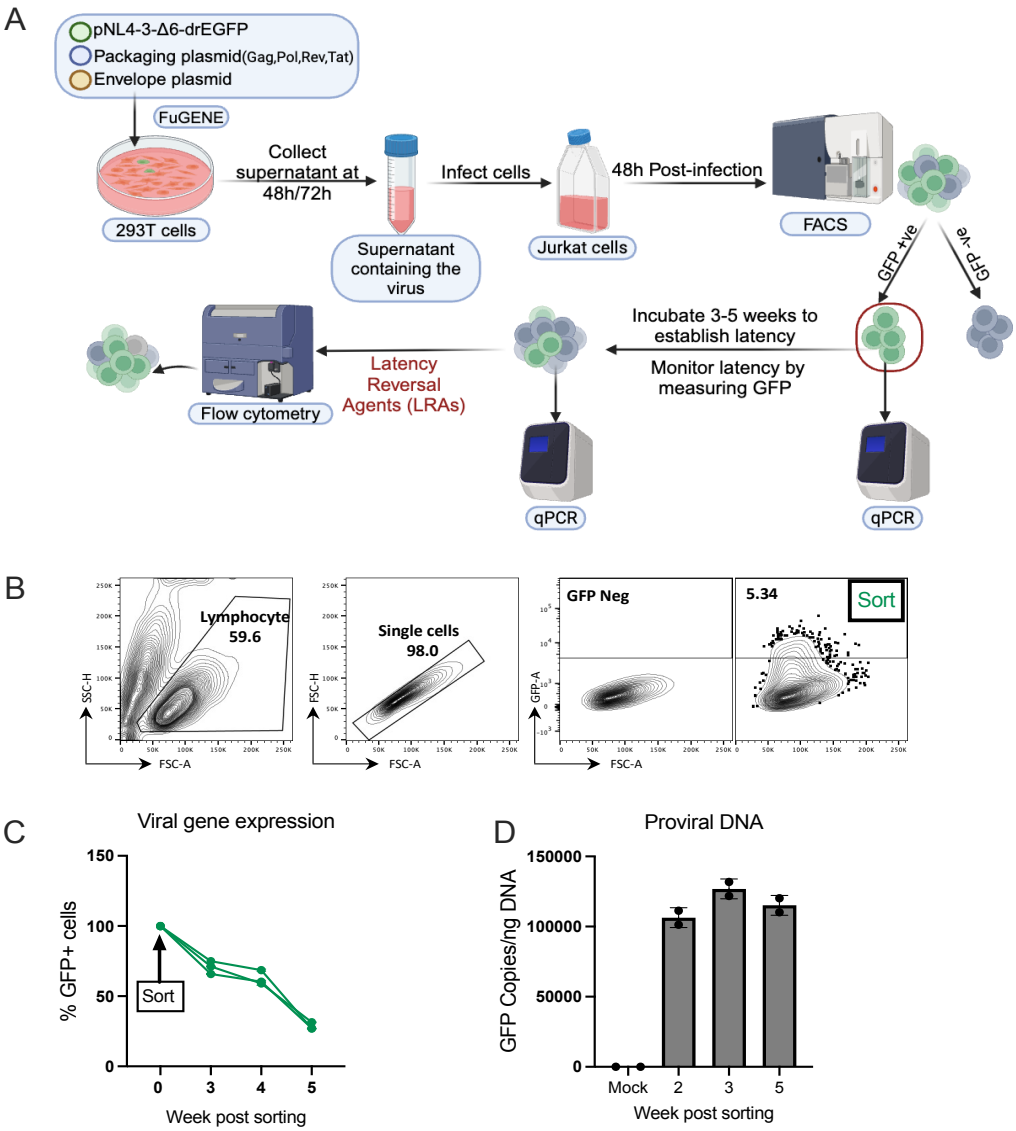

Figure 3.1: Schematic description of the generation of the latent Jurkat cell model. (A) An HIV-1 reporter virus encoding for GFP under the control of the HIV-1 promoter/enhancer (LTR) was used to differentiate between active and latently infected cells. pNL4-3-Δ6-drEGFP is an HIV-1 construct with deletions in *env* and *nef*, and contains six premature stop codons in *gag*, *vif*, *vpr*, and *vpu*. It expresses a destabilized GFP with a half-life of approximately 4 hours. The virus only allows for one round of infection. The VSV-G pseudotyped HIV-1 vector was produced by FuGENE transfection into 293T cells. The produced virus was used to infect Jurkat cells, and infection was confirmed by flow cytometry (FACS). Forty-eight hours post-infection, GFP+ (infected) cells were sorted and maintained until latent infection was established (usually at least half of the sorted GFP+ Jurkat cells becomes latent within 2-3 weeks). (B) sorting gating strategy (C) FACS analysis for GFP expression at different time points after sorting the infected cells. (D) Quantification by qPCR of proviral DNA copies (using GFP primers) in mock-infected cells and sorted GFP+ cells at different weeks post-sorting.

Table 3.1 LRAs used to reactivate HIV-1 in latently infected Jurkat cells.

Stimuli	Physiological activity	Signaling pathway	Ref.
Phorbol myristate acetate (PMA)	PKC activation	PKC/NF-kB;PKC/MAPK	[166]
Phytohaemagglutinin (PHA)	PHA binds to sugars on glycosylated surface proteins, including T cell receptor (TCR)	Lck/Calcineurin/NFAT and PKC/NF-kB	[166]
***α*-CD3/CD28 Abs**	TCR engagement	Lck/Calcineurin/NFAT and PKC/NF-kB	[166]
Ionomycin	Ca^{++} influx	Calcineurin	[166]
TLR 7 agonist (imiquimod) **TLR 8 agonist (CL75)**	The natural ligands of TLR7 and TLR8 were identified as single-stranded RNA (ssRNA), recognize ssRNA viruses	MyD88 leading to the activation of NF-kB and other transcription factors	[172]
FOXO-1 (FOXO-1 inhibitor)	Transcription factor	-Regulates metabolism (Glucose-6-phosphate, Phosphoenolpyruvate carboxykinase PGC1,Apolipoprotein C-III) -Oxidative stress (Glutathion,selenoprotein P,manganese superoxide dismutase,and peroxiredoxin III)	[170]
TNF-α	TRAF recruitment	NF-kB/AP-1	[166,169]
IL-6	Glycoprotein 130 receptor engagement	JAK/STAT; PI3K/AKT/NF-kB and PKC/MAPK	[169]
IL7	Common gamma-chain receptor engagement	JAK/STAT and PI3K/AKT/NF-kB	[166]
IL15	Common gamma-chain receptor engagement	JAK/STAT and PI3K/AKT/NF-kB	[168]
IL-2	Cell surface receptor complex consisting of IL2 R alpha/CD25, IL-2/IL15 R beta, and the common gamma-chain/IL-2R gamma subset	JAK1, JAK3/STAT/ AKT/ MAPK	[166,169]

Table 3.2. Concentrations of compounds used to reactivate latent HIV-1 in Jurkat T cells.

LRA	Conc. 1	Conc. 2	Conc. 3	Conc.4	Conc. 5	Ref. For first conc.
PMA	[10ng/ml]	[3ng/ml]	[0.9ng/ml]	[0.27ng/ml]	[0.08ng/ml]	[158]
PHA	[10 µg/ml]	[3 µg/ml]	[0.9 µg/ml]	[0.27µg/ml]	[0.08µg/ml]	[166]
***α*-CD3+** ***α*-CD28**	3µg/ml 4µg/ml	1µg/ml 2µg/ml	0.3µg/ml 1µg/ml	01µg/ml 0.5µg/ml	0.03µg/ml 0.25µg/ml	[166]
Ionomycin	[1µg/ml]	[0.1µg/ml]	[0.01µg/ml]	[0.001µg/ml]	[0.0001µg/ml]	[166]
TLR7 agonist	[5 µg/ml]	[3 µg/ml]	[1 µg/ml]	[0.2µg/ml]	--------	[172]
TLR8 agonist	[5 µg/ml]	[3 µg/ml]	[1 µg/ml]	[0.2µg/ml]	--------	[172]
FOXO-1 inhibitor	[200nM]	[150nM]	[100nM]	[50nM]	[25nM]	[101,170]
TNF-α	[5 ng/ml]	[1.5ng/ml]	[0.45ng/ml]	[0.135ng/ml]	[0.04ng/ml]	[101]
IL-6	[20ng/ml]	[6ng/ml]	[1.8ng/ml]	[0.54ng/ml]	[0.16ng/ml]	[169]
IL7	[20ng/ml]	[6ng/ml]	[1.8ng/ml]	[0.54ng/ml]	[0.16ng/ml]	[173]
IL15	[20ng/ml]	[6ng/ml]	[1.8ng/ml]	[0.54ng/ml]	[0.16ng/ml]	[166,168]
IL-2	[20ng/ml]	[6ng/ml]	[1.8ng/ml]	[0.54ng/ml]	[0.16ng/ml]	[166]

3.2.1.1 PMA.

PMA is a chemical compound often used to achieve maximal activation of latent proviruses in CD4 T cells [159]. PMA has the ability to strongly activate protein kinase C (PKC), an enzyme that is essential for intracellular signalling cascades. PKC

affects the kinase Raf, which in turn causes the activation of ERK [174]. A variety of downstream targets are then activated by ERK. The PKC pathway also activates the NF-kB pathway by inducing IKK-dependent phosphorylation and IκBα degradation. As a result, free NF-kB may bind and translocate to locations within the HIV-1 LTR enhancer region [174]. This was shown to promote HIV-1 activation from latency [166,175,176].

To test the effect of PMA in our model of latency, cells were treated with increasing concentrations of the compound, or DMSO as control, and analysed by flow cytometry 24 hours after treatment. HIV-1 reactivation from latency may result in de-novo viral gene expression in cells in which the provirus was previously silent, or in greater viral gene expression in those cells in which the provirus was already active at low levels. Therefore, for greater accuracy, HIV-1 reactivation needs to be evaluated by measuring both the percentage of GFP+ cells and the levels of expression of GFP by calculating the mean fluorescence intensity (MFI).

PMA induced significant HIV-1 reactivation from latency above background in a dose-dependent way as detected by both the percentage of GFP+ cells **(Figure 3.2C)** and the GFP MFI **(Figure 3.2D)** with no impact on cell viability as measured by the viability dye (LIVE/DEAD™ Fixable Blue Dead Cell Stain Kit) **(Figure 3.2E)**. To determine if treatment with PMA also induced cell activation, surface expression of CD69, an early CD4+ T cell activation marker [177,178] was measured by flow cytometry in parallel. As expected, PMA stimulated CD69 surface expression in a dose-dependent way **(Figure 3.2F-G)**. These results agree with previous studies showing that PMA potently reactivated latent HIV-1 in cell lines and primary cells

[166] and demonstrated that our polyclonal latency model was responding as expected.

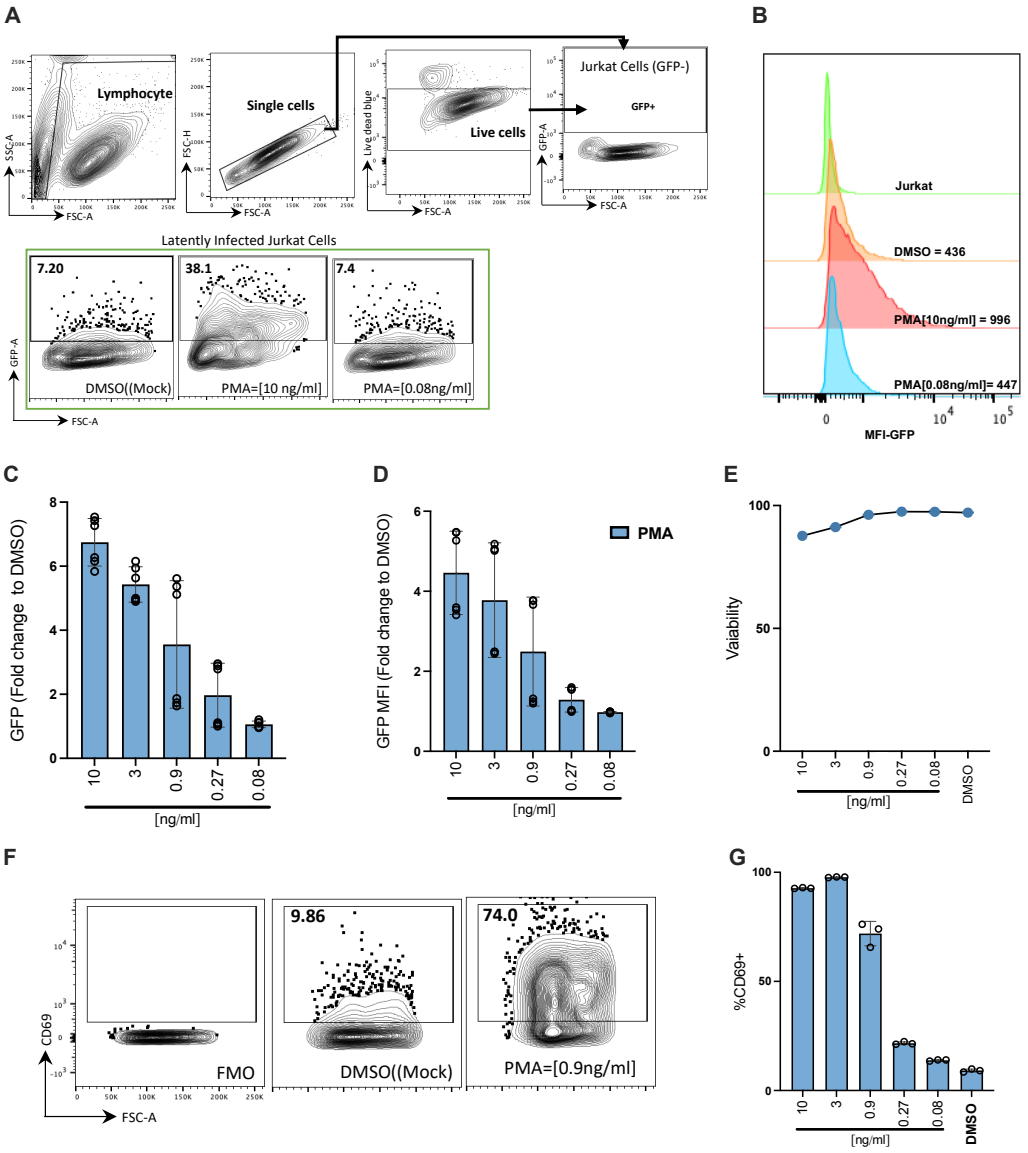

Figure 3.2. Titration of PMA to reactivate HIV-1 in latently infected Jurkat cells. (A) Gating strategy; latently infected Jurkat cells were activated with five different concentrations of PMA [10, 3, 0.9, 0.27 and 0.08 ng/ml] or 0.1 % DMSO for 24h; figure shows an example of PMA at the highest and lowest concentrations used. The frequency of GFP+ cells was quantified using flow cytometry; lower panels, representative dot plots of untreated (DMSO) and treated latent Jurkat cells. (B) Histogram showing an example of GFP MFI measured using FlowJo software (C) Bar graphs showing GFP fold change relative to control DMSO. (D) Bar graphs showing MFI fold change relative to DMSO after exposure to the indicated concentrations of PMA. (E) Viability was measured using Live dead stain and flow cytometry used to gate on live cells. (F) Gating strategy for CD69+ cells from live cells; the figure shows an example of DMSO, TNF-α and PMA-treated samples at the indicated concentrations. (G) Bar graph showing the percentage of CD69+ cells. Bar graphs show the average values ± SD, n=6 except for panels E and G where n=3.

3.2.1.2 TCR activation (PHA, anti-CD3/anti-CD28).

Phytohemagglutinin (PHA) is a plant-derived lectin that is commonly used to activate T cells. It has the capacity to attach itself to certain carbohydrate molecules found on T cell surfaces. These carbohydrates molecules, such as TCRs, function as PHA receptors [166]. By attaching to the carbohydrate receptors on the surface of T cells, PHA cross-links them, which then stimulates signalling cascades leading to calcineurin and NFAT activation, as well as PKC stimulation leading to NF-kB activation.

Anti-CD3 and anti-CD28 Abs are monoclonal antibodies [179] that mimic natural signals that T cells receive during antigen recognition and co-stimulation, leading to T cell activation, proliferation, and cytokine production. Anti-CD3 Abs specifically bind to the CD3 complex associated with the TCR on the surface of T cells while anti-CD28 bind to the coreceptor CD28 to stabilize the signal [180].

Upon TCR engagement, the immunoreceptor tyrosine-based activation motifs (ITAMs) on the cytosolic side of the TCR/CD3 complex is phosphorylated by lymphocyte protein tyrosine kinase (Lck), which allows ZAP70 to be recruited and become activated. Linker for T cell activation (LAT) is a transmembrane adaptor protein that ZAP70 phosphorylates, causing the recruitment of several adaptor and effector molecules as well as the creation of the LAT signalosome. LAT binds to and activates Phospholipase C1 (PLC1) [181], which in turn causes the paracaspase MALT1 and the CARD domain proteins CARMA1 and BCL10 to bind and activate TRAF6. The ubiquitin-ligase TRAF6, in turn, ubiquitinates and activates transforming-growth-factor- β-activated kinase-1 (TAK1) [181,182] , which regulates both the NF-kB pathway by activating the IKK complex, and the mitogen-activated protein kinase (MAPK) pathway. The MAPK causes actin polymerization and the activation of the transcription factors FOS, JUN, and activator protein complex 1 (AP-1) through JNK or ERK [183] **(Figure 3.3).**

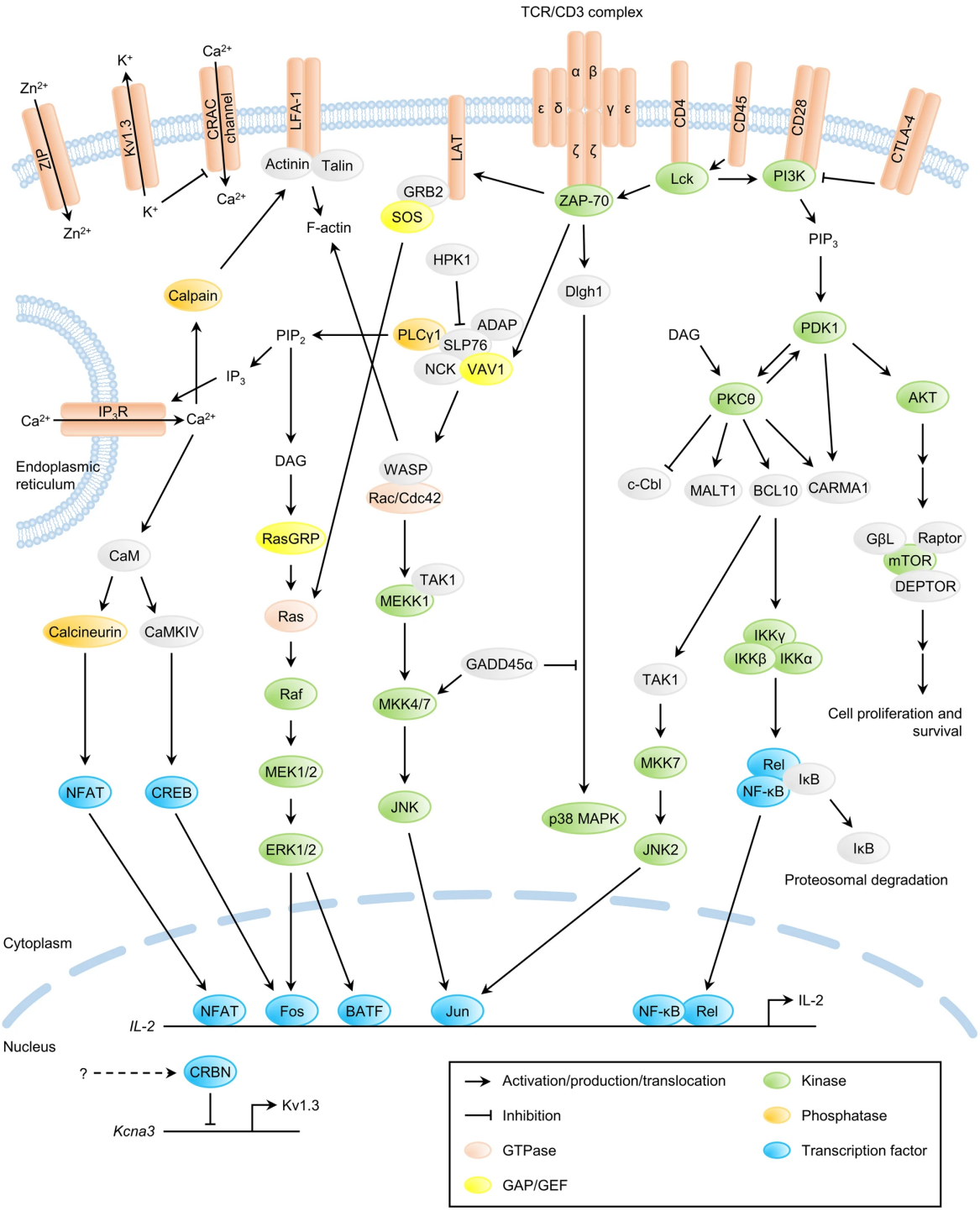

Figure 3.3. Overview of T cell receptor signaling cascades. Taken from Hwang et al. 2020 [181]

It has been demonstrated that the administration of anti-CD3/CD28 Abs or PHA on its own can activate T cells and trigger cytokine production, which can promote a setting that is favourable for HIV-1 reactivation from latency [166,180,184].

The activity of PHA or anti-CD3/CD28 Abs was therefore tested in our latency model to see if they can induce HIV-1 reactivation. To test the effect of PHA in our model of latency, cells were treated with increasing concentrations of the compound, or DMSO as control, and analysed by flow cytometry 24 hours after treatment. PHA induced significant HIV-1 reactivation from latency above background in a dose-dependent way as detected by both the percentage of GFP+ cells **(Figure 3.4A)** and the GFP MFI **(Figure 3.4B)**. To determine if treatment with PHA also induced cell activation, surface expression of CD69 was measured by flow cytometry in parallel. The result showed that PHA stimulated CD69 surface expression in a dose-dependent way **(Figure 3.4C)**. Except at the highest two concentrations used, no impact on cell viability was detected **(Figure 3.2D)**.

Next, we tested the anti-CD3/CD28 Abs for their ability to induce viral expression from latent state. Tissue culture plates were coated with increasing concentrations of anti-CD3 Ab and incubated for 30mins then cells were added to the plates along with increasing concentrations of soluble anti-CD28 Ab, or DMSO as control, and analysed by flow cytometry 24 hours after treatment. Anti-CD3/CD28 Abs induced HIV-1 reactivation from latency above background at all concentrations tested as detected by the percentage of GFP+ cells **(Figure 3.4E)** and, to a lesser extent, the GFP MFI **(Figure 3.4F)**. To determine if treatment with anti-CD3/CD28 Abs also induced T cell activation, surface expression of CD69 was measured by flow

cytometry in parallel. The result showed that CD69 expression was induced in dose-depended manner compared to control latent Jurkat cells **(Figure 3.4G)**. No impact on cell viability was detected **(Figure 3.4H).**

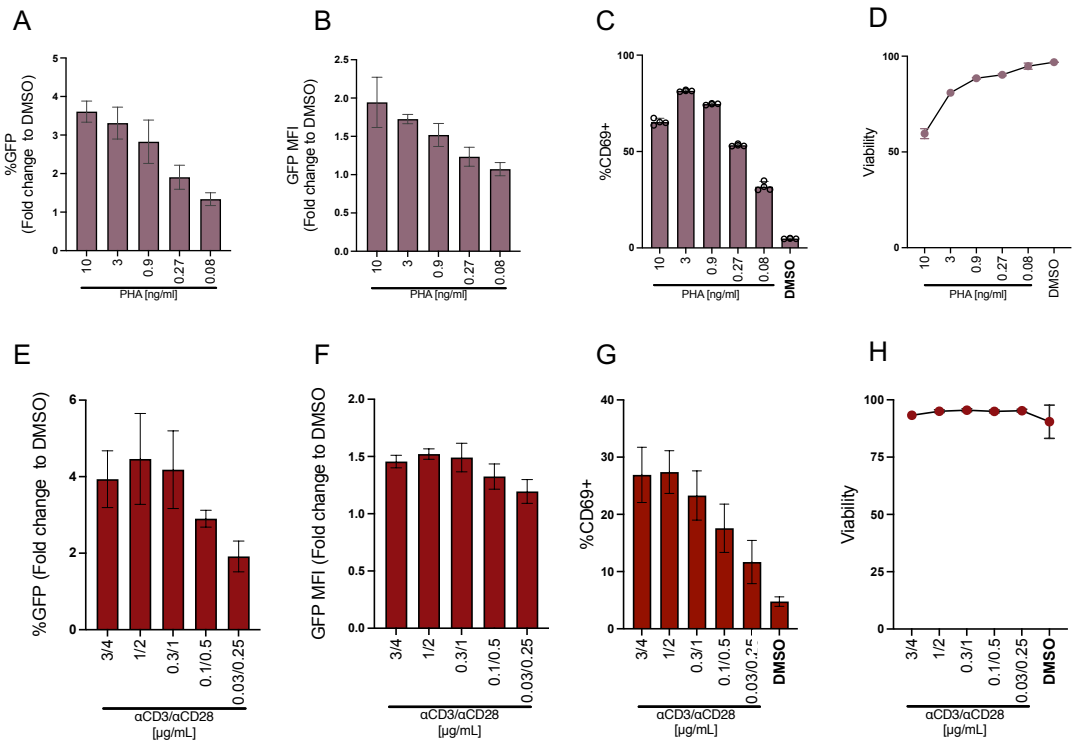

Figure 3.4. Optimization of PHA, and anti-CD3/CD28 Abs to reactivate HIV-1 in latently infected Jurkat cells. The same gating strategy shown in Figure 3.2-A was applied here. (A-D) Latent infected Jurkat cells were stimulated with different concentrations of anti-CD3/CD28 Abs for 24h then analysed by Flow cytometry (A) Bar graphs showing GFP fold change relative to control DMSO. (B) Bar graphs showing GFP MFI fold change relative to DMSO after exposure to the indicated concentration of stimulant. (C) The same gating strategy shown in Figure 3.2-D was applied to panel C, showing the percentage of CD69+ cells. (D) Cell viability was measured by Live dead stain and flow cytometry used to gate on live cells. (E-H) Laten-t infected Jurkat cells were stimulated with different concentrations of PHA for 24h then analysed by Flow cytometry (E) Bar graphs showing GFP fold change relative to control DMSO. (F) Bar graphs showing GFP MFI fold change relative to DMSO after exposure to the indicated concentration of stimulant. (G) showing the percentage of CD69+ cells (H) Cell viability. Bar graphs show the average values ± SD, n=6 except for % of CD69+ cells and viability where n=3.

3.2.1.3 Calcium ionophore activation (Ionomycin).

Ionomycin is a membrane permeable calcium ionophore which promotes the entry and exit of calcium ions (Ca2+) from cells. Ionomycin can activate the T cell bypassing TCR engagement by inducing a rapid increase in intracellular calcium levels and activate Ca2+/calmodulin-dependent signaling pathways. It induces the hydrolysis of phosphoinositides and leads to the activation of the calcineurin enzyme, which eventually activates NFAT by dephosphorylating it [185]. The HIV-1 LTR promoter region contains binding sites for NFAT. When NFAT is activated and translocated into the nucleus, it can bind to the HIV-1 LTR and enhance viral transcription and reactivation [186].

Ionomycin, in combination with PHA, is often used to study the mechanisms of HIV latency and to reactivate the latent provirus [159,186]. To better dissect the pathways for HIV-1 reactivation that might be dependent on Hsp90, PHA and Ionomycin were tested independently.

Cells were treated with different concentrations of Ionomycin or DMSO for 24 hours; then GFP expression was analysed by flow cytometry. The results showed that the highest concentrations of ionomycin [1 and 2 μg/ml] could induce a 2.5-fold increase in the percentage of GFP+ cells and the GFP MFI showed comparable results at 2 μg/ml (**Figure 3.5 A-B)**. To determine if treatment with ionomycin alone can also induce T cell activation, surface expression of CD69 was measured by flow cytometry in parallel. Similar to GFP expression, 1 and 2 μg/ml ionomycin induced CD69 expression compared to control DMSO-treated cells **(Figure 3.5C)**. T-cell activation through ionomycin relies on the accumulation of calcium ions and the

hydrolysis of phosphoinositides which could explain why the lower concentration did not activate the T cell. Of note, even though phosphoinositide hydrolysis increases with rising ionomycin concentrations, the optimal activation of T-cells occurs within a specific, narrow range of ionomycin concentrations [187]. No toxicity was detected at the tested concentrations **(Figure 3.5D)**.

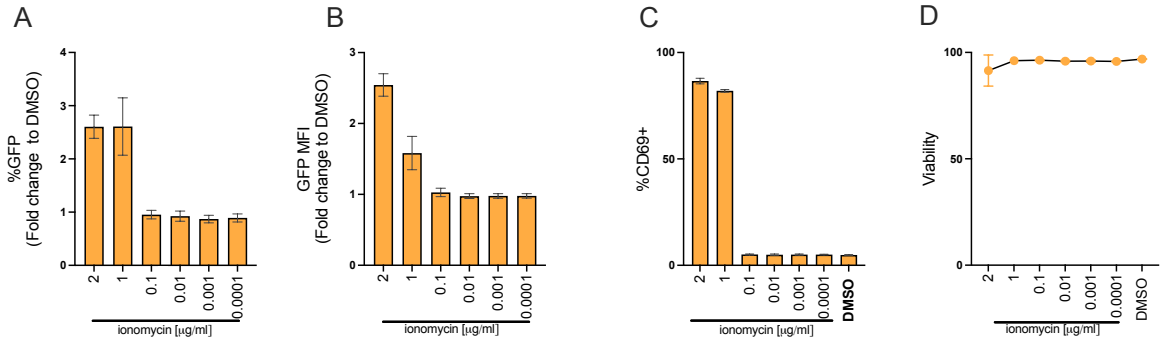

Figure 3.5. Optimization of Ionomycin to reactivate HIV-1 in latently infected Jurkat cells. The same gating strategy shown in Figure 3.2-A was used for panels A and B. Latent infected Jurkat cells were stimulated with different concentrations of ionomycin for 24h before analysis by Flow cytometry (A) Bar graphs showing the fold change in the percentage of GFP+ cells relative to control DMSO-treated cells and (B) bar graphs showing GFP MFI fold change relative to DMSO after exposure to the indicated concentration of ionomycin. (C) The same gating strategy shown in Figure 3.2-D was for panel C, which shows the percentage of CD69+ cells. (D) Cell viability was measured by using the Live dead stain and flow cytometry used to gate on live cells. Bar graphs show the average values ± SD, n=6 except for panels C and D where n=3.

3.2.1.4 Toll-like receptor 7 and 8 agonists.

Toll-like receptors (TLRs) belong to a group of pattern recognition receptors (PRRs) that have a critical function in the innate immune system's identification of microbial invaders [188]. TLRs are present on a range of immune and non-immune cells and are responsible for initiating immune responses against pathogens by detecting

common microbial molecules like bacterial lipopolysaccharide, lipopeptides, and viral and bacterial RNA and DNA [188,189]. The activation of TLRs triggers signalling pathways that lead to either the activation of the transcription factor NF-kB or the activation of mitogen-activated protein kinases p38 and JNK [184,188–190].

TLR7 and TLR8 agonists are artificial substances made to resemble the RNA structures that these receptors can identify and stimulate the receptors when they are delivered into the cells [191]. Growing evidence suggests that TLR8 activation promotes HIV-1 viral replication and latency reversal in human primary CD4+ T cells, and that CD4+ T cells can release cytokines in response to TLR7 and TLR8 ligands [191].

Here I tested whether a synthetic ligand selective for TLR7 (CL264), TLR8 (CL75) or shared between TLR7 and TLR8 (TLR7/8) (R848) can activate the latent provirus in our model. To this end, the latent Jurkat cells were treated with increasing concentrations of TLR agonists and examined HIV-1 reactivation by flow cytometry, as described. The results show that the TLR agonists tested were less potent than other stimuli and induced only a modest increase in the percentage of GFP+ cells (approximately 1-2 fold change) at the highest concentration tested **(Figure 3.6A)**. The GFP MFI showed only modest increases with the TLR7 and TLR8 agonists and no change with the TLR7/8 agonist **(Figure 3.6B)**; additionally, no increase in CD69 expression was observed relative to control DMSO **(Figure 3.6C)**. No toxicity was detected at the tested concentrations **(Figure 3.6D)**.

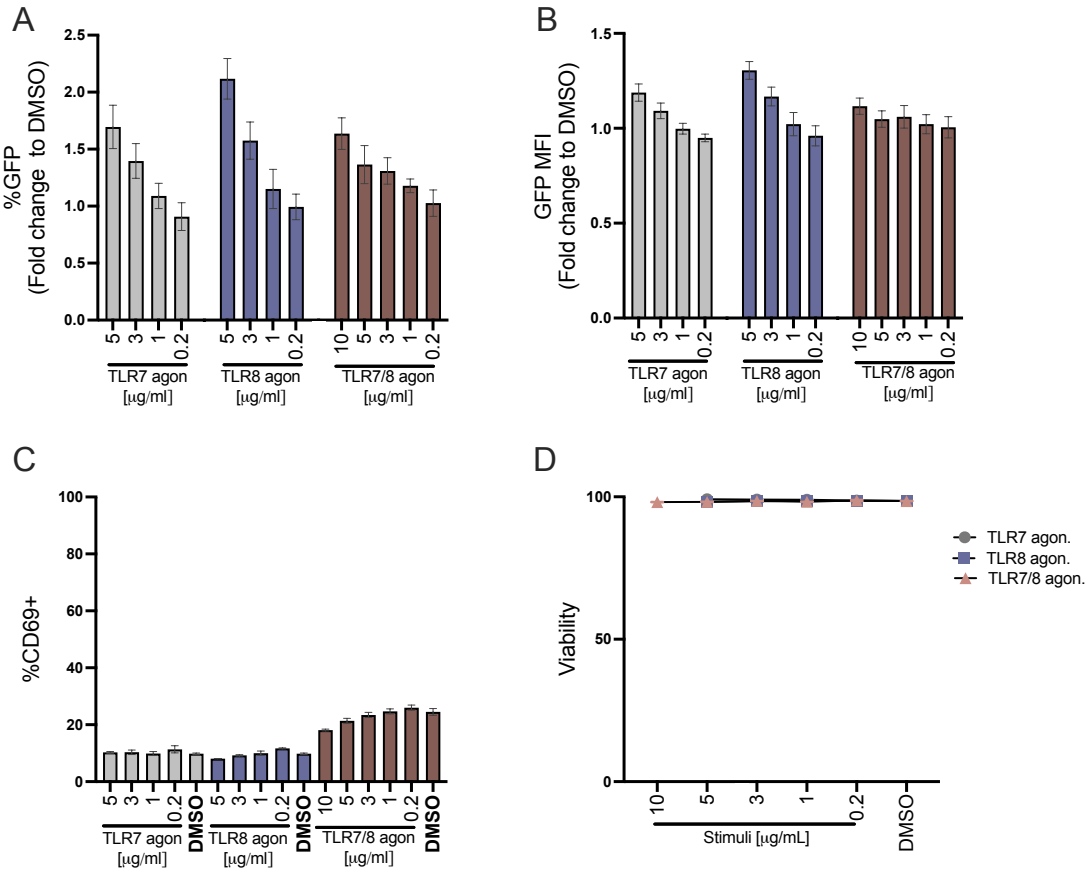

Figure 3.6. Optimization of TLR7 agonist, and TLR8 agonist to reactivate HIV-1 in latently infected Jurkat cells. The same gating strategy shown in Figure 3.2-A was applied here. (A-D) Latent infected Jurkat cells were stimulated with different concentrations of TLR7 agonist or TLR8 agonist for 24h then analysed by Flow cytometry (A) Bar graphs showing GFP fold change relative to control DMSO and (B) bar graphs showing GFP MFI fold change relative to DMSO after exposure to the indicated concentration of stimulant. (C) The same gating strategy shown in Figure 3.2-D was applied to panel C, showing the percentage of CD69+ cells. (D) Cell viability was measured by Live dead stain and flow cytometry used to gate on live cells. Bar graphs show the average values ± SD, n=6 except for % CD69+ cells, viability where n=3.

3.2.1.5 Cytokine activation (TNF-α, IL7, IL15, IL6 and IL2).

Several cytokines and cytokine combinations have been shown to reactivate latent HIV-1 [192]. Here, I tested TNF-α, IL7, IL15, IL-6, and IL-2 for their ability to reactivate the latent provirus in our latency model. Each cytokine was added at different concentrations and HIV-1 reactivation was analysed by flow cytometry. TNF-α induced a dose-dependent reactivation, with approximately 4-fold increase in the percentage of GFP+ cells at highest concentration tested relative to DMSO (**Figure 3.7A),** and the GFP MFI showed a 1.8 fold increase relative to DMSO (**Figure 3.7A).** However, TNF-α did not affect CD69 expression **(Figure 3.7A).** No toxicity was detected at the tested concentrations.

In contrast to TNF-α, IL7, IL15, IL7+15, IL2, or IL6 did not reactivate HIV-1 compared to control DMSO at any of the tested concentrations **(Figure 3.7 B-C).** No cell toxicity was observed with the tested cytokines **(Figure 3.7D).**

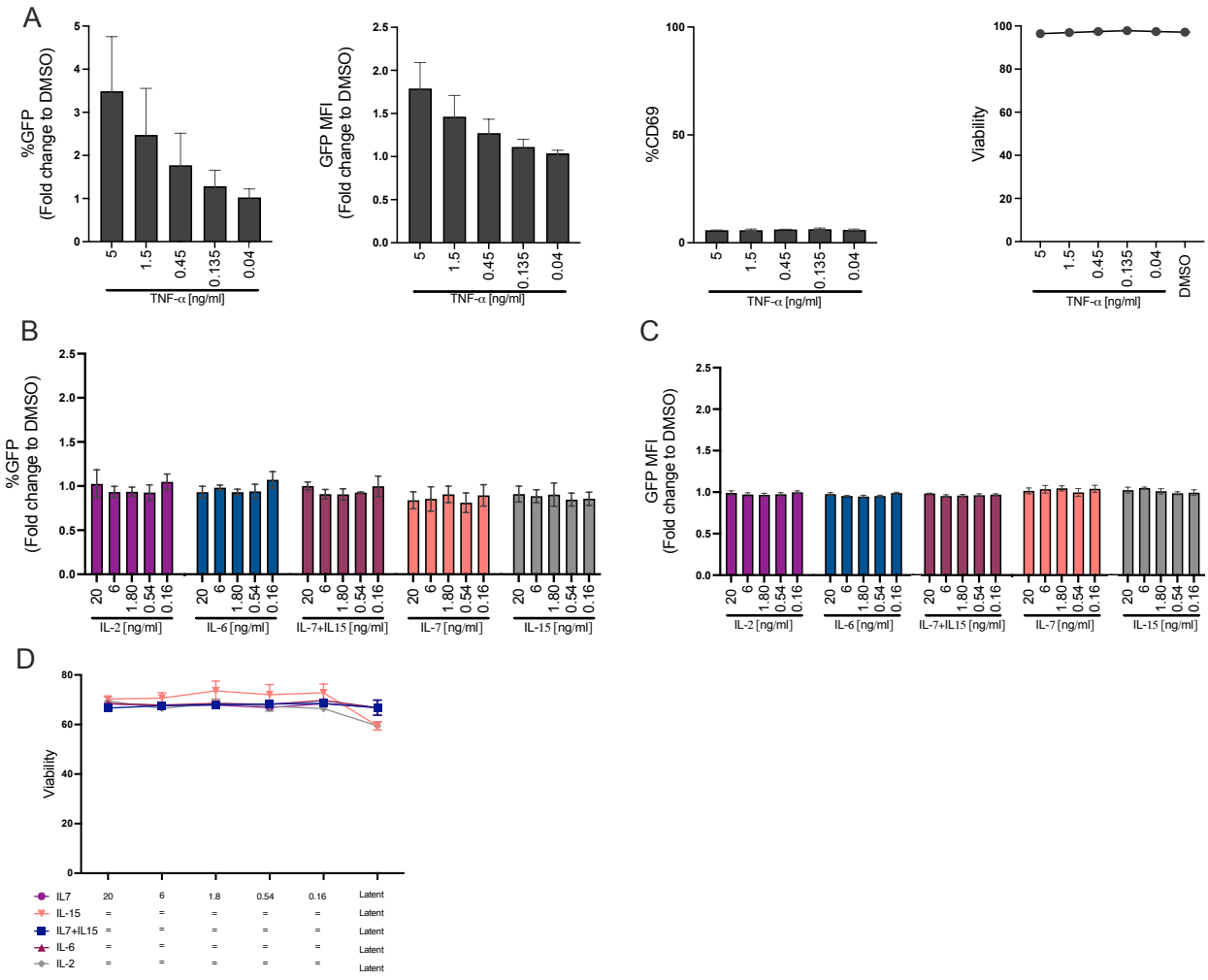

Figure 3.7. Optimisation of cytokines to reactivate HIV-1 in latently infected Jurkat cells. (A) Latently infected Jurkat cells were activated for 24 hours with different concentrations of TNF-α and analysed by flow cytometry to measure, from left to right, the percentage of GFP+ cells, GFP MFI, the percentage of CD69+ cells and cell viability using the same gating strategy shown in Fig (3.2A, D) E, n=6 for GFP and n = 3 for viability and activation markers. (B) latently infected cells were stimulated with different concentrations of IL2, IL6, IL7+IL15, IL7 alone or IL15 alone and analysed by flow cytometry to measure the percentage of GFP+ cells and (C) the GFP MFI (right panel). Bar graphs show the average values ± SD, n = 3. (D) Cell toxicity was analysed by flow cytometry using forward vs. side-scatter profiles.

IL7 have been shown to reactivate the latent provirus in other latency models [193], therefore, I asked why IL7 was inactive in our model. I speculated that it might be due to the lack of expression of the IL7 receptor (CD127) in Jurkat cells and so I used an anti- CD127 antibody to label Jurkat cells. Primary CD4+ T cells obtained by magnetic sorting from PBMCs, known to express the IL7 receptor [193] were used as control. The results indicated that Jurkat cells express much lower amounts of CD127 in comparison to primary cells **(Figure 3.8).** We therefore concluded that Jurkat cells do not express enough CD127 to obtain meaningful results and decided to repeat these experiments in primary cells (see Chapter 5).

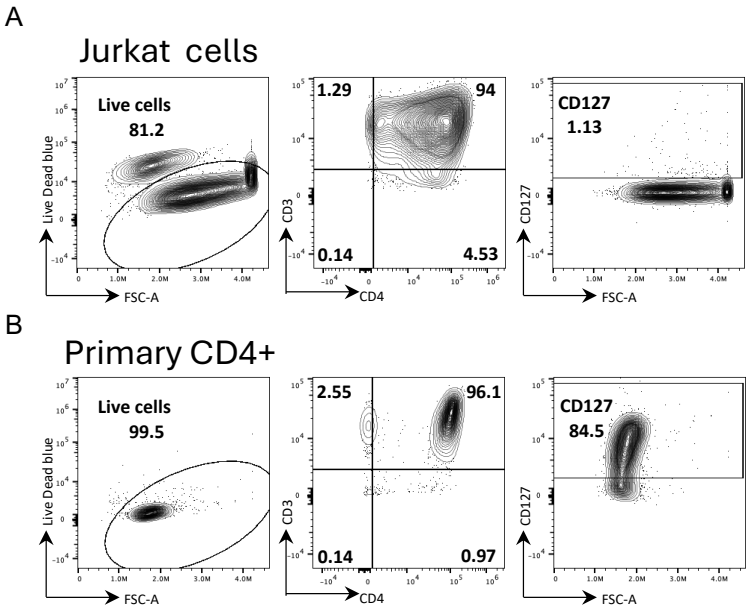

Figure 3.8: **Flow cytometry to detect CD127.** (A) Jurkat cells were stained with an anti-CD127 antibody and analysed by flow cytometry. Live cells were gated using CD3 and CD4 and CD127 was measured in CD4 T cells. (B) same as the upper panels but primary CD4+ T cells were purified from PBMCs using magnetic sorting.

3.2.1.6 FOXO-1 inhibition.

FOXO-1, also known as Forkhead Box O1, is a transcription factor that plays a crucial role in regulating various cellular processes, including cell growth, differentiation, metabolism, and stress response [170]. FOXO-1 can contribute to the maintenance of HIV-1 latency by promoting a quiescent state in infected CD4+ T cells and FOXO-1 inhibitor reactivate the latent virus in T cell [170]. In a study by Vallejo-Gracia et al, FOXO-1 inhibition caused ER stress in resting T cells, reducing the activation of transcription factor 4 (ATF4) and increasing NFAT activity. Both transcription factors contributed to HIV reactivation and were found to be associated with HIV chromatin [194–196] . Furthermore, inhibition of FOXO-1 by AS1842856 was shown to induce HIV-1 latency reactivation [170]. Hence, the effect of the same FOXO-1 inhibitor (AS1842856) in our latency model was tested.

Latently infected Jurkat cells were incubated with five different concentrations of AS1842856 for 48h then the percentage of GFP+ and CD71+ cells measured by flow cytometry. CD71 is a transferrin receptor that is upregulated when cell metabolism increases and is known to be induced by FOXO-1 inhibition in CD4 T cells [170]. In terms of percentage of GFP+ cells, the results showed that AS1842856 was capable of reactivating the latent virus approximately 2.5-fold at concentrations from 100nM to 500nM **(Figure 3.9A)**; AS1842856 also modestly increased the GFP MFI, reaching a plateau at concentrations >100 nM **(Figure 3.9B)**. However, almost 100% of Jurkat cells expressed CD71 in control DMSO samples and adding the FOXO-1 inhibitor did not lead to further increases in expression **(Figure 3.9C)**. Elevated baseline CD71 levels may be attributed to the constitutive activation of specific

metabolic pathways in Jurkat cells that have undergone transformation. AS1842856 did not seem to cause any cell toxicity at the tested concentrations **(Figure 3.9D)**.

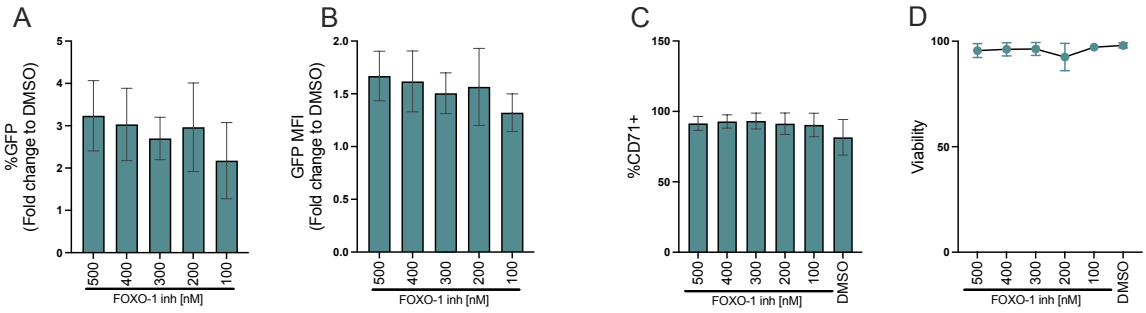

Figure 3.9. Optimization of FOXO-1 inhibitor AS1842856 to reactivate HIV-1 in latently infected Jurkat cells. The gating strategy shown in Figure 3.2A was used to collect data in panels A and B. (A) Bar graphs showing the fold change of the percentage of GFP+ cells relative to control DMSO. (B) Bar graphs showing the GFP MFI fold change relative to DMSO after exposure to the indicated concentration of AS1842856. (C) Bar graphs showing the percentage of CD71. (D) Viability measured by using the live dead stain and flow cytometry. Bar graphs show the average values ± SD, n=6 except for viability where n=3.

In summary, of the 12 stimuli that were tested, 9 (antiCD3/CD28, PMA, PHA, FOXO-1 inh, TNF-α, ionomycin, TLR7 agonist, TLR8 agonist, and TLR7/8 agonist) were able to reactivate HIV-1 in our latency model albeit to a different degree. This is consistent with previous studies that showed PMA, PHA, anti-CD3/CD28 Abs to be potent LRAs [166] whereas the other stimuli were relatively less potent [172,197] . These results demonstrated that our Jurkat latency model was able to recapitulate many physiological patthways for HIV-1 reactivation from latency.

Next, I sought to test if any of these stimuli were dependent on Hsp90. Previous work showed that stimulus saturation impacts negatively on the effect of selective Hsp90 antagonists and has a toxic effect when combined with drug treatment [101].

Therefore, for each stimulus, an optimal concentration was chosen that was both below saturation and was not toxic. Within these parameters, the most efficient stimulant was PMA, followed by anti-CD3/CD28 Abs, the FOXO-1 inhibitor, TNF-α, Ionomycin, PHA and TLR7/8 agonists **(Figure 3.9).** Whereas PMA and TNF-α have been previously shown to be dependent on Hsp90, six LRAs, namely PHA, Ionomycin, anti-CD3/CD28 Abs, FOXO-1 inhibitor, TLR7 and TLR8 agonists needed further investigation.

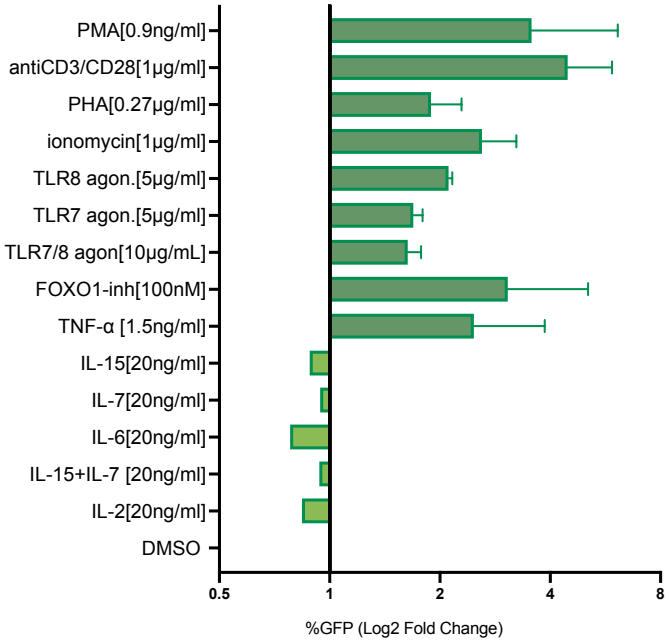

Figure 3.10. Latent HIV-1 reactivation in Jurkat cells by the different stimuli. Bar graphs showing Log_2 fold changes in the percentage GFP+ cells over DMSO (negative control) for the specified concentration of stimuli, which was not toxic and was below saturation. Bar graphs show the average values ± SD, n=2 independent experiments.

3.2.2 Identification of Hsp90-dependent pathways.

To test if the LRAs shown in Figure 3.10 were dependent on Hsp90, two selective antagonists were used: AUY922 and 17-AAG [136] **(Figure 3.11).** 17-AAG and

AUY922 are structurally different small molecules that bind to the N-term ATPase pocket of Hsp90 and compete with ATP, selectively inactivating the chaperone [101]. In humans, 17-AAG causes hepatotoxicity whereas AUY922 has a significantly better toxicity profile, its pharmacologic and pharmacodynamics characteristics are well understood, and it has been used in Phase II clinical trials mainly to treat haematological malignancies [198,199].

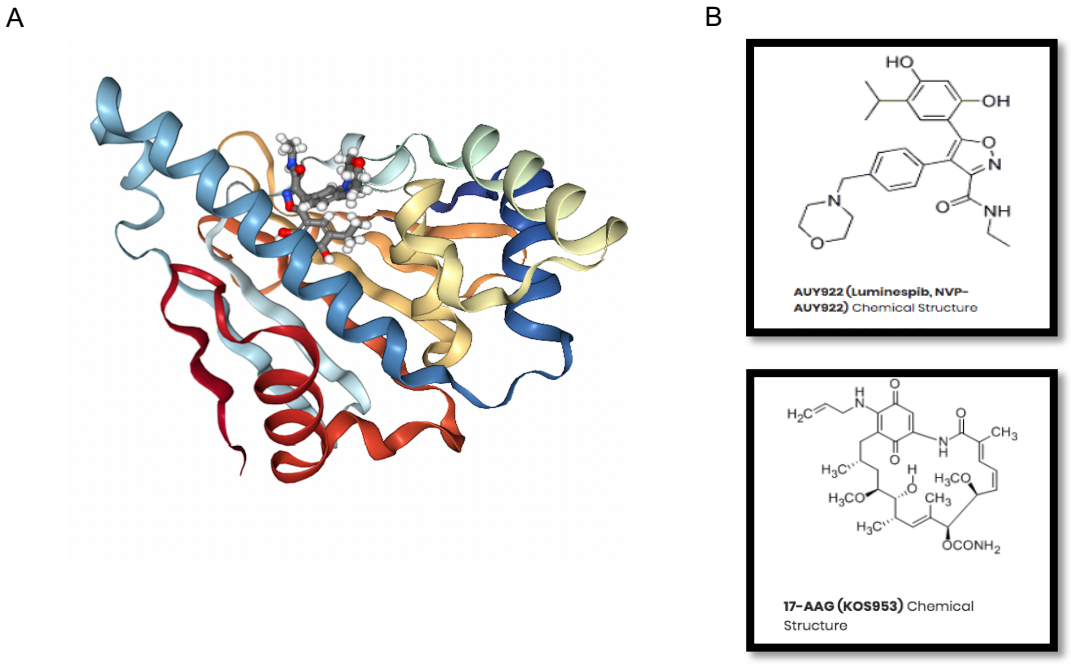

Figure 3.11 Hsp90 inhibitors bound to ATPase. (A) Crystal structure of AUY922 bound to the N-terminal ATPase pocket of Hsp90 (Protein Data Bank (6LTI). Cao, H.L. (B) Chemical structures of AUY922 and 17-AAG.

Latently infected cells were treated with a fixed concentration of stimulants for 24 hours, except for FOXO-1 inhibitor which was for 48 hours, in the presence of increasing concentrations of AUY922, or DMSO as control. Cell toxicity was assessed by flow cytometry using the Live/dead stain. Simultaneously, I measured

expression of CD69 to monitor T cell activation in the presence of TNF-α, PMA, PHA, Ionomycin and anti-CD3/CD28 Abs.

PMA robustly reactivated latent HIV-1 and AUY922 reduced in a dose-dependent way the percentage of GFP+ cells, as previously described although the effect with PHA was less marked compared to PMA and there was no effect on the GFP MFI for the latter **(Figure 3.12 A-B).** Ionomycin did not seem significantly affected by AUY922, arguing against its Hsp90 dependency **(Figure 3.12C).** AUY922 inhibited the percentage GFP+ cells after treatment with TNF-α. AUY did not reduce did not the percentage of CD69+ cells induced by TNF-α **(Figure 3.12D).** Additionally, CD69 expression triggered by exposure to PMA, PHA and ionomycin was reduced by AUY922 **(Figure 3.12A-C)**. Treatment of the stimulated cells with AUY922 did not induce cell toxicity as measured by the live/dead staining and flow cytometry (**Figure 3.12E**).

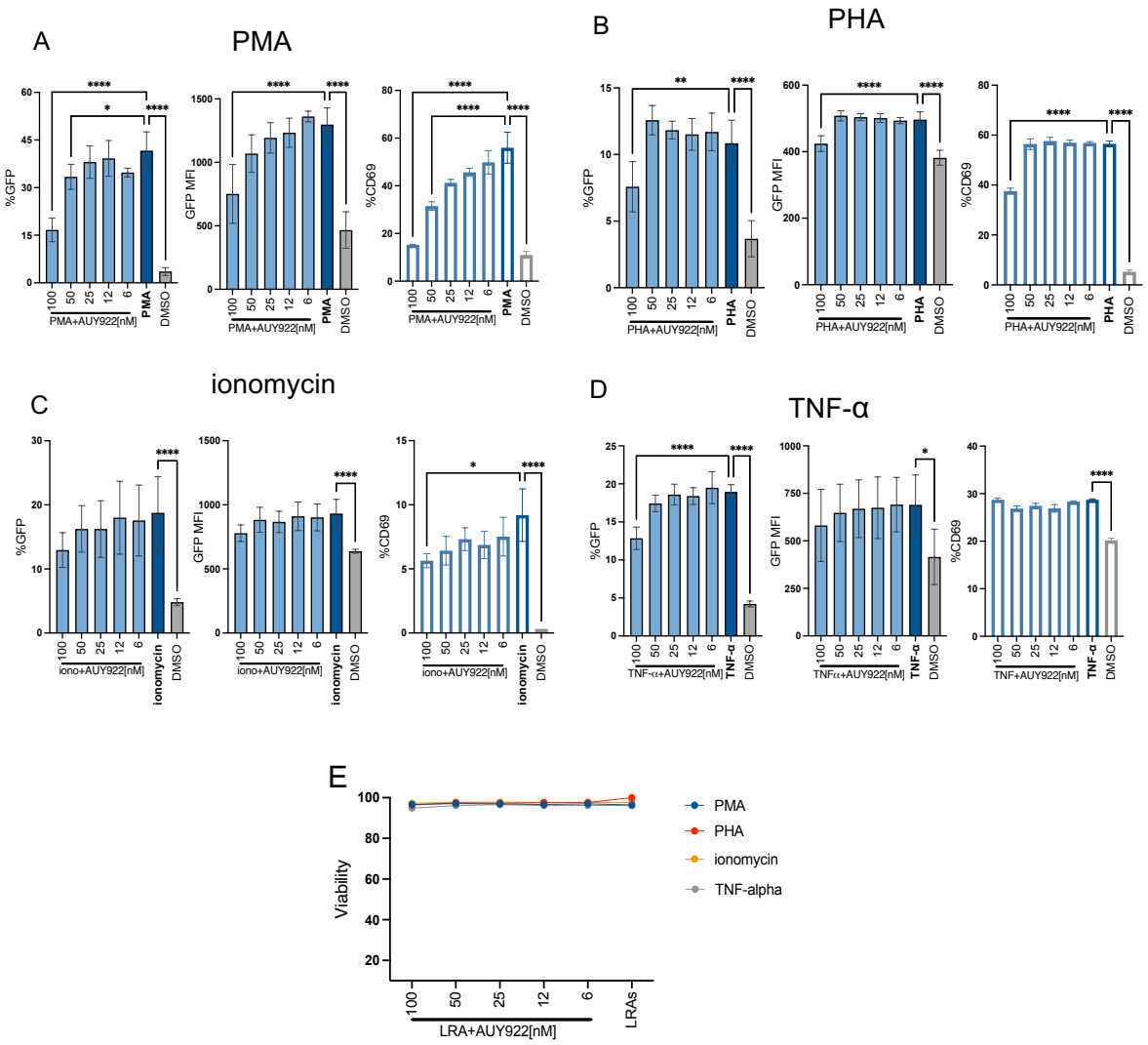

Figure 3.12. AUY922 represses HIV-1 reactivation induced by PMA and TNF-α but not PHA or ionomycin in latently infected Jurkat cells. Latently infected Jurkat cells were treated with a fixed concentration of stimulant in the presence of increasing concentrations of AUY922 for 24h and analysed by flow cytometry: stimuli used: (A) PMA [0.9 ng/ml], (B) PHA [0.3 µg/ml], (C) Ionomycin [1 µg/ml] (D) TNF-α [1.5ng/ml]. At the time of stimulation, cells were also treated with the indicated concentrations of AUY922 for 24h and analysed by flow cytometry. In (A-D), bar plots in the left panels show the average percentage ± SD (n=6) of GFP+ cells, middle panels show the average GFP MFI ± SD (n=6), and right panels show the average percentage ± SD (n=3) of $CD69^{+}$ cells. (E) Cell viability. Statistical significance was calculated using one-way ANOVA with Dunnett's correction. *=p≤0.05; **=p≤0.01; ***=p≤0.001;****=p<0.0001.

In addition, AUY922 inhibited HIV-1 reactivation induced by anti-CD3/CD28 Abs **(Figure 3.13 A)**, both in terms of percentage of GFP+ cells and GFP MFI. The TLR7, TLR8 and TLR7/8 agonists did induce moderate but significant HIV-1 reactivation and AUY922 inhibited this effect **(Figure 3.13 B-D)**. Likewise, AUY922 blunted the induction of CD69 expression induced by anti-CD3/CD28 Abs (**Figure 3.13A)**. Treatment of the stimulated cells with AUY922 did not increase cell toxicity at the tested concentrations, except for the TLR8 agonist at 100 nM **(Figure 3.13E)**.

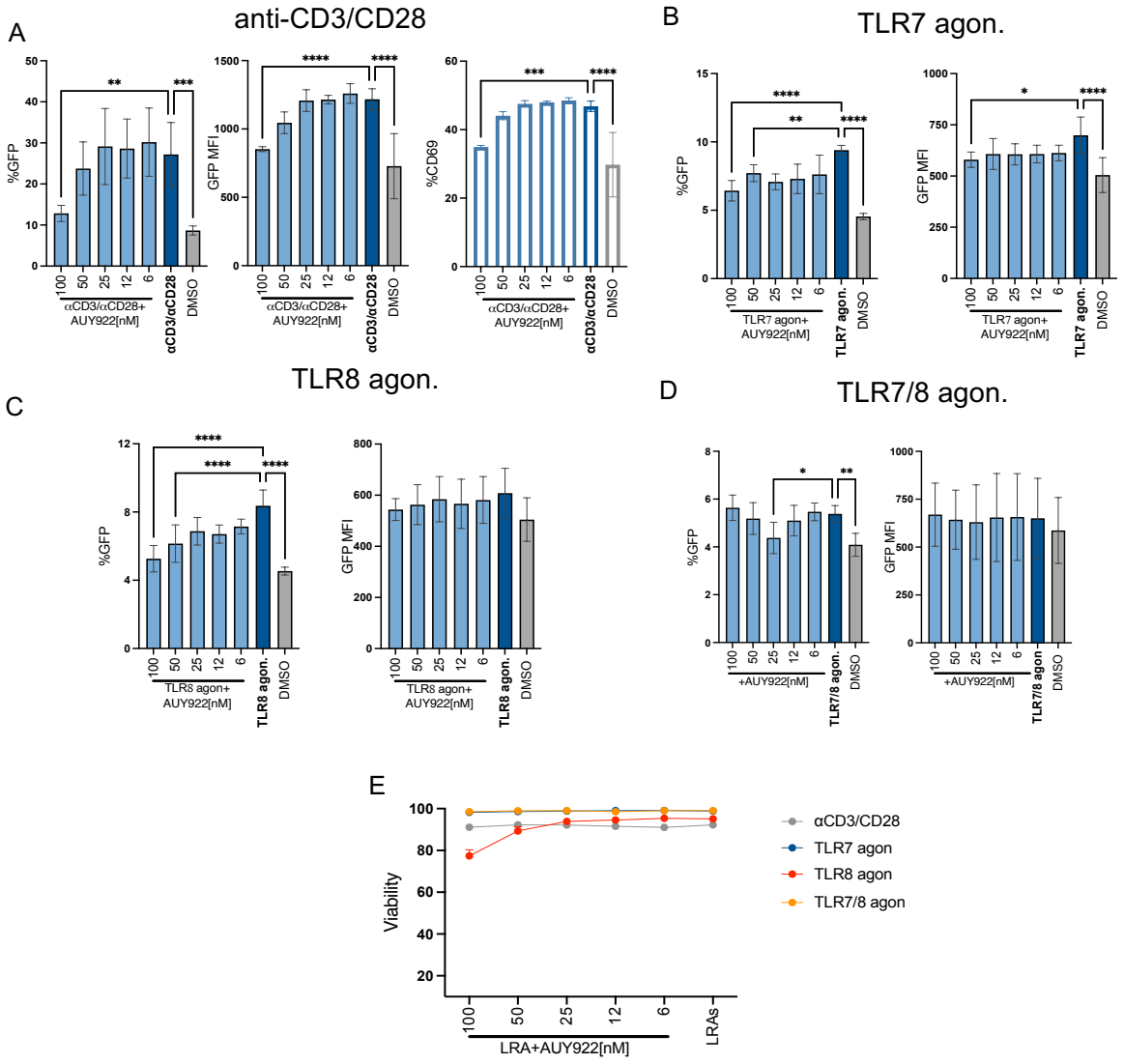

Figure 3.13. AUY922 represses HIV-1 reactivation induced by anti-CD3/CD28 Abs and TLRs agonist in latently infected Jurkat cells. Latently infected Jurkat cells were treated with a fixed concentration of stimulant in the presence of increasing concentrations of AUY922 for 24h and analysed by flow cytometry; stimuli used (A) anti-CD3 [1 µg/ml] /anti CD28 Abs [2 µg/ml]. (B) TLR7 agonist [5µg/ml], (C) TLR8 agonist, (D) TLR7/8 agonist. At the time of stimulation, cells were also treated with the indicated concentrations of AUY922 for 24h and analysed by flow cytometry. In (A), bar plots in the left panels show the average percentage ± SD (n=6) of GFP+ cells, middle panels show the average GFP MFI ± SD (n=6), and right panels show the average percentage ± SD (n=6) of $CD69^+$ cells. (B-D), bar plots in the left panels show the average percentage ± SD (n=6) of GFP+ cells, right panels show the average GFP MFI ± SD (n=6). (E) Cell viability. Statistical significance was calculated using one-way ANOVA with Dunnett's correction. *=p≤0.05; **=p≤0.01; ***=p≤0.001;****=p<0.0001.

Moreover, I tested the FOXO-1 inhibitor in the presence of different concentrations of AUY922. The results showed that AUY922 reduced HIV-1 reactivation induced by the FOXO-1 inhibitor, both in term of percentage of GFP+ cells and MFI **(Figure 3.14 A-B).** Treatment with AUY922 did not cause detectable cell toxicity **(Figure 3.14C)**.

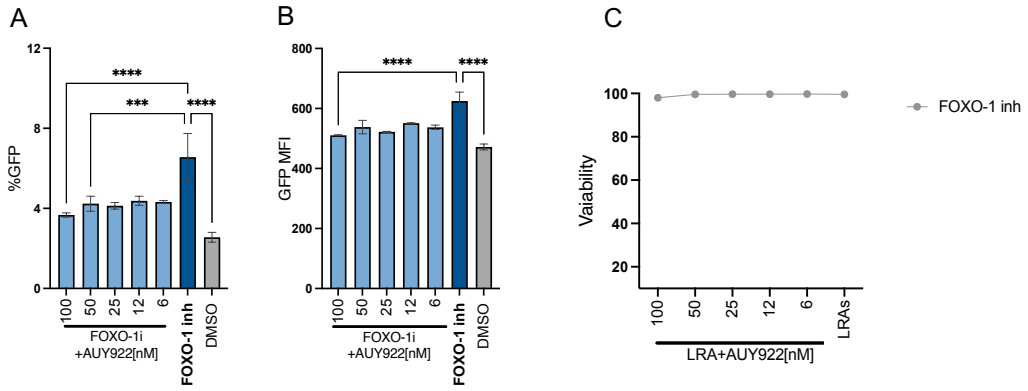

Figure 3.14. AUY922 could repress HIV-1 reactivation triggered by the FOXO-1 inhibitor in latently infected Jurkat cells. Latently infected Jurkat cells were treated with a fixed concentration of FOXO-1 inhibitor [200 nM] in the presence of increasing concentrations of AUY922 for 24h and analysed by flow cytometry; (A) Bar graphs show the percentage of GFP+ cells; (B) Bar graphs show the GFP MFI. (C) Cell toxicity was analysed by flow cytometry using the live/dead staining. Bar graphs show the average values ± SD, n=6. Significance was calculated using one-way ANOVA with Dunnett's correction, *=p≤0.05; **=p≤0.01;***=p≤0.001;****=p<0.0001

3.2.3 Specificity of Hsp90 Inhibition.

To test the specificity of the results obtained with AUY922, 17-AAG was used [200]. 17-AAG has a different chemical structure than AUY922 **(Figure 3.9)**, and it likewise inhibits Hsp90 function by binding to the ATPase pocket of Hsp90 and out-competing ATP. I examined 17-AAG ability to prevent provirus reactivation in response to the stimuli tested with AUY922. Simultaneously, I measured expression of CD69 to monitor T cell activation when applicable.

The results showed that 17-AAG repressed viral reactivation in a dose-dependent manner after stimulation with PMA **(Figure 3.15A**). Additionally, 17-AAG inhibit the reactivation by PHA, ionomycin and TNF-α **(Figure 3.15 B-D**). 17-AAG did decrease the expression of CD69 after stimulation with PHA and ionomycin **(Figure 3.15A-C**).

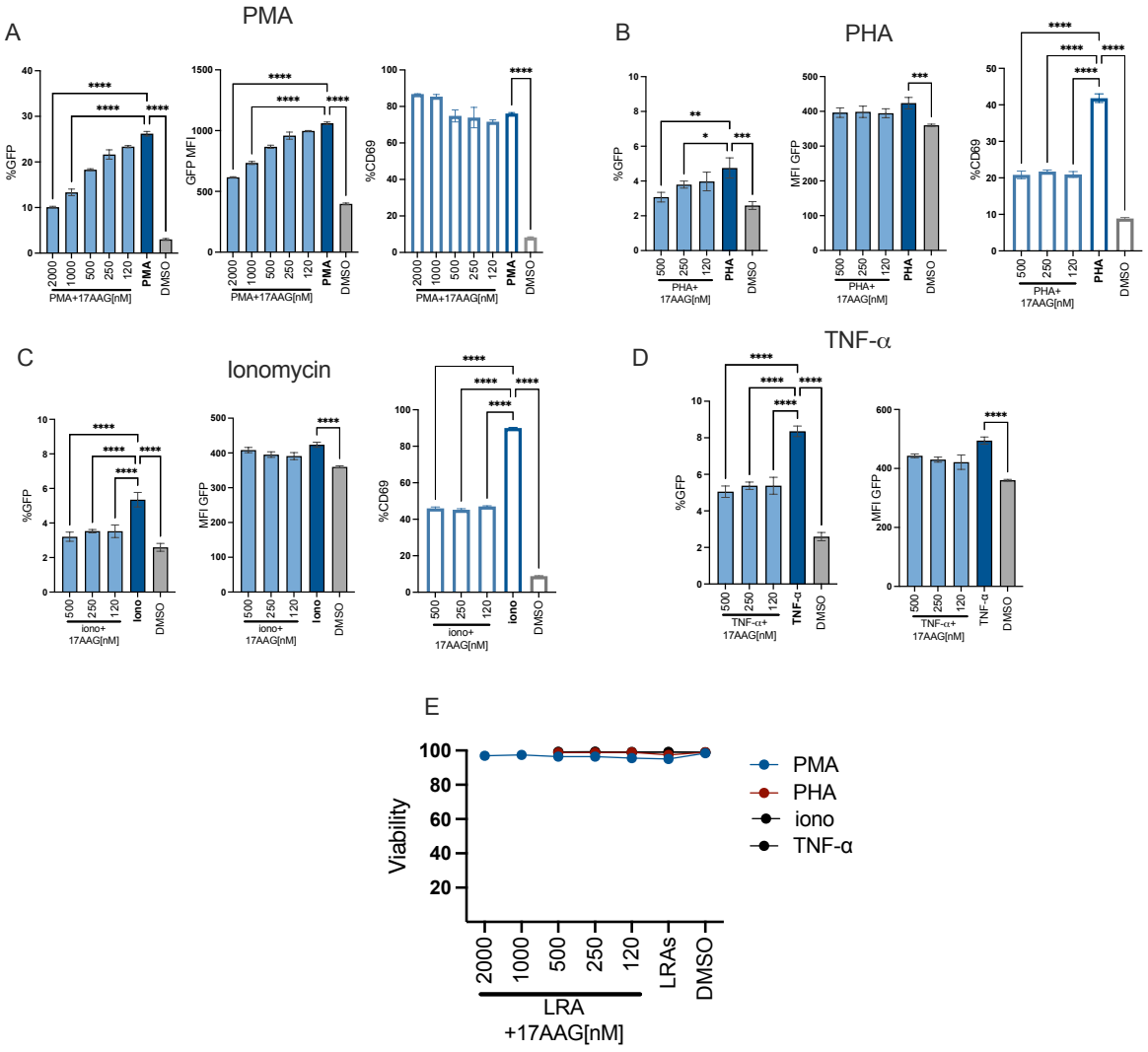

Figure 3.15 17-AAG represses HIV-1 reactivation induced by PMA, PHA, ionomycin, TNF-α in latently infected Jurkat cells. (A, B), latently infected Jurkat cells were stimulated with (A) PMA [0.9 ng/ml], (B) PHA (C) Ionomycin (D)TNF-α. At the time of stimulation, cells were also treated with the indicated concentrations of 17-AAG for 24h and analysed by flow cytometry. In (A-C), bar plots in the left panels show the average percentage ± SD (n=3) of GFP+ cells, middle panels show the average GFP MFI ± SD (n=3), and right panels show the average percentage ± SD (n=3) of $CD69^{+}$ cells. (D), bar plots in the left panels show the average percentage ± SD (n=3) of GFP+ cells, right panels show the average GFP MFI ± SD (n=3). (E) Cell viability. Statistical significance was calculated using one-way ANOVA with Dunnett's correction. *=p≤0.05; **=p≤0.01; ***=p≤0.001;****=p<0.0001.(E) Cell viability was monitored by flow cytometry using the live/dead stain.

In addition**,** 17-AAG inhibited HIV-1 reactivation induced by anti-CD3/CD28 Abs in a dose-dependent manner **(Figure 3.16 A)**, both in terms of percentage of GFP+ cells and GFP MFI. Furthermore, 17-AAG showed a better inhibitory profile than AUY922 against TLR8 agonists **(Figure 3.16 B**). with no significant cell toxicity at the tested concentrations **(Figure 3.16 E).** However, 17-AAG did not inhibit the activation by FOXO-1 inhibitor **(Figure 3.16 D)**

Taken together, the results demonstrate that Hsp90 broadly regulates HIV-1 reactivation, including that one triggered by TLR7 agonist and TLR8 agonist activation and inhibition of FOXO-1, which has not been reported before.

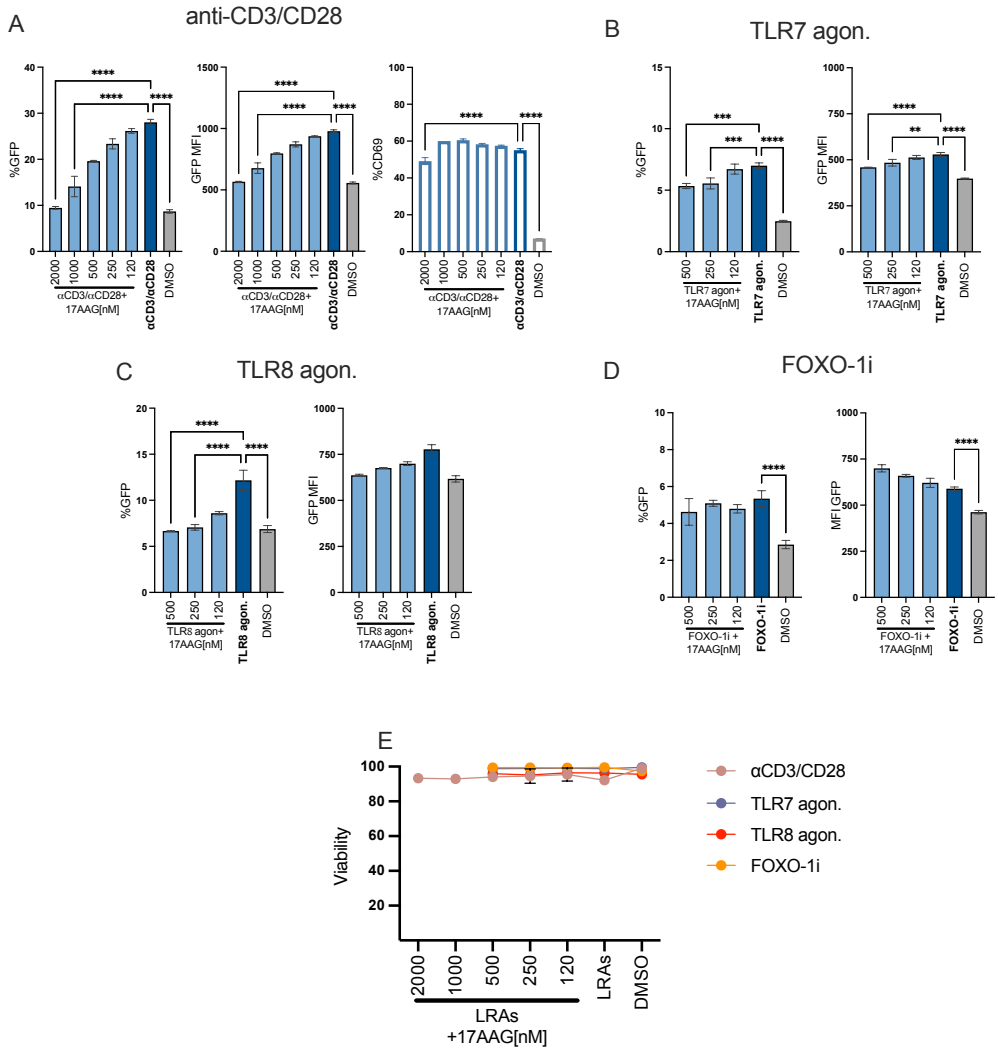

Figure 3.16 17-AAG represses HIV-1 reactivation induced by ati-CD3/CD28 Abs and TLR but not FOXO-1i in latently infected Jurkat cells. (A, D), latently infected Jurkat cells were stimulated with (A) anti-CD3/CD28 Abs (B) TLR7 agon. (C) TLR8 agon. (D) FOXO-1i. At the time of stimulation, cells were also treated with the indicated concentrations of 17-AAG for 24h and analysed by flow cytometry. In (A), bar plots in the left panels show the average percentage ± SD (n=3) of GFP+ cells, middle panels show the average GFP MFI ± SD (n=3), and right panels show the average percentage ± SD (n=3) of $CD69^{+}$ cells. (B-D), bar plots in the left panels show the average percentage ± SD (n=3) of GFP+ cells, right panels show the average GFP MFI ± SD (n=3). (E) Cell viability. Statistical significance was calculated using one-way ANOVA with Dunnett's correction. *=p≤0.05; **=p≤0.01; ***=p≤0.001;****=p<0.0001.

3.4.1 Discussion.

Previous studies demonstrated that Hsp90 is important for HIV-1 reactivation from latency, but these studies only investigated a few pathways [101,201]. HIV-1 latency depends on multiple factors that act in combination to repress, or stimulate viral gene expression [156]. Furthermore, viral latency is also linked to the quiescent state of the latently infected CD4+ T cell [202]. Conversely, activation of T cells can trigger the reactivation of latent HIV-1, which is a key challenge in curing HIV [203]. T cell stimulation tends to trigger HIV-1 reactivation via different signalling and epigenetic pathways, often working in combination [156,204]. This multi-factorial mechanism highlights the importance of identifying master regulators that can be targeted to control HIV-1 reactivation from latency, regardless of the specific stimuli that initiate it. Reactivating latent HIV-1 could potentially lead to viral eradication by enabling the immune system to clear infected cells [176,184,205].

Here I have tested the hypothesis that Hsp90 may be a master regulator of HIV-1 latency. I used different stimuli previously reported to reactivate HIV-1 from latency in models of latency and *ex-vivo* in patients' cells [156,166,196,206]. A screening was performed in a Jurkat model of latency and detected PMA, TNF-α, TCR, TLR7, TLR8, and FOXO-1 pathways to be Hsp90-dependent. Initially, I tested several LRAs on their own to confirm their activity in the Jurkat latency model and to find the optimal concentration that would reactivate HIV-1 without detectable cell toxicity. In the next step, a specific concentration of each LRA was chosen to test the activity of the Hsp90 inhibitors. This two-step approach was critical to reduce artefacts caused by saturating doses of LRAs and toxic effects.

To test the specificity of the results, careful drug titrations were performed and two inhibitors with different chemical structures but targeting the same Hsp90 ATPase pocket were tested, namely AUY922 and 17-AAG. Ideally, genetic depletion of Hsp90 could have further confirmed the specificity of the results, however it was previously shown that only a modest reduction in Hsp90 levels is compatible with cell survival [100] and the existence of various Hsp90 isoforms [119] makes the genetic experiments challenging. Nonetheless, the results based on the pharmacological approach showed that that AUY922 and 17-AAG had similar activity, and it is therefore unlikely that the observed phenotypes are due to off-target effects.

Using this approach, I confirmed the Hsp90 dependency of PMA and TNF-α for HIV-1 reactivation [101] and I identified TCR stimulation, TLR7/8 stimulation, and FOXO-1 inhibition as new Hsp90-dependent reactivation pathways. Because TCR stimulation is a more physiological stimulus than PMA or PHA, its dependence on Hsp90 may be relevant to modulate HIV-1 latency *in-vivo*. Notably, Ionomycin was not dependent on Hsp90. Ionomycin induces activation of NFAT [207], which suggests that NFAT activity is not dependent on Hsp90. These negative results further confirmed that the AUY922 activity was not due to off-target effects. TCR stimulation, PMA and PHA triggered upregulation of CD69 in parallel with HIV-1 reactivation, consistent with the notion that virus reactivation goes hand in hand with CD4+T cell activation.

Treatment with the Hsp90 inhibitors also reduced CD69 expression, suggesting that the drugs target pathways shared between HIV-1 and CD69. NF-kB is involved in

the transcriptional regulation of CD69 [208,209] and the CD69 promoter region harbours a binding site for NF-kB. When NF-kB becomes activated and translocates into the nucleus, it binds to this site within the CD69 promoter, resulting in an increase in CD69 expression [208]. Additionally, reducing the levels of CD69 expression by treatment with AUY922 might be advantageous because this marker has been shown to be induced by HIV-1 in cell-to-cell spread, promoting a resident memory-like transcriptional signature [210]. This HIV-1-induced reprogramming may shape the latent reservoir by increasing the proportion of latently infected CD4+ T cells that remain within lymph nodes, and potentially make them less susceptible to antiretrovirals [210].

The Jurkat model of latency developed in our lab is different from the well-characterised J-Lat latency model in that it is polyclonal hence more representative of the situation *in-vivo* [211]. Our polyclonal model is expected to include latently infected cells with many different proviral integration sites, and we are currently analysing the integration sites distribution in these cells. This is relevant because the site of proviral integration influences viral latency, its ability to reactivate and its response to drugs [212,213].

The screening in the Jurkat model detected TLR7, TLR8 and FOXO-1 reactivation pathways to be Hsp90-dependent. The presence of TLR7 and TLR8 receptors in T cell is controversial; while some studies found TLR7 and TLR8 receptors to be expressed in T cells [172,214–216], other studies did not confirm this claim [217] and TLR7/8 activation may be primarily triggered in monocytes or macrophages,

resulting in the production of pro-inflammatory cytokines that indirectly reactivate latent HIV-1 in infected CD4 T cells [172]. Our findings showed a moderate reactivation of HIV- compared to the other stimuli such as TCR, which could be due to the low expression of these TLR receptors. Moreover, it has been demonstrated that FOXO-1 inhibition causes HIV reactivation in CD4+ T cells [170], which is consistent with our results [194–196]. I found that the FOXO-1 inhibitor was able to reactivate the latent provirus in our model of latency in an Hsp90 dependent manner. However, more pathway analysis is needed to find which specific Hsp90 client proteins are involved in the phenotype.

Although the Jurkat model was useful to screen the Hsp90-dependency of different LRAs, it also has several limitations because it is a transformed cell line and may not fully recapitulate the behaviour of primary cells. For example, CD127, the IL7 receptor, was downregulated in Jurkat cells compared to primary cells and the Jurkat cells did not respond to most cytokine stimulation. Another limitation is that we used a modified HIV-1 vector instead of the wild-type virus. The modified single cycle virus we used is well-established and useful to study HIV-1 latency because it does not express viral proteins and therefore does not cause cell toxicity [158]. Furthermore, a single cycle virus made by cell transfection should eliminate problems related to the presence of defective proviruses that may appear to be latent but are in fact deleted or grossly rearranged. Nonetheless, our model does not have the accessory protein vpr which was found to be important for reprograming infected T cells and changing the expression of some markers of T cell activation, such as CD69 [210].

A recent study showed that the Hsp90 inhibitor tanespimycin (17-AAG) effectively suppressed HIV-1 transcription and latency reactivation in *ex-vivo* PBMCs from individuals with HIV, suggesting its potential as a therapeutic agent [143]. Hsp90 is an abundant chaperone with many client proteins [160]. Hence it will be important to focus mechanistic studies on selected key targets that are shared across different reactivation pathways.

Chapter 4: Identification of the key components of the signaling pathways that depend on Hsp90

4.1 Introduction

Hsp90 plays a crucial role in assisting a diverse array of client proteins by facilitating their proper folding, stabilization, and activation, many of which are essential components of critical cellular pathways [113,119,160] .

Client proteins often interact with Hsp90 via specific recognition motifs or sequences, which become accessible when these proteins are partly folded or unstable [119,160]. Hsp90's most important clients are those involved in signal transduction [119], which includes a range of protein kinases and transcription factors [119]. These include ligand-dependent transcription factors such as steroid hormone receptors (e.g., the oestrogen receptor), which require Hsp90 for proper folding and activation, as well as ligand-independent transcription factors like MyoD, crucial for muscle differentiation.

Hsp90 also plays a critical role in stabilizing and activating several key kinases within signaling pathways [119,123,134]. For instance, Hsp90 is important for the function of Akt (also known as Protein Kinase B), a critical player in the PI3K/Akt signalling pathway that controls cell survival and metabolism. Moreover, Hsp90 supports the activation of transcription factors such p53, which is often destabilized in its mutated form in cancer cells. Other important clients include the HIF-1α (Hypoxia-Inducible Factor 1-alpha), which is crucial for cellular response to low oxygen levels, and the TGF-β (Transforming Growth Factor-beta) receptor, which plays a significant role in cell growth and differentiation.

In the context of HIV-1, Hsp90 client proteins are essential for processes that are necessary for both latent provirus reactivation and viral replication [100–

102,117,141]. In the TCR pathway, Hsp90, along with its co-chaperone Cdc37, plays a critical role in stabilizing key kinases such as ZAP-70 [218] ,which is essential for initiating downstream signaling cascades required for T-cell activation and subsequent HIV-1 transcriptional activation. Cdc37 specifically facilitates the recruitment and stabilization of kinase clients, including IKK, further supporting pathways that regulate NF-kB activation, a key transcription factor driving HIV-1 gene expression [101]. Similarly, in the TLR pathway, Hsp90 supports kinases like IRAK4 and IKK, which are central to NF-kB activation and the regulation of immune responses [219]. Both pathways converge on transcription factors such as NF-kB, NFAT, and AP-1, which directly regulate the HIV-1 promoter within the 5′ LTR, driving viral gene expression and reactivation of latent proviruses.

The PMA pathway also plays a critical role in HIV-1 reactivation and involves Hsp90 client proteins. PMA bypasses receptor-level interactions and directly activates PKC, an Hsp90 client protein [220]. PKC activation leads to the phosphorylation and activation of downstream targets such as IKK, which drives NF-kB activation, and the MAPK pathways, including the JNK and p38 cascades, which contribute to AP-1 activation. These transcription factors, along with NFAT, regulate the transcriptional of HIV-1 within the LTR, making the PMA pathway a key mechanism for latency reactivation.

The purpose of the experiments described in this chapter is to identify common Hsp90 client proteins, specifically those involved in the TCR, PMA, and TLR pathways, and to explore their contribution to HIV-1 reactivation. This includes identifying potential targets for therapeutic intervention to disrupt latency and enhance strategies for viral eradication.

4.2 Results

4.2.1 TAK1 may regulate HIV-1 reactivation

Having established that the reactivation of HIV-1 from latency, induced by various LRAs, are dependent on Hsp90, the next step was to investigate the underlying mechanisms involved. To achieve this, I conducted an in-depth review of the literature and utilized the comprehensive list of Hsp90 interactors created by the Picard Laboratory [221]; focusing on three key signaling pathways (TCR, TLR pathways, and PMA) aiming to identify potential factors that are known to be Hsp90 client proteins and are shared across these pathways. These findings would then be experimentally validated using our latency model.

I began by exploring the TCR pathway and PMA, which share significant overlap. When T cells are activated via anti-CD3/CD28 Abs or PMA, both pathways ultimately converge at critical downstream signaling nodes **(Figure 4.1)**, particularly the activation of TAK1, an Hsp90 client protein [222,223]. Anti-CD3/CD28 Abs engage the TCR complex, triggering the activation of proximal signaling molecules such as Lck and ZAP-70, which then initiate a cascade involving LAT phosphorylation and the subsequent activation of PLC-γ1, ultimately leading to TAK1 activation [224,225]. Similarly, PMA bypasses receptor-level interactions, directly activating PKC, which also results in TAK1 activation **(Figure 4.1)**.

Once activated, TAK1 phosphorylates and activates the IKK complex (IκB kinase complex), which in turn leads to the degradation of IκB, an inhibitor of NF-kB [226]. This degradation allows NF-kB to translocate into the nucleus, where it promotes the transcription of genes involved in T cell survival, proliferation, and cytokine

production. Additionally, TAK1 activates the MAPK pathways, including the JNK and p38 MAPK cascades, which lead to the activation of transcription factors like AP-1 [181,227,228]. NFAT, which can also be activated by ionomycin in combination with PMA, is activated through a parallel pathway involving the dephosphorylation of NFAT by calcineurin [185] **(Figure 4.1)**. NFAT, NF-kB, and AP-1 regulate the expression of genes critical for T cell effector functions [229,230] and are key regulators of HIV-1 gene expression [39].

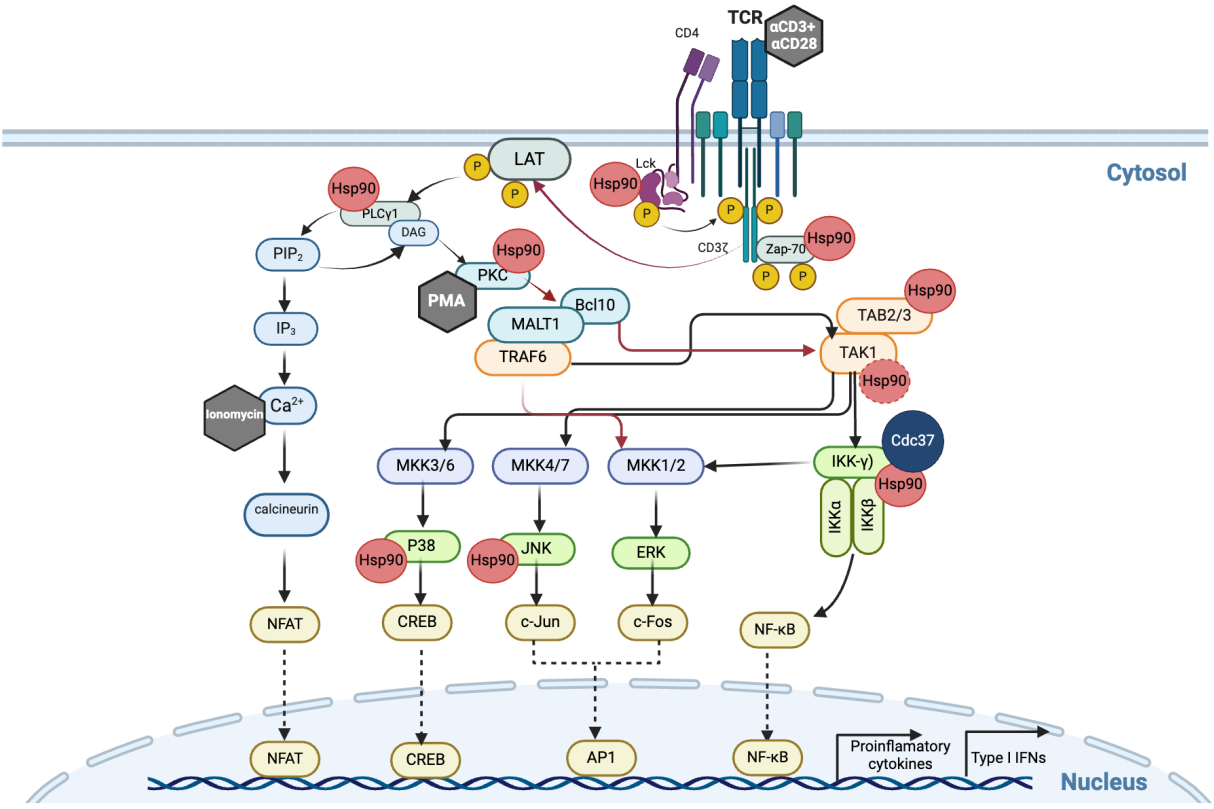

Figure 4.1 Schematic description of the TCR signal transduction pathways and the factors that are targeted by the LRAs. LRAs (grey hexagon) or that are known Hsp90 client proteins (red circles).

Despite the differences in upstream pathways, anti-CD3/CD28 Abs and PMA converge on TAK1, linking them to a similar downstream pathway that regulates the activation of several transcription factors.

TAK1 has been identified as a client protein of Hsp90 and its co-chaperone Cdc37 [221,231].The interaction between Hsp90 and TAK1 predominantly occurs through the N-terminal domain of Hsp90, which stabilizes TAK1 and protects it from proteasomal degradation [222]. This stabilization mechanism ensures that TAK1 remains functional within the cell, thereby sustaining its critical role in mediating inflammatory responses [232,233].

Interestingly, although Hsp90 maintains TAK1's stability, it is not required for the activation of TAK1 in response to inflammatory stimuli [222,229]. This suggests that Hsp90's role is more focused on preserving TAK1's structural integrity rather than directly modulating its activation. Inhibition of Hsp90 using compounds such as geldanamycin or 17-AAG has been shown to result in the degradation of TAK1, leading to diminished activity in downstream inflammatory signaling pathways [223]. To confirm previous results that TAK1 is a client protein for Hsp90, latent Jurkat cells were stimulated with anti-CD3/CD28 Abs with or without AUY922 and TAK1 protein levels were measured by Western blot **(Figure 4.2)**. The results showed that total TAK1 increased in anti-CD3/CD28 Abs only treated cells which was reduced after AUY922 treatment. These results confirm that Hsp90 is important for TAK1 and that TAK1 is a client protein for Hsp90 in agreement with the earlier reports. Given these findings, I decided to experimentally investigate whether TAK1 regulates HIV-1 reactivation.

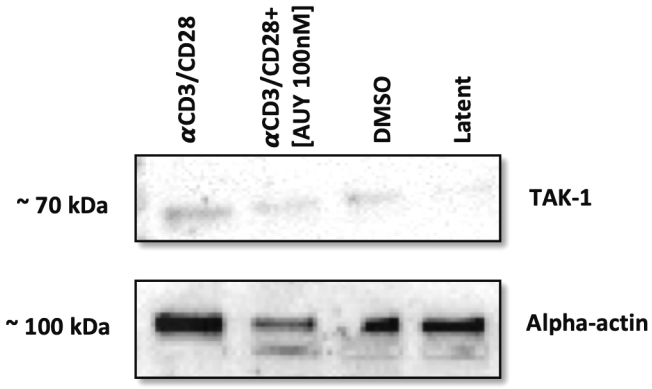

Figure 4.2. Western blot to detect total TAK1 in latently infected Jurkat cells. $1x10^6$ latently infected cells were stimulated with anti-CD3 [1μg/mL] /anti-CD28 [2μg/mL] Abs in the presence or absence of AUY922 [100nM] for 24h, then the lysate was collected for WB analysis to detect TAK1 protein/ Alpha actin (loading control).

4.2.2 Assisting the role of TAK1 in HIV-1 reactivation.

To test whether TAK1 is required for HIV-1 reactivation, I used 5Z-7-Oxozeaenol (5Z), a resorcylic acid lactone and a potent and selective inhibitor of TAK1 [234]. The mechanism of action of 5Z involves the irreversible inhibition of TAK1 by covalently modifying a cysteine residue within the ATP-binding pocket of the kinase, thereby blocking its activity [234]. Latent Jurkat cells were stimulated with a fixed concentration of PMA for 24 hours in the presence of 5Z, or DMSO as control. Cells were analysed then by flow cytometry to measure the percentage of GFP+ cells, expression of activation markers CD69 and CD25, and cell viability. Stimulation with PMA triggered viral reactivation, which was significantly suppressed by 5Z in a dose-dependent manner, as evidenced by reductions in both the percentage of GFP+ cells and GFP MFI **(Figure 4.3B-C)**. Additionally, the surface expression of activation markers CD69 and CD25 was markedly inhibited by 5Z **(Figure 4.3E-F)** and except

at the highest concentration tested, no cytotoxic effects were observed **(Figure 4.3D)**.

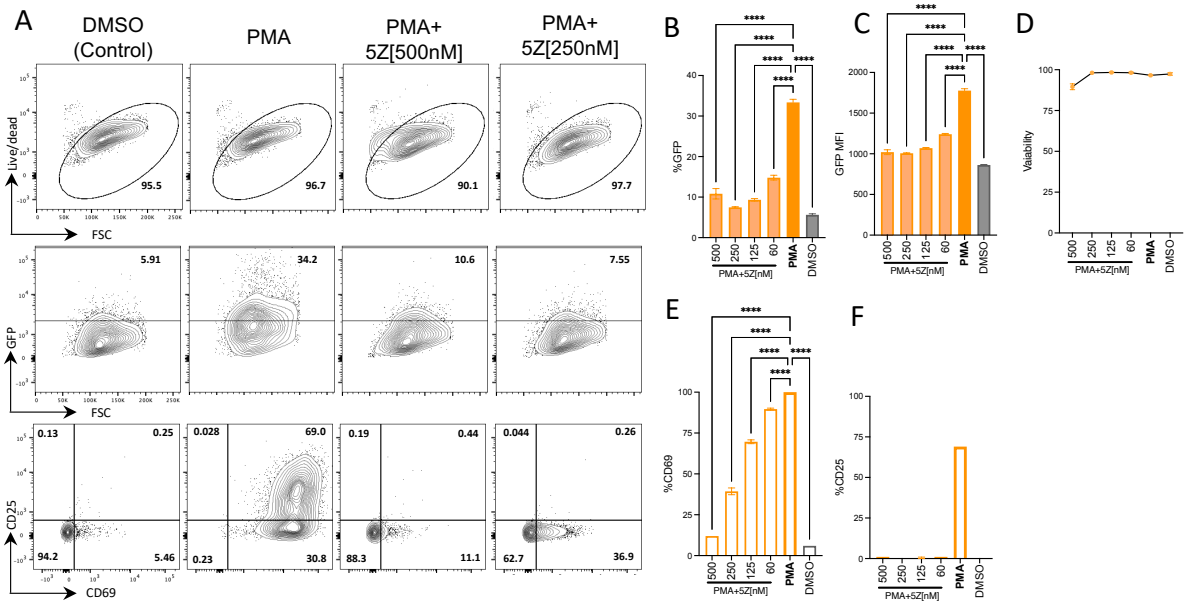

Figure 4.3. **5Z inhibits the reactivation of HIV-1 by PMA.** Latently infected Jurkat cells were stimulated with PMA [0.9ng/ml] for 24 hours in the presence of the indicated concentrations of TAK1 inhibitor 5Z and analyzed by FACS. (A) Representative flow cytometry plots for live/dead (top panels), percentage of GFP+ cells (middle panel) and CD25+ and CD69+ cells (bottom panel). (B) Bar graphs showing the average percentage ± SD of GFP+ cells, (C) Average GFP MFI ± SD, (D) Cell viability (E) average percentage ± SD of CD69+ cells, (F) Average percentage ± SD of CD25+ cells and. N = 6. Significance was calculated using one-way ANOVA with Dunnett's correction. *=p≤0.05; **=p≤0.01; ***=p≤0.001; ****=p<0.0001.

To further explore the potential of 5Z to inhibit HIV-1 in a more physiologically relevant stimuli, latent Jurkat cells were reactivated with anti-CD3/CD28 Abs for 24 hours in the presence of 5Z. The results demonstrated that 5Z effectively inhibited activation induced by anti-CD3/CD28 Abs in a dose-dependent manner **(Figure 4.4)**. This inhibition was comparable to the effects observed with AUY922 on HIV-1

reactivation, indicating that 5Z can similarly suppress HIV-1 reactivation under these conditions **(Figure 4.4)**.

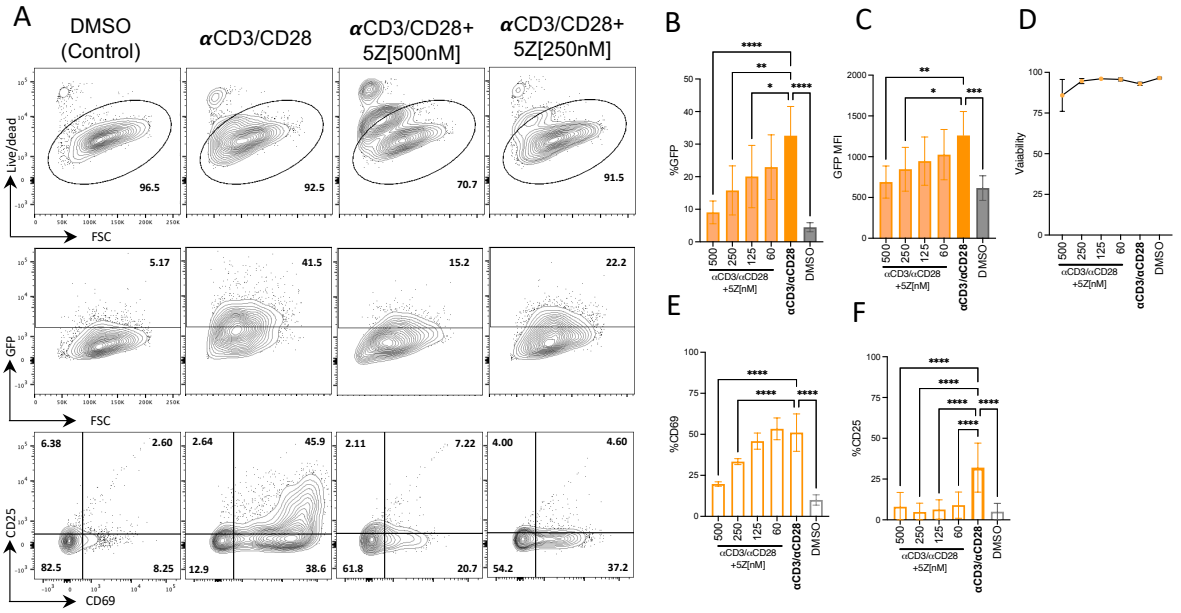

Figure 4.4. **5Z inhibits the reactivation of HIV-1 by anti-CD3/CD28 Abs**. Latently infected Jurkat cells were stimulated with anti-CD3/CD28 Abs [1µg/ml/2µg/ml] in the presence of the indicated concentrations of 5Z for 24 hours and analyzed by FACS. (A) Representative flow cytometry plots for live/dead (top panels), percentage of GFP+ cells (middle panel) and CD25+ and CD69+ cells (bottom panel) (B) Bar graphs showing average percentage ± SD of GFP+ cells, (C) average GFP MFI ± SD, (D) cell viability (E) average percentage ± SD of CD69+ cells, (F) average percentage ± SD of CD25+ cells. N = 6. Significance was calculated using one-way ANOVA with Dunnett's correction. *=p≤0.05; **=p≤0.01; ***=p≤0.001; ****=p<0.0001.

TAK1 is critical for IL-2 expression and 5Z has been reported to lower IL-2 gene transcription [235]. Therefore, to validate the specific activity of 5Z in our model, I treated the latent Jurkat cells with anti-CD3/CD28 Abs for 24h with AUY922 or 5Z and measured IL-2 mRNA by RT-qPCR. TCR engagement potently stimulated IL-2 gene expression. DMSO and AUY922 inhibited IL-2 gene expression but it is

presently unclear why DMSO should show such an effect, nonetheless 5Z at 500nM showed the greatest inhibitory activity, well above both DMSO and AUY922 **(Figure 4.5)**.

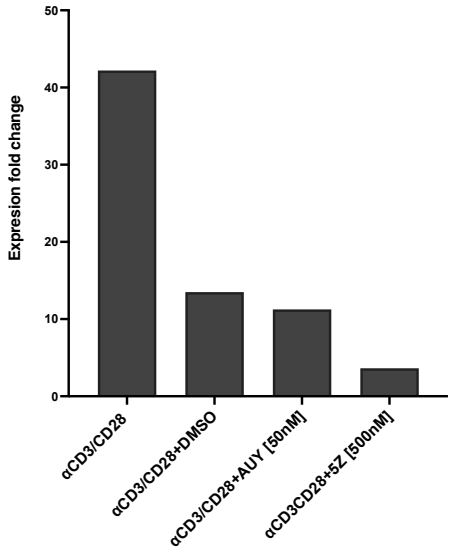

Figure 4.5. Quantitative real-time (qRT–PCR) analysis to measure changes in IL-2 mRNA gene expression fold changes relative to no treatment. Cells were stimulated with anti-CD3/CD28 Abs [1µg/ml/2µg/ml] in the presence of the indicated concentrations of 5Z, AUY922 or DMSO for 24 hour and the cells collected for RNA extraction.

4.2.3 Investigating the effect of AUY922 and 5Z on the NF-kB, NFAT and AP-1 signal transduction pathways

Next, I sought to evaluate the effects of AUY922 and 5Z on the individual transcription factors NF-kB, AP-1, and NFAT. For this purpose, I utilized triple parameter reporter (TPR) indicator cells [236], generously provided by Prof. Peter Steinberger, University of Vienna. These TPR cells are a Jurkat cell line engineered such that the response elements for NF-kB, NFAT, and AP-1 drive the expression of fluorescent proteins eCFP, eGFP, and mCherry, respectively [236]. This setup

enabled us to monitor the activation of these transcription factors simultaneously through flow cytometry. To begin, I titrated PMA, ionomycin, or a combination of PMA and ionomycin to assess their toxicity and ability to stimulate the response elements. As expected, PMA strongly activated NF-kB and AP-1, while exerting a more moderate effect on NFAT across all tested concentrations compared to the DMSO control **(Figure 4.6A).** In contrast, ionomycin alone failed to induce activation of NF-kB, NFAT, and AP-1 across all tested concentrations compared to the DMSO control **(Figure 4.6B).**

PMA and ionomycin are often used together to achieve maximal stimulation of downstream pathways, particularly NFAT. Therefore, I proceeded to test the combination of PMA and ionomycin. As expected, this combination activated all three response elements: NF-kB, NFAT, and AP-1. The combination notably enhanced the activation of NFAT and AP-1 compared to PMA alone, while NF-kB activation remained unchanged **(Figure 4.6C).**

Given that all tested concentrations of PMA were effective in stimulating the three transcription factors, the lowest concentrations were selected for further experiments with AUY922. Additionally, the highest concentration of ionomycin did not exhibit any toxic effects; therefore, this concentration was chosen for use for the combined treatment (PMA + ionomycin).

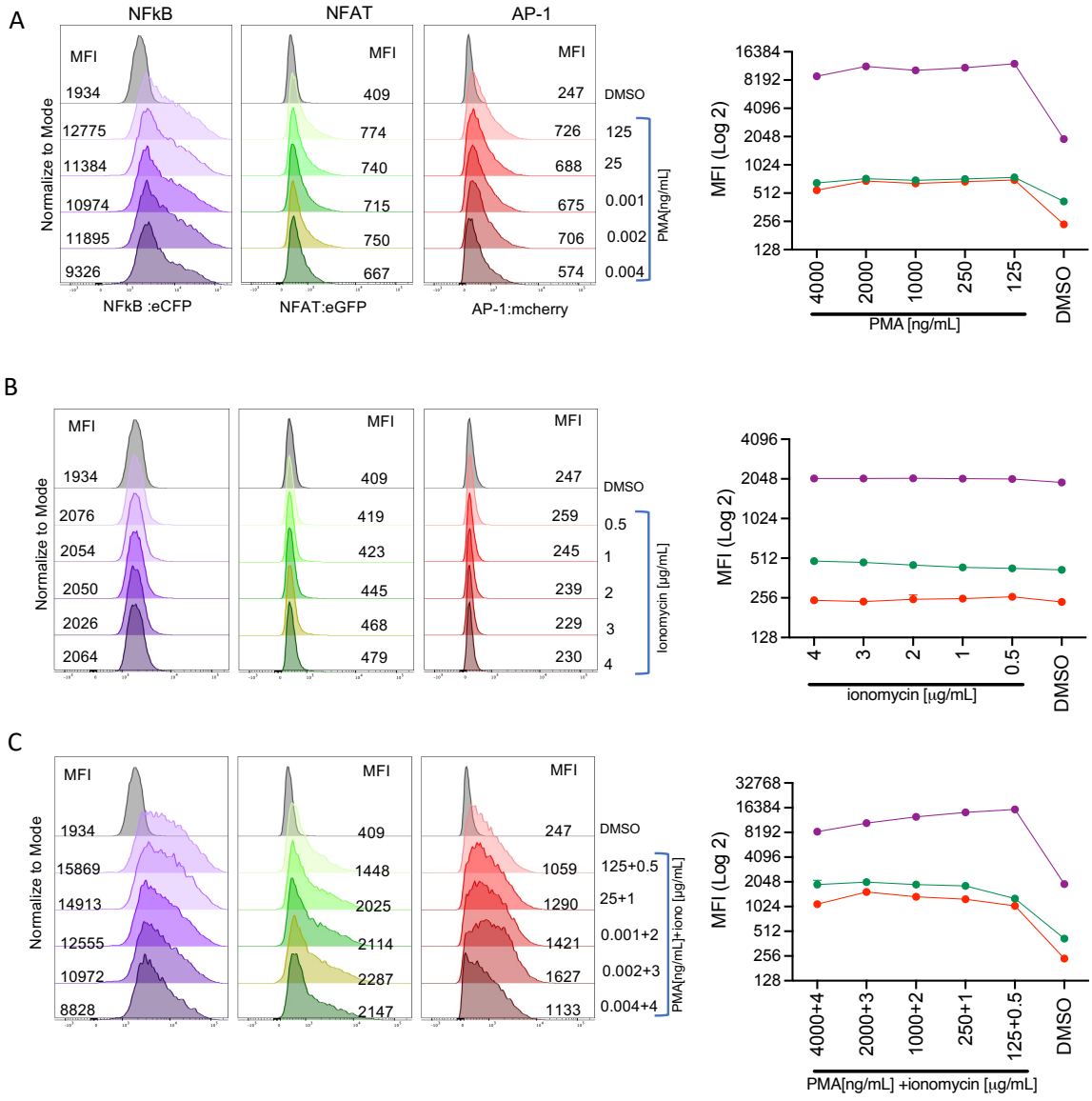

Figure 4.6. **Titration of stimuli in TPR cells**. MFI was measured by flow cytometry after stimulation of TPR cells with different indicated concentrations of (A) PMA (B) ionomycin (C) PMA+ ionomycin or DMSO (control).

Next, to investigate whether AUY922 and 5Z can influence the activation of the NF-kB, NFAT, and AP-1 response elements, TPR cells were stimulated as before with a fixed concentration of PMA **(Figure 4.7A)**, or PMA combined with ionomycin **(Figure 4.7B)** in the presence of AUY922 **(Figure 4.7C).** Flow cytometry was

performed after 24 hours to assess the results. The data revealed that AUY922 reduced in a dose-dependent manner the activation of NF-kB, AP-1, and, weakly, NFAT in cells stimulated with PMA or PMA and ionomycin **(Figure 4.7)**. These findings confirm the role of Hsp90 in the activation of several key transcription factors linked to HIV-1 latency. Interestingly, the inhibitory effect of AUY922 on NFAT was less pronounced compared to NF-kB and AP-1, with a plateau observed between 25 and 50 nM. This suggests that the activation of the NF-kB, AP-1 and NFAT pathways is not entirely dependent on Hsp90, which may account for the absence of cell toxicity at the concentrations tested.

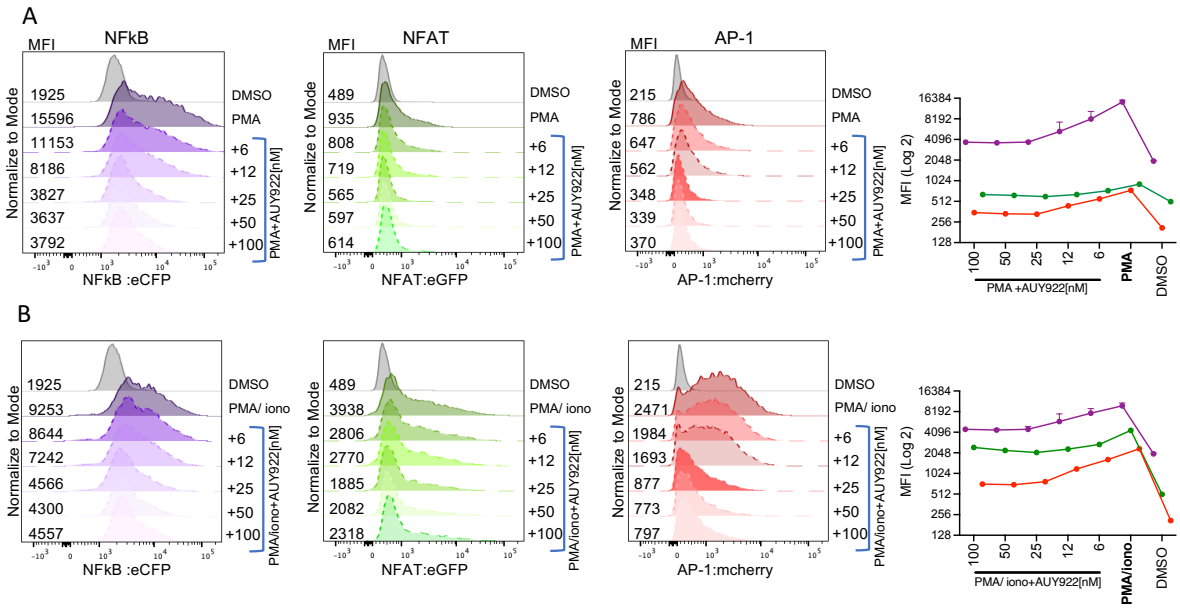

Figure 4.7. AUY922 inhibitor suppresses NFAT, NF-kB, and AP-1. MFI was measured by flow cytometry after stimulation of TPR cells with either (A) PMA [125 ng/mL] or (B) PMA [125 ng/mL] + ionomycin [4 µg/ml] in the presence or absence of different concentrations of AUY922.

I replicated these experiments in the presence of the TAK1 inhibitor 5Z and observed a dose-dependent repression of NF-kB and AP-1 activation following

PMA stimulation **(Figure 4.8)**. NFAT showed lower sensitivity to 5Z, mirroring the observations made with AUY922 **(Figure 4.7)**. Additionally, stimulation with PMA and ionomycin was significantly reduced by 5Z in a dose-dependent manner **(Figure 4.8)**. Collectively, these results suggest that the pharmacological inhibition of Hsp90 mimics TAK1 inhibition, indicating that AUY922 and 5Z share the same downstream effects, reinforcing the idea that TAK1 is a key Hsp90 chaperone involved in regulating HIV-1 reactivation.

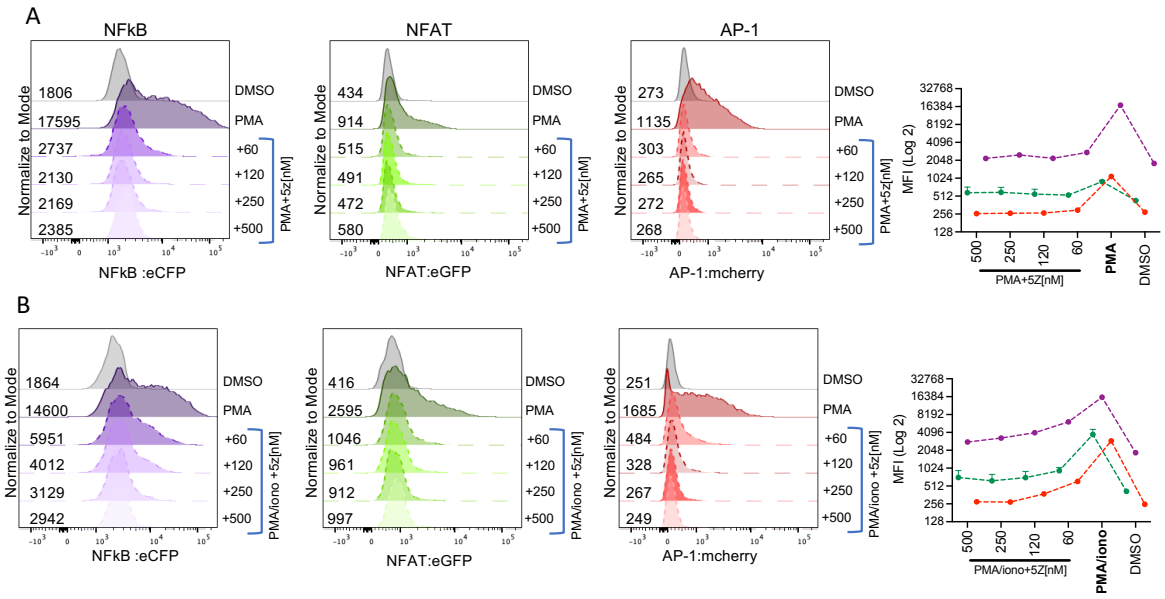

Figure 4.8. TAK1 inhibitor suppresses NFAT, NF-kB, and AP-1. MFI was measured by flow cytometry after stimulation of TPR cells with either (A) PMA [125 ng/mL] or (B) PMA [125 ng/mL] + ionomycin [4 µg/ml] in the presence or absence of different concentrations of TAK1 inhibitor (5Z).

These TPR cells lack the endogenous TCR α-chain. To evaluate the effect of TCR stimulation, we utilized a TPR derivative in which the α-chain had been reintroduced via lentiviral transduction (kind gift of Prof. Hans Stauss, UCL). I stimulated the cells with anti-CD3/CD28 Abs to assess their toxicity and ability to stimulate the response

elements **(Figure 4.9).** In these modified cells, stimulation with anti-CD3/CD28 Abs resulted in modest activation of NF-kB and AP-1, but not NFAT. This activation was slightly attenuated by AUY922 **(Figure 4.9B).** The limited response observed in these TPR cells following TCR stimulation may be attributed to incomplete reconstitution of a fully functional TCR complex. 5Z also reduced the activation of NF-kB, AP-1 and NFAT triggered by TCR stimulation **(Figure 4.9 C-D**).

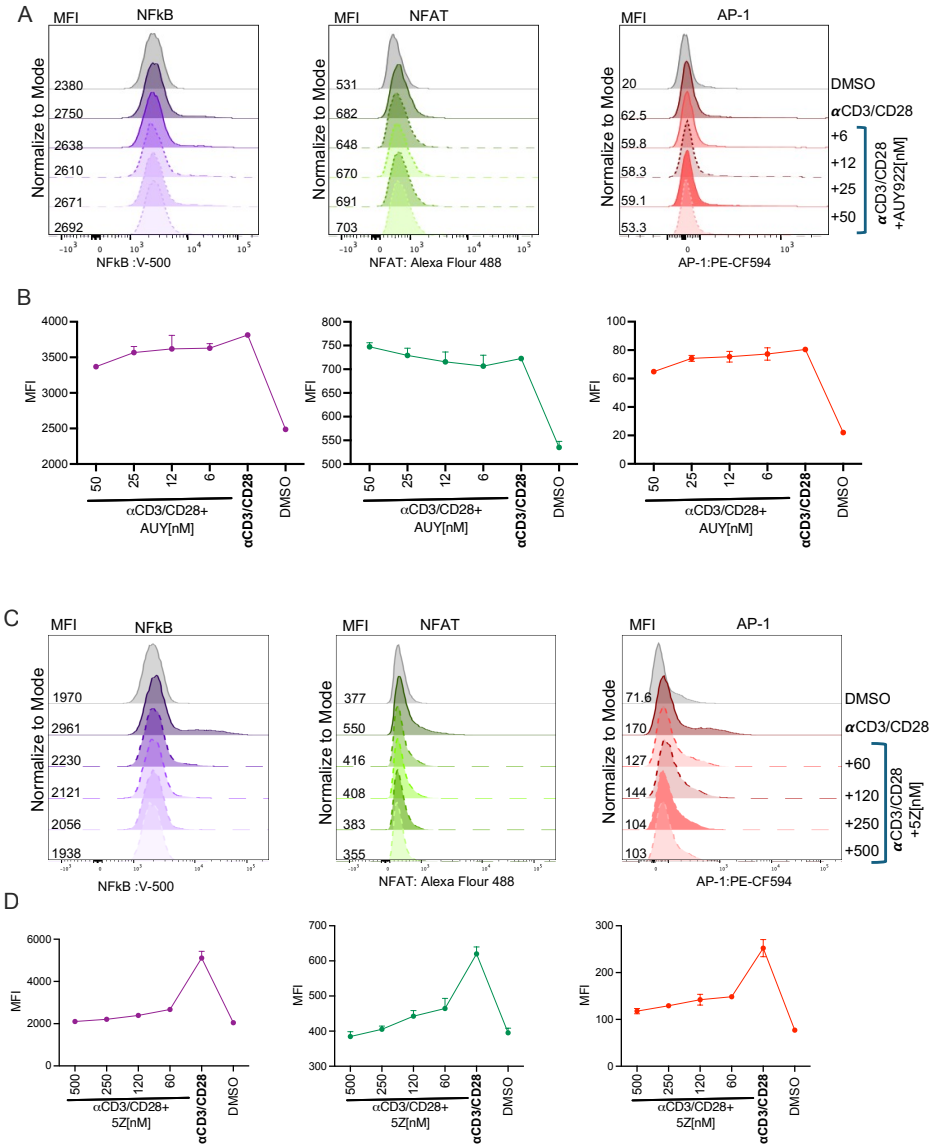

Figure 4.9 TPR cells activation with anti-CD3CD28 Abs +/- AUY922 or 5Z. TPR cells that express a reconstituted TCR were stimulated with anti- CD3 [1μg/ml]/ anti CD28 [2μg/ml antibodies in the presence of the indicated concentrations of AUY922 (A-B) or 5Z (C-D). (A) MFI was measured by flow cytometry to detect activation of NF-kB (left panel), NFAT (middle panel) and AP-1 (right panel). (B) Graph showing average MFI values ± SD for each transcription factor (n= 3). (C-D) Same as above in the presence of the indicated concentrations of 5Z.

Taken together, these results indicate that pharmacological inhibition of Hsp90 and TAK1 have a similar effect on activation of NF-kB and AP-1, supporting the idea that TAK1 is a Hsp90 chaperone that may contribute HIV-1 reactivation. However, we cannot exclude that 5Z mimicked AUY922 by a different mechanism, or by targeting other cellular factors.

4.2.4 investigate the AUY922 effect on Phosphorylation of Key Components in the TAK1 Downstream Pathway.

Next, I sought to determine if the inhibition of Hsp90 would affect the phosphorylation of key factors downstream of TAK1, specifically MAPK (p38), NF-kB (p-65), JNK(p-JNK), and ERK-1/2 (p-ERK-1/2). To investigate this, I used primary CD4+ cells isolated from the PBMCs of four different donors. CD4+ cells were pretreated with either DMSO (as a control) or AUY922 at concentrations of 100 nM or 200 nM for 1 hour, followed by activation with anti-CD3/CD28 Abs for 10 minutes. Next, cells were fixed, permeabilized, and stained with fluorophore antibodies against p-38 (pT180/pY182), p-65 (pS529), p-JNK (pT183/pY185) and p-ERK1/2 (pT202/pY204). Data were acquired on a flow cytometer and analyzed using FlowJo. The results

revealed a significant increase in p-ERK1/2 levels in cells treated with anti-CD3/CD28 Abs + DMSO compared to untreated controls. Similar results were observed for p65, p-JNK and to a lesser extent p-38. However, treatment with AUY922 for 1h did not appear to result in a significant reduction of the phosphorylation level of these molecules **(Figure 4.10)**.

These results suggest that phosphorylation of the tested signal transduction molecules may not depend on Hsp90, and this may reflect the fact that Hsp90 is important for TAK1 stability but not function [222,229]. Degradation of TAK1 is likely to take longer than 1 hour treatment with AUY922 hence the lack of detectable effects on phosphorylation of downstream molecules. However, these experiments have limitations because there was no effective positive control for the inhibition of phosphorylation, and the timing may be critical. Future work is needed to address this limitation.

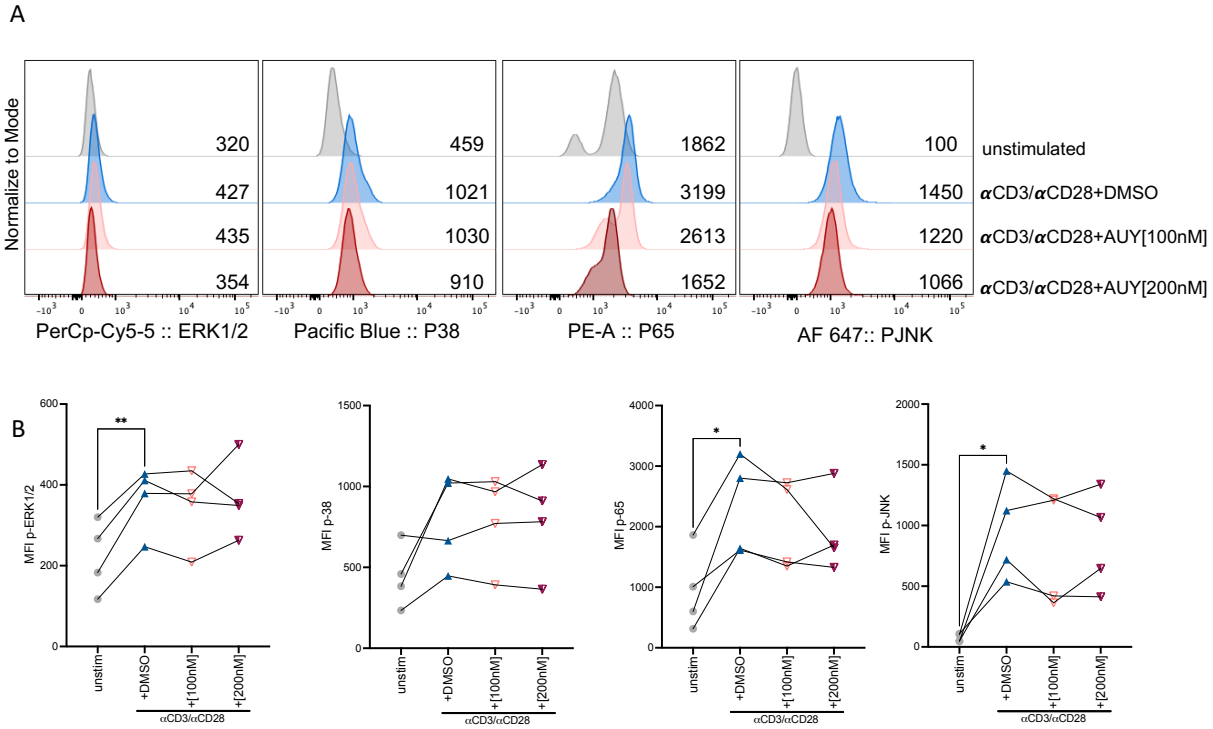

Figure 4.10. AUY922 effect on the Phosphorylation of Key Components downstream TAK1. ERK1/2, P-38, P65, and JNK phosphorylation were measured by flow cytometry in CD4+ isolated from healthy donors. Cells were pretreated with DMSO, AUY922 [100 nM], or AUY922 [200 nM] for 1 h and then stimulated with anti-CD3/CD28 Abs [1 µg/ml/2 µg/ml] for 10 mins. (A) shows a representative histogram of one donor (B) shows MFI of phosphor-ERK1/2, P-38, P65, and JNK for all donors. Statistical significance was calculated using two-tailed paired t-Test: *=p≤0.05; **=p≤0.01; ***=p≤0.001; ****=p<0.0001.

4.3 Discussion

The aim of this chapter was to identify a common Hsp90 client protein, specifically involved in the TCR, PMA, and TLR pathways, and to explore its contribution to HIV-1 reactivation. In this chapter, I specifically tested whether TAK1, a known Hsp90 client protein, is required for HIV-1 reactivation in latently infected Jurkat cells by employing a TAK1 inhibitor, 5Z. Additionally, TPR cells, engineered to express the transcription factors NFAT, NF-kB, and AP-1, were used to assess the effects of both AUY922 and 5Z on these transcription factors, which are critical regulators of HIV-1 transcription. Furthermore, I examined the effect of AUY922 on the phosphorylation of key components downstream of the TAK1 pathway in primary CD4+ T cells.

I found that TAK1 contributes to HIV-1 reactivation, as its inhibition by 5Z significantly reduced viral reactivation. Similarly, AUY922 and TAK1 inhibition in TPR cells effectively suppressed the activation of NF-kB, AP-1, and, to a lesser extent, NFAT. These results suggest that Hsp90 and TAK1 are essential for the full activation of these transcription factors, all of which are critical for HIV-1 gene expression.

The mechanism by which NFAT is inhibited by the TAK1 inhibitor remains unclear, as TAK1 is not directly connected to the NFAT signaling pathway. However, emerging evidence indicates that TAK1 may regulate the calcineurin-NFAT pathway indirectly through its interaction with RCAN1 (Regulator of Calcineurin 1), a key modulator of this pathway. TAK1, activated by stimuli such as PMA or TCR signaling, can form a signaling complex with RCAN1, which influences calcineurin-NFAT signaling by phosphorylating RCAN1. This phosphorylation converts RCAN1 from an inhibitor

into a facilitator of calcineurin activity, enhancing NFAT nuclear translocation and transcriptional activity [237].

Interestingly, as demonstrated in Chapter 3 (Figure 3.5), AUY922 did not inhibit HIV-1 reactivation induced by ionomycin alone. This lack of inhibition likely reflects the fact that ionomycin specifically activates the NFAT pathway through a single, direct mechanism, without crosstalk involving TAK1. In contrast, PMA and TCR activation enhance NFAT activation via multiple pathways, including TAK1-mediated calcium influx, which promotes NFAT nuclear translocation. These distinctions underscore the complexity of NFAT regulation and its dependence on the specific context of upstream signaling events.

Our results also revealed that Hsp90 inhibition by AUY922 did not significantly affect the phosphorylation of key signaling molecules downstream of TAK1, such as MAPK (p38), NF-kB (p-p65), JNK (p-JNK), and ERK-1/2 (p-ERK-1/2), in primary CD4+ T cells. This would confirm our and others' findings that Hsp90 primarily influences TAK1 stability rather than its immediate phosphorylation activity.

However, this study has limitations that should be addressed in future work. One limitation is the absence of a positive control in the phospho-assays performed on primary CD4+ T cells. Including a known TAK1 activator or inhibitor, such as 5Z, would have provided a more robust baseline for validating the phosphorylation changes observed downstream of TAK1.

In conclusion, the findings in this chapter suggest that Hsp90 and TAK1 are required for the reactivation of HIV-1 and that their influence on downstream signaling pathways is context-dependent. Further studies are needed to explore these

alternative mechanisms and to better understand the broader implications of Hsp90 and TAK1 inhibition in the context of HIV-1 latency and reactivation. Understanding these pathways could inform new therapeutic strategies for targeting latent HIV-1 reservoirs, addressing a major barrier to HIV-1 eradication.

Chapter 5: The effect of Hsp90 inhibitor on CD4+ T cell phenotype and activation status.

5.1 Introduction

Many ongoing research efforts are focused on developing new therapeutic strategies to address the limitations of existing HIV-1 treatments [106,238]. cART has transformed HIV-1 from a life-threatening condition into a manageable chronic disease, allowing PLWH who are virologically suppressed to have life expectancies close to those of uninfected individuals [239]. However, issues such as drug resistance, side effects, and the persistence of latent viral reservoirs developed the urgent need for new therapeutic approaches.

One of the most difficult aspects of HIV-1 treatment is the survival of latent viral reservoirs, particularly in memory CD4+ T cells, which are a primary target of HIV-1 infection. These reservoirs allow the virus to avoid the immune system and stay hidden from the effects of cART, making complete eradication difficult [238].

Memory CD4+ T cells are critical components of the immune system, providing long-term immunity by responding rapidly to previously encountered antigens. Their longevity is attributed to their ability to maintain a quiescent state, undergo homeostatic proliferation, and resist apoptosis [240]. HIV-1 preferentially infects proliferating activated CD4+ T effector cells and those transitioning to a resting memory state, as these cells express higher levels of CCR5 and CXCR4 co-receptors, which facilitate viral entry [39,241]. Once infected, some memory CD4+ T cells harbour latent proviruses, allowing the virus to persist in a dormant state that evades immune surveillance and ART [242,243]. It is estimated that approximately

one in a million CD4+ T cells in ART-treated individuals carries a latent provirus, presenting a significant challenge to HIV-1 eradication [39].

In-vitro models of HIV-1 latency in memory CD4+ T cells are essential tools for investigating the mechanisms of latency establishment, maintenance, and reactivation [243,244]. These models often involve activating naïve or total CD4+ T cells through the T-cell receptor (TCR) to create conditions conducive to HIV-1 infection [39,241]. Following infection, cells are driven into a quiescent state to adopt a resting memory phenotype, which is essential for latency establishment [241].

Moreover, *in-vivo*, effector CD4+ T cells are particularly vulnerable to HIV-1 infection, as their activated state provides a favourable environment for viral replication [39]. *Ex-vivo* models enable detailed exploration of how HIV-1 manipulates host cellular pathways to persist, providing a valuable framework for studying the polarization, differentiation, and activation states of memory CD4+ T cells [241–244]. These models also facilitate the testing of LRAs, which are designed to reactivate and eliminate latent reservoirs.

Subsets such as central memory (Tcm), transitional memory (Ttm), and effector memory (Tem) CD4+ T cells exhibit distinct contributions to the latent reservoir [242,244]. Among these, Tem cells are the largest contributors to the inducible reservoir due to their transcriptionally active state, making them particularly responsive to LRAs [242]. Polarized subsets, such as Th1 cells, which are known for their antiviral properties, and Th17 cells, crucial for mucosal immunity, also harbour

latent HIV-1, highlighting the diverse cellular niches exploited by the virus [245,246]. In addition to cellular subsets, markers of activation or inhibition, such as CD25, CD69, PD-1 and TIGIT, as well as epigenetic modifications, play crucial roles in regulating latency and reactivation [39,244].

Building on these discoveries could offer critical insights into the mechanisms underlying HIV-1 persistence, potentially leading to new therapeutic strategies for targeting latent reservoirs and advancing efforts toward achieving a functional or complete cure for HIV-1. Inhibiting HIV-1 gene expression presents an alternative approach to managing the virus by preventing reactivation and reducing chronic inflammation in PLWH. Despite its promise, no approved drugs currently target this stage of the viral life cycle. However, several compounds, including PKC, PI3K, and MEK inhibitors, are in development or pre-clinical stages. These compounds have shown potential *in-vitro* by suppressing TCR-mediated stimulation of latently infected CD4+ T cells and could represent a significant advancement in HIV-1 therapeutic strategies [39,58,101,156,169,247].

Another approach involves targeting master regulators that govern multiple parallel pathways essential for HIV-1 reactivation as long the overall T cell function is not disrupted. In this context, I evaluated the effectiveness of the Hsp90 inhibitor AUY922 in reducing HIV-1 activation in a primary cell model, and assessed its impact on T cell phenotype and different subsets.

5.2 Results

5.2.1 Optimization of AUY922 for use in primary CD4+ T cells

Our previous results (Chapter 3) showed that AUY922 and 17-AAG were able to inhibit the reactivation of HIV- 1 in latently infected Jurkat cells model induced by various stimuli. This indicates that Hsp90 may be a master regulator of latency controlling the activity of multiple signaling pathways. Of note, AUY922 and 17-AAG were more potent at inhibiting HIV-1 reactivation than CD69 expression (Figures 3.12-3.15), suggesting a degree of specificity, which is important if these inhibitors are to be tested in pre-clinical models and in clinical trials. Jurkat cells are a well-established model of latency [158,166], but the relevance of Hsp90 in regulating HIV-1 latency also needs to be tested in primary CD4+ T cells. Furthermore, agents that suppress HIV-1 reactivation should have minimal effect on the phenotypic and function of host CD4+ T cells when used in clinical settings. Therefore, I initially investigated whether blocking Hsp90 with AUY922 was toxic in primary cells or affected their phenotype and differentiation state.

To optimize conditions, initial experiments were performed to titrate AUY922 in uninfected primary CD4+ T cells and determine the best drug concentration showing little or no toxicity and little or no perturbation of the activated cellular phenotype initially measured using expression levels of CD3, CD4, CD69, CD25 and the proportion of live cells.

CD4+ T cells were isolated from peripheral blood mononuclear cells (PBMCs) of a healthy donor using magnetic sorting and were either incubated in the presence of IL-2 (no stim) or were activated for three days with a combination of anti-CD3/CD28 Abs, followed by different concentrations of AUY922 or DMSO on the third day. After 24 hours of AUY922 treatment, cells were analysed by flow cytometry **(Figure 5.1).**

The results showed that AUY922 did not affect expression of CD3 and CD4 and it was not toxic at concentrations up to 100 nM **(Figure 5.1A)**. Expression of CD25 and CD69 was potently induced by treatment with anti-CD3/CD28 Abs relative to IL-2 (no stim) alone **(Figure 5.1B-C)**. At 50nM or greater, AUY922 reduced the percentage of CD25+ and double positive CD25+CD69+ cells relative to control. At concentrations of 6,12 and 25nM, the effect of AUY922 on the percentage of CD25+CD69+ cells were less pronounced than at >50nM and was minimal for either CD25+ or CD69+ cells **(Figure 5.1B)**. Therefore, due to its lack of cell toxicity and modest impact on CD69, I chose to use 25 nM AUY922 in subsequent experiments.

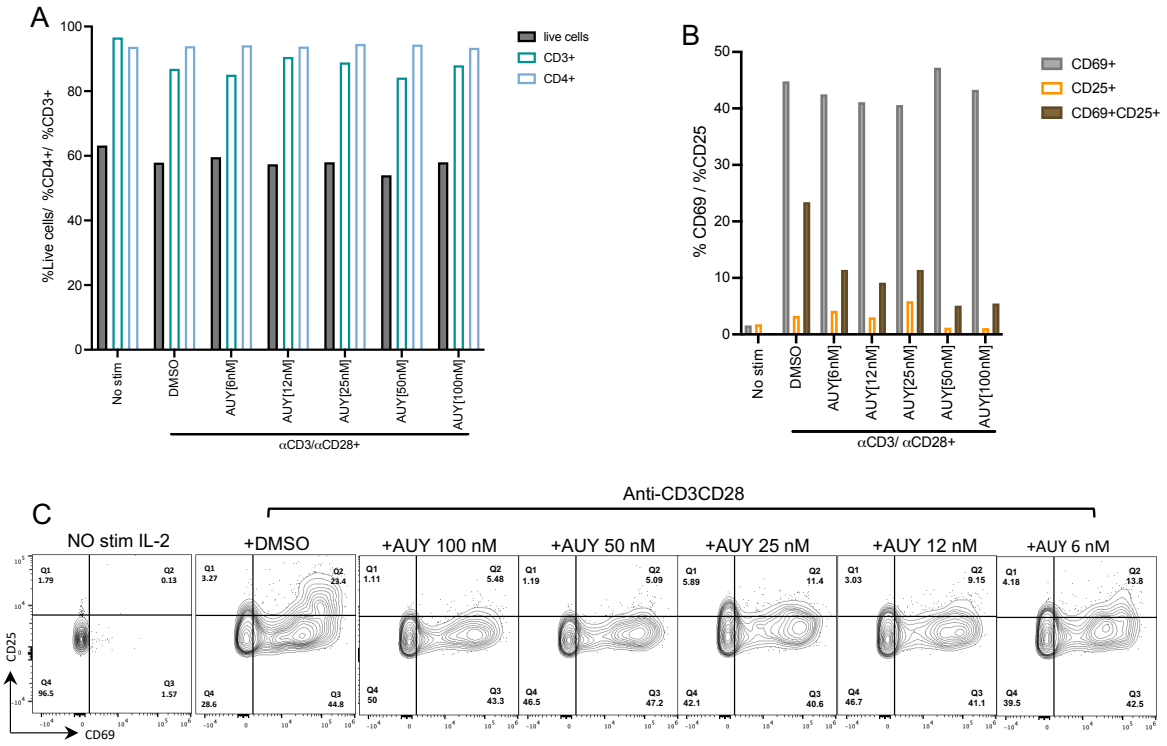

Figure 5.1. Optimization of the AUY922 concentration in primary CD4 T cells. CD4+ T cells were isolated from frozen PBMCs and were either treated with IL-2 or activated for 3 days with anti-CD3/CD28 Abs. On day 3, different concentration of AUY922 were added to the samples for 24h and cells were analysed by flow cytometry to detect CD3, CD4, CD69 and CD25. (A) Bar graphs showing the percentage of live CD3+ and CD4+ cells. (B) Bar graphs showing the percentage of CD25+, CD69+ and CD25+CD69+ cells. (C) Flow cytometry plots for CD69 and CD25 gated from live cells and CD3+CD4+ cells.

5.2.2 AUY922 has little impact on the phenotype of CD4+ T cells.

To extend the analysis to critical cell surface markers defining CD4 +T cell subsets, CD4+ T lymphocytes were stimulated with anti-CD3/CD28 Abs for 72h in the presence or absence of AUY922 (25nM) and analysed by a spectral Cytek Aurora cytometer. An 18-colour antibody panel was used that was carefully selected on the

basis of published protocols [248–255] **(Table 5.1)**. In studying the role of CD4+ T cells in HIV-1 latency, specific markers were chosen to characterize different subsets and their contributions to viral persistence, four main CD4+ T cell subsets were identified as following: naïve (CD3+CD4+, CD45RA+, CCR7+), T central memory (Tcm) (CD3+CD4+, CD45RA-, CCR7+), T effector memory (Tem) (CD3+CD4+, CD45RA-, CCR7-), T effector (CD3+CD4+, CD45RA+, CCR7-), T cell subsets Th17 (CD194+, CD196+), Th1 (CD194- and CD183+), and Th2 (CD194+, CD196). Markers of T cell activation (CD25, CD69, HLA-DR, CD38) were included to identify subsets with enhanced susceptibility to HIV-1 infection due to their activated state [244]. Inhibitory markers (PD-1, TIGIT, Tim-3) were selected to assess T cell exhaustion, a hallmark of cells within the HIV-1 reservoir that may contribute to immune evasion. Together, these markers provide a comprehensive framework for investigating how HIV-1 establishes and maintains latency within different CD4+ T cell populations [244] **(Table 5.2)**. The gating strategy is shown in **(Figure 5.2).** To precisely gate the correct population, Fluorescence Minus One (FMO) gating was performed for each of the antibodies on stimulated cells with no AUY922**.** The parameters set for this FMO staining were subsequently used to gate the samples **(Figure 5.2).**

Table 5.1. Markers used to define CD4+ T cell populations

Name	Marker for	Ref.	Name	Marker for	Ref.
CD3	Pan T cell receptor	[248,254]	**CXCR3 (CD183)**	Th1, Negative marker for Th2 and Th17	[248,250,254]
CD4	T helper (Th)	[248,250,252,254]	**HLA-DR**	Activation marker	[248,250]
CD45RA	T naïve, T effector	[248,252,254]	**CD69**	Activation marker	[248,250,254]
CCR7 (CD197)	T naïve, T memory	[248,250,254]	**CD38**	Activation marker	[248]
CD45RO	T memory	[248,250,252,254]	**CD71**	Activation marker	[170]
CD127	T memory, T naïve	[248,250,252]	**PD-1**	Inhibitory marker	[248]
CD25	Activation marker, negative marker for T naïve	[248,250]	**Tim-3**	Inhibitory marker	[248]
CCR4 (CD194)	Th2, Th17, negative marker for Th1	[248,254]	**TIGIT**	Inhibitory marker	[248]
CCR6 (CD196)	TH17, negative marker for Th2 and Th1	[248,254]			

Table 5.2 Markers used to identify T cell subset, activation and inhibition

Name	**Marker for**	**Ref.**
T naïve	CD3+ CD4+ CD45RA+ CCR7+	[243,244,252,254]
T central memory (Tcm)	CD3+ CD4+ CD45RA- CCR7+	[243,244,252,254]
T effector (Teff)	CD3+ CD4+ CD45RA+ CCR7-	[243,244,252,254]
T effector memory (Tem)	CD3+ CD4+CD45RA- CCR7-	[243,244,252,254]
T memory	CD3+ CD4+ CD45RO+ CD127+	[243,244,252,254]
Th17	CD194+ CD196+	[244,248,254]
Th1	CD194- CD183+	[244,248,254]
Th2	CD194+ CD196-	[244,248,254]
T cell activation markers	CD25, CD69, CD38, HLA-DR, CD71	[170,196,243,244,248,254]
T cell inhibitory markers	PD-1, TIGIT, Tim-3	[243,244,248,254]

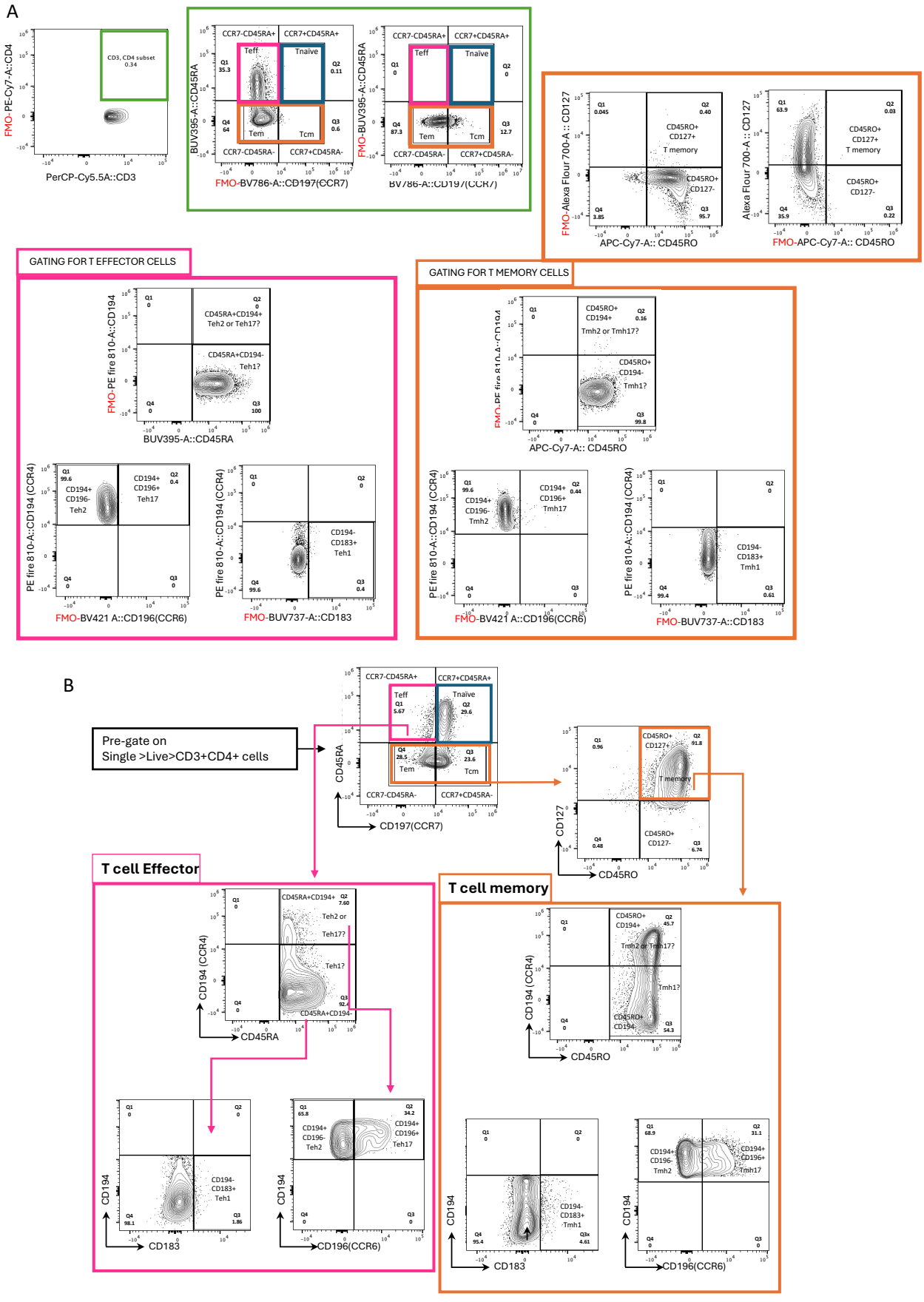
A
FMO-PE-Cy7-A::CD4
PerCP-Cy5.5A::CD3
CD3, CD4 subset
0.34
BUV395-A::CD45RA
FMO-BV786-A::CD197(CCR7)
CCR7-CD45RA+
CCR7+CD45RA+
Teff
Tnaive
Tem
Tcm
CCR7-CD45RA-
CCR7+CD45RA-
FMO-BUV395-A::CD45RA
BV786-A::CD197(CCR7)
FMO-Alexa Flour 700-A :: CD127
APC-Cy7-A:: CD45RO
CD45RO+
CD127+
T memory
CD45RO+
CD127-
Alexa Flour 700-A :: CD127
FMO-APC-Cy7-A:: CD45RO
GATING FOR T EFFECTOR CELLS
FMO-PE fire 810-A::CD194
BUV395-A::CD45RA
CD45RA+CD194+
Teh2 or Teh17?
CD45RA+CD194-
Teh1?
PE fire 810-A::CD194 (CCR4)
FMO-BV421 A::CD196(CCR6)
CD194+
CD196-
Teh2
CD194+
CD196+
Teh17
FMO-BUV737-A::CD183
CD194-
CD183+
Teh1
GATING FOR T MEMORY CELLS
FMO-PE fire 810-A::CD194
APC-Cy7-A:: CD45RO
CD45RO+
CD194+
Tmh2 or Tmh17?
CD45RO+
CD194-
Tmh1?
PE fire 810-A::CD194 (CCR4)
FMO-BV421 A::CD196(CCR6)
CD194+
CD196-
Tmh2
CD194+
CD196+
Tmh17
FMO-BUV737-A::CD183
CD194-
CD183+
Tmh1
B
Pre-gate on
Single >Live>CD3+CD4+ cells
CD45RA
CD197(CCR7)
CD127
CD45RO
T cell Effector
CD194 (CCR4)
CD45RA
CD45RA+CD194+
Teh2 or
Teh17?
Teh1?
CD45RA+CD194-
CD194
CD183
CD194-
CD183+
Teh1
CD196(CCR6)
CD194+
CD196-
Teh2
CD194+
CD196+
Teh17
T cell memory
CD194 (CCR4)
CD45RO
CD45RO+
CD194+
Tmh2 or Tmh17?
Tmh1?
CD45RO+
CD194-
CD194
CD183
CD194-
CD183+
Tmh1
CD196(CCR6)
CD194+
CD196-
Tmh2
CD194+
CD196+
Tmh17

Figure 5.2. Gating strategy and FMO. (A) Primary CD4+ T cells were analysed by spectral flow cytometry and positive gates were established by staining with the 18-antibody panel minus one (fluorescence minus one or FMO). (B) Representative flow cytometry plots and gating strategy of T cell subsets from one donor gated from live CD3+CD4+ cells.

Next, CD4+ T cells were isolated from 4 different donors. Cells were split into 3 aliquots; one aliquot was stimulated with anti-CD3/CD28 Abs for 48h before addition of DMSO (control) for another 24h, the second aliquot was stimulated as before and AUY922 (25nM) was added at 48h post-stimulation, and the last aliquot was not stimulated (IL-2 only). Then, cells were antibody-stained and analysed by flow cytometry based on the gating established using the FMO parameters **(Figure 5.2)**.

The flow cytometry high-dimensional data were processed using t-distributed stochastic neighbour embedding (tSNE), a dimensionality reduction technique that visualizes complex high-dimensional data in two- or three-dimensional space. tSNE preserves the relationships between data points by placing similar points close together in the reduced space, making it especially useful for identifying clusters or patterns in complex datasets [256]. Our tSNE plots revealed no consistent changes in the main cell types, including samples treated with the Hsp90 inhibitor, except for a pattern of lower Tim3+ cells in stimulated relative to control samples but AUY922 did not change this **(Figure 5.3).** The expression of the activation markers CD69 and CD25 were higher in stimulated cells, and AUY922 lowered CD69 levels in two out of four donors. The late activation markers HLA-DR and CD38 were unchanged **(Figure 5.3)**.

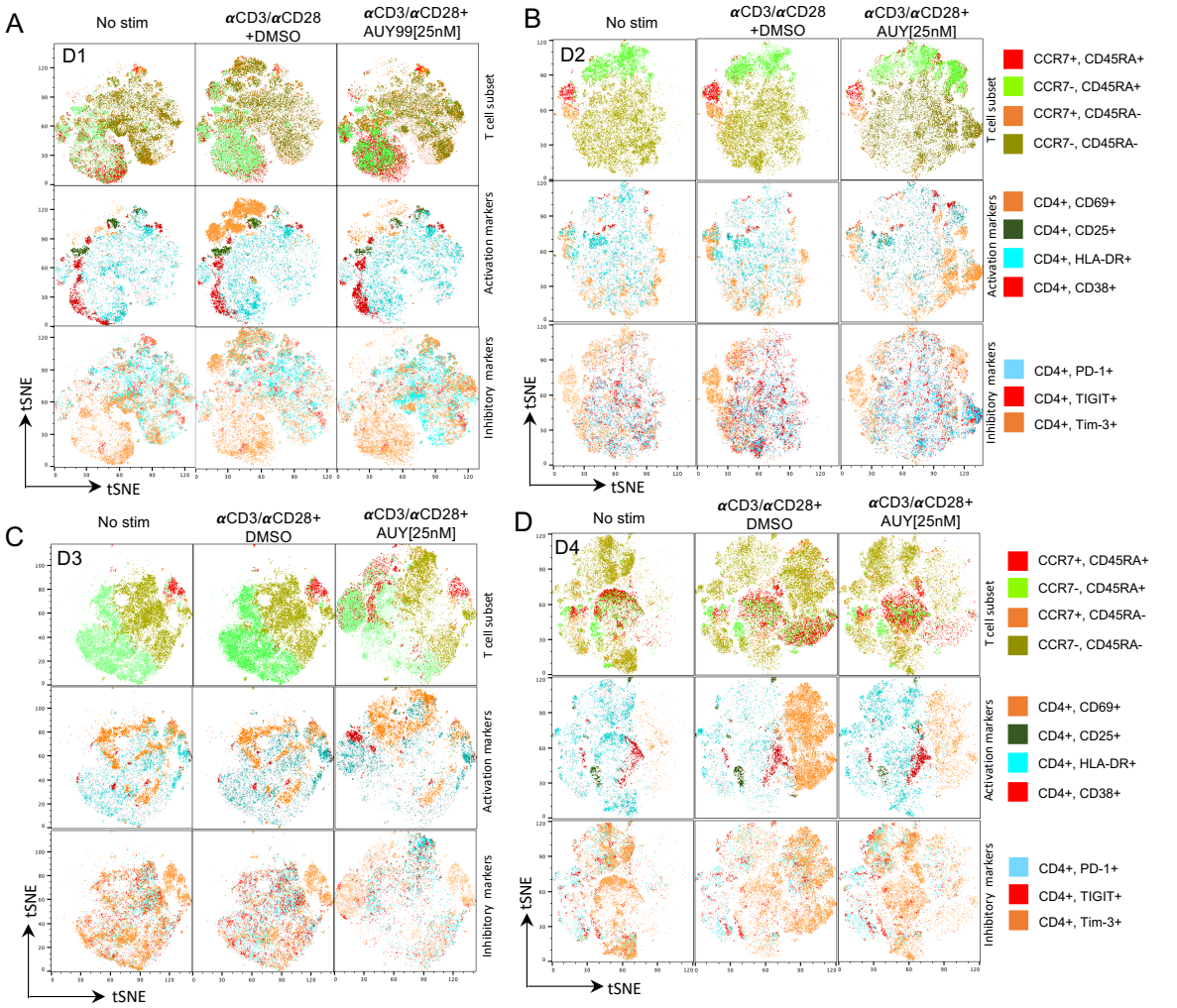

Figure 5.3. **The effect of AUY922 treatment on different CD4+ T cell populations tSNE plots**. CD4+ T cells were isolated from PBMCs and treated with IL-2 only (no stim) or anti-CD3/CD28 Abs + IL-2 for 72 hours, and AUY922 [25 nM] or DMSO added 48 hours post stimulation. Cells were analysed by flow cytometry 24 hours after the addition of AUY922. tSNE data of the T subsets, activation, and inhibitory markers were generated by FlowJo. A) tSNE plot for donor 1. B) tSNE plot for donor 2. C) tSNE plot for donor 3. D) tSNE plot for donor 4.

Quantification and statistical analysis of the flow cytometry data confirmed that AUY922 treatment did not significantly impact the proportion of the various cell

populations **(Figure 5.4)**, or their activation state, although a trend toward reduced CD25+ cells was observed **(Figure 5.4).** In two of the 4 donors, TCR stimulation increased the percentage of CD69+ cells and AUY922 treatment abrogated that effect **(Figure 5.4),** suggesting that AUY922 may reduce CD4+ T cell activation in a subset of donors that better respond to TCR stimulation. However, overall, the data indicate that the Hsp90 inhibitor did not detectably perturb the CD4+ T cell phenotype, at least at the concentration and time of exposure tested.

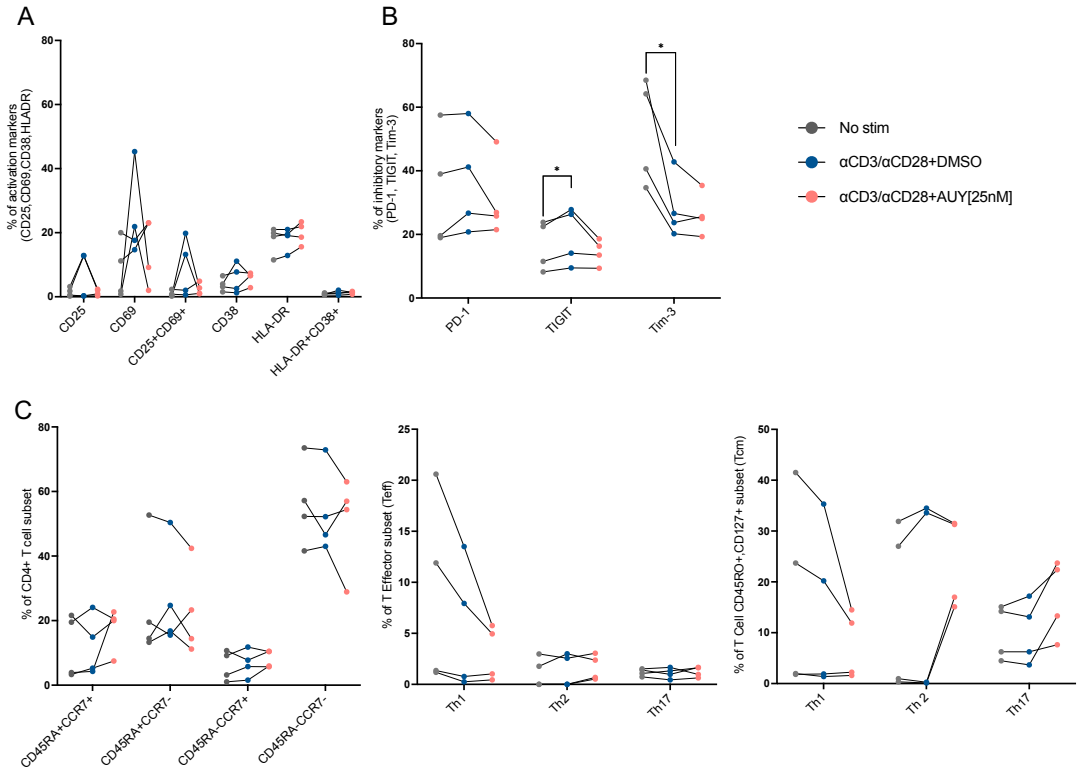

Figure 5.4. The effect of AUY922 treatment on different CD4+ T cell populations. Primary CD4+ T cells were treated with IL-2 only (no stim) or with anti-CD3/CD28 Abs and IL-2 for 72 hours, and AUY922 [25 nM] or DMSO added at 48 hours post-stimulation. Cells were analysed by spectral flow cytometry using a panel of 18 antibodies 24 hours after the addition of AUY922. (A) Results for T cell activation markers (B) Inhibitory markers (C) cell subset markers. Subsets were identified according to the combination of surface markers shown in Table 5.2 and the gating strategy shown in Figure 5.2. Statistical significance was calculated using two-tailed paired t-Test: *=p≤0.05; **=p≤0.01; ***=p≤0.001; ****=p<0.0001.

5.2.3 Inhibition of Hsp90 suppresses HIV-1 reactivation without affecting the differentiation phenotype of primary CD4+ T cells

Next, I examined the selectivity of AUY922 in a primary model of HIV-1 latency **(Figure 5.5A).** CD4+ T cells were isolated from PBMCs of 5 different donors, stimulated with anti-CD3/CD28 Abs for 72h before infection with the same single cycle NL4.3Δ6-drGFP virus used to generate the latent Jurkat cells (see Figure 3.1). Aliquots of uninfected cells were maintained in media containing 50 μg/ml IL-2 and the percentage of GFP+ cells and MFI GFP was monitored by flow cytometry from infection day until day 6 or 8 post infection. Once latency was established, samples were re-stimulated with anti-CD3/CD28 Abs in the presence of AUY922 and HIV-1 reactivation measured by flow cytometry **(Figure 5.5A and 5.5B).** In the latency phase, there was a progressive loss of viral gene expression, which was more marked when measured as GFP MFI than percentage of GFP+ cells **(Figure 5.5C)**. To monitor T cell activation, the activation markers CD69+ and CD25+ were measured. Two days post-infection, >80% of the cells were still expressing at least one activation marker. Progressively, cells lost expression of the activation markers in parallel with GFP such that by the day of reactivation, only approx. 10-20% of the cells expressed at least one activation marker, indicating that infected cells progressively returned to a more resting state, except for donor 5 **(Figure 5.5D)**.

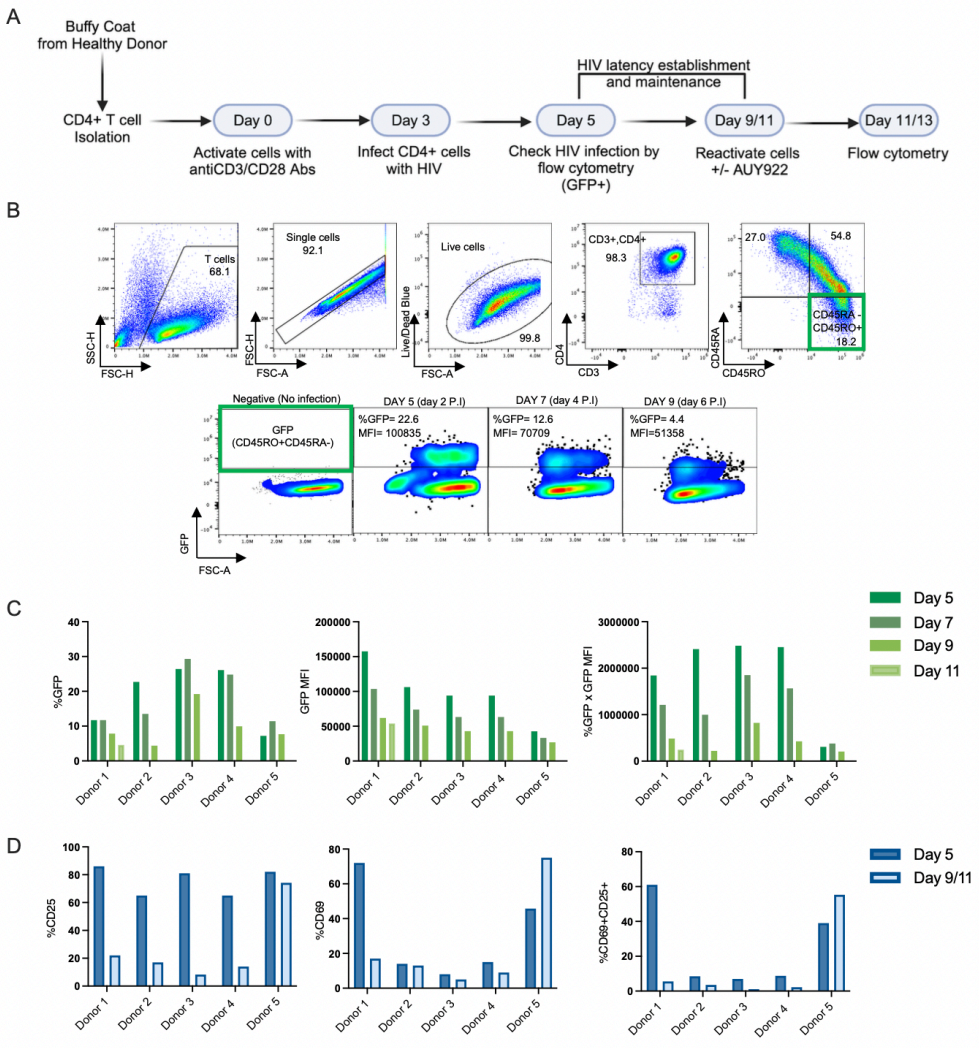

Figure 5.5. Generation of the *ex-vivo* latency infected primary CD4+ T cells. (A) Schematic depiction of the experimental set-up to generate latently infected cells *ex-vivo*. Cells were infected at day 3 post-stimulation with a VSV-G pseudotyped, single cycle HIV-1 reporter virus (pNL4-3-Δ6-drEGFP). (B) Representative flow cytometry plots showing the gating strategy used to detect the GFP+ cells in the CD45RA- CD45RO+ memory population. Cells were analysed by flow cytometry for GFP expression at regular intervals. (C) Bar graphs showing the GFP MFI (left panel), the percentage of GFP+ cells (middle panel), and combined % GFP x MFI (right panel) measured for each donor on the indicated days. (D) Bar graphs showing the percentage of CD25+ cells (left panel), CD69+ cells (middle panel), and double CD25+CD69+ cells (right panel) for each donor measured by flow cytometry on the indicated days. Schematic in (A) was created with BioRender.com.

To ensure that the virus integrated into the cells' genome and that it was not lost during cell culture, DNA was extracted on day 5 and day 9 or 11 and used for Alu-LTR PCR. **(Figure 5.6).** The well-established Alu-LTR method is based on TaqMan qPCR amplification using one primer for Alu repetitive elements, which are distributed throughout the genome, and a second primer specific for the HIV- 1 LTR [213]. Successful amplification happens only when the LTR is integrated near an Alu element. Although flow cytometry showed a decrease in the percentage of GFP+ cells between day 5 and day 9 or 11 **(Figure 5.5C)**, little or no loss of proviral DNA was found, arguing against a selective loss of infected cells during culture and supporting the notion that, like in the Jurkat cells, our model in primary cells measured real latency.

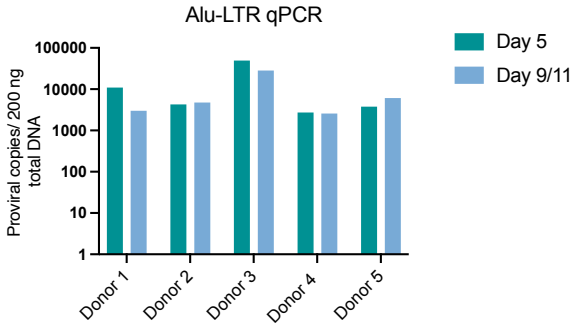

Figure 5.6. Alu-LTR qPCR. DNA was extracted from the CD4+ T cells on the indicated days and used to quantify integrated proviral DNA copies by Alu-LTR qPCR.

To investigate which stimuli were Hsp90-dependent in this model, we had to prioritize LRAs due to the limited number of cells available. We selected anti-CD3/CD28 Abs, a FOXO-1 inhibitor, IL7/IL15, and TLR7 agonists because these stimuli represent diverse mechanisms of latency reversal, targeting key pathways relevant to HIV-1 reactivation. Anti-CD3/CD28 Abs mimic T-cell receptor (TCR) engagement, directly

activating signaling pathways essential for T-cell activation and HIV-1 reactivation [76]. The FOXO-1 inhibitor was chosen due to its role in modulating transcriptional regulation linked to latency maintenance [170,196]. IL7/IL15 were selected as they are known to promote T-cell survival and proliferation, enhancing HIV-1 reactivation in latency models [173]. Finally, TLR7 agonists were prioritized for their ability to activate innate immune pathways, which have been shown to contribute to latency disruption [172].

On day 9 or 11, latently infected cells were re-stimulated with the specific stimuli in the presence of 25 nM or 50 nM AUY922 or DMSO for 48h and analysed by multiparameter flow cytometry on a Cytek Aurora using the same antibody panel and gating strategy described in (Table 5.2 and Figure 5.2). Also, here CD71 (the transferrin receptor) was added to the Abs panel as a metabolic activation marker which is induced by inhibition of FOXO-1 [170].

5.2.3.1 anti-CD3/CD28 Abs

Cells were stimulated with anti-CD3 [1μg/mL] + CD28 [2μg/mL] Abs and treated with either DMSO or AUY922 [25nM] or AUY922 [50nM] for 48h. Treated cells were analysed by spectral flow cytometry to measure the percentage of GFP+ cells and its MFI both in the CD45RA- CD45RO+ population and in each CD4+ T cell sub-type. The results showed that in CD45RA- CD45RO+ memory cells, anti-CD3/CD28 Abs triggered significant reactivation, as measured by the GFP MFI, which was inhibited by AUY922 in a dose-dependent way **(Figure 5.7A-B)**. TCR stimulation did not appear to appreciably increase the percentage of GFP+ cells, nonetheless when

both the GFP MFI and the percentage of GFP+ cells were combined, TCR stimulation was found to be effective, and this effect was partially abrogated by AUY922 at 50nM **(Figure 5.7A-B)**. We then assessed HIV-1 reactivation and the effect of AUY922 in the other CD4+ T cell sub-sets. Within specific CD4+ T cell populations, CD45RA+ CCR7+ “naïve” cells showed the greatest susceptibility to AUY922, followed by CD45RA- CCR7+ central memory cells [257] **(Figure 5.7C-D)**, although the latter trend did not reach statistical significance.

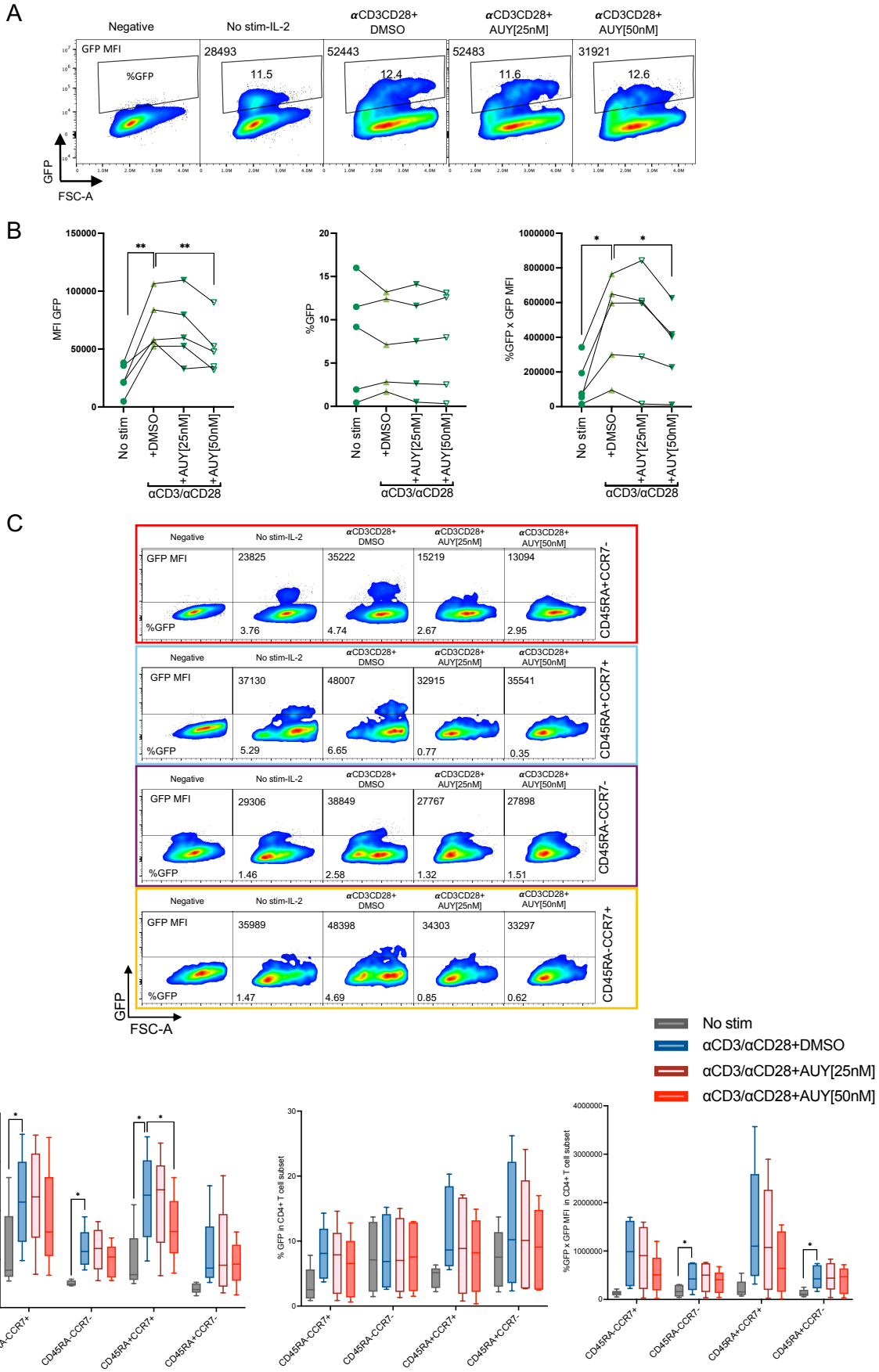
A
Negative
No stim-IL-2
αCD3CD28+ DMSO
αCD3CD28+ AUY[25nM]
αCD3CD28+ AUY[50nM]
GFP MFI
28493
52443
52483
31921
%GFP
11.5
12.4
11.6
12.6
GFP
FSC-A
B
MFI GFP
%GFP
%GFP x GFP MFI
No stim
+DMSO
+AUY[25nM]
+AUY[50nM]
αCD3/αCD28
C
GFP MFI
%GFP
CD45RA+CCR7-
CD45RA+CCR7+
CD45RA-CCR7-
CD45RA-CCR7+
23825
35222
15219
13094
3.76
4.74
2.67
2.95
37130
48007
32915
35541
5.29
6.65
0.77
0.35
29306
38849
27767
27898
1.46
2.58
1.32
1.51
35989
48398
34303
33297
1.47
4.69
0.85
0.62
GFP
FSC-A
No stim
αCD3/αCD28+DMSO
αCD3/αCD28+AUY[25nM]
αCD3/αCD28+AUY[50nM]
D
GFP MFI in CD4+ T cell subset
% GFP in CD4+ T cell subset
%GFP x GFP MFI in CD4+ T cell subset
CD45RA-CCR7+
CD45RA-CCR7-
CD45RA+CCR7+
CD45RA+CCR7-

Figure 5.7. Effect of AUY922 on HIV-1 reactivation induced by anti-CD3/CD28 Abs in primary CD4+ T cell subsets. Latently infected primary CD4+ T cells were generated *ex-vivo,* as described in Figure 5.5. Cells were re-stimulated on day 9 or 11 with anti-CD3/CD28 Abs with or without AUY922 [25 nM or 50 nM] or DMSO. Cells were analysed by spectral flow cytometry using the same antibody panel used in Figure 5.4, in addition to GFP and CD71. (A) Representative flow plots showing the GFP MFI before (no stim-IL-2) and after re-stimulation with anti-CD3 /CD28 Abs or AUY922 [25 or 50 nM]. (B) Graphs showing the results for 5 donors: GFP MFI (left panel), percentage of GFP+ cells (middle panel), and combined % GFP x MFI in the CD45RA- CD45RO+ population. (C) Representative flow plots showing the gating for GFP+ in different T cell subsets with different conditions (no stim-IL-2) and after re-stimulation with anti-CD3/CD28 Abs or AUY922 [25 or 50 nM]. (D) Results from five donors are shown for the GFP MFI (right panel), percentage of GFP+ cells (middle panel) and combined % GFP x MFI (right panel) in each CD4+ T cell subset. Bar plots show 1st quartile, 3rd quartile and median for five donors. Statistical significance was calculated using a two-tailed paired t-Test comparing anti-CD3/CD28 Abs versus no stim-IL-2, and anti-CD3/CD28 Abs versus 50 nM AUY922, *=p≤0.05; **=p≤0.01; ***=p≤0.001; ****=p<0.0001.

We also examined if inhibition of Hsp90 at levels sufficient to reduce viral gene expression affected the differentiation and phenotype of CD4+ T cells. In cells stimulated twice by anti-CD3/CD28 Abs, we found a significant upregulation of activation markers CD69 , CD25, CD38 and CD71 [258] **(Figure 5.8 A)**, with simultaneous upregulation of inhibitory markers PD-1, TIGIT and Tim-3 (the latter showed a trend but did not reach statistical significance), which suggested a degree of exhaustion after two rounds of stimulation in a relatively short time interval. Additionally, TIGIT and PD-1 have been linked to HIV-1 latency, with their expression strongly associated with latent HIV-1 reservoirs in memory CD4+ T cells highlighting their potential as targets for reducing the viral reservoir [60].

(Figure 5.8B). Treatment with AUY922 did not appreciably affect expression of these markers, except for a noticeable reduction in TIGIT surface expression **(Figure**

5.8B). This decrease may be attributed to AUY922 reducing the size of the HIV-1 reservoir, which is known to be enriched in cells with high TIGIT expression [60]. The results also showed a significant reduction in the proportion of markers of Th1 cells against a significant increase in the proportion of markers of Th2 cells upon TCR stimulation but treatment with AUY922 did not change this **(Figure 5.8C)**. The observed changes in Th1 and Th2 markers may be influenced by the strength and context of TCR signaling [259]. Robust TCR signals are known to support Th1 differentiation by increasing responsiveness to IL-12 and promoting the expression of T-bet, the key transcription factor for Th1 cells. In contrast, weaker or prolonged TCR stimulation, particularly in the presence of specific cytokines, can suppress Th1 pathways and favour Th2 differentiation by enhancing IL-4 signaling, which drives Th2 lineage commitment. This suggests that the balance between Th1 and Th2 differentiation is regulated by the intensity of TCR signaling and the surrounding cytokine environment [259].

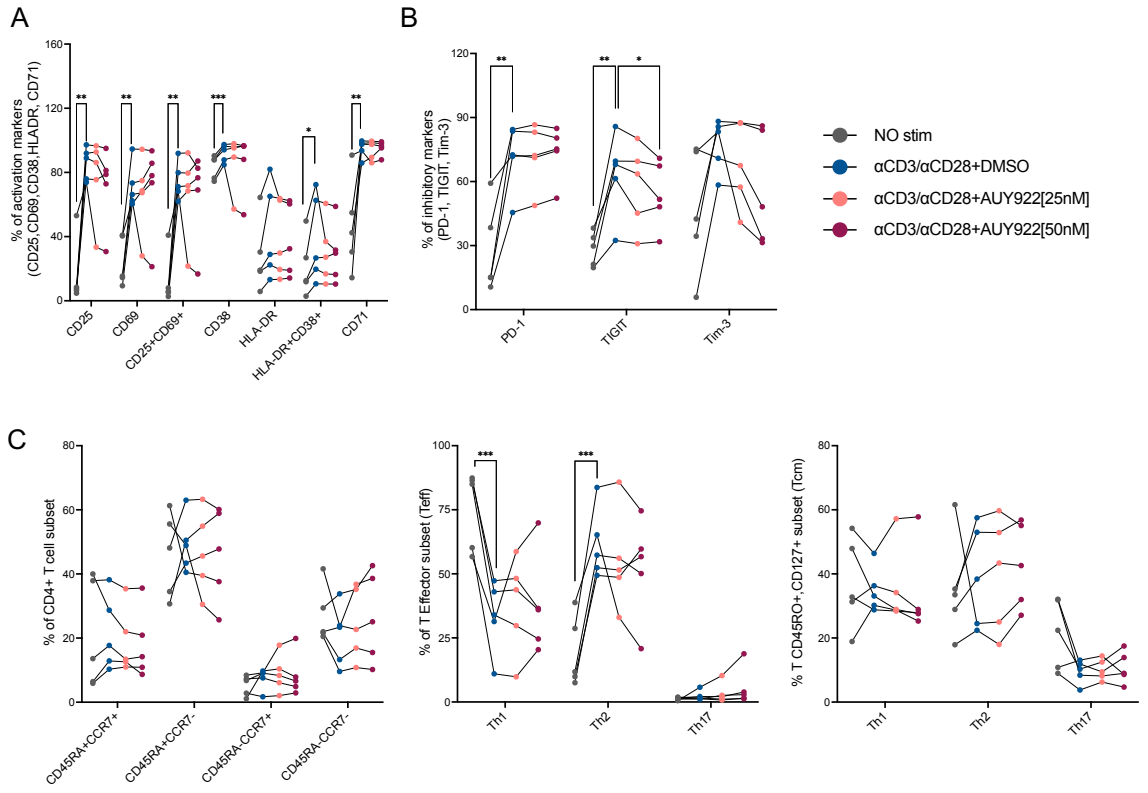

Figure 5.8. AUY922 does not significantly change the CD4+ T cell phenotype or activation state upon anti-CD3/CD28 Abs activation. Latently infected primary CD4+ T cells were re-stimulated on day 9 or 11 with the indicated LRA with or without AUY922 [25 nM or 50 nM] or DMSO. Cells were analysed by spectral flow cytometry using the same antibody panel used in Figure 5.4 with the addition of CD71. (A) T cell activation markers (B) inhibitory markers (C) CD4 T cell subsets, effector subsets and memory subsets after re-stimulation with anti-CD3 [1 µg/ml] and anti-CD28 [2 µg/ml] antibodies plus AUY922 [25 or 50 nM] or DMSO. Results were obtained from five different donors. Statistical significance was calculated using a two-tailed paired t-Test comparing, within each cell sub-type, anti-CD3/CD28 Abs versus no stim (IL-2), anti-CD3/CD28 Abs versus 50 nM AUY922, *=p≤0.05; **=p≤0.01; ***=p≤0.001; ****=p<0.0001.

5.2.3.2 IL7/IL15

Latent cells were stimulated with IL7 [20ng/mL] + IL15 [20ng/mL] and treated with either DMSO or AUY922 [25nM] or AUY922 [50nM] for 48h. Treated cells were analysed as previously described in anti-CD3/CD28 Abs stimulation. Cells treated with IL7 and IL15 did not show appreciable reactivation, however inhibition of Hsp90 significantly reduced residual viral gene expression below the baseline (unstimulated cells) in CD45RA- CD45RO+ memory cells and this effect was significant for GFP MFI, percentage of GFP+ cells and the combination of GFP MFI and % GFP+ cells **(Figure 5.9)**. Within specific CD4+ T cell subsets, the greatest susceptibility to AUY922 was detected in CD45RA+ CCR7+ cells, followed by CD45RA- CCR7+ cells, and CD45RA- CCR7- effector memory cells **(Figure 5.9)**.

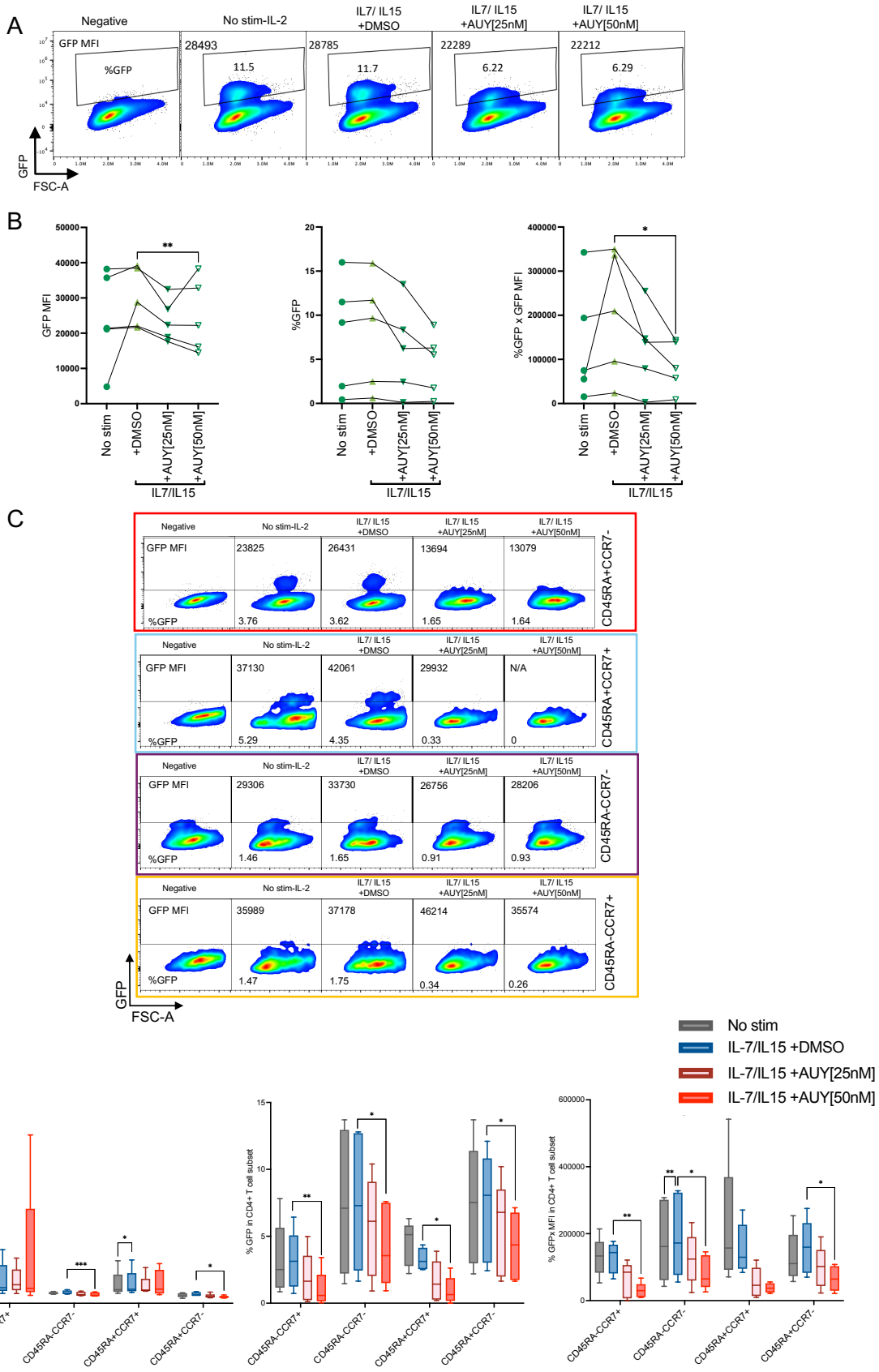
A
Negative
No stim-IL-2
IL7/ IL15 +DMSO
IL7/ IL15 +AUY[25nM]
IL7/ IL15 +AUY[50nM]
GFP MFI
%GFP
28493
11.5
28785
11.7
22289
6.22
22212
6.29
GFP
FSC-A
B
GFP MFI
%GFP
%GFP x GFP MFI
No stim
+DMSO
+AUY[25nM]
+AUY[50nM]
IL7/IL15
C
CD45RA+CCR7-
CD45RA+CCR7+
CD45RA-CCR7-
CD45RA-CCR7+
GFP MFI
%GFP
23825
3.76
26431
3.62
13694
1.65
13079
1.64
37130
5.29
42061
4.35
29932
0.33
N/A
0
29306
1.46
33730
1.65
26756
0.91
28206
0.93
35989
1.47
37178
1.75
46214
0.34
35574
0.26
GFP
FSC-A
D
No stim
IL-7/IL15 +DMSO
IL-7/IL15 +AUY[25nM]
IL-7/IL15 +AUY[50nM]
GFP MFI of CD4+ T cell subset
% GFP in CD4+ T cell subset
% GFPx MFI in CD4+ T cell subset
CD45RA-CCR7+
CD45RA-CCR7-
CD45RA+CCR7+
CD45RA+CCR7-

Figure 5.9. Effect of AUY922 on HIV-1 reactivation induced by IL7/IL15 in primary CD4+ T cell subsets. Latently infected primary CD4+ T cells were generated *ex-vivo*, as described in Figure 5.5. Cells were re-stimulated on day 9 or 11 with IL7/IL15 with or without AUY922 [25 nM or 50 nM] or DMSO. Cells were analysed by spectral flow cytometry using the same antibody panel used in Figure 5.4, in addition to GFP and CD71. (A) Representative flow plots showing the GFP MFI before (no stim-IL-2) and after re-stimulation IL7/IL15 or AUY922 [25 or 50 nM]. (B) Graphs showing the results for 5 donors: GFP MFI (left panel), percentage of GFP+ cells (middle panel), and combined % GFP x MFI in the CD45RA- CD45RO+ population. (C) Representative flow plots showing the gating for GFP+ in different T cell subsets with different conditions (no stim-IL-2) and after re-stimulation with IL7/IL15 or AUY922 [25 or 50 nM]. (D) Results from five donors are shown for the GFP MFI (right panel), percentage of GFP+ cells (middle panel) and combined % GFP x MFI (right panel) in each CD4+ T cell subset. Bar plots show 1st quartile, 3rd quartile and median for five donors. Statistical significance was calculated using a two-tailed paired t-Test comparing IL7/IL15 versus no stim-IL-2, and IL7/IL15 versus 50 nM AUY922, *=p≤0.05; **=p≤0.01; ***=p≤0.001; ****=p<0.0001.

In terms of T cell phenotype, treatment with IL7/IL15 significantly upregulated HLA-DR and CD71, confirming activity of the cytokines, and AUY922 significantly reduced expression of CD71 **(Figure 5.10)**. In terms of T cell subsets there were no significant changes shown after activation, or after treatment with AUY922.

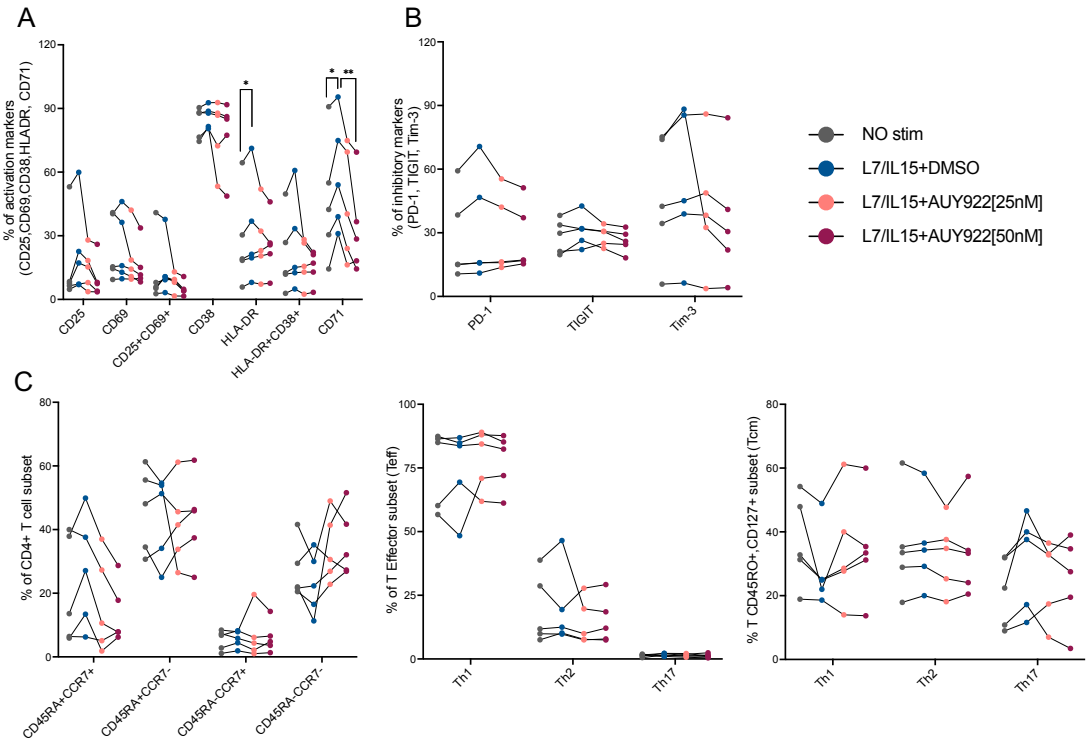

Figure 5.10. AUY922 does not significantly change the CD4+ T cell phenotype or activation state upon IL7/IL15 activation. Latently infected primary CD4+ T cells were re-stimulated on day 9 or 11 with the IL7/IL15 with or without AUY922 [25 nM or 50 nM] or DMSO. Cells were analysed by spectral flow cytometry using the same antibody panel used in Figure 5.4 with the addition of CD71. A) show T cell activation markers B) inhibitory markers C) CD4 T cell subsets, effector subsets and memory subsets after re-stimulation with anti-CD3 [1 µg/ml] and anti-CD28 [2 µg/ml] antibodies plus AUY922 [25 or 50 nM] or DMSO. Results were obtained from five different donors. Statistical significance was calculated using a two-tailed paired t-Test comparing, within each cell sub-type, IL7/IL15 versus no stim (IL-2), IL7/IL15 versus 50 nM AUY922, *=p≤0.05; **=p≤0.01; ***=p≤0.001; ****=p<0.0001.

5.2.3.3 FOXO-1 inhibitor

Cells were stimulated with the FOXO-1 inh (AS1842856) [200nM] and treated with either DMSO or AUY922 [25nM or 50nM] for 48h and analysed as previously described. Treatment with the FOXO-1 inhibitor failed to induce viral reactivation,

however, AUY922 was able to significantly reduce residual viral gene expression below the baseline of unstimulated CD45RA- CD45RO+ cells **(Figure5.11)**. In term of HIV-1 inhibition in other T cell subsets, the results showed strong response to AUY922 in the CD45RA- CCR7+ and CD45RA+ CCR7- populations, followed by the CD45RA+ CCR7+ population **(Figure 5.11)**.

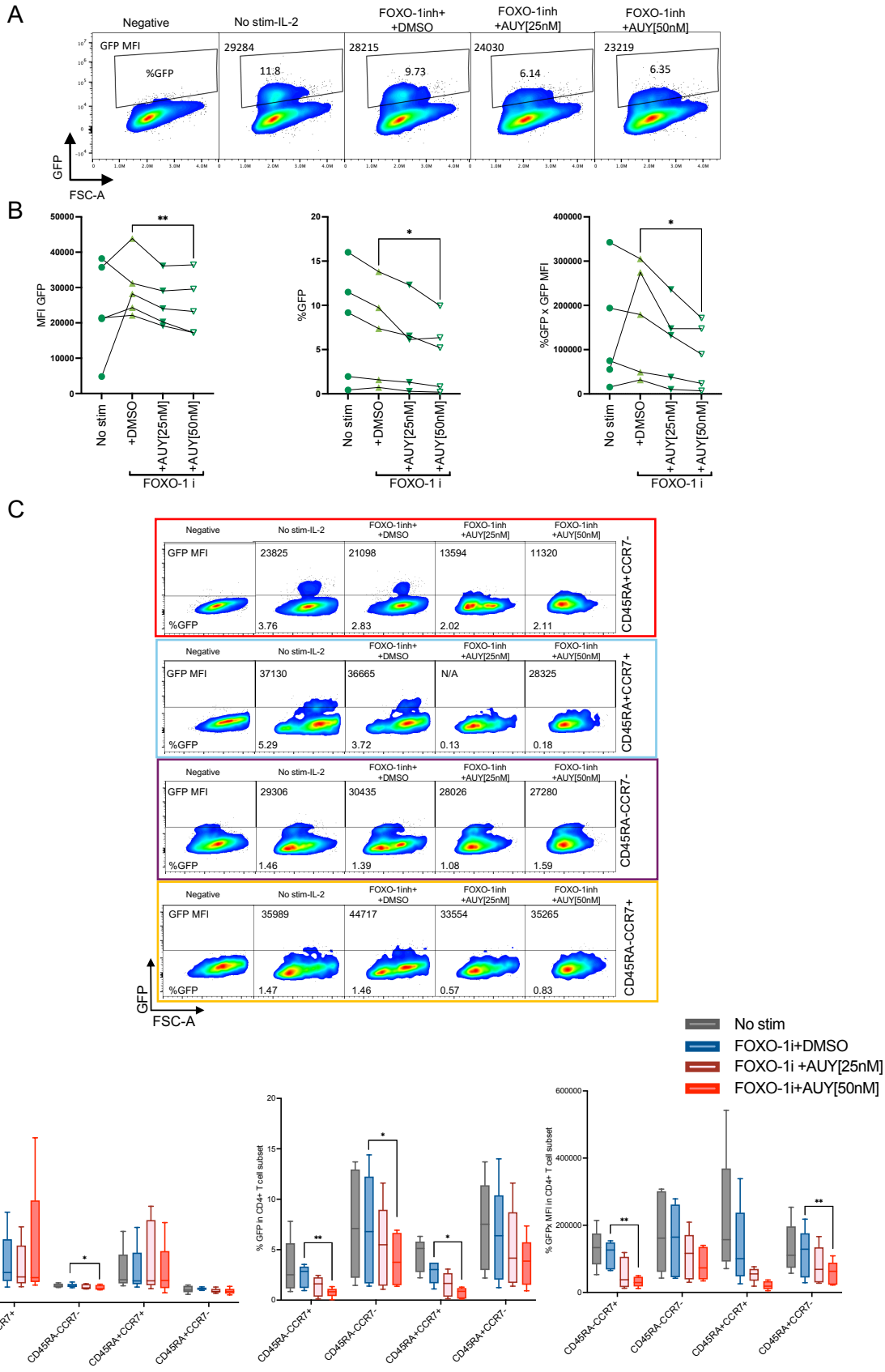
A
Negative
No stim-IL-2
FOXO-1inh+ +DMSO
FOXO-1inh +AUY[25nM]
FOXO-1inh +AUY[50nM]
GFP MFI
%GFP
29284
11.8
28215
9.73
24030
6.14
23219
6.35
GFP
FSC-A
B
MFI GFP
%GFP
%GFP x GFP MFI
No stim
+DMSO
+AUY[25nM]
+AUY[50nM]
FOXO-1 i
C
GFP MFI
%GFP
23825
3.76
21098
2.83
13594
2.02
11320
2.11
CD45RA+CCR7-
37130
5.29
36665
3.72
N/A
0.13
28325
0.18
CD45RA+CCR7+
29306
1.46
30435
1.39
28026
1.08
27280
1.59
CD45RA-CCR7-
35989
1.47
44717
1.46
33554
0.57
35265
0.83
CD45RA-CCR7+
GFP
FSC-A
D
No stim
FOXO-1i+DMSO
FOXO-1i +AUY[25nM]
FOXO-1i+AUY[50nM]
GFP MFI of CD4+ T cell subset
% GFP in CD4+ T cell subset
% GFPx MFI in CD4+ T cell subset
CD45RA-CCR7+
CD45RA-CCR7-
CD45RA+CCR7+
CD45RA+CCR7-

Figure 5.11. Effect of AUY922 on HIV-1 reactivation induced by FOXO-1 inhibitor in primary CD4+ T cell subsets. Latently infected primary CD4+ T cells were generated *ex-vivo*, as described in Figure 5.5. Cells were re-stimulated on day 9 or 11 with FOXO-1 inhibitor with or without AUY922 [25 nM or 50 nM] or DMSO. Cells were analysed by spectral flow cytometry using the same antibody panel used in Figure 5.4, in addition to GFP and CD71. (A) Representative flow plots showing the GFP MFI before (No stim-IL-2) and after re-stimulation FOXO-1 inhibitor or AUY922 [25 or 50 nM]. (B) Graphs showing the results for 5 donors: GFP MFI (left panel), percentage of GFP+ cells (middle panel), and combined % GFP x MFI in the CD45RA- CD45RO+ population. (C) Representative flow plots showing the gating for GFP+ in different T cell subsets with different conditions (no stim-IL-2) and after re-stimulation with FOXO-1i or AUY922 [25 or 50 nM]. (D) Results from five donors are shown for the GFP MFI (right panel), percentage of GFP+ cells (middle panel) and combined % GFP x MFI (right panel) in each CD4+ T cell subset. Bar plots show 1st quartile, 3rd quartile and median for five donors. Statistical significance was calculated using a two-tailed paired t-Test comparing FOXO-1 inhibitor versus no stim-IL-2, and FOXO-1 inhibitor versus 50 nM AUY922, *=p≤0.05; **=p≤0.01; ***=p≤0.001; ****=p<0.0001.

Additionally, the FOXO-1 inhibitor significantly upregulated CD25, downregulated CD69 and showed a trend for CD71 upregulation **(Figure5.12)**. It is not clear how the FOXO-1 inhibitor downregulated CD69 expression. No other significant change in T cell subset except the significant increase in Teh2 after stimulation.

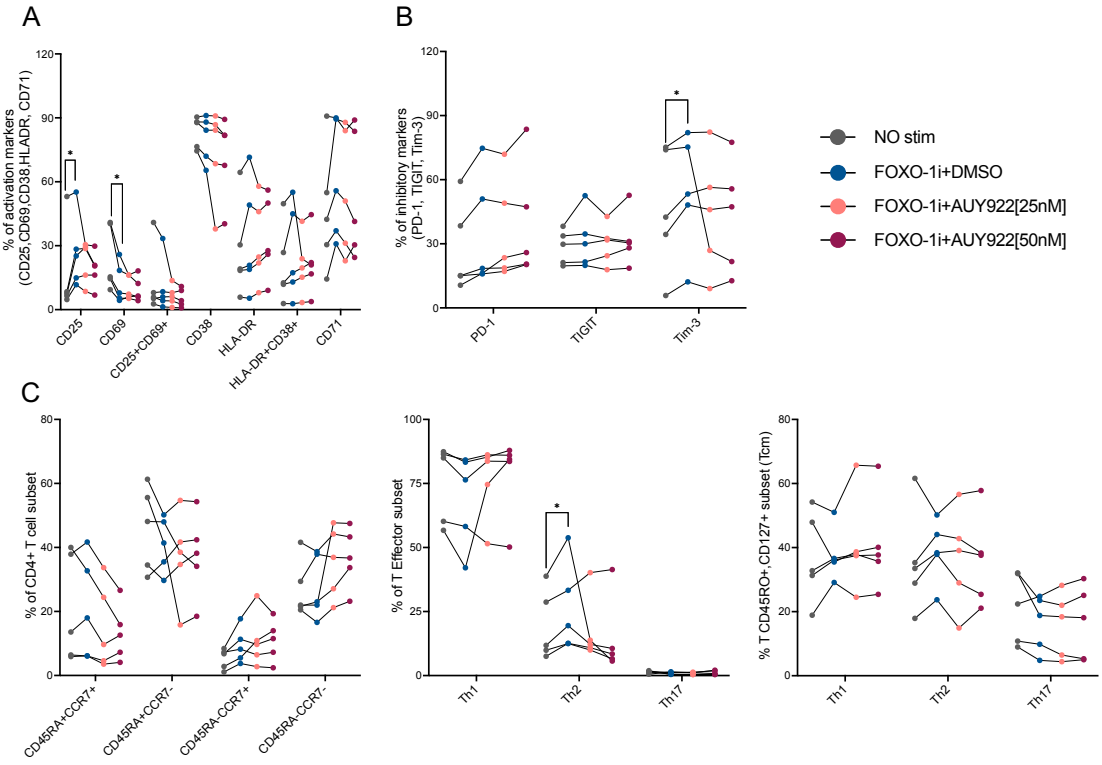

Figure 5.12. AUY922 does not significantly change the CD4+ T cell phenotype or activation state upon FOXO-1i activation. Latently infected primary CD4+ T cells were re-stimulated on day 9 or 11 with the FOXO-1 inhibitor with or without AUY922 [25 nM or 50 nM] or DMSO. Cells were analysed by spectral flow cytometry using the same antibody panel used in Figure 5.4 with the addition of CD71. (A) show T cell activation markers B) inhibitory markers (C) CD4 T cell subsets, effector subsets and memory subsets after re-stimulation FOXO-1i plus AUY922 [25 or 50 nM] or DMSO. Results were obtained from five different donors. Statistical significance was calculated using a two-tailed paired t-Test comparing, within each cell sub-type, FOXO-1 inhibitor versus no stim (IL-2), FOXO-1 inhibitor versus 50 nM AUY922, *=p≤0.05; **=p≤0.01; ***=p≤0.001; ****=p<0.0001.

5.2.3.4 TLR7 agonist

To test the Hsp90 dependence of the TLR7 signal transduction pathways, latently infected cells from 4 different donors were stimulated with TLR7 agonist [5μg/mL] and treated with either DMSO or AUY922 [25nM or 50nM] for 48h. Treated cells were analysed by flow cytometry as previously described.

Upon TLR7 stimulation, one donor showed an increase in both the GFP MFI and the percentage of GFP+ cells measured in CD45RA- CD45RO+ cells, indicating virus reactivation, and AUY922 abrogated this effect. However, the other donors failed to induce viral reactivation and yet AUY922 reduced viral reactivation below the baseline of unstimulated CD45RA- CD45RO+ cells in 3 out of 4 donors. Within specific CD4+ T cell subsets, we noticed a trend for AUY922-mediated inhibition of viral gene expression (% GFP x MFI) in CD45RA+ CCR7+ cells, followed by CD45RA+ CCR7- cells and CD45RA- CCR7+ although the results were not statistically significant mostly due to the noticeable variation between the donors **(Figure 5.13)**.

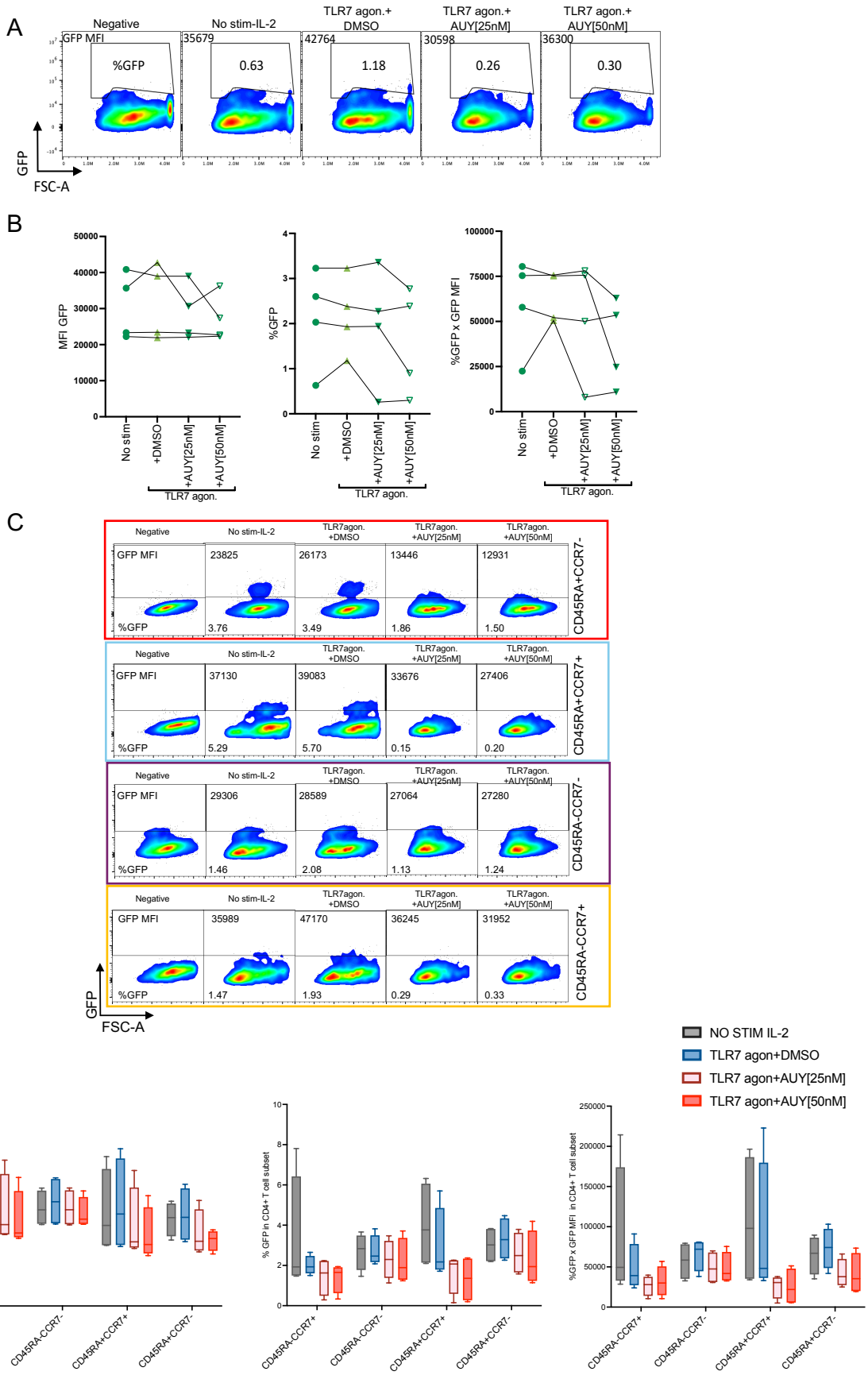
A
Negative
No stim-IL-2
TLR7 agon.+ DMSO
TLR7 agon.+ AUY[25nM]
TLR7 agon.+ AUY[50nM]
GFP MFI
35679
42764
30598
36300
%GFP
0.63
1.18
0.26
0.30
GFP
FSC-A
B
MFI GFP
%GFP
%GFP x GFP MFI
No stim
+DMSO
+AUY[25nM]
+AUY[50nM]
TLR7 agon.
C
Negative
No stim-IL-2
TLR7agon. +DMSO
TLR7agon. +AUY[25nM]
TLR7agon. +AUY[50nM]
GFP MFI
%GFP
23825
26173
13446
12931
3.76
3.49
1.86
1.50
CD45RA+CCR7-
37130
39083
33676
27406
5.29
5.70
0.15
0.20
CD45RA+CCR7+
29306
28589
27064
27280
1.46
2.08
1.13
1.24
CD45RA-CCR7-
35989
47170
36245
31952
1.47
1.93
0.29
0.33
CD45RA-CCR7+
GFP
FSC-A
D
NO STIM IL-2
TLR7 agon+DMSO
TLR7 agon+AUY[25nM]
TLR7 agon+AUY[50nM]
GFP MFI in CD4+ T cell subset
% GFP in CD4+ T cell subset
%GFP x GFP MFI in CD4+ T cell subset
CD45RA-CCR7+
CD45RA-CCR7-
CD45RA+CCR7+
CD45RA+CCR7-

Figure 5.13. Effect of AUY922 on HIV-1 reactivation induced by TLR7 agonist name in primary CD4+ T cell subsets. Latently infected primary CD4+ T cells were generated *ex-vivo*, as described in Figure 5.5. Cells were re-stimulated on day 9 or 11 with TLR7 agon. with or without AUY922 [25 nM or 50 nM] or DMSO. Cells were analysed by spectral flow cytometry using the same antibody panel used in Figure 5.4, in addition to GFP and CD71. (A) Representative flow plots showing the GFP MFI before (no stim-IL-2) and after re-stimulation TLR7 agon. or AUY922 [25 or 50 nM]. (B) Graphs showing the results for 4 donors: GFP MFI (left panel), percentage of GFP+ cells (middle panel), and combined % GFP x MFI in the CD45RA- CD45RO+ population. (C) Representative flow plots showing the gating for GFP+ in different T cell subsets with different conditions (no stim-IL-2) and after re-stimulation with TLR7 agon. or AUY922 [25 or 50 nM]. (D) Results from 4 donors are shown for the GFP MFI (right panel), percentage of GFP+ cells (middle panel) and combined % GFP x MFI (right panel) in each CD4+ T cell subset. Statistical significance was calculated using a two-tailed paired t-Test comparing TLR7 agon. versus no stim-IL-2, and TLR7 agon. versus 50 nM AUY922, *=p≤0.05; **=p≤0.01; ***=p≤0.001; ****=p<0.0001.

Regarding T cell phenotype, significant variability was observed among the four donors when treated with the TLR7 agonist, with no notable upregulation of activation or inhibitory markers **(Figure 5.14).** Similarly, analysis of T cell subsets revealed no significant changes following activation or treatment with the TLR agonist and AUY922.

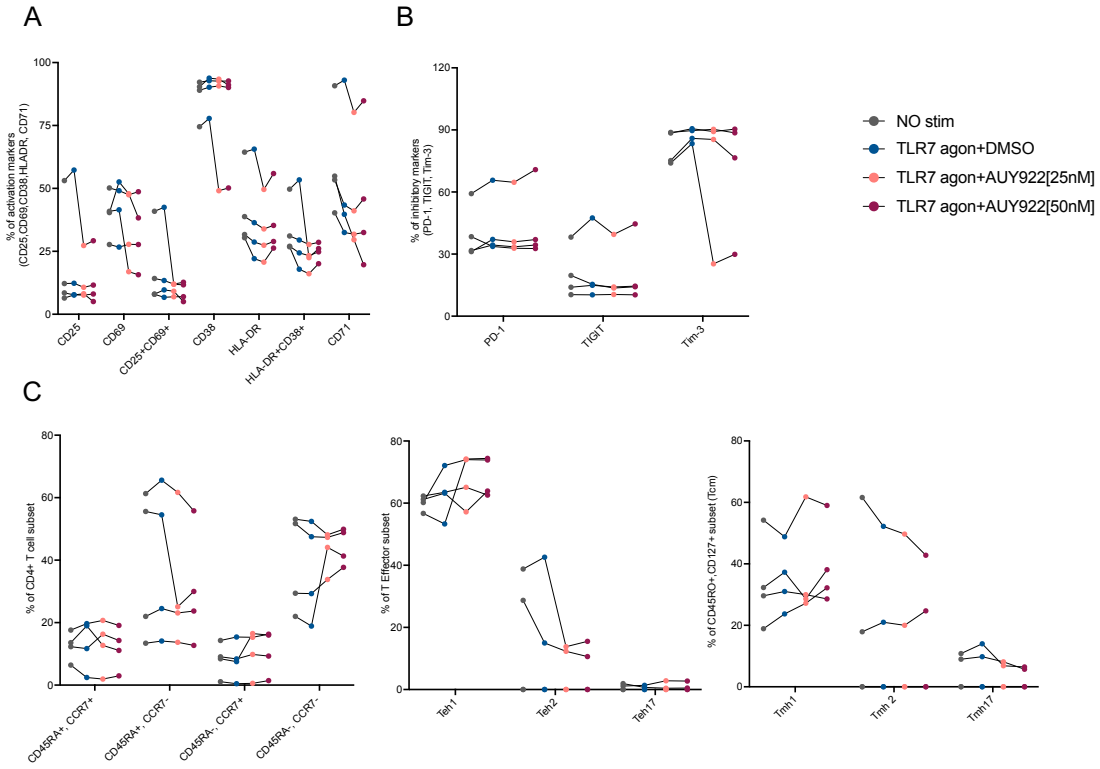

Figure 5.14. AUY922 does not significantly change the CD4+ T cell phenotype or activation state upon TLR7 agonist activation. Latently infected primary CD4+ T cells were re-stimulated on day 9 or 11 with the TLR7 agon. with or without AUY922 [25 nM or 50 nM] or DMSO. Cells were analysed by spectral flow cytometry using the same antibody panel used in Figure 5.4 with the addition of CD71. (A) show T cell activation markers B) inhibitory markers (C) CD4 T cell subsets, effector subsets and memory subsets after re-stimulation TLR7agon. plus AUY922 [25 or 50 nM] or DMSO. Results were obtained from 4 different donors. Statistical significance was calculated using a two-tailed paired t-Test comparing, within each cell sub-type, TLR7agon.versus no stim (IL-2), TLR7agon. versus 50 nM AUY922, *=p≤0.05; **=p≤0.01; ***=p≤0.001; ****=p<0.0001.

It is not clear why IL7 + IL15, the FOXO-1 inhibitor and TLR7 agonist. did not trigger appreciable viral reactivation however we note that the conditions of the experiments on Jurkat cells and on primary CD4+ T cells were different, mainly because the primary cells had been pre-stimulated with anti-CD3/CD28 Abs to make them permissive to HIV-1 infection 10 days before re-stimulation, which might have

affected their response to the LRAs themselves. Furthermore, the threshold for the response to LRAs might be different between Jurkat and primary cells. Nonetheless, the results confirmed that targeting Hsp90 reduced TCR-induced reactivation and inhibited baseline viral gene expression in latently infected cells even in the presence of IL7 and IL15, the FOXO-1 inhibitor or TLR7 agon. Notably, in our experimental conditions, the Hsp90 antagonists did not significantly affect the phenotype of CD4+ T cells, suggesting that they have a good level of selectivity for HIV.

The presence of IL-2 at all stages was essential for cell survival in our experimental conditions and so we were unable to control for its effects. However, we found that treatment with AUY922 did not reduce baseline HIV-1 gene expression in the presence of IL-2 alone **(Figure 5.15)**. Thus, background activity of IL-2 might have partially masked the reactivating effect of IL7/IL15, the FOXO-1 inhibitor, and TLR7 agon., but the effect of AUY922 appeared to depend on the addition of these LRAs.

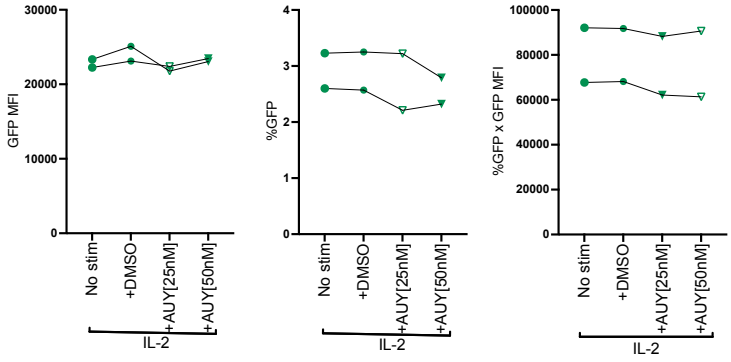

Figure 5.15 Effect of AUY922 on latently infected primary CD4+ T cells treated with IL-2 only. Latently infected primary CD4+ T cells were generated *ex-vivo* as described in Figure 5.5 A. On day 9 or 11, cells were treated with AUY922 [25 nM or 50 nM] or DMSO in the presence of IL-2. Graphs showing the results for 2 donors: GFP MFI (left panel), percentage of GFP+ cells (middle panel), and combined % GFP x MFI in the CD45RA-CD45RO+ population.

5.2.4 The effect of AUY922 treatment on different cytokine production.

Next, to gain further insight into the effect of AUY922 on CD4+ T cells, we investigated if treatment with the drug affected cytokines production from activated CD4+ T cells. To this end, the supernatant from the cell cultures of the same 5 donors described in **(Figure 5.16)** was collected 48h post-re-stimulation with anti-CD3/CD28 Abs. The levels of cytokines were quantified using the LEGENDplex Multi-Analyte Flow Assay Kit from BioLegend. This multiple bead-based immunoassay is based on the basic ELISA-type sandwich-assay principle. Each bead is coated with a specific antibody for the cytokine or chemokine of interest [260]. Subsequently, these beads were differentiated by size and internal fluorescence intensity using a flow cytometer and the concentration of 5 cytokines that define specific subsets of effector CD4+ T cells was measured: IFN-γ and TNF-α (Th1), IL-4 and IL-10 (Th2) and IL-17A (Th17) [240]. The results showed that TCR stimulation was able to significantly increase the production of all tested cytokines, however AUY922 at 25 nM or 50 nM significantly but modestly inhibited only IL-4 and IL-10 production **(Figure 5.16)**. There was a downward trend for the other cytokines in the AUY922-treated samples compared to untreated, but it did not reach statistical significance. These results confirmed that inhibition of Hsp90 did not broadly perturb CD4+ T cell function, although it might modestly reduce production of some Th2 and Th1 cytokines.

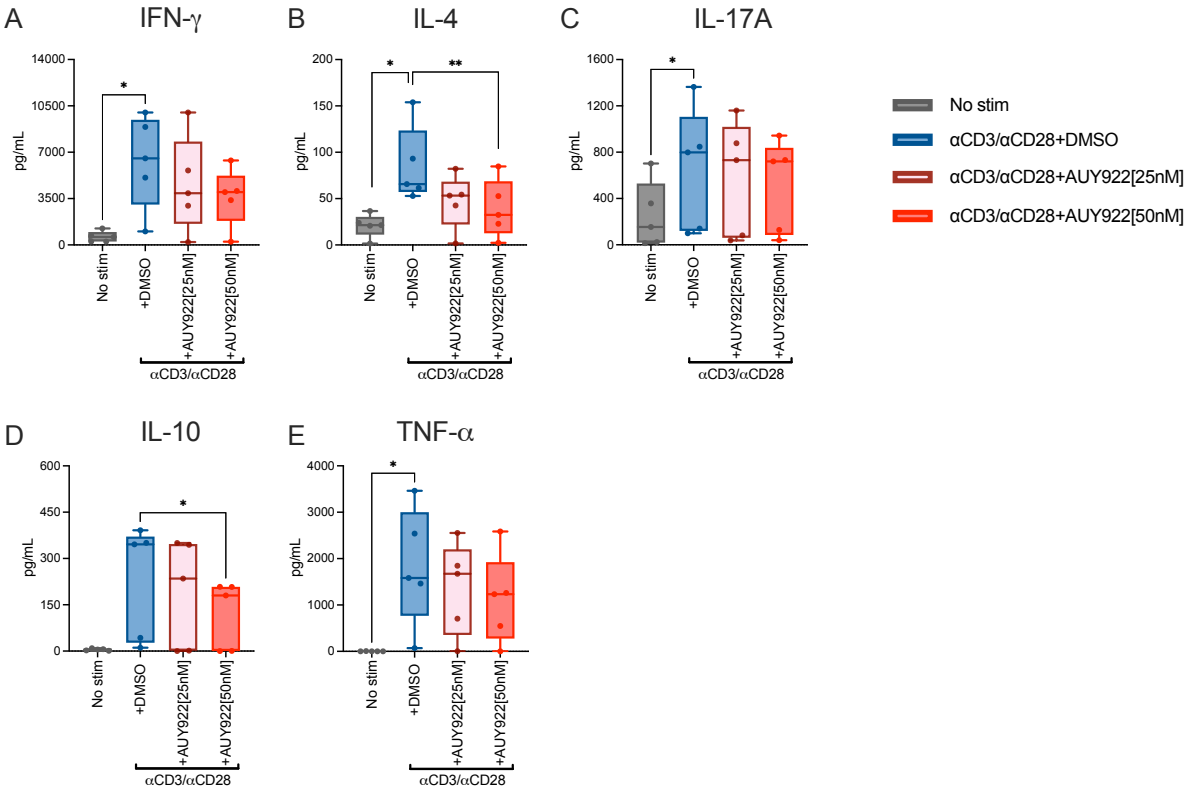

Figure 5.16 The effect of AUY922 treatment on different cytokine production. Supernatant from latently infected CD4+ T cells, which were re-stimulated with anti-CD3/CD28 Abs in the presence or absence of DMSO (control), AUY922 (25 nM), or AUY922 (50 nM), was collected 48 hours after re-stimulation and used to measure different cytokines concentration. (A) IFN-γ, (B) IL-4, (C) IL-17A, (D) IL-10, and (E) TNF-α. Data are presented as mean ± standard error of the mean (SEM) n=5. Concentrations are shown in pg/ml. Statistical significance was determined using a Paired two-tailed Student's t-test. *P < 0.05, **P < 0.01, ***P < 0.001. Pairwise comparisons were: No stim-IL-2 and anti-CD3/CD28 Abs;; anti-CD3/CD28 Abs and AUY922 50 nM.

5.3 Discussion

Although the Jurkat model was useful to screen the Hsp90-dependency of different LRAs, it also has several limitations because it is a transformed cell line and may not fully recapitulate the behaviour of primary cells. For example, IL7 did not reactivate latent HIV-1 in Jurkat cells despite it being a known LRA in primary cells [206].

Therefore, I have extended the screening to primary CD4+T cells. One important aspect for LRAs and for LPAs is their selectivity towards the integrated provirus, and whether they substantially perturb T cell function, which is undesirable. To examine this aspect, I have employed multi-parameter flow cytometry to assess the effect of a short course AUY922 treatment *in-vitro* on the phenotype of CD4+ T cells before proceeding to the more complex experiment with latently infected cells. I characterized different T cell subsets and analysed markers of activation and inhibitory “exhaustion” in the primary cells isolated from healthy donors before and after stimulation and upon addition of AUY922. I found that although stimulation changed the T cell population distribution in some donors tested, AUY922 did not significantly affect the T cell subset distribution compared to stimulated cells; however, CD69, and CD25 showed a trend of reduction after AUY922 treatment in 2 out of 4 donors.

The multicolour panel that we used depends only on surface markers to distinguish between T cell types, which could be considered as a drawback. However, with our model, we could not include intracellular markers because to stain for intracellular

cytokines, cells would need to be fixed and permeabilized, which could affect detection of surface markers and possibly the GFP signal. Nonetheless, in the future we could verify our results using more advanced techniques such single cell sequencing analysis, which would give us a more comprehensive insight into the effect of AUY922 on T cell biology.

The analysis was extended to *ex-vivo* infected latent primary cells. This was achieved by activating cells by TCR stimulation, infection with a single cycle HIV-1 virus and allowing the cells to return to a state of semi-quiescence, which was accompanied by HIV-1 latency. Then some of the LRAs that were tested in the Jurkat model were tested in primary cells. The results from latently infected primary T cell showed promise, as AUY922 was able to inhibit HIV-1 reactivation by anti-CD3/CD28 Abs, without inducing broad changes in T cell activation or differentiation. Nonetheless, even when the specific LRA (IL7/IL15, FOXO-1i or TLR7agonist) was not able to reactivate the latent virus, AUY922 was able to reduce viral gene expression to level below base line (unstimulated). This indicated that Hsp90 is required for basal HIV-1 gene expression and is consistent with findings in Jurkat cells showing that Hsp90 localizes with the actively transcribing provirus [101].

Our results showed that distinct CD4+ T cell subsets responded differently to LRAs and AUY922, with the strongest reactivation observed in CD45RA+ CCR7+ cells “naïve T cells”. Central memory (CD45RA- CCR7+) and effector memory (CD45RA-CCR7-) subsets also showed reactivation, though to a lesser extent, consistent with earlier findings [243,255]. While variability in LRA responses across subsets is

documented, the precise mechanisms remain unclear [242,261]. Our findings point to a subtype-specific sensitivity to Hsp90 inhibition, highlighting the need for more research on how Hsp90 and LRAs interact to control HIV-1 latency in various CD4+ T cell subsets.

Overall, the reactivation level of the virus was different from one stimulus to another, and this could be because each stimulus reactivates the virus through a unique pathway which involve different cellular factors. Another reason could be that some stimuli are weak and could be used as an adjuvant instead of using them individually. We chose to use individual stimuli in order to determine whether they are Hsp90-dependent and to dissect the pathways involved, which could help identify new targets for inhibiting HIV-1 reactivation. However, we could use a combination of stimuli in the future. Partial reactivation of latent HIV-1, regardless of the stimulus tested, remains a challenge. One explanation may be related to the integration site of the provirus. Proviruses integrated into highly condensed chromatin regions, such as centromeric satellite DNA, may become “superlatent” and fail to respond to LRAs [262].

Other epigenetic factors, such as DNA methylation, may also play a role in suppressing reactivation. Methylation of CpG islands in the HIV-1 promoter could reduce transcriptional activity and contribute to latency [263,264]. To assess the role of methylation, techniques such as bisulfite sequencing could be employed to analyse the methylation status of the LTR region in latent proviruses [264]. It is also important to consider that some proviruses may be defective, containing mutations

or deletions that render them incapable of producing functional virus even upon reactivation. This could explain why partial reactivation is observed in patients' cells [265]. Quantifying intact proviruses could be achieved through methods like intact proviral DNA assays (IPDA), which distinguish between intact and defective proviruses [266]. Monitoring these variables in primary cells from ART patients may help identify the drawbacks of latency-reversing techniques and open the door to more focused methods of eradicating latent reservoirs.

Chapter 6: Discussion

HIV-1 latency is a dynamic and multifaceted phenomenon influenced by various molecular and cellular factors that together suppress viral gene expression. One critical aspect of latency is its reliance on the quiescent state of CD4+ T cells, which allows the virus to evade immune detection and persist in a dormant state. However, the activation of these resting T cells can disrupt latency and reactivating viral replication, presenting a challenge for achieving an HIV-1 cure. T cell activation triggers latent HIV-1 reactivation through diverse signaling pathways, including those linked to epigenetic remodelling and transcriptional activation, often acting synergistically to amplify viral gene expression.

This complexity suggests the necessity of identifying and targeting key molecular regulators that can override latency and effectively control HIV reactivation. Approaches such as latency-reversing agents aim to induce reactivation, facilitating immune-mediated clearance of infected cells. However, this strategy must be carefully managed to avoid undesired consequences, such as the expansion of viral reservoirs or incomplete immune clearance, which could further complicate viral eradication. Advances in our understanding of the cellular and molecular mechanisms controlling latency offer opportunities to design more precise therapeutic interventions that balance reactivation and clearance, ultimately advancing the goal of an HIV cure.

Here, we have confirmed that inhibiting Hsp90 antagonises HIV-1 reactivation triggered by LRAs previously reported to reactivate HIV-1 in models of latency and *ex-vivo* in patients' cells [156,166,173,196] such as TCR, PMA, PHA and TNF-α [101,267] and showed, for the first time to our knowledge, that Hsp90 is also required for HIV-1 reactivation induced by TLR7 and TLR8 stimulation and FOXO-1 inhibition. No significant loss of cell viability was detected in our experimental conditions and similar results were obtained using AUY922 or 17-AAG, two structurally different Hsp90 inhibitors that bind to the same ATPase pocket in the N-terminal region of the chaperone, supporting the specificity of the effect. AUY922 was chosen for our experiments because it is a well-characterized drug that has been used in phase II and III clinical trials [135].

The Jurkat latency model established in our laboratory distinguishes from the widely studied J-Lat model due to its polyclonal nature, which better mirrors the complexity of *in-vivo* latency. Unlike monoclonal models, our polyclonal system incorporates latently infected cells harbouring a diverse array of proviral integration sites. This diversity provides a more comprehensive representation of the factors influencing latency and reactivation. Ongoing investigations are focused on mapping the distribution of these integration sites to better understand their role in maintaining latency.

The location of proviral integration is a critical determinant of viral latency, as it significantly affects the virus's capacity for reactivation and its susceptibility to pharmacological interventions [212,213]. In the future, by studying individual clones

with known viral integration sites within this polyclonal model, we aim to uncover new insights into the mechanisms that influence HIV-1 reactivation and its requirement for Hsp90.

The inhibitory effect of AUY922 on HIV-1 reactivation appears to be extensive, impacting multiple pathways that are naturally involved in reactivating latent viruses. This broad effect is likely attributable to the diverse array of client proteins that rely on Hsp90 for proper folding and functional assembly, many of which are critical components in the signaling pathways necessary for HIV-1 reactivation. Previous studies, including our own, have demonstrated that Hsp90 is an integral part of the IKK complex, where it supports its activity, and that it stabilizes P-TEFb, which is essential for efficient viral transcription [101] .

Our findings build on these observations, revealing that Hsp90 plays a pivotal role in regulating key signaling pathways such as NF-kB and AP-1, while exerting a more moderate effect on NFAT signaling. This underscores Hsp90's central role in coordinating multiple processes required for viral reactivation. We confirmed that AUY922 treatment reduced total TAK1 levels in stimulated cells, and that direct targeting of TAK1 recapitulated the effects of AUY922 in latently infected cells. These results suggest that the anti-reactivation activity of AUY922 may, at least in part, be mediated through its impact on TAK1. However, it remains possible that 5Z exerts additional effects through other unidentified targets, leaving room for further investigation into the precise mechanisms underlying AUY922's broad inhibitory action.

Our findings indicate that both Hsp90 and TAK1 are essential for the reactivation of HIV-1; however, their roles in downstream signaling pathways may vary depending on the cellular context. This context-dependent influence suggests the existence of alternative mechanisms that require further exploration. By dissecting the interplay between Hsp90, TAK1, and the signaling pathways involved in viral reactivation, we may identify new avenues for therapeutic intervention to better manage or potentially eradicate latent HIV-1.

Our results support the notion that Hsp90 is a master regulator of HIV-1 latency. But does inhibition of Hsp90 address the second problem related to the effect of latency potentiating agents on the physiology of the infected CD4+ T cells?

To examine this aspect, multi-parameter flow cytometry was employed to understand the effect of a short course AUY922 treatment *in-vitro* on the phenotype of activated CD4+ T cells before proceeding to the more complex experiment with latently infected cells. The panel of markers were chosen to identify several subsets of CD4+ T cells, including naïve, effector, central memory, effector memory and subtypes Th1, Th2 and Th17. We have also employed surface markers of activation, whose expression changed depending on the applied LRA in agreement with its known physiological effect. Overall, the results of these experiments revealed no significant change in any of the cell phenotypes, suggesting that the degree of Hsp90 inhibition applied to inhibit HIV-1 reactivation was well tolerated.

The analysis was then extended to latent primary cells. To this end we generated the *ex-vivo* CD4+ latently infected cells, which was achieved by activating cells by TCR stimulation to make the cells permissive to HIV-1 infection, and then allowing the cells to return to a state of semi-quiescence and establishing the viral latency by passaging the cells and a second round of stimulation with LRAs to trigger viral reactivation in the presence of AUY922.

In this model, we successfully established viral latency, although variability was observed between donors in the extent of latency and reactivation. Treatment with AUY922 demonstrated an inhibitory effect on viral reactivation, reducing the levels of viral gene expression as indicated by the GFP MFI. However, AUY922 did not completely block reactivation, as evidenced by the percentage of GFP+ cells remaining relatively stable. This response contrasted with results from Jurkat cells, where AUY922 reduced both GFP MFI and the proportion of GFP+ cells, indicating a stronger drug effect in the Jurkat cell line. This difference could be attributed to the increased sensitivity of cancer cells, such as Jurkat cells, to Hsp90 inhibitors. This heightened sensitivity in cancer cells has been associated with their elevated dependence on Hsp90 to support higher rates of protein synthesis and metabolic activity. Additionally, it has been suggested that cancer cells may possess specific Hsp90 complexes [268,269] with a conformation that enhances drug targeting, though this remains controversial. These differences highlight the unique responses between primary CD4+ T cells and Jurkat cells when exposed to Hsp90 inhibitors like AUY922 [269].

IL7 and IL15 did not enhance the viral reactivation in primary cells or the Jurkat model of latency. While the lack of an effect in the Jurkat cells is explained by the lack of the IL7 receptor, our expectation was that this cytokine would work in the primary cells since it has been shown to activate latent HIV-1 in human CD4+ T cells from humanized mice and in patient cells at the same concentrations we tested [166,206]. However, this effect was found to be proviral-strain specific, it varied from donor to donor and was seen after several days of exposure to IL7 [167,206]. Furthermore, significant IL7 induced reactivation is not universally observed [270,271]. We detected upregulation of HLA-DR, as previously described [173], and CD71 upon treatment with IL7/IL15 which confirmed the activity of the IL7/IL15 on the cells, but we did not detect viral reactivation. We speculate that the shorter treatment period used in our experiments compared to the other studies might explain the different results [167,206]. It is also possible that IL-2, by partly stimulating HIV-1 gene expression, masked the activating effect of IL7/IL15. Notably, AUY922 suppressed viral gene expression below the baseline even in the presence of IL7/IL15, confirming its activity on the HIV-1 promoter [101].

Exposure of the primary cells to the FOXO-1 inhibitor also failed to induce detectable HIV-1 reactivation, but increased surface expression of CD71, consistent with prior studies [170]. This finding contrasts with the reactivation reported in other studies [170,196]. As in the case of IL7/IL15, it is possible that this difference is attributable to the limited time of exposure to the FOXO-1 inhibitor. Unfortunately, our primary latency model could not be extended beyond 12–13 days due to a significant decline in cell viability beyond this timeframe. Despite these limitations, AUY922 further

suppressed viral reactivation, reducing it to levels below the baseline of untreated cells, even in the presence of the FOXO-1 inhibitor.

TCR stimulation showed strong reactivation of the viral HIV-1 which was significantly inhibited by AUY922. Different cell subsets showed different responses to the LRAs and AUY922. Overall, the strongest viral reactivation after TCR stimulation and the greatest susceptibility to AUY922 was detected in CD45RA+ CCR7+ cells, which is largely made of naïve cells but can also contain a small proportion of T memory stem cells (Tscm) [272] followed by CD45RA- CCR7+ central memory cells, and CD45RA- CCR7- effector memory cells, which agrees with a previous study [194]. Certain CD4+ T cell subsets have been shown to be more susceptible to specific LRAs but the reasons for this behaviour are not clear [242,244,261,273]. Our results extend these observations to include CD4+ T cell subtype-specific responses to Hsp90 inhibition and it will be interesting to investigate the mechanistic reason for this phenotype and how different LRAs and Hsp90 intersect in the different CD4+ T cell subtypes.

Interestingly, AUY922 treatment did not significantly affect the distribution of CD4+ T cell subtypes within the population and only had a minor impact on Th1 and Th2 cytokine production. These findings suggest that inhibiting Hsp90 can reduce HIV-1 reactivation without substantially altering CD4+ T cell differentiation or activation status under the conditions tested. Additionally, the slight reduction in Th1 cytokine production could be beneficial for PLWH, as they often experience elevated levels of systemic inflammation. TCR stimulation enhanced surface expression of activation

and inhibitory markers and reduced the relative proportion of the markers for Th1 cells, indicating that our readout was able to detect phenotypic changes in the samples.

Considering that Hsp90 participates in a wide variety of cellular pathways, these results may seem surprising. Selectivity is usually a function of the drug concentration and time of exposure, which in our case was limited to 48 hours. It is possible that a longer incubation time in the presence of the drug may affect the phenotype of CD4+ T cells, and it should be possible to evaluate this aspect in patients who are being treated with AUY922 or other Hsp90 inhibitors in clinical trials [274].

Our study has some limitations. One key limitation is the use of a modified HIV-1 vector instead of the wild-type virus. While the single-cycle virus employed in our experiments is a well-established and widely accepted model for studying HIV-1 latency, it does not produce viral proteins, thereby reducing cell toxicity and addressing concerns about defective proviruses, which often appear latent due to significant deletions or rearrangements generated during multiple rounds of replication. However, this modified virus lacks the accessory protein Vpr, which has been shown to reprogramme infected T cells and modulate activation markers like CD69. The absence of Vpr represents a potential drawback, as it may not fully capture the natural dynamics of HIV-1 infection and latency. Future investigations should explore whether latency in a more replication-competent virus remains susceptible to Hsp90 inhibition. Additionally, using primary cells from HIV-1-infected

individuals could provide a more physiologically relevant understanding of the effects of Hsp90 inhibitors on latent reservoirs. Notably, recent studies have demonstrated that 17-AAG significantly inhibited HIV-1 reactivation in cells from patients with latent infection [143].

Moreover, in this study, T cell activation was achieved using anti-CD3 and anti-CD28 antibodies, a widely utilized method for polyclonal T cell stimulation. While this approach is effective in inducing robust T cell activation, it is inherently artificial and does not accurately mimic physiological TCR engagement. Specifically, anti-CD3 stimulation bypasses natural antigen recognition by directly cross-linking the CD3 complex, leading to broad, non-specific activation of T cells regardless of their antigen specificity [180]. This limitation reduces the ability to assess antigen-specific responses and may not fully reflect the dynamics of T cell activation as they occur *in-vivo.*

To address this, future experiments should consider more physiological methods, such as stimulating T cells with HIV-1 specific peptides presented by autologous or HLA-matched antigen-presenting cells (APCs), including dendritic cells, B cells, or monocytes. This strategy allows for selective activation of HIV-specific T cells through engagement of the native TCR–peptide–MHC interaction. In this approach, short peptides derived from immunodominant regions of HIV-1 proteins such as Gag, Pol, Nef, or Env are pulsed onto APCs and presented via MHC class I or class II molecules to CD8+ or CD4+ T cells, respectively. Such antigen-specific stimulation provides a more accurate representation of immune responses observed during

natural infection and is particularly valuable in evaluating the functional capacity of HIV-specific T cells [275–277].

Another limitation lies in the multicolour panel used to distinguish T cell subtypes, which relied solely on surface markers. Nonetheless, in the future we could verify our results using more advanced techniques such single cell sequencing analysis, which would give us a more comprehensive insight into the effect of AUY922 on T cell biology.

Our findings offer potential relevance to functional cure strategies. Notably, a study using a humanized mouse model demonstrated that short-term treatment with AUY922 prevented long-term HIV-1 rebound [102]. This supports the idea that AUY922 could contribute to a block-and-lock approach by reinforcing the latent state of the virus. Including AUY922 in HIV-1 treatment regimens could theoretically help maintain latency more permanently. Importantly, AUY922 has undergone phase II clinical trials (www.clinicaltrials.gov) for cancer treatment. While its anti-cancer efficacy was limited, these trials provided valuable insights into the drug's therapeutic index and manageable side effects, such as blue-color vision disturbances and gastrointestinal symptoms [278]. Interestingly, our results suggest that AUY922 concentrations well below the lowest doses used in clinical trials are sufficient to inhibit HIV-1 reactivation.

Hsp90 also supports the replication of various RNA and DNA viruses [117], including early gene expression in human cytomegalovirus (HCMV) [279] making it a broad-

spectrum antiviral target that could benefit people living with HIV who often experience co-infections [280].

While AUY922 shows promise, translating these findings into clinical applications remains a challenge. Its inclusion in ART regimens could benefit individuals struggling to achieve complete viral suppression. Further research is needed to evaluate the pharmacokinetics, safety, and tolerability of AUY922 in combination with ART. Additionally, its minimal impact on CD4+ T cell phenotypes and limited effects on cytokine production suggest that it may suppress HIV-1 reactivation without causing significant immune dysregulation. Exploring potential synergies between AUY922 and agents like Tat inhibitors [281] or AhR (The aryl hydrocarbon receptor) agonists [282], could enhance its ability to provide durable viral suppression. Overall, Hsp90 inhibitors such as AUY922 represent an exciting avenue for advancing functional cure strategies, offering hope for bridging the gap between experimental findings and clinical applications.

References

1. UNAIDS website. Global HIV & AIDS statistics—Fact sheet. In: https://www.unaids.org/en/resources/fact-sheet. 2023.
2. Sharp PM, Hahn BH. Origins of HIV and the AIDS pandemic. Cold Spring Harb Perspect Med. 2011;1. doi:10.1101/cshperspect.a006841
3. Simon V, Ho DD, Abdool Karim Q. HIV/AIDS epidemiology, pathogenesis, prevention, and treatment. Lancet. Elsevier B.V.; 2006. pp. 489–504. doi:10.1016/S0140-6736(06)69157-5
4. Woodburn B, Emery A, Swanstrom R. Human Immunodeficiency Virus (Retroviridae). Encyclopedia of Virology: Volume 1-5, Fourth Edition. Elsevier; 2020. pp. 460–474. doi:10.1016/B978-0-12-814515-9.00042-4
5. Merson MH, Rey O'malley J, Serwadda D, Apisuk C. HIV Prevention 1 The history and challenge of HIV prevention. www.thelancet.com. 2008;372: 475. doi:10.1016/S0140
6. Bekker LG, Beyrer C, Mgodi N, Lewin SR, Delany-Moretlwe S, Taiwo B, et al. HIV infection. Nature Reviews Disease Primers. Nature Research; 2023. doi:10.1038/s41572-023-00452-3
7. Geretti AM. HIV-1 subtypes: epidemiology and significance for HIV management. Curr Opin Infect Dis. 2006.
8. Menéndez-Arias L, Álvarez M. Antiretroviral therapy and drug resistance in human immunodeficiency virus type 2 infection. Antiviral Research. 2014. pp. 70–86. doi:10.1016/j.antiviral.2013.12.001
9. Sleasman JW, Goodenow MM. 13. HIV-1 infection. Journal of Allergy and Clinical Immunology. Mosby Inc.; 2003. doi:10.1067/mai.2003.91
10. Cohen MS, Shaw GM, McMichael AJ, Haynes BF. Acute HIV-1 Infection. New England Journal of Medicine. 2011;364: 1943–1954. doi:10.1056/nejmra1011874
11. Kaur G, Mehra N. Genetic determinants of HIV-1 infection and progression to AIDS: Immune response genes. Tissue Antigens. 2009. pp. 373–385. doi:10.1111/j.1399-0039.2009.01337.x
12. Smoleń-Dzirba J, Rosińska M, Janiec J, Beniowski M, Cycoń M, Bratosiewicz-Wąsik J, et al. HIV-1 Infection in Persons Homozygous for CCR5-Δ32 Allele: The Next Case and the Review. Reviews. 2017. Available: www.permanyer.com
13. van Heuvel Y, Schatz S, Rosengarten JF, Stitz J. Infectious RNA: Human Immunodeficiency Virus (HIV) Biology, Therapeutic Intervention, and the Quest for a Vaccine. Toxins. MDPI; 2022. doi:10.3390/toxins14020138
14. Goto T, Nakai M, Ikutat K. The Life-cycle of Human Immunodeficiency Virus Type. 1998.
15. Le Douce V, Herbein G, Rohr O, Schwartz C. Open Access REVIEW BioMed Central Molecular mechanisms of HIV-1 persistence in the monocyte-macrophage lineage. 2010. Available: http://www.retrovirology.com/content/7/1/32

16. Sattentau QJ, Stevenson M. Macrophages and HIV-1: An Unhealthy Constellation. Cell Host and Microbe. Cell Press; 2016. pp. 304–310. doi:10.1016/j.chom.2016.02.013
17. Brenchley JM, Hill BJ, Ambrozak DR, Price DA, Guenaga FJ, Casazza JP, et al. T-Cell Subsets That Harbor Human Immunodeficiency Virus (HIV) In Vivo: Implications for HIV Pathogenesis. J Virol. 2004;78: 1160–1168. doi:10.1128/jvi.78.3.1160-1168.2004
18. Rucker J, Edinger AL, Sharron M, Samson M, Lee B, Berson JF, et al. Utilization of Chemokine Receptors, Orphan Receptors, and Herpesvirus-Encoded Receptors by Diverse Human and Simian Immunodeficiency Viruses. J Virol. 1997. Available: https://journals.asm.org/journal/jvi
19. Dwivedi R, Prakash P, Kumbhar BV, Balasubramaniam M, Dash C. HIV-1 capsid and viral DNA integration. mBio. American Society for Microbiology; 2024. doi:10.1128/mbio.00212-22
20. Taylor IA, Fassati A. The capsid revolution. Journal of Molecular Cell Biology. Oxford University Press; 2023. doi:10.1093/jmcb/mjad076
21. Ruelas DS, Greene WC. An integrated overview of HIV-1 latency. Cell. Elsevier B.V.; 2013. p. 519. doi:10.1016/j.cell.2013.09.044
22. Kok YL, Vongrad V, Shilaih M, Di Giallonardo F, Kuster H, Kouyos R, et al. Monocyte-derived macrophages exhibit distinct and more restricted HIV-1 integration site repertoire than CD4 + T cells. Sci Rep. 2016;6. doi:10.1038/srep24157
23. Barr SD, Ciuffi A, Leipzig J, Shinn P, Ecker JR, Bushman FD. HIV Integration Site Selection: Targeting in Macrophages and the Effects of Different Routes of Viral Entry. Molecular Therapy. 2006;14: 218–225. doi:10.1016/j.ymthe.2006.03.012
24. Alburtamani N, Paul A, Fassati A. The role of capsid in the early steps of hiv-1 infection: New insights into the core of the matter. Viruses. MDPI; 2021. doi:10.3390/v13061161
25. Rossi E, Meuser ME, Cunanan CJ, Cocklin S. Structure, function, and interactions of the hiv-1 capsid protein. Life. MDPI AG; 2021. pp. 1–25. doi:10.3390/life11020100
26. Toccafondi E, Lener D, Negroni M. HIV-1 Capsid Core: A Bullet to the Heart of the Target Cell. Frontiers in Microbiology. Frontiers Media S.A.; 2021. doi:10.3389/fmicb.2021.652486
27. Jang S, Engelman AN. Capsid–host interactions for HIV-1 ingress. Microbiology and Molecular Biology Reviews. 2023;87. doi:10.1128/mmbr.00048-22
28. Rossi E, Meuser ME, Cunanan CJ, Cocklin S. Structure, function, and interactions of the hiv-1 capsid protein. Life. MDPI AG; 2021. pp. 1–25. doi:10.3390/life11020100
29. Menéndez-Arias L, Sebastián-Martín A, Álvarez M. Viral reverse transcriptases. Virus Research. Elsevier B.V.; 2017. pp. 153–176. doi:10.1016/j.virusres.2016.12.019
30. Krupkin M, Jackson LN, Ha B, Puglisi EV. Advances in understanding the initiation of HIV-1 reverse transcription. Current Opinion in Structural Biology. Elsevier Ltd; 2020. pp. 175–183. doi:10.1016/j.sbi.2020.07.005

31. Aiken C, Rousso I. The HIV-1 capsid and reverse transcription. Retrovirology. BioMed Central Ltd; 2021. doi:10.1186/s12977-021-00566-0
32. Peng Y, Zong Y, Wang D, Chen J, Chen ZS, Peng F, et al. Current drugs for HIV-1: from challenges to potential in HIV/AIDS. Frontiers in Pharmacology. Frontiers Media SA; 2023. doi:10.3389/fphar.2023.1294966
33. Lapaillerie D, Lelandais B, Mauro E, Lagadec F, Tumiotto C, Miskey C, et al. Modulation of the intrinsic chromatin binding property of HIV-1 integrase by LEDGF/p75. Nucleic Acids Res. 2021;49: 11241–11256. doi:10.1093/nar/gkab886
34. Martin-Gayo E, Yu XG. Role of dendritic cells in natural immune control of HIV-1 infection. Frontiers in Immunology. Frontiers Media S.A.; 2019. doi:10.3389/fimmu.2019.01306
35. Burnett JC, Miller-Jensen K, Shah PS, Arkin AP, Schaffer D V. Control of stochastic gene expression by host factors at the HIV promoter. PLoS Pathog. 2009;5. doi:10.1371/journal.ppat.1000260
36. Pereira LA, Bentley K, Peeters A, Churchill MJ, Deacon NJ. A compilation of cellular transcription factor interactions with the HIV-1 LTR promoter. Nucleic Acids Res. 2000.
37. Tripathy MK, Abbas W, Herbein G. Epigenetic regulation of HIV-1 transcription. Epigenomics. 2011. pp. 487–502. doi:10.2217/epi.11.61
38. Williams SA, Kwon H, Chen L-F, Greene WC. Sustained Induction of NF-κB Is Required for Efficient Expression of Latent Human Immunodeficiency Virus Type 1. J Virol. 2007;81: 6043–6056. doi:10.1128/jvi.02074-06
39. Mbonye U, Karn J. The cell biology of HIV-1 latency and rebound. Retrovirology. BioMed Central Ltd; 2024. doi:10.1186/s12977-024-00639-w
40. Donahue DA, Wainberg MA. Cellular and molecular mechanisms involved in the establishment of HIV-1 latency. 2013. Available: http://www.retrovirology.com/content/10/1/11
41. Rölling MD, Stoszko M, Mahmoudi T. Molecular Mechanisms Controlling HIV Transcription and Latency – Implications for Therapeutic Viral Reactivation. Advances in Molecular Retrovirology. InTech; 2016. doi:10.5772/61948
42. Purcell DFJ, Martin MA. Alternative Splicing of Human Immunodeficiency Virus Type 1 mRNA Modulates Viral Protein Expression, Replication, and Infectivity. J Virol. 1993. Available: https://journals.asm.org/journal/jvi
43. Li W, Huang Y, Yuan H, Han J, Li Z, Tong A, et al. Characterizing transcripts of HIV-1 different substrains using direct RNA sequencing. Heliyon. 2024;10. doi:10.1016/j.heliyon.2024.e39474
44. Emery A, Swanstrom R. Hiv-1: To splice or not to splice, that is the question. Viruses. MDPI AG; 2021. doi:10.3390/v13020181
45. Nasioulas G, Zolotukhin AS, Tabernero C, Solomin L, Cunningham,' CP, Pavlakis GN, et al. Elements Distinct from Human Immunodeficiency Splice Sites Are Responsible for the Rev Dependence of env mRNA Virus Type 1. J Virol. 1994.
46. McGraw A, Hillmer G, Medehincu SM, Hikichi Y, Gagliardi S, Narayan K, et al. Exploring HIV-1 Maturation: A New Frontier in Antiviral Development. Viruses. 2024;16: 1423. doi:10.3390/v16091423

47. Berman PW, Nunes WM, Haffar OK. Expression of Membrane-Associated and Secreted Variants of gpl60 of Human Immunodeficiency Virus Type 1 In Vitro and in Continuous Cell Lines. J Virol. 1988.
48. Freed EO. HIV-1 assembly, release and maturation. Nat Rev Microbiol. 2015;13: 484–496. doi:10.1038/nrmicro3490
49. Ono A, Ablan SD, Lockett SJ, Nagashima K, Freed EO. Phosphatidylinositol (4,5) bisphosphate regulates HIV-1 Gag targeting to the plasma membrane. Available: www.pnas.orgcgidoi10.1073pnas.0405596101
50. Gottlinger HG, Dorfman T, Sodroski JG, Haseltine WA. Effect of mutations affecting the p6 gag protein on human immunodeficiency virus particle release (capsid assembly/budding/cell surface attachment/interferon a). Proc Natl Acad Sci USA. 1991. Available: https://www.pnas.org
51. Kmiec D, Kirchhoff F. Antiviral factors and their counteraction by HIV-1: many uncovered and more to be discovered. Journal of Molecular Cell Biology. Oxford University Press; 2024. doi:10.1093/jmcb/mjae005
52. Delviks-Frankenberry KA, Desimmie BA, Pathak VK. Structural insights into APOBEC3-mediated lentiviral restriction. Viruses. MDPI AG; 2020. doi:10.3390/v12060587
53. Ramirez PW, Sharma S, Singh R, Stoneham CA, Vollbrecht T, Guatelli J. Plasma membrane-associated restriction factors and their counteraction by HIV-1 accessory proteins. Cells. MDPI; 2019. doi:10.3390/cells8091020
54. D`Urbano V, De Crignis E, Re MC. Host Restriction Factors and Human Immunodeficiency Virus (HIV-1): A Dynamic Interplay Involving All Phases of the Viral Life Cycle. Curr HIV Res. 2018;16: 184–207. doi:10.2174/1570162x16666180817115830
55. Cano-Ortiz L, Luedde T, Münk C. HIV-1 restriction by SERINC5. Medical Microbiology and Immunology. Springer Science and Business Media Deutschland GmbH; 2023. pp. 133–140. doi:10.1007/s00430-022-00732-x
56. Zotova AA, Atemasova AA, Filatov A V., Mazurov D V. HIV Restriction Factors and Their Ambiguous Role during Infection. Molecular Biology. Pleiades Publishing; 2019. pp. 212–226. doi:10.1134/S0026893319020171
57. Gibbons JM, Marno KM, Pike R, Lee WJ, Jones CE, Ogunkolade BW, et al. HIV-1 Accessory Protein Vpr Interacts with REAF/RPRD2 To Mitigate Its Antiviral Activity. J Virol. 2020;94. doi:10.1128/jvi.01591-19
58. Van Lint C, Bouchat S, Marcello A. HIV-1 transcription and latency: An update. Retrovirology. 2013;10: 1–38. doi:10.1186/1742-4690-10-67
59. Siliciano RF, Greene WC. HIV latency. Cold Spring Harb Perspect Med. 2011;1. doi:10.1101/cshperspect.a007096
60. Fromentin R, Bakeman W, Lawani MB, Khoury G, Hartogensis W, DaFonseca S, et al. CD4+ T Cells Expressing PD-1, TIGIT and LAG-3 Contribute to HIV Persistence during ART. PLoS Pathog. 2016;12. doi:10.1371/journal.ppat.1005761
61. Chun T, Finzi D, Margolick jOSEPH, Chadwick K, Schwartz D, S RF. In vivo fate of HIV-1-infected T cells: Quantitative analysis of the transition to stable latency. 1995. Available: http://www.nature.com/naturemedicine
62. Sáez-Cirión A, Bacchus C, Hocqueloux L, Avettand-Fenoel V, Girault I, Lecuroux C, et al. Post-Treatment HIV-1 Controllers with a Long-Term

Virological Remission after the Interruption of Early Initiated Antiretroviral Therapy ANRS VISCONTI Study. PLoS Pathog. 2013;9. doi:10.1371/journal.ppat.1003211
63. Reuschl AK, Mesner D, Shivkumar M, Whelan MVX, Pallett LJ, Guerra-Assunção JA, et al. HIV-1 Vpr drives a tissue residency-like phenotype during selective infection of resting memory T cells. Cell Rep. 2022;39. doi:10.1016/j.celrep.2022.110650
64. Chen J, Zhou T, Zhang Y, Luo S, Chen H, Chen D, et al. The reservoir of latent HIV. Frontiers in Cellular and Infection Microbiology. Frontiers Media S.A.; 2022. doi:10.3389/fcimb.2022.945956
65. Wong JK, Yukl SA. Tissue reservoirs of HIV. Current Opinion in HIV and AIDS. Lippincott Williams and Wilkins; 2016. pp. 362–370. doi:10.1097/COH.0000000000000293
66. Astrid R.W. Schro¨der PSHCCBJREFB. HIV-1 Integration in the Human Genome Favors Active Genes and Local Hotspots. Cell. 2002;110, 521–529.
67. He G, Margolis DM. Counterregulation of Chromatin Deacetylation and Histone Deacetylase Occupancy at the Integrated Promoter of Human Immunodeficiency Virus Type 1 (HIV-1) by the HIV-1 Repressor YY1 and HIV-1 Activator Tat. Mol Cell Biol. 2002;22: 2965–2973. doi:10.1128/mcb.22.9.2965-2973.2002
68. Tyagi M, Karn J. CBF-1 promotes transcriptional silencing during the establishment of HIV-1 latency. EMBO Journal. 2007;26: 4985–4995. doi:10.1038/sj.emboj.7601928
69. Moranguinho I, Valente ST. Block-and-lock: New horizons for a cure for HIV-1. Viruses. MDPI AG; 2020. doi:10.3390/v12121443
70. Varin A, Decrion AZ, Sabbah E, Quivy V, Sire J, Van Lint C, et al. Synthetic Vpr protein activates activator protein-1, c-Jun N-terminal kinase, and NF-κB and stimulates HIV-1 transcription in promonocytic cells and primary macrophages. Journal of Biological Chemistry. 2005;280: 42557–42567. doi:10.1074/jbc.M502211200
71. Wallet C, Rohr O, Schwartz C. Evolution of a concept: From accessory protein to key virulence factor, the case of HIV-1 Vpr. Biochemical Pharmacology. Elsevier Inc.; 2020. doi:10.1016/j.bcp.2020.114128
72. Amini S, Saunders M, Kelley K, Khalili K, Sawaya BE. Interplay between HIV-1 Vpr and Sp1 modulates p21WAF1 gene expression in human astrocytes. Journal of Biological Chemistry. 2004;279: 46046–46056. doi:10.1074/jbc.M403792200
73. Weichseldorfer M, Reitz M, Latinovic OS. Past hiv-1 medications and the current status of combined antiretroviral therapy options for hiv-1 patients. Pharmaceutics. MDPI; 2021. doi:10.3390/pharmaceutics13111798
74. Hütter G, Nowak D, Mossner M, Ganepola S, Müig A, Allers K, et al. Long-Term Control of HIV by CCR5 Delta32/ Delta32 Stem-Cell Transplantation. N Engl J Med. 2009.
75. Gupta RK, Abdul-Jawad S, McCoy LE, Mok HP, Peppa D, Salgado M, et al. HIV-1 remission following CCR5Δ32/Δ32 haematopoietic stem-cell transplantation. Nature. 2019;568: 244–248. doi:10.1038/s41586-019-1027-4

76. Jensen BEO, Knops E, Cords L, Lübke N, Salgado M, Busman-Sahay K, et al. In-depth virological and immunological characterization of HIV-1 cure after CCR5Δ32/Δ32 allogeneic hematopoietic stem cell transplantation. Nat Med. 2023;29: 583–587. doi:10.1038/s41591-023-02213-x
77. Hsu J, Van Besien K, Glesby MJ, Pahwa S, Coletti A, Warshaw MG, et al. HIV-1 remission and possible cure in a woman after haplo-cord blood transplant. Cell. 2023;186: 1115-1126.e8. doi:10.1016/j.cell.2023.02.030
78. Capa L, Ayala-Suárez R, De La Torre Tarazona HE, González-García J, del Romero J, Alcamí J, et al. Elite controllers long-term non progressors present improved survival and slower disease progression. Sci Rep. 2022;12. doi:10.1038/s41598-022-19970-3
79. Walker BD, Yu XG. Unravelling the mechanisms of durable control of HIV-1. Nature Reviews Immunology. 2013. pp. 487–498. doi:10.1038/nri3478
80. Bone B, Lichterfeld M. “block and lock” viral integration sites in persons with drug-free control of HIV-1 infection. Curr Opin HIV AIDS. 2024;19: 110–115. doi:10.1097/COH.0000000000000845
81. Kim Y, Anderson JL, Lewin SR. Getting the “Kill” into “Shock and Kill”: Strategies to Eliminate Latent HIV. Cell Host Microbe. 2018;23: 14–26. doi:10.1016/j.chom.2017.12.004
82. Jean MJ, Fiches G, Hayashi T, Zhu J. Current Strategies for Elimination of HIV-1 Latent Reservoirs Using Chemical Compounds Targeting Host and Viral Factors. AIDS Research and Human Retroviruses. Mary Ann Liebert Inc.; 2019. pp. 1–24. doi:10.1089/aid.2018.0153
83. Tanaka K, Kim Y, Roche M, Lewin SR. The role of latency reversal in HIV cure strategies. Journal of Medical Primatology. John Wiley and Sons Inc; 2022. pp. 278–283. doi:10.1111/jmp.12613
84. Rasmussen TA, Lewin SR. Shocking HIV out of hiding: Where are we with clinical trials of latency reversing agents? Current Opinion in HIV and AIDS. Lippincott Williams and Wilkins; 2016. pp. 394–401. doi:10.1097/COH.0000000000000279
85. Zerbato JM, Purves H V., Lewin SR, Rasmussen TA. Between a shock and a hard place: challenges and developments in HIV latency reversal. Current Opinion in Virology. Elsevier B.V.; 2019. pp. 1–9. doi:10.1016/j.coviro.2019.03.004
86. Archin NM, Liberty AL, Kashuba AD, Choudhary SK, Kuruc JD, Crooks AM, et al. Administration of vorinostat disrupts HIV-1 latency in patients on antiretroviral therapy. Nature. 2012;487: 482–485. doi:10.1038/nature11286
87. Archin NM, Kirchherr JL, Sung JAM, Clutton G, Sholtis K, Xu Y, et al. Interval dosing with the HDAC inhibitor vorinostat effectively reverses HIV latency. Journal of Clinical Investigation. 2017;127: 3126–3135. doi:10.1172/JCI92684
88. Rasmussen TA, Tolstrup M, Brinkmann CR, Olesen R, Erikstrup C, Solomon A, et al. Panobinostat, a histone deacetylase inhibitor, for latent virus reactivation in HIV-infected patients on suppressive antiretroviral therapy: A phase 1/2, single group, clinical trial. Lancet HIV. 2014;1: e13–e21. doi:10.1016/S2352-3018(14)70014-1

89. Søgaard OS, Graversen ME, Leth S, Olesen R, Brinkmann CR, Nissen SK, et al. The Depsipeptide Romidepsin Reverses HIV-1 Latency In Vivo. PLoS Pathog. 2015;11. doi:10.1371/journal.ppat.1005142
90. Gutiérrez C, Serrano-Villar S, Madrid-Elena N, Pérez-EÍas MJ, Martń ME, Barbas C, et al. Bryostatin-1 for latent virus reactivation in HIV-infected patients on antiretroviral therapy. AIDS. 2016;30: 1385–1392. doi:10.1097/QAD.0000000000001064
91. Marsden MD, Loy BA, Wu X, Ramirez CM, Schrier AJ, Murray D, et al. In vivo activation of latent HIV with a synthetic bryostatin analog effects both latent cell “kick” and “kill” in strategy for virus eradication. PLoS Pathog. 2017;13. doi:10.1371/journal.ppat.1006575
92. Vibholm LK, Konrad C V., Schleimann MH, Frattari G, Winckelmann A, Klastrup V, et al. Effects of 24-week Toll-like receptor 9 agonist treatment in HIV type 1+ individuals. AIDS. 2019;33: 1315–1325. doi:10.1097/QAD.0000000000002213
93. Vansant G, Bruggemans A, Janssens J, Debyser Z. Block-and-lock strategies to cure HIV infection. Viruses. MDPI AG; 2020. doi:10.3390/v12010084
94. Mousseau G, Clementz MA, Bakeman WN, Nagarsheth N, Cameron M, Shi J, et al. An Analog of the Natural Steroidal Alkaloid Cortistatin A Potently Suppresses Tat-Dependent HIV Transcription. Cell Host Microbe. 2012;12: 97–108. doi:10.1016/j.chom.2012.05.016
95. Mousseau G, Kessing CF, Fromentin R, Trautmann L, Chomont N, Valente ST. The tat inhibitor didehydro-cortistatin a prevents HIV-1 reactivation from latency. mBio. 2015;6. doi:10.1128/mBio.00465-15
96. Kessing CF, Nixon CC, Li C, Tsai P, Takata H, Mousseau G, et al. In Vivo Suppression of HIV Rebound by Didehydro-Cortistatin A, a “Block-and-Lock” Strategy for HIV-1 Treatment. Cell Rep. 2017;21: 600–611. doi:10.1016/j.celrep.2017.09.080
97. Bisgrove DA, Mahmoudi T, Henklein P, Verdin E. Conserved P-TEFb-interacting domain of BRD4 inhibits HIV transcription. 2007. Available: www.pnas.orgcgidoi10.1073pnas.0705053104
98. Niu Q, Liu Z, Alamer E, Fan X, Chen H, Endsley J, et al. Structure-guided drug design identifies a BRD4-selective small molecule that suppresses HIV. Journal of Clinical Investigation. 2019;129: 3361–3373. doi:10.1172/JCI120633
99. Besnard E, Hakre S, Kampmann M, Lim HW, Hosmane NN, Martin A, et al. The mTOR Complex Controls HIV Latency. Cell Host Microbe. 2016;20: 785–797. doi:10.1016/j.chom.2016.11.001
100. Vozzolo L, Loh B, Gane PJ, Tribak M, Zhou L, Anderson I, et al. Gyrase B inhibitor impairs HIV-1 replication by targeting Hsp90 and the capsid protein. Journal of Biological Chemistry. 2010;285: 39314–39328. doi:10.1074/jbc.M110.155275
101. Anderson I, Low JS, Weston S, Weinberger M, Zhyvoloup A, Labokha AA, et al. Heat shock protein 90 controls HIV-1 reactivation from latency. Proc Natl Acad Sci U S A. 2014;111. doi:10.1073/pnas.1320178111

102. Joshi P, Maidji E, Stoddart CA. Inhibition of heat shock protein 90 prevents HIV rebound. Journal of Biological Chemistry. 2016;291: 10332–10346. doi:10.1074/jbc.M116.717538
103. Vranckx LS, Demeulemeester J, Saleh S, Boll A, Vansant G, Schrijvers R, et al. LEDGIN-mediated Inhibition of Integrase-LEDGF/p75 Interaction Reduces Reactivation of Residual Latent HIV. EBioMedicine. 2016;8: 248–264. doi:10.1016/j.ebiom.2016.04.039
104. Vansant G, Vranckx LS, Zurnic I, Van Looveren D, Van De Velde P, Nobles C, et al. Impact of LEDGIN treatment during virus production on residual HIV-1 transcription. Retrovirology. 2019;16. doi:10.1186/s12977-019-0472-3
105. Debyser Z, Vansant G, Bruggemans A, Janssens J, Christ F. Insight in HIV integration site selection provides a block-and-lock strategy for a functional cure of HIV infection. Viruses. MDPI AG; 2019. doi:10.3390/v11010012
106. Pham HT, Mesplède T. The latest evidence for possible HIV-1 curative strategies. Drugs in Context. Bioexcel Publishing LTD; 2018. doi:10.7573/dic.212522
107. Magro G, Calistri A, Parolin C. Targeting and understanding hiv latency: The crispr system against the provirus. Pathogens. MDPI; 2021. doi:10.3390/pathogens10101257
108. Perreau M, Banga R, Pantaleo G. Targeted Immune Interventions for an HIV-1 Cure. Trends in Molecular Medicine. Elsevier Ltd; 2017. pp. 945–961. doi:10.1016/j.molmed.2017.08.006
109. Hoter A, El-Sabban ME, Naim HY. The HSP90 family: Structure, regulation, function, and implications in health and disease. International Journal of Molecular Sciences. MDPI AG; 2018. doi:10.3390/ijms19092560
110. Lindquist S. THE HEAT-SHOCK RESPONSE. 1986. Available: www.annualreviews.org.
111. Pirkkala L, Sistonen L. Heat Shock Proteins (HSPs): Structure, Function and Genetics. Encyclopedia of Life Sciences. Wiley; 2006. doi:10.1038/npg.els.0006130
112. Chen B, Zhong D, Monteiro A. Comparative genomics and evolution of the HSP90 family of genes across all kingdoms of organisms. BMC Genomics. 2006;7. doi:10.1186/1471-2164-7-156
113. Wei H, Zhang Y, Jia Y, Chen X, Niu T, Chatterjee A, et al. Heat shock protein 90: biological functions, diseases, and therapeutic targets. MedComm. John Wiley and Sons Inc; 2024. doi:10.1002/mco2.470
114. Birbo B, Madu EE, Madu CO, Jain A, Lu Y. Role of hsp90 in cancer. International Journal of Molecular Sciences. MDPI; 2021. doi:10.3390/ijms221910317
115. Whitesell L, Lindquist SL. HSP90 and the chaperoning of cancer. Nature Reviews Cancer. 2005. pp. 761–772. doi:10.1038/nrc1716
116. Bohush A, Bieganowski P, Filipek A. Hsp90 and its co-chaperones in neurodegenerative diseases. International Journal of Molecular Sciences. MDPI AG; 2019. doi:10.3390/ijms20204976
117. Geller R, Taguwa S, Frydman J. Broad action of Hsp90 as a host chaperone required for viral replication. Biochimica et Biophysica Acta - Molecular Cell Research. 2012. pp. 698–706. doi:10.1016/j.bbamcr.2011.11.007

118. Li Y, Dong J, Qin JJ. Small molecule inhibitors targeting heat shock protein 90: An updated review. European Journal of Medicinal Chemistry. Elsevier Masson s.r.l.; 2024. doi:10.1016/j.ejmech.2024.116562
119. Schopf FH, Biebl MM, Buchner J. The HSP90 chaperone machinery. Nature Reviews Molecular Cell Biology. Nature Publishing Group; 2017. pp. 345–360. doi:10.1038/nrm.2017.20
120. Pearl LH, Prodromou C, Workman P. The Hsp90 molecular chaperone: An open and shut case for treatment. Biochemical Journal. 2008. pp. 439–453. doi:10.1042/BJ20071640
121. Sima S, Richter K. Regulation of the Hsp90 system. Biochimica et Biophysica Acta - Molecular Cell Research. Elsevier B.V.; 2018. pp. 889–897. doi:10.1016/j.bbamcr.2018.03.008
122. Eckl JM, Richter K. Functions of the Hsp90 chaperone system: lifting client proteins to new heights. Int J Biochem Mol Biol. 2013. Available: http://www.picard.ch/
123. Zuehlke A, Johnson JL. Hsp90 and co-chaperones twist the functions of diverse client proteins. Biopolymers. 2010. pp. 211–217. doi:10.1002/bip.21292
124. Li L, Wang L, You QD, Xu XL. Heat Shock Protein 90 Inhibitors: An Update on Achievements, Challenges, and Future Directions. Journal of Medicinal Chemistry. American Chemical Society; 2020. pp. 1798–1822. doi:10.1021/acs.jmedchem.9b00940
125. Taldone T, Gozman A, Maharaj R, Chiosis G. Targeting Hsp90: small-molecule inhibitors and their clinical development. Current Opinion in Pharmacology. 2008. pp. 370–374. doi:10.1016/j.coph.2008.06.015
126. Li Y, Zhang T, Schwartz SJ, Sun D. New developments in Hsp90 inhibitors as anti-cancer therapeutics: Mechanisms, clinical perspective and more potential. Drug Resistance Updates. 2009;12: 17–27. doi:10.1016/j.drup.2008.12.002
127. Li ZN, Luo Y. HSP90 inhibitors and cancer: Prospects for use in targeted therapies (Review). Oncol Rep. 2023;49. doi:10.3892/or.2022.8443
128. Cheung KMJ, Matthews TP, James K, Rowlands MG, Boxall KJ, Sharp SY, et al. The identification, synthesis, protein crystal structure and in vitro biochemical evaluation of a new 3,4-diarylpyrazole class of Hsp90 inhibitors. Bioorg Med Chem Lett. 2005;15: 3338–3343. doi:10.1016/j.bmcl.2005.05.046
129. Brough PA, Aherne W, Barril X, Borgognoni J, Boxall K, Cansfield JE, et al. 4,5-Diarylisoxazole Hsp90 chaperone inhibitors: Potential therapeutic agents for the treatment of cancer. J Med Chem. 2008;51: 196–218. doi:10.1021/jm701018h
130. Eccles SA, Massey A, Raynaud FI, Sharp SY, Box G, Valenti M, et al. NVP-AUY922: A novel heat shock protein 90 inhibitor active against xenograft tumor growth, angiogenesis, and metastasis. Cancer Res. 2008;68: 2850–2860. doi:10.1158/0008-5472.CAN-07-5256
131. Jensen MR, Schoepfer J, Radimerski T, Massey A, Guy CT, Brueggen J, et al. NVP-AUY922: A small molecule HSP90 inhibitor with potent antitumor

activity in preclinical breast cancer models. Breast Cancer Research. 2008;10. doi:10.1186/bcr1996
132. Sessa C, Shapiro GI, Bhalla KN, Britten C, Jacks KS, Mita M, et al. First-in-human phase I dose-escalation study of the HSP90 inhibitor AUY922 in patients with advanced solid tumors. Clinical Cancer Research. 2013;19: 3671–3680. doi:10.1158/1078-0432.CCR-12-3404
133. Barrott JJ, Haystead TAJ. Hsp90, an unlikely ally in the war on cancer. FEBS Journal. 2013. pp. 1381–1396. doi:10.1111/febs.12147
134. Goetz MP, Toft DO, Ames MM, Erlichman C. The Hsp90 chaperone complex as a novel target for cancer therapy. Annals of Oncology. 2003. pp. 1169–1176. doi:10.1093/annonc/mdg316
135. Kim Y, Alarcon S, Lee S, Lee M-J, Giaccone G, Neckers L, et al. Update on Hsp90 Inhibitors in Clinical Trial. Curr Top Med Chem. 2009;9: 1479–1492. doi:10.2174/156802609789895728
136. Neckers L, Workman P. Hsp90 molecular chaperone inhibitors: Are we there yet? Clinical Cancer Research. 2012. pp. 64–76. doi:10.1158/1078-0432.CCR-11-1000
137. Albakova Z. HSP90 multi-functionality in cancer. Frontiers in Immunology. Frontiers Media SA; 2024. doi:10.3389/fimmu.2024.1436973
138. Boukli NM, Shetty V, Cubano L, Ricaurte M, Coelho-Dos-Reis J, Nickens Z, et al. Unique and differential protein signatures within the mononuclear cells of HIV-1 and HCV mono-infected and co-infected patients. 2012. Available: http://www.clinicalproteomicsjournal.com/content/9/1/11
139. Ringrose JH, Jeeninga RE, Berkhout B, Speijer D. Proteomic Studies Reveal Coordinated Changes in T-Cell Expression Patterns upon Infection with Human Immunodeficiency Virus Type 1. J Virol. 2008;82: 4320–4330. doi:10.1128/jvi.01819-07
140. Roesch F, Meziane O, Kula A, Nisole S, Porrot F, Anderson I, et al. Hyperthermia stimulates HIV-1 replication. PLoS Pathog. 2012;8: 35. doi:10.1371/journal.ppat.1002792
141. Pan XY, Zhao W, Zeng XY, Lin J, Li MM, Shen XT, et al. Heat Shock Factor 1 Mediates Latent HIV Reactivation. Sci Rep. 2016;6: 1–12. doi:10.1038/srep26294
142. Wang C, Chen C, Pan Z, He Y, Zhang Z, Liu R, et al. Quantitative Proteomics of the CDK9 Interactome Reveals a Function of the HSP90-CDC37-P-TEFb Complex for BETi-Induced HIV-1 Latency Reactivation. J Proteome Res. 2023;22: 2880–2889. doi:10.1021/acs.jproteome.3c00162
143. Janssens J, Kim P, Kim SJ, Wedrychowski A, Kadiyala GN, Hunt PW, et al. Mechanisms and efficacy of small molecule “latency promoting agents” to inhibit HIV reactivation ex vivo. JCI Insight. 2024. doi:10.1172/jci.insight.183084
144. Lubkowska A, Pluta W, Strońska A, Lalko A. Role of heat shock proteins (Hsp70 and hsp90) in viral infection. International Journal of Molecular Sciences. MDPI; 2021. doi:10.3390/ijms22179366
145. Tsou YL, Lin YW, Chang HW, Lin HY, Shao HY, Yu SL, et al. Heat Shock protein 90: Role in Enterovirus 71 Entry and Assembly and Potential Target for Therapy. PLoS One. 2013;8. doi:10.1371/journal.pone.0077133

146. Reyes-del Valle J, Chávez-Salinas S, Medina F, del Angel RM. Heat Shock Protein 90 and Heat Shock Protein 70 Are Components of Dengue Virus Receptor Complex in Human Cells. J Virol. 2005;79: 4557–4567. doi:10.1128/jvi.79.8.4557-4567.2005
147. Geller R, Andino R, Frydman J. Hsp90 Inhibitors Exhibit Resistance-Free Antiviral Activity against Respiratory Syncytial Virus. PLoS One. 2013;8. doi:10.1371/journal.pone.0056762
148. Connor JH, Mckenzie MO, Parks GD, Lyles DS. Antiviral Activity and RNA Polymerase Degradation Following Hsp90 Inhibition in a Range of Negative Strand Viruses. 2007.
149. Smith DR, McCarthy S, Chrovian A, Olinger G, Stossel A, Geisbert TW, et al. Inhibition of heat-shock protein 90 reduces Ebola virus replication. Antiviral Res. 2010;87: 187–194. doi:10.1016/j.antiviral.2010.04.015
150. Wyler E, Mösbauer K, Franke V, Diag A, Gottula LT, Arsiè R, et al. Transcriptomic profiling of SARS-CoV-2 infected human cell lines identifies HSP90 as target for COVID-19 therapy. iScience. 2021;24. doi:10.1016/j.isci.2021.102151
151. Ujino S, Yamaguchi S, Shimotohno K, Takaku H. Heat-shock protein 90 is essential for stabilization of the hepatitis C virus nonstructural protein NS3. Journal of Biological Chemistry. 2009;284: 6841–6846. doi:10.1074/jbc.M806452200
152. Waxman L, Whitney M, Pollok BA, Kuo LC, Darke PL. Host cell factor requirement for hepatitis C virus enzyme maturation. 2001. Available: www.pnas.orgcgidoi10.1073pnas.241510898
153. Momose F, Naito T, Yano K, Sugimoto S, Morikawa Y, Nagata K. Identification of Hsp90 as a stimulatory host factor involved in influenza virus RNA synthesis. Journal of Biological Chemistry. 2002;277: 45306–45314. doi:10.1074/jbc.M206822200
154. Hakre S, Chavez L, Shirakawa K, Verdin E. HIV latency: Experimental systems and molecular models. FEMS Microbiology Reviews. 2012. pp. 706–716. doi:10.1111/j.1574-6976.2012.00335.x
155. K. Jones, B. Peterli. Control of RNA initiation and elongation at the HIV-1 promoter. Annu Rev Biochem. 1994;63: 717–43. doi:10.1146/annurev.bi.63.070194.003441
156. Brooks DG, Arlen PA, Gao L, Kitchen CMR, Zack JA. Identification of T cell-signaling pathways that stimulate latent HIV in primary cells. 2003. doi:10.1073/pnas.2233345100
157. Folks TM, Clouset KA, Justement J, Rabsonf A, Duho E, Kehrl JH, et al. Tumor necrosis factor a induces expression of human immunodeficiency virus in a chronically infected T-cell clone (pathogenesis/virus latency/long terminal repeat/transfection). Immunology. 1989. doi:10.1073/pnas.86.7.2365
158. Yang H, Xing S, Shan L, Connell KO, Dinoso J, Shen A, et al. Small-molecule screening using a human primary cell model of HIV latency identifies compounds that reverse latency without cellular activation. 2009;119. doi:10.1172/JCI39199DS1

159. McKernan LN, Momjian D, Kulkosky J. Protein kinase C: One pathway towards the eradication of latent HIV-1 Reservoirs. Advances in Virology. 2012. doi:10.1155/2012/805347
160. Taipale M, Jarosz DF, Lindquist S. HSP90 at the hub of protein homeostasis: Emerging mechanistic insights. Nature Reviews Molecular Cell Biology. 2010. pp. 515–528. doi:10.1038/nrm2918
161. Kim H, Choi MS, Inn KS, Kim BJ. Inhibition of HIV-1 reactivation by a telomerase-derived peptide in a HSP90-dependent manner. Sci Rep. 2016;6. doi:10.1038/srep28896
162. Agosto LM, Henderson AJ. CD4+ T Cell Subsets and Pathways to HIV Latency. AIDS Research and Human Retroviruses. Mary Ann Liebert Inc.; 2018. pp. 780–789. doi:10.1089/aid.2018.0105
163. Bosque A, Planelles V. Induction of HIV-1 latency and reactivation in primary memory CD4 T cells. 2009. doi:10.1182/blood-2008-07
164. Khanal S, Schank M, Gazzar M el, Moorman JP, Yao ZQ. Hiv-1 latency and viral reservoirs: Existing reversal approaches and potential technologies, targets, and pathways involved in hiv latency studies. Cells. MDPI; 2021. pp. 1–23. doi:10.3390/cells10020475
165. Garon EB, Finn RS, Hamidi H, Dering J, Pitts S, Kamranpour N, et al. The HSP90 inhibitor NVP-AUY922 potently inhibits non-small cell lung cancer growth. Mol Cancer Ther. 2013;12: 890–900. doi:10.1158/1535-7163.MCT-12-0998
166. Spina CA, Anderson J, Archin NM, Bosque A, Chan J, Famiglietti M, et al. An In-Depth Comparison of Latent HIV-1 Reactivation in Multiple Cell Model Systems and Resting CD4+ T Cells from Aviremic Patients. PLoS Pathog. 2013;9: 1–15. doi:10.1371/journal.ppat.1003834
167. Saleh S, Wightman F, Ramanayake S, Alexander M, Kumar N, Khoury G, et al. Expression and reactivation of HIV in a chemokine induced model of HIV latency in primary resting CD4+ T cells. Retrovirology. 2011;8: 80. doi:10.1186/1742-4690-8-80
168. Covino DA, Desimio MG, Doria M. Impact of IL-15 and latency reversing agent combinations in the reactivation and NK cell-mediated suppression of the HIV reservoir. Sci Rep. 2022;12. doi:10.1038/s41598-022-23010-5
169. Chun TW, Engel D, Mizell SB, Ehler LA, Fauci AS. Induction of HIV-1 replication in latently infected CD4+ T cells using a combination of cytokines. Journal of Experimental Medicine. 1998;188: 83–91. doi:10.1084/jem.188.1.83
170. Roux A, Leroy H, De Muylder B, Bracq L, Oussous S, Dusanter-Fourt I, et al. FOXO1 transcription factor plays a key role in t cell—HIV-1 interaction. PLoS Pathog. 2019;15: 1–23. doi:10.1371/journal.ppat.1007669
171. Meås HZ, Haug M, Beckwith MS, Louet C, Ryan L, Hu Z, et al. Sensing of HIV-1 by TLR8 activates human T cells and reverses latency. Nat Commun. 2020;11. doi:10.1038/s41467-019-13837-4
172. Meås HZ, Haug M, Beckwith MS, Louet C, Ryan L, Hu Z, et al. Sensing of HIV-1 by TLR8 activates human T cells and reverses latency. Nat Commun. 2020;11. doi:10.1038/s41467-019-13837-4

173. Wang FX, Xu Y, Sullivan J, Souder E, Argyris EG, Acheampong EA, et al. IL-7 is a potent and proviral strain-specific inducer of latent HIV-1 cellular reservoirs of infected individuals on virally suppressive HAART. Journal of Clinical Investigation. 2005;115: 128–137. doi:10.1172/JCI200522574
174. McKernan LN, Momjian D, Kulkosky J. Protein kinase C: One pathway towards the eradication of latent HIV-1 Reservoirs. Advances in Virology. 2012. doi:10.1155/2012/805347
175. Jamal I, Paudel A, Thompson L, Abdelmalek M, Khan IA, Singh VB. Sulforaphane prevents the reactivation of HIV-1 by suppressing NFκB signaling. J Virus Erad. 2023;9. doi:10.1016/j.jve.2023.100341
176. Lopes JR, Chiba DE, Dos Santos JL. HIV latency reversal agents: A potential path for functional cure? European Journal of Medicinal Chemistry. Elsevier Masson s.r.l.; 2021. doi:10.1016/j.ejmech.2021.113213
177. Nisnboym M, Vincze SR, Xiong Z, Sneiderman CT, Raphael RA, Li B, et al. Immuno-PET Imaging of CD69 Visualizes T-Cell Activation and Predicts Survival Following Immunotherapy in Murine Glioblastoma. Cancer Research Communications. 2023;3: 1173–1188. doi:10.1158/2767-9764.crc-22-0434
178. Simms PE, Ellis TM. Utility of Flow Cytometric Detection of CD69 Expression as a Rapid Method for Determining Poly-and Oligoclonal Lymphocyte Activation. Clin Diagn Lab Immunol. 1996. Available: https://journals.asm.org/journal/cdli
179. Trickett A, Kwan YL. T cell stimulation and expansion using anti-CD3/CD28 beads. J Immunol Methods. 2003;275: 251–255. doi:10.1016/S0022-1759(03)00010-3
180. Tong-Starkesen SE, Luciw PA, Peterlin BM. Signaling through T lymphocyte surface proteins, TCR/CD3 and CD28, activates the HIV-1 long terminal repeat. The Journal of Immunology. 1989;142: 702–707. doi:10.4049/jimmunol.142.2.702
181. Hwang JR, Byeon Y, Kim D, Park SG. Recent insights of T cell receptor-mediated signaling pathways for T cell activation and development. Experimental and Molecular Medicine. Springer Nature; 2020. pp. 750–761. doi:10.1038/s12276-020-0435-8
182. Paul S, Schaefer BC. A new look at T cell receptor signaling to nuclear factor-κB. Trends in Immunology. 2013. pp. 269–281. doi:10.1016/j.it.2013.02.002
183. Huse M. The T-cell-receptor signalling network. J Cell Sci. 2009;122: 1269–1273. doi:10.1242/jcs.042762
184. Spivak AM, Planelles V. Novel Latency Reversal Agents for HIV-1 Cure. Annual Review of Medicine. Annual Reviews Inc.; 2018. pp. 421–436. doi:10.1146/annurev-med-052716-031710
185. Galron D, Tamir A, Altman A, Isakov N. Mechanisms of T cell activation by the calcium ionophore ionomycin. Cell Immunol. 1994.
186. Acchioni C, Remoli AL, Marsili G, Acchioni M, Nardolillo I, Orsatti R, et al. Alternate NF-κB-Independent Signaling Reactivation of Latent HIV-1 Provirus. J Virol. 2019;93. doi:10.1128/jvi.00495-19
187. Chatila,' T, Silverman L, Miller,' And R, Geha R. MECHANISMS OF T CELL ACTIVATION BY IONOMYCIN' THE CALCIUM IONOPHORE. 1989.

188. Sharma S, TenOever BR, Grandvaux N, Zhou GP, Lin R, Hiscott J. Toll-Like Receptor Signaling Pathways. Science (1979). 2003;300: 1148–1151. doi:10.1126/science.1081315
189. Kabelitz D. Expression and function of Toll-like receptors in T lymphocytes. Current Opinion in Immunology. 2007. pp. 39–45. doi:10.1016/j.coi.2006.11.007
190. Kawai T, Akira S. Signaling to NF-κB by Toll-like receptors. Trends in Molecular Medicine. 2007. pp. 460–469. doi:10.1016/j.molmed.2007.09.002
191. Meås HZ, Haug M, Beckwith MS, Louet C, Ryan L, Hu Z, et al. Sensing of HIV-1 by TLR8 activates human T cells and reverses latency. Nat Commun. 2020;11. doi:10.1038/s41467-019-13837-4
192. Chun T-W, Engel D, Mizell SB, Ehler LA, Fauci AS. Induction of HIV-1 Replication in Latently Infected CD4 T Cells Using a Combination of Cytokines. The Journal of Experimental Medicine •. 1998. Available: http://www.jem.org
193. Spina CA, Anderson J, Archin NM, Bosque A, Chan J, Famiglietti M, et al. An In-Depth Comparison of Latent HIV-1 Reactivation in Multiple Cell Model Systems and Resting CD4+ T Cells from Aviremic Patients. PLoS Pathog. 2013;9: 1–15. doi:10.1371/journal.ppat.1003834
194. Bosque A, Planelles V. Induction of HIV-1 latency and reactivation in primary memory CD4 T cells. 2009. doi:10.1182/blood-2008-07
195. Caselli E, Benedetti S, Gentili V, Grigolato J, di Luca D. Short communication: Activating transcription factor 4 (ATF4) promotes HIV type 1 activation. AIDS Res Hum Retroviruses. 2012;28: 907–912. doi:10.1089/aid.2011.0252
196. Vallejo-Gracia A, Chen IP, Perrone R, Besnard E, Boehm D, Battivelli E, et al. FOXO1 promotes HIV latency by suppressing ER stress in T cells. Nat Microbiol. 2020;5: 1144–1157. doi:10.1038/s41564-020-0742-9
197. Novis CL, Archin NM, Buzon MJ, Verdin E, Round JL, Lichterfeld M, et al. Reactivation of latent HIV-1 in central memory CD4+ T cells through TLR-1/2 stimulation. Retrovirology. 2013;10. doi:10.1186/1742-4690-10-119
198. Oki Y, Younes A, Knickerbocker J, Samaniego F, Nastoupil L, Hagemeister F, et al. Experience with HSP90 inhibitor AUY922 in patients with relapsed or refractory non-Hodgkin lymphoma. Haematologica. Ferrata Storti Foundation; 2015. pp. e272–e274. doi:10.3324/haematol.2015.126557
199. Taniguchi H, Hasegawa H, Sasaki D, Ando K, Sawayama Y, Imaizumi Y, et al. Heat Shock Protein 90 Inhibitor NVP-AUY922 Has Potent Anti-Tumor Activity With Adult T-Cell Leukemia-Lymphoma Cells. Blood. 2013;122: 1829–1829. doi:10.1182/blood.v122.21.1829.1829
200. Anderson I, Low JS, Weston S, Weinberger M, Zhyvoloup A, Labokha AA, et al. Heat shock protein 90 controls HIV-1 reactivation from latency. Proc Natl Acad Sci U S A. 2014;111. doi:10.1073/pnas.1320178111
201. Li T, Jiang HL, Tong YG, Lu JJ. Targeting the Hsp90-Cdc37-client protein interaction to disrupt Hsp90 chaperone machinery. Journal of Hematology and Oncology. BioMed Central Ltd.; 2018. doi:10.1186/s13045-018-0602-8

202. Bukrinsky MI, Stanwick TL, Dempsey MP, Stevenson M. Quiescent T lymphocytes as an inducible virus reservoir in HIV-1 infection. Science (1979). 1991;254: 423–427. doi:10.1126/science.1925601
203. Walker-Sperling VEK, Cohen VJ, Tarwater PM, Blankson JN. Reactivation Kinetics of HIV-1 and Susceptibility of Reactivated Latently Infected CD4 + T Cells to HIV-1-Specific CD8 + T Cells . J Virol. 2015;89: 9631–9638. doi:10.1128/jvi.01454-15
204. Spina CA, Anderson J, Archin NM, Bosque A, Chan J, Famiglietti M, et al. An In-Depth Comparison of Latent HIV-1 Reactivation in Multiple Cell Model Systems and Resting CD4+ T Cells from Aviremic Patients. PLoS Pathog. 2013;9: 1–15. doi:10.1371/journal.ppat.1003834
205. Elsheikh MM, Tang Y, Li D, Jiang G. Deep latency: A new insight into a functional HIV cure. EBioMedicine. 2019;45: 624–629. doi:10.1016/j.ebiom.2019.06.020
206. Wang F-X, Xu Y, Sullivan J, Souder E, Argyris EG, Acheampong EA, et al. IL-7 is a potent and proviral strain–specific inducer of latent HIV-1 cellular reservoirs of infected individuals on virally suppressive HAART. Journal of Clinical Investigation. 2005;115: 128–137. doi:10.1172/jci22574
207. Rao A, Luo C, Hogan PG. TRANSCRIPTION FACTORS OF THE NFAT FAMILY: Regulation and Function. Annu Rev Immunol. 1997. Available: www.annualreviews.org
208. Ló Pez-Cabrera M, Muñ Oz E, Valle Blá Zquez § M, Ursa MA, Santis AG, Sá Nchez-Madrid F. Transcriptional Regulation of the Gene Encoding the Human C-type Lectin Leukocyte Receptor AIM/CD69 and Functional Characterization of Its Tumor Necrosis Factor-responsive Elements*. 1995.
209. Vazquez BN, Laguna T, Carabana J, Krangel MS, Lauzurica P. CD69 Gene Is Differentially Regulated in T and B Cells by Evolutionarily Conserved Promoter-Distal Elements. The Journal of Immunology. 2009;183: 6513–6521. doi:10.4049/jimmunol.0900839
210. Reuschl AK, Mesner D, Shivkumar M, Whelan MVX, Pallett LJ, Guerra-Assunção JA, et al. HIV-1 Vpr drives a tissue residency-like phenotype during selective infection of resting memory T cells. Cell Rep. 2022;39. doi:10.1016/j.celrep.2022.110650
211. Jordan A, Bisgrove D, Verdin E. HIV reproducibly establishes a latent infection after acute infection of T cells in vitro. EMBO Journal. 2003;22: 1868–1877. doi:10.1093/emboj/cdg188
212. Rezaei SD, Cameron PU. Human Immunodeficiency Virus (HIV)-1 Integration Sites in Viral Latency. Current HIV/AIDS Reports. Current Medicine Group LLC 1; 2015. pp. 88–96. doi:10.1007/s11904-014-0241-9
213. Zhyvoloup A, Melamed A, Anderson I, Planas D, Lee CH, Kriston-Vizi J, et al. Digoxin reveals a functional connection between HIV-1 integration preference and T-cell activation. PLoS Pathog. 2017;13. doi:10.1371/journal.ppat.1006460
214. Tezcan FA, Kaiser JT, Mustafi D, Walton MY, Howard JB, Rees DC. Toll-Like Receptor 8–Mediated Reversal of CD4+ Regulatory T cell Function. Science (1979). 2005;309: 1377–1380. doi:10.1126/science.1115653

215. Dominguez-Villar M, Gautron AS, de Marcken M, Keller MJ, Hafler DA. TLR7 induces anergy in human CD4+ T cells. Nat Immunol. 2015;16: 118–128. doi:10.1038/ni.3036
216. Kabelitz D. Expression and function of Toll-like receptors in T lymphocytes. Current Opinion in Immunology. 2007. pp. 39–45. doi:10.1016/j.coi.2006.11.007
217. Mansson A, Adner M, Cardell LO. Toll-like receptors in cellular subsets of human tonsil T cells: Altered expression during recurrent tonsillitis. Respir Res. 2006;7. doi:10.1186/1465-9921-7-36
218. Castro JE, Prada CE, Loria O, Kamal A, Chen L, Burrows FJ, et al. ZAP-70 is a novel conditional heat shock protein 90 (Hsp90) client: Inhibition of Hsp90 leads to ZAP-70 degradation, apoptosis, and impaired signaling in chronic lymphocytic leukemia. Blood. 2005;106: 2506–2512. doi:10.1182/blood-2005-03-1099
219. Fan CS, Chen CC, Chen LL, Chua KV, Hung HC, Hsu JTA, et al. Extracellular HSP90α Induces MyD88−IRAK Complex-Associated IKKα/β−NF-κB/IRF3 and JAK2/TYK2−STAT-3 Signaling in Macrophages for Tumor-Promoting M2-Polarization. Cells. 2022;11. doi:10.3390/cells11020229
220. Lu XA, Wang X, Zhuo W, Jia L, Jiang Y, Fu Y, et al. The regulatory mechanism of a client kinase controlling its own release from Hsp90 chaperone machinery through phosphorylation. Biochemical Journal. 2014;457: 171–183. doi:10.1042/BJ20130963
221. Picard. HSP90 INTERACTORS. 2023.
222. Liu XY, Seh CC, Cheung PCF. HSP90 is required for TAK1 stability but not for its activation in the pro-inflammatory signaling pathway. FEBS Lett. 2008;582: 4023–4031. doi:10.1016/j.febslet.2008.10.053
223. Shi L, Zhang Z, Fang S, Xu J, Liu J, Shen J, et al. Heat shock protein 90 (Hsp90) regulates the stability of transforming growth factor β-activated kinase 1 (TAK1) in interleukin-1β-induced cell signaling. Mol Immunol. 2009;46: 541–550. doi:10.1016/j.molimm.2008.07.019
224. Brownlie RJ, Zamoyska R. T cell receptor signalling networks: Branched, diversified and bounded. Nature Reviews Immunology. 2013. pp. 257–269. doi:10.1038/nri3403
225. Balagopalan L, Kortum RL, Coussens NP, Barr VA, Samelson LE. The linker for activation of T Cells (LAT) signaling hub: From signaling complexes to microclusters. Journal of Biological Chemistry. American Society for Biochemistry and Molecular Biology Inc.; 2015. pp. 26422–26429. doi:10.1074/jbc.R115.665869
226. Espada CE, St. Gelais C, Bonifati S, Maksimova V V., Cahill MP, Kim SH, et al. TRAF6 and TAK1 Contribute to SAMHD1-Mediated Negative Regulation of NF-κB Signaling. J Virol. 2021;95: 1–14. doi:10.1128/jvi.01970-20
227. Shah K, Al-Haidari A, Sun J, Kazi JU. T cell receptor (TCR) signaling in health and disease. Signal Transduction and Targeted Therapy. Springer Nature; 2021. doi:10.1038/s41392-021-00823-w

228. Zhang W, Liu HT, Tu H. MAPK signal pathways in the regulation of cell proliferation in mammalian cells. Cell Res. 2002. Available: http://www.cell-research.com
229. Shim JH, Xiao C, Paschal AE, Bailey ST, Rao P, Hayden MS, et al. TAK1, but not TAB1 or TAB2, plays an essential role in multiple signaling pathways in vivo. Genes Dev. 2005;19: 2668–2681. doi:10.1101/gad.1360605
230. Sun L, Deng L, Ea C-K, Xia Z-P, Chen ZJ. The TRAF6 Ubiquitin Ligase and TAK1 Kinase Mediate IKK Activation by BCL10 and MALT1 in T Lymphocytes mediates binding, either directly or indirectly, to specific microbial components, and an intracellular signaling do-main that is conserved among Toll and interleukin-1. Mol Cell. 2004.
231. Bouwmeester T, Bauch A, Ruffner H, Angrand PO, Bergamini G, Croughton K, et al. A physical and functional map of the human TNF-α/NF-κB signal transduction pathway. Nat Cell Biol. 2004;6: 97–105. doi:10.1038/ncb1086
232. Sakurai H. Targeting of TAK1 in inflammatory disorders and cancer. Trends in Pharmacological Sciences. 2012. pp. 522–530. doi:10.1016/j.tips.2012.06.007
233. Xu YR, Lei CQ. TAK1-TABs Complex: A Central Signalosome in Inflammatory Responses. Front Immunol. 2021;11: 1–12. doi:10.3389/fimmu.2020.608976
234. Wu J, Powell F, Larsen NA, Lai Z, Byth KF, Read J, et al. Mechanism and in vitro pharmacology of TAK1 inhibition by (5 Z)-7-oxozeaenol. ACS Chem Biol. 2013;8: 643–650. doi:10.1021/cb3005897
235. Sakurai H, Singhirunnusorn P, Shimotabira E, Chino A, Suzuki S, Koizumi K, et al. TAK1-mediated transcriptional activation of CD28-responsive element and AP-1-binding site within the IL-2 promoter in Jurkat T cells. FEBS Lett. 2005;579: 6641–6646. doi:10.1016/j.febslet.2005.10.059
236. Jutz S, Leitner J, Schmetterer K, Doel-Perez I, Majdic O, Grabmeier-Pfistershammer K, et al. Assessment of costimulation and coinhibition in a triple parameter T cell reporter line: Simultaneous measurement of NF-κB, NFAT and AP-1. J Immunol Methods. 2016;430: 10–20. doi:10.1016/j.jim.2016.01.007
237. Liu Q, Busby JC, Molkentin JD. Interaction between TAK1-TAB1-TAB2 and RCAN1-calcineurin defines a signalling nodal control point. Nat Cell Biol. 2009;11: 154–161. doi:10.1038/ncb1823
238. Liu C, Ma X, Liu B, Chen C, Zhang H. HIV-1 functional cure: Will the dream come true? BMC Med. 2015;13. doi:10.1186/s12916-015-0517-y
239. Trickey A, Sabin CA, Burkholder G, Crane H, d'Arminio Monforte A, Egger M, et al. Life expectancy after 2015 of adults with HIV on long-term antiretroviral therapy in Europe and North America: a collaborative analysis of cohort studies. Lancet HIV. 2023;10: e295–e307. doi:10.1016/S2352-3018(23)00028-0
240. Farber DL, Yudanin NA, Restifo NP. Human memory T cells: Generation, compartmentalization and homeostasis. Nature Reviews Immunology. 2014. pp. 24–35. doi:10.1038/nri3567
241. Chavez L, Calvanese V, Verdin E. HIV Latency Is Established Directly and Early in Both Resting and Activated Primary CD4 T Cells. PLoS Pathog. 2015;11. doi:10.1371/journal.ppat.1004955

242. Kulpa DA, Talla A, Brehm JH, Ribeiro SP, Yuan S, Bebin-Blackwell A-G, et al. Differentiation into an Effector Memory Phenotype Potentiates HIV-1 Latency Reversal in CD4 + T Cells . J Virol. 2019;93. doi:10.1128/jvi.00969-19
243. Xie G, Luo X, Ma T, Frouard J, Neidleman J, Hoh R, et al. Characterization of HIV-induced remodeling reveals differences in infection susceptibility of memory CD4+ T cell subsets in vivo. Cell Rep. 2021;35. doi:10.1016/j.celrep.2021.109038
244. Pardons M, Baxter AE, Massanella M, Pagliuzza A, Fromentin R, Dufour C, et al. Single-cell characterization and quantification of translation-competent viral reservoirs in treated and untreated HIV infection. PLoS Pathog. 2019;15. doi:10.1371/journal.ppat.1007619
245. Sun H, Kim D, Li X, Kiselinova M, Ouyang Z, Vandekerckhove L, et al. Th1/17 Polarization of CD4 T Cells Supports HIV-1 Persistence during Antiretroviral Therapy. J Virol. 2015;89: 11284–11293. doi:10.1128/jvi.01595-15
246. Lee GQ, Orlova-Fink N, Einkauf K, Chowdhury FZ, Sun X, Harrington S, et al. Clonal expansion of genome-intact HIV-1 in functionally polarized Th1 CD4+ T cells. Journal of Clinical Investigation. 2017;127: 2689–2696. doi:10.1172/JCI93289
247. Mbonye U, Leskov K, Shukla M, Valadkhan S, Karn J. Biogenesis of P-TEFb in CD4+ T cells to reverse HIV latency is mediated by protein kinase C (PKC)-independent signaling pathways. PLoS Pathog. 2021;17. doi:10.1371/journal.ppat.1009581
248. Mousset CM, Hobo W, Woestenenk R, Preijers F, Dolstra H, van der Waart AB. Comprehensive Phenotyping of T Cells Using Flow Cytometry. Cytometry Part A. Wiley-Liss Inc.; 2019. pp. 647–654. doi:10.1002/cyto.a.23724
249. Van Den Broek T, Borghans JAM, Van Wijk F. The full spectrum of human naive T cells. Nature Reviews Immunology. Nature Publishing Group; 2018. pp. 363–373. doi:10.1038/s41577-018-0001-y
250. Kumar B V., Connors TJ, Farber DL. Human T Cell Development, Localization, and Function throughout Life. Immunity. Cell Press; 2018. pp. 202–213. doi:10.1016/j.immuni.2018.01.007
251. Jameson SC, Masopust D. Understanding Subset Diversity in T Cell Memory. Immunity. Cell Press; 2018. pp. 214–226. doi:10.1016/j.immuni.2018.02.010
252. Golubovskaya V, Wu L. Different subsets of T cells, memory, effector functions, and CAR-T immunotherapy. Cancers. MDPI AG; 2016. doi:10.3390/cancers8030036
253. Raphael I, Nalawade S, Eagar TN, Forsthuber TG. T cell subsets and their signature cytokines in autoimmune and inflammatory diseases. Cytokine. Academic Press; 2015. pp. 5–17. doi:10.1016/j.cyto.2014.09.011
254. Maecker HT, McCoy JP, Nussenblatt R. Standardizing immunophenotyping for the Human Immunology Project. Nature Reviews Immunology. 2012. pp. 191–200. doi:10.1038/nri3158
255. Pardons M, Baxter AE, Massanella M, Pagliuzza A, Fromentin R, Dufour C, et al. Single-cell characterization and quantification of translation-competent

viral reservoirs in treated and untreated HIV infection. PLoS Pathog. 2019;15. doi:10.1371/journal.ppat.1007619
256. Ferrer-Font L, Mayer JU, Old S, Hermans IF, Irish J, Price KM. High-Dimensional Data Analysis Algorithms Yield Comparable Results for Mass Cytometry and Spectral Flow Cytometry Data. Cytometry Part A. 2020;97: 824–831. doi:10.1002/cyto.a.24016
257. Geginat J, Lanzavecchia A, Sallusto F. Proliferation and differentiation potential of human CD8+ memory T-cell subsets in response to antigen or homeostatic cytokines. Blood. 2003;101: 4260–4266. doi:10.1182/blood-2002-11-3577
258. Shipkova M, Wieland E. Surface markers of lymphocyte activation and markers of cell proliferation. Clinica Chimica Acta. 2012. pp. 1338–1349. doi:10.1016/j.cca.2011.11.006
259. Bhattacharyya ND, Feng CG. Regulation of T Helper Cell Fate by TCR Signal Strength. Frontiers in Immunology. Frontiers Media S.A.; 2020. doi:10.3389/fimmu.2020.00624
260. Aguilar-Vazquez A, Chavarria-Avila E, Gutiérrez-Hernández JM, Toriz-González G, Salazar-Paramo M, Medrano-Ramirez G, et al. Increased Cytokine Levels in Seronegative Myositis: Potential Th17 Immune Response Implications. Int J Mol Sci. 2024;25. doi:10.3390/ijms252011061
261. Grau-Expósito J, Luque-Ballesteros L, Navarro J, Curran A, Burgos J, Ribera E, et al. Latency reversal agents affect differently the latent reservoir present in distinct CD4+ t subpopulations. PLoS Pathog. 2019;15. doi:10.1371/journal.ppat.1007991
262. Jiang C, Lian X, Gao C, Sun X, Einkauf KB, Chevalier JM, et al. Distinct viral reservoirs in individuals with spontaneous control of HIV-1. Nature. 2020;585: 261–267. doi:10.1038/s41586-020-2651-8
263. Blazkova J, Trejbalova K, Gondois-Rey F, Halfon P, Philibert P, Guiguen A, et al. CpG methylation controls reactivation of HIV from latency. PLoS Pathog. 2009;5. doi:10.1371/journal.ppat.1000554
264. Mantovani N, Defelicibus A, da Silva IT, Cicero MF, Santana LC, Arnold R, et al. Latency-associated DNA methylation patterns among HIV-1 infected individuals with distinct disease progression courses or antiretroviral virologic response. Sci Rep. 2021;11. doi:10.1038/s41598-021-02463-0
265. Ho YC, Shan L, Hosmane NN, Wang J, Laskey SB, Rosenbloom DIS, et al. Replication-competent noninduced proviruses in the latent reservoir increase barrier to HIV-1 cure. Cell. 2013;155: 540. doi:10.1016/j.cell.2013.09.020
266. Peluso MJ, Bacchetti P, Ritter KD, Beg S, Lai J, Martin JN, et al. Differential decay of intact and defective proviral DNA in HIV-1–infected individuals on suppressive antiretroviral therapy. JCI Insight. 2020;5. doi:10.1172/jci.insight.132997
267. Mbonye U, Wang B, Gokulrangan G, Shi W, Yang S, Karn J. Cyclin-dependent kinase 7 (CDK7)-mediated phosphorylation of the CDK9 activation loop promotes P-TEFb assembly with Tat and proviral HIV reactivation. Journal of Biological Chemistry. 2018;293: 10009–10025. doi:10.1074/jbc.RA117.001347

268. Kamal A, Thao L, Sensintaffar J, Zhang L, Boehm MF, Fritz LC, et al. A high-affinity conformation of Hsp90 confers tumour selectivity on Hsp90 inhibitors. Nature. 2003;425: 407–410. doi:10.1038/nature01913
269. Chiosis G, Neckers L. Tumor selectivity of Hsp90 inhibitors: the explanation remains elusive. ACS chemical biology. 2006. pp. 279–284. doi:10.1021/cb600224w
270. Bosque A, Famiglietti M, Weyrich AS, Goulston C, Planelles V. Homeostatic proliferation fails to efficiently reactivate HIV-1 latently infected central memory CD4+ T cells. PLoS Pathog. 2011;7. doi:10.1371/journal.ppat.1002288
271. Mohammadi P, di Iulio J, Muñoz M, Martinez R, Bartha I, Cavassini M, et al. Dynamics of HIV Latency and Reactivation in a Primary CD4+ T Cell Model. PLoS Pathog. 2014;10. doi:10.1371/journal.ppat.1004156
272. Gattinoni L, Speiser DE, Lichterfeld M, Bonini C. T memory stem cells in health and disease. Nature Medicine. Nature Publishing Group; 2017. pp. 18–27. doi:10.1038/nm.4241
273. Fromentin R, Chomont N. HIV persistence in subsets of CD4+ T cells: 50 shades of reservoirs. Seminars in Immunology. Academic Press; 2021. doi:10.1016/j.smim.2020.101438
274. Magyar CTJ, Vashist YK, Stroka D, Kim-Fuchs C, Berger MD, Banz VM. Heat shock protein 90 (HSP90) inhibitors in gastrointestinal cancer: where do we currently stand?—A systematic review. Journal of Cancer Research and Clinical Oncology. Springer Science and Business Media Deutschland GmbH; 2023. pp. 8039–8050. doi:10.1007/s00432-023-04689-z
275. Huang XL, Fan Z, Borowski LA, Mailliard RB, Rolland M, Mullins JI, et al. Dendritic cells reveal a broad range of MHC class I epitopes for HIV-1 in persons with suppressed viral load on antiretroviral therapy. PLoS One. 2010;5. doi:10.1371/journal.pone.0012936
276. Rgen J, Walter B, Brander C, Mammen M, Garboczi DN, Kalams SA, et al. Stimulation of human cytotoxic T cells with HIV-1-derived peptides presented by recombinant HLA-A2 peptide complexes. Int Immunol. 1997.
277. Boritz E, Rapaport EL, Campbell TB, Koeppe JR, Wilson CC. CD4+ T cell targeting of human immunodeficiency virus type 1 (HIV-1) peptide sequences present in vivo during chronic, progressive HIV-1 disease. Virology. 2007;361: 34–44. doi:10.1016/j.virol.2006.10.040
278. Kong A, Rea D, Ahmed S, Beck JT, López López R, Biganzoli L, et al. Phase 1B/2 study of the HSP90 inhibitor AUY922 plus trastuzumab in metastatic HER2-positive breast cancer patients who have progressed on trastuzumab-based regimen. Available: www.impactjournals.com/oncotarget
279. Basha W, Kitagawa R, Uhara M, Imazu H, Uechi K, Tanaka J. Geldanamycin, a potent and specific inhibitor of Hsp90, inhibits gene expression and replication of human cytomegalovirus. Antivir Chem Chemother. 2005;16: 135–146.
280. Acchioni C, Sandini S, Acchioni M, Sgarbanti M. Co-Infections and Superinfections between HIV-1 and Other Human Viruses at the Cellular Level. Pathogens. Multidisciplinary Digital Publishing Institute (MDPI); 2024. doi:10.3390/pathogens13050349

281. Li C, Mousseau G, Valente ST. Tat inhibition by didehydro-Cortistatin A promotes heterochromatin formation at the HIV-1 long terminal repeat. Epigenetics Chromatin. 2019;12. doi:10.1186/s13072-019-0267-8
282. Chatterjee D, Zhang Y, Ngassaki-Yoka CD, Dutilleul A, Khalfi S, Hernalsteens O, et al. Identification of aryl hydrocarbon receptor as a barrier to HIV-1 infection and outgrowth in CD4+ T cells. Cell Rep. 2023;42. doi:10.1016/j.celrep.2023.112634